



Publishing House NAPOCA STAR

ISBN 978-973-647-596-2



**4<sup>th</sup> CONFERENCE ON ELEMENTARY  
PROCESSES IN ATOMIC SYSTEMS**

**CLUJ-NAPOCA, ROMANIA  
JUNE 18-20, 2008**

**BOOK OF ABSTRACTS**

**EDITED BY**

**KATALIN PÓRA, VASILE CHIȘ and LADISLAU NAGY**

## *Conference sponsored by*



**European Physical Society – *www.eps.org***

This publication was supported by the Romanian National Plan for Research (PN II) under contract No. ID 539

## *Organizers*



**Babeş–Bolyai University  
Cluj–Napoca, Romania  
*www.ubbcluj.ro***



**Institute of Nuclear Research of the  
Hungarian Academy of Sciences (ATOMKI)  
Debrecen, Hungary – *www.atomki.hu***

The Conference on Elementary Processes in Atomic Systems (CEPAS) is held every three years. The conference focuses on all aspects of processes and phenomena stimulated by interactions of electrons, positrons, ions, atoms, molecules, photons and other constituents of matter with gaseous, liquid, and condensed matter at low and intermediate energy. The scientific program of the conference includes invited review talks and progress reports. The contributed papers are presented during poster sessions but some were selected for oral presentations as hot topics.

CEPAS hosts a special SPARC session, as the last session of the conference on Friday afternoon. The SPARC – Stored Particles Atomic physics Research Collaboration – has been formed within the project FAIR – Facility for Antiproton and Ion Research – to be built at GSI, Darmstadt – Germany. The particular session is organized by the SPARC Collaboration Board.

## ORGANIZING COMMITTEE

**Dénes Berényi** - *honorary chairman*

ATOMKI, Debrecen, Hungary

**Ladislau Nagy** - *chairman*

Babeş-Bolyai University, Cluj, Romania

**Vasile Chiş** - *secretary*

Babeş-Bolyai University, Cluj, Romania

**Onuc Cozar**

Babeş-Bolyai University, Cluj, Romania

**Titus Beu**

Babeş-Bolyai University, Cluj, Romania

**Simion Aştilean**

Babeş-Bolyai University, Cluj, Romania

**Leontin David**

Babeş-Bolyai University, Cluj, Romania

**Sándor Ricz**

ATOMKI, Debrecen, Hungary

**Károly Tókési**

ATOMKI, Debrecen, Hungary

## ADVISORY BOARD

**Lorenzo Avaldi**

CNR-Istituto di Metodologie Inorganiche  
e dei Plasmi, Roma, Italy

**Raúl Barrachina**

Centro Atómico, Bariloche, Argentina

**Joachim Burgdörfer**

Institut für Theoretische Physik,  
Technische Universität Wien, Austria

**Robert DuBois**

Department of Physics, University  
Missouri-Rolla, USA

**Viorica Florescu**

University of Bucharest, Romania

**Ákos Kövér**

ATOMKI, Debrecen, Hungary

**Azzeddine Lahmam-Bennani**

Laboratoire des Collisions Atomiques et  
Moléculaires, Université Paris XI, Orsay  
Cedex, France

**Takeshi Mukoyama**

Institute for Chemical Research, Kyoto  
University, Japan

**Ágnes Nagy**

Department of Theoretical Physics,  
University of Debrecen, Hungary

**Béla Paripás**

Department of Physics, University of  
Miskolc, Hungary

**Gheorghe Popa**

University A.I. Cuza, Iaşi, Romania

**László Sarkadi**

ATOMKI, Debrecen, Hungary

**Béla Sulik**

ATOMKI, Debrecen, Hungary

**Joachim Ullrich**

Max-Planck-Institut für Kernphysik,  
Heidelberg, Germany

**Colm Whelan**

Department of Physics, College of  
Sciences, Norfolk, USA

**Mariusz Zubek**

Gdańsk University of Technology,  
Poland



## 4TH CONFERENCE ON ELEMENTARY PROCESSES IN ATOMIC SYSTEMS

CLUJ-NAPOCA, ROMANIA, JUNE 18-20, 2008

### Conference Program

---

#### June 17

---

- 17.00 – 20.00 Registration,  
Hotel Universitas
- 19.00 Welcome party,  
Restaurant near Hotel Universitas
- 

---

#### June 18

---

- 9.00 – 9.30 Opening, Central Building, Aula Magna

**Chair: Takeshi Mukoyama – Central Building, Aula Magna**

- 9.35 – 10.10 Dénes Berényi,  
*Fundamental information in atomic physics*
- 10.10 – 10.30 Karl-Ontjes Groeneveld  
*Planetary orbits in atomic physics*
- 10.30 – 11.00 Coffee break

**Chair: Robert DuBois – Central Building, Aula Augustin Maior**

- 11.00 – 11.35 Michael Schulz,  
*Kinematically complete experiments in atomic collisions*
- 11.35 – 12.10 Stefan Schippers,  
*Relativistic, QED and nuclear effects in highly charged ions revealed by resonant electron-ion recombination in storage rings*
- 12.10 – 12.35 Adnan Naja,  
*Fully differential experiments for electron impact ionisation of small atoms and molecules*
- 12.35 – 12.55 Angela Braeuning-Demian,  
*SPARC's flair at FAIR: new perspectives for atomic physics research with highly charged ions and antiprotons at the future FAIR facility*
- 12.55 – 14.30 Lunch break

**Chair: Stefan Facsko – Central Building, Aula Augustin Maior**

- 14.30 – 15.05** Yasunori Yamazaki,  
*Interaction of charged particles with insulators*
- 15.05 – 15.30** John R. Sabin,  
*Molecular fragmentation on swift ion collision*
- 15.30 – 15.55** Oksana Plekan,  
*Photoemission spectroscopy of DNA base tautomers*
- 15.55 – 16.15** Coffee break

**Chair: Raul Barrachina – Central Building, Aula Augustin Maior**

- 16.15 – 16.50** John Tanis,  
*Interferences in coherent electron emission from diatomic molecules*
- 16.50 – 17.15** Jean-Yves Chesnel,  
*Fast oscillating structures in electron spectra following slow  $He^{q+} + He$  collisions: search for electron interferences*
- 17.15 – 17.40** Francois Fremont,  
*Young interferences using a single electron source and an atomic-size two center interferometer*
- 17.40 – 19.10** Poster session
- 19.15** Meeting of the Scientific Committee and Organizing Committee,  
Pyramid Restaurant

---

## June 19

**Chair: Günther Werth – Central Building, Aula Augustin Maior**

- 8.45 – 9.20** Fernando Martin,  
*The role of nuclear dynamics in  $H_2$  ionization and dissociation by synchrotron radiation and laser pulses*
- 9.20 – 9.45** Robert Moshhammer,  
*Atomic and molecular fragmentation dynamics in intense laser fields*
- 9.45 – 10.10** Juan Fiol,  
*Detailed description of collision dynamics in atomic ionization processes*
- 10.10 – 10.35** Zejun Ding,  
*Monte Carlo simulation of electron interaction with solids and surfaces*
- 10.35 – 11.05** Coffee break

**Chair: Viorica Florescu – Central Building, Aula Augustin Maior**

- 11.05 – 11.40** Joachim Burgdorfer,  
*Atomic dynamics on the attosecond scale: photons and charged particles*



- 11.40 – 12.15** Mihai Gavrilă,  
*Atomic stabilization in superintense LASER fields, then and now*
- 12.15 – 12.40** Matjaz Zitnik,  
*X-ray resonant Raman scattering from noble gas atoms and beyond*
- 12.40 – 13.00** Sándor Borbély,  
*Over-the-barrier ionization of the hydrogen atom by intense ultrashort laser pulses*
- 13.00 – 14.30** Lunch break

**Chair: Gheorghe Popa – Central Building, Aula Augustin Maier**

- 14.30 – 15.05** Friedrich Aumayr,  
*Highly charged ion-induced nanostructures on surfaces*
- 15.05 – 15.40** Nikolaus Stolterfoht,  
*Scaling laws for guided transmission of highly-charged ions through nanocapillaries in a PET polymer*
- 15.40 – 16.05** Fumihiko Koike,  
*Temporal aspects in atomic ionizations initiated by electron or photon impact*
- 16.05 – 16.25** Juana L. Gervasoni,  
*Dispersion relation and plasmon excitation in nanostructures by charged particles*
- 16.25 – 17.55** Poster session
- 18.15** Visit of the Art Museum of Cluj-Napoca (Bánffy Palace)
- 19.00** Concert, Flauto Dolce Ensemble

**June 20**

**Chair: Titus Beu – Central Building, Aula Augustin Maier**

- 8.45 – 9.20** Colm Whelan,  
*Fragmentation processes*
- 9.20 – 9.55** Udo Buck,  
*The solvated electron in recent cluster experiments*
- 9.55 – 10.20** Kevin Prince,  
*Inner shell spectroscopy and the shapes of biomolecules*
- 10.20 – 10.40** Edward Parilis,  
*Interaction of Highly Charged Clusters with Surface*
- 10.40 – 11.20** Coffee break

**Chair: Ákos Kövér – Central Building, Aula Augustin Maier**

- 11.20 – 11.55** James Walters,  
*Atomic Collisions Involving Antimatter*
- 11.55 – 12.20** Gaetana Laricchia,  
*Ionizing collisions by positrons and positronium impact*

- 12.20 – 12.45** Radu Campeanu,  
*Positron impact ionization of atoms and molecules*
- 12.45 – 13.10** Helge Knudsen,  
*Ionization of noble gas atoms in slow antiproton collisions*
- 13.10 – 13.30** Alexander Glushkov,  
*QED theory of radiation emission and absorption lines for atoms and ions in a strong laser field*
- 13.30 – 15.00** Lunch break

**SPARC – Chair: Stephan Fritzsche – Central Building, Aula Augustin Maier**

- 15.00 – 15.25** Alex Gumberidze,  
*X-ray spectroscopy of highly-charged heavy ions at FAIR*
- 15.25 – 15.50** Christopher Kozhuharov,  
*Ultra-cold electron target for recombination experiments at the new experimental storage ring, NESR*
- 15.50 – 16.15** Andrey Surzhykov,  
*Recent theoretical progress in studying x-ray emission from highly-charged, heavy ions*
- 16.15 – 16.40** Daniel Ursescu,  
*High power lasers and X-ray lasers for experiments within SPARC collaboration*
- 16.40 – 17.05** Daniel Fischer,  
*Reaction Microscopes in heavy-ion storage rings - results and prospects*
- 19.00** Banquet, Pyramid restaurant
-

## List of Posters

<b>We-1</b>	T → V, R ENERGY EXCHANGE FOR INELASTIC COLLISIONS OF COLD MOLECULES IN THE SYSTEM CSBR + CSBR <b>V.M. Azriel</b> , L.Yu. Rusin	59
<b>We-2</b>	IONIZATION OF METASTABLE THALLIUM ATOMS <b>I.I. Shafranyosh</b> , V.I. Marushka, R.O. Fedorko, T.A. Snegurskaya, V. Perehanets	60
<b>We-3</b>	EXTRACTING INTERACTION PARAMETERS FROM NEAR THRESHOLD EXPERIMENTS P. A. Macri and <b>R. O. Barrachina</b>	61
<b>We-4</b>	LOW-ENERGY ELECTRON SCATTERING FROM CALCIUM <b>S. Gedeon</b> and V. Lazur	62
<b>We-5</b>	ANGULAR DISTRIBUTION OF X-RAY SATELLITES FOLLOWING THE DIELECTRONIC RECOMBINATION OF HIGH-Z IONS <b>S. Fritzsche</b> , N. M. Kabachnik, A. Surzhykov and Th. Stöhlker	63
<b>We-6</b>	RESONANT AUGER DECAY OF AR 2p HOLE INDUCED BY ELECTRON IMPACT <b>M. Žitnik</b> , M. Kavčič, K. Bučar, B. Paripás, B. Palásthy, K. Tőkési	64
<b>We-7</b>	PROPERTIES OF AUGER ELECTRONS FOLLOWING EXCITATION OF POLARIZED ATOMS BY POLARIZED ELECTRONS <b>A. Kupliauskienė</b> , V. Tutlys	65
<b>We-8</b>	FLUORESCENCE OF POLARIZED ATOMS EXCITED BY POLARIZED ELECTRONS <b>A. Kupliauskienė</b>	66
<b>We-9</b>	MODELLING ELECTRON KINETICS IN BF <sub>3</sub> <b>O. Šašić</b> , Z. Raspopović, Ž. Nikitović, V. Stojanović and Z. Lj. Petrović	67
<b>We-10</b>	STUDY OF THE ELECTRON-ELECTRON CORRELATION VIA OBSERVING THE TWO-ELECTRON CUSP L. Sarkadi and A. Orbán	68
<b>We-11</b>	POST-COLLISION INTERACTION AFTER ELECTRON IMPACT MEASURED BY (e,2e) COINCIDENCE TECHNIQUE B. Paripás and B. Palásthy	69
<b>We-12</b>	INTERPLAY OF INITIAL AND FINAL STATES FOR (e; 3e) AND (γ; 2e) PROCESSES ON HELIUM <b>L.U. Ancarani</b> , G. Gasaneo, F.D. Colavecchia and C. Dal Cappello	70

<b>We-13</b>	NEAR-THRESHOLD EXCITATION OF THE RESONANCE $\lambda$ 158.6 nm LINE IN ELECTRON-INDIUM ION COLLISIONS A. Gomonai, A. Imre, <b>E. Ovcharenko</b> , Yu. Hutych	71
<b>We-14</b>	MECHANISM INVESTIGATION IN COLLISION OF CLOSED ELECTRON SHELL ATOMIC PARTICLES <b>R. Lomsadze</b> , M. Gochitashvili, B. Lomsadze, N. Tsiskarishvili, O. Taboridze	72
<b>We-15</b>	INNER-SHELL PHOTODETACHMENT OF IRON AND RUTHENIUM NEGATIVE IONS <b>I. Dumitriu</b> , René C. Bilodeau, T. Gorczyca, G. Ackerman, C. W. Walter, N. D. Gibson, A. Aguilar, Z. Pesic, D. Rolles, and N. Berrah	73
<b>We-16</b>	GENERALIZED OSCILATOR STRENGTHS FOR ELECTRON SCATTERING BY In ATOM AT SMALL ANGLES <b>M. S. Rabasović</b> , S. D. Tošić, V. Pejčev, D. Šević, D. M. Filipović and B. P. Marinković	74
<b>We-17</b>	ELASTIC ELECTRON SCATTERING BY SILVER ATOMS <b>S. D. Tošić</b> , V. I. Kelemen, D. Šević, V. Pejčev, D. M. Filipović, E. Yu. Remeta and B. P. Marinković	75
<b>We-18</b>	ELASTIC ELECTRON SCATTERING BY Zn , Cd AND Hg ATOMS IN THE OPTICAL POTENTIAL APPROACH <b>V. Kelemen</b> , M. Dovhanych, E. Remeta	76
<b>We-19</b>	COLLISIONS IN TERMS OF QUANTUM TRAJECTORIES M. Acuña, and <b>J. Fiol</b>	77
<b>We-20</b>	THEORETICAL AND EXPERIMENTAL INVESTIGATIONS OF ELECTRON EMISSION DURING WATER IONIZATION BY LIGHT ION IMPACT <b>C. Champion</b> , H. Lekadir and C. Dal Cappello	78
<b>We-21</b>	ELECTRONIC RELATIVISTIC EFFECT IN BINARY-ENCOUNTER APPROXIMATION FOR ION-ATOM COLLISIONS <b>Takeshi Mukoyama</b>	79
<b>We-22</b>	INNER-SHELL IONIZATION IN ION-ATOM COLLISIONS AT MeV/u ENERGIES <b>M.M. Gugu</b> , C. Ciortea, A. Enulescu, I. Piticu, D.E. Dumitriu, D. Fluerașu, A.C. Scafes, M.C. Pentia, C. Ciocarlan, and M.D. Pena	80
<b>We-23</b>	A SETUP FOR ELECTRON-ION COLLISIONS STUDIES EMPLOYING HIGH-RESOLUTION ELECTRON SPECTROSCOPY <b>K. Holste</b> , S. Schippers, A. Müller and S. Riez	81
<b>We-24</b>	PULSE HEIGHT DISTRIBUTION MEASUREMENTS ON POLYCRYSTALLINE CVD-DIAMOND WITH HEAVY IONS AT ENERGIES OF 11 MeV/u AND 50 MeV/u A. Braeuning – Demian, <b>D. Fluerașu</b> , D. Dumitriu	82

<b>We-25</b>	PRODUCTION OF MOLECULAR HYDROGEN IONS FROM C <sub>2</sub> H <sub>4</sub> AND C <sub>2</sub> H <sub>6</sub> UNDER ELECTRON CAPTURE AND LOSS COLLISIONS OF 2MeV Si IONS <b>Akio Itoh</b> , Takahiro Yamada, Tomoya Mizuno, Hidetsugu Tsuchida	83
<b>We-26</b>	DIFFERENTIAL CROSS SECTIONS FOR ELECTRON-IMPACT SCATTERING ON BORON <b>L. Bandurina</b> , V. Gedeon	84
<b>We-27</b>	IMPACT PARAMETER METHOD CALCULATIONS FOR FULLY DIFFERENTIAL IONIZATION CROSS SECTIONS <b>F. Járαι-Szabó</b> and L. Nagy	85
<b>We-28</b>	CROSS SECTIONS AND TRANSPORT PROPERTIES OF F <sup>+</sup> IONS IN Ar, Kr AND Xe <b>J.V. Jovanović</b> , Z.Lj. Petrović and V. Stojanović	86
<b>We-29</b>	Z <sub>2</sub> STRUCTURE OF THE STOPPING POWER FOR ELECTRON BEAMS Hasan Gümüş, Önder Kabadayi	87
<b>We-30</b>	DESIGN, SIMULATION AND CONSTRUCTION OF MULTI-FIELD LINEAR TIME-OF-FLIGHT MASS SPECTROMETERS Erengil Z, Kaymak N, Yildirim M, Sise O, Dogan M and Kilic HS	88
<b>We-31</b>	MONTE CARLO CALCULATIONS OF THE SECONDARY ELECTRON EMISSION INDUCED BY IONS <b>A. Nina</b> , M. Radmilović-Radjenović, V. Stojanović and Z. Lj. Petrović	89
<b>We-32</b>	MEASUREMENTS AND ANALYSIS OF SECONDARY ELECTRON YIELDS IN TOWNSEND DARK DISCHARGES <b>G. Malović</b> , D. Marić , S. Živanov, M. Radmilović- Radjenović and Z.Lj. Petrović	90
<b>We-33</b>	ENERGY-BAND STRUCTURE AND INELASTIC SCATTERING EFFECTS IN THE LOW-ENERGY ABSORBED CURRENT AND SECONDARY-ELECTRON EMISSION SPECTROSCOPIES <b>O.F. Panchenko</b> and L.K. Panchenko	91
<b>We-34</b>	WATER VAPOUR UV DISCHARGE SOURCE <b>V.A. Kelman</b> , A.A. Heneral, Yu.V. Zhmenyak, Yu.O. Shpenik, <b>O.I. Plekan</b>	92
<b>We-35</b>	JONES EFFECT ON Li AND Na ATOMS <b>V.V. Chernushkin</b> , V.D. Ovsiannikov	93
<b>We-36</b>	ON RYDBERG SERIES OF AUTOIONIZING RESONANCES <b>V. Stancalie</b>	94
<b>We-37</b>	THERMAL IONIZATION OF Cs RYDBERG STATES <b>Glukhov I. L.</b> and Ovsiannikov V. D.	95

<b>We-38</b>	THE ELECTRONIC g-FACTOR OF HYDROGEN-LIKE IONS AS TEST OF BOUND-STATE QUANTUM ELECTRODYNAMICS G. Werth, K. Blaum, B. Schabinger, S. Sturm	96
<b>We-39</b>	QED APPROACH TO THE PHOTON-PLASMON TRANSITIONS AND DIAGNOSTICS OF THE SPACE PLASMA TURBULENCE A. Glushkov, O. Khetselius and A. Svinarenko	97
<b>We-40</b>	QUANTUM DYNAMICS OF THE RESONANT LEVELS FOR ATOMIC AND NUCLEAR ENSEMBLES IN A LASER PULSE: OPTICAL BI-STABILITY EFFECT AND NUCLEAR QUANTUM OPTICS O. Khetselius	98
<b>We-41</b>	RELATIVISTIC CALCULATING THE HYPERFINE STRUCTURE PARAMETERS IN THE HEAVY-ELEMENTS AND LASER SEPARATION OF ISOTOPES AND NUCLEAR ISOMERS O. Khetselius	99
<b>We-42</b>	GENERATION OF X-RAY RADIATION AT THE INTERACTION OF CHARGE PARTICLES WITH DIELECTRICS V.P. Petukhov	100
<b>We-43</b>	ELECTRON-IMPACT EXCITATION OF Yb RESONANCE LINE O.B. Shpenik, M.M. Erdevdy, J.E. Kontros	101
<b>We-44</b>	LOW-ENERGY ELECTRON SPECTROSCOPY OF Bi FILMS O.B. Shpenik, T.Yu. Popik, R.O. Ortikov	102
<b>We-45</b>	ON SURFACE ELEMENTARY PROCESSES AND POLYMER SURFACE MODIFICATIONS INDUCED BY DOUBLE PULSED DBD A. S. Chiper, A. V. Nastuta, G. B Rusu and G. Popa	103
<b>We-46</b>	MONOATOMIC DEEP NANOSTRUCTURES ON ALKALI HALIDE SURFACES INDUCED BY HIGHLY CHARGED IONS S. Facsko, R. Heller, R. Wilhelm, Z. Pešić and W. Möller	104
<b>We-47</b>	TRANSMISSION OF 4.5 keV Ar <sup>9+</sup> IONS THROUGH A SINGLE MACROSCOPIC GLASS-CAPILLARY R.J. Berezky, G. Kowarik, F. Aumayr, K. Tőkési	105
<b>We-48</b>	MCP IMAGES OF IONS TRANSMITTED THROUGH ION GUIDING ALUMINA CAPILLARIES Z. Juhász, B. Sulik, Gy. Víkor, S. Biri, I. Iván, K. Tőkési, E. Takács, S. Mátéfi-Tempfli, M. Mátéfi-Tempfli, L. Piraux, J. Pálinkás	106
<b>We-49</b>	INTERPLAY OF COULOMB EXPLOSION AND BINARY PROCESSES IN FRAGMENTATION OF MOLECULES BY HIGHLY CHARGED ION IMPACT Z. Juhász, J.-Y. Chesnel, F. Frémont, A. Hajaji, B. Sulik	107

<b>We-50</b>	THERMALLY INDUCED FRAGMENTATION OF NEUTRAL AND CHARGED C <sub>60</sub> Titus Adrian Beu, Lóránd Horváth, Ioan Ghişoiu	108
<b>We-51</b>	FRAGMENTATION OF GLYCINE MOLECULE BY LOW-ENERGY ELECTRONS V. S. Vukstich, A.I. Imre, <b>A. V. Snegursky</b>	109
<b>We-52</b>	ABOVE-THRESHOLD IONIZATION OF CALCIUM BY LINEARLY AND CIRCULARLY POLARIZED LASER PULSES <b>G. Buica</b>	110
<b>We-53</b>	ANGULAR MOMENTUM IN ATOMIC IONIZATION BY SHORT LASER PULSES: MULTIPHOTON VERSUS SEMICLASSICAL TUNNELING MODEL <b>D. G. Arbó</b> , K. I. Dimitriou, E. Persson, and J. Burgdörfer	111
<b>We-54</b>	POLARISATION EFFECTS IN EXCITATION OF STRONG PERTURBED ATOMIC STATES <b>Bondar I. I.</b> , Suran V. V.	112
<b>We-55</b>	OBSERVATION OF NEW TYPE RESONANT MAXIMA AT FORMATION OF DOUBLY CHARGED IONS UPON MULTIPHOTON IONIZATION OF BARIUM ATOMS BY LINEARLY AND CIRCULARLY POLARIZED RADIATION <b>Suran V. V.</b> , Bondar I. I.	113
<b>We-56</b>	MULTIPHOTON IONIZATION OF ATOMS WITH SHORT INTENSE LASER PULSES CLOSE TO RESONANCE CONDITIONS <b>V. D. Rodríguez</b> , D. G. Arbó and P. A. Macri	114
<b>We-57</b>	NON-INVASIVE MARKERS MEASUREMENTS <b>M.Culea</b> , O. Cozar ,E. Culea	115
<b>We-58</b>	RESIDUAL CHARACTERIZATION OF SOME PESTICIDES IN WINE <b>M. Culea</b> , C. Lehene, O. Cozar	116
<b>We-59</b>	CHARACTERIZATION OF SOME PLANT EXTRACTS BY GC-MS <b>A. Iordache</b> , M. Culea, O. Cozar	117
<b>We-60</b>	STATISTICAL STUDY OF DATA FOR CIRRHOSIS DIAGNOSIS BY GC/MS <b>C. Mesaros</b> , M. Culea, O. Cozar	118

<b>Th-1</b>	LASER SPECTROSCOPIC STUDIES OF COLLISIONAL DYNAMICS IN ANTIPROTONIC HELIUM <b>M. Hori</b>	119
<b>Th-2</b>	INTERACTION OF POSITRONIUM ATOMS WITH PARAMAGNETIC MOLECULES MEASURED BY PERTURBED ANGULAR DISTRIBUTION IN 3 - GAMMA ANNIHILATION DECAY E.A. Ivanov, <b>I. Vata</b> , S.Toderian, D. Dudu, I.Rusen and S. Nitisor	120
<b>Th-3</b>	NEGATIVE DIFFERENTIAL CONDUCTIVITY OF POSITRONS IN GASES <b>A. Banković</b> , Z.Lj. Petrović, G. Malović, J.P. Marler and R. E. Robson	121
<b>Th-4</b>	ANNIHILATION OF PROTONIUM BY CHARGED PARTICLE IMPACT A. Igarashi and <b>L. Gulyás</b>	122
<b>Th-5</b>	INFORMATION ABOUT TS-1 AND TS-2 DOUBLE IONIZATION MECHANISMS FOR POSITRON AND ELECTRON IMPACT IONIZATION OF ARGON <b>R.D. DuBois</b> , J. Gavin, O. G. de Lucio	123
<b>Th-6</b>	IONIZATION OF MOLECULES BY POSITRON AND ELECTRON IMPACT <b>I. Tóth</b> , R. I. Campeanu, V. Chiş and L. Nagy	124
<b>Th-7</b>	CROSS SECTION OF POSITIVE IONS PRODUCTION IN ELECTRON COLLISION WITH ADENINE MOLECULES M.I. Sukhoviya, V.V. Stecovych., M.I. Shafranyosh, O.V. Pavlyuchok, L.L. Shimon, I.I Shafranyosh	125
<b>Th-8</b>	IONIZATION OF GUANINE MOLECULES BY ELECTRON IMPACT NEAR THRESHOLD A.N. Zavilopulo, O.B. Shpenik, A.S. Agafonova	126
<b>Th-9</b>	IONIZATION AND DISSOCIATIVE IONIZATION OF A POPOP MOLECULE L.G.Romanova, A.N.Zavilopulo, A.S.Agafonova, O.B.Shpenik, M.I.Mykyta	127
<b>Th-10</b>	RADIATIVE CHARACTERISTICS OF POPOP MOLECULES AT LOW-ENERGY ELECTRON-IMPACT EXCITATION M.M. Erdevdy, <b>O.B. Shpenik</b> , J.E. Kontros	128
<b>Th-11</b>	ELECTRON SPECTROSCOPY OF POPOP MOLECULES I.V.Chernyshova, J.E.Kontros, <b>O.B.Shpenik</b>	129
<b>Th-12</b>	ELECTRON-IMPACT IONIZATION OF GLUCOSE AND VITAMIN C J.E.Kontros, I.V.Chernyshova, <b>O.B.Shpenik</b>	130



<b>Th-13</b>	THEORETICAL CROSS SECTIONS FOR IONIZING PROCESSES OF DNA BASES IMPACTED BY $H^+$ , $He^{2+}$ AND $C^{6+}$ IONS: A CLASSICAL MONTE CARLO APPROACH <b>C. Champion</b> , H. Lekadir, I. Abbas and J. Hanssen	131
<b>Th-14</b>	THE EFFECT OF INTERNAL STATE OF DIATOMIC MOLECULES ON THE DYNAMICS OF ENERGY EXCHANGE <b>V.M. Azriel</b> , L.Yu. Rusin	132
<b>Th-15</b>	OFF-SHELL CONTINUUM-DISTORTED-WAVE THEORY FOR POSITRONIUM FORMATION FROM NOBLE GAS ATOMS P. A. Macri and <b>R. O. Barrachina</b>	133
<b>Th-16</b>	YOUNG-TYPE INTERFERENCE WITH SINGLE ELECTRONS IN THE AUTOIONIZATION OF ATOMS BY THE IMPACT OF MOLECULES: AN INDEPENDENT MEASUREMENT IN THE BACKWARD DIRECTION S. Suárez, D. Fregenal, G. Bernardi, P. Focke, F. Frémont, J.-Y. Chesnel, A. Hajaji and <b>R. O. Barrachina</b>	134
<b>Th-17</b>	MOLECULAR ORIENTATION INFLUENCE ON THE INTERFERENCE PATTERN <b>K. Póra</b> , L. Nagy	135
<b>Th-18</b>	INTERFERENCES IN ELECTRON EMISSION FROM $O_2$ BY 30 MEV $O^{9+}$ IMPACT <b>M. Winkworth</b> , P. D. Fainstein, M. E. Galassi, J. Baran, B.S. Dassanayake, S. Das, T. Elkafrawy, D. Cassidy, A. Kayani and J.A. Tanis	136
<b>Th-19</b>	ELECTRON TRANSPORT COEFFICIENTS IN $N_2O$ IN RF FIELDS <b>O. Šašić</b> , S. Dupljanin, S. Dujko and Z. Lj. Petrović	137
<b>Th-20</b>	FIELD-INDUCED ENHANCEMENTS OF DIELECTRONIC RECOMBINATION IN Na -LIKE S AND Na-LIKE Ar <b>I. Orban</b> , S. Böhm, S. Trotsenko, and R. Schuch	138
<b>Th-21</b>	PHOTOIONIZATION OF $Li^+$ ION ABOVE THE EXCITED ION FORMATION THRESHOLD <b>T. Zajak</b> , A. Opachko and V Simulik	139
<b>Th-22</b>	STUDY OF LEFT-RIGHT ASYMMETRY IN PHOTOIONIZATION <b>T. Ricsóka</b> , S. Riez, Á. Kövér, K. Holste, A. A. Borovyk Jr., D. Varga, S. Schippers and A. Müller	140
<b>Th-23</b>	THE INFLUENCE OF Zn ATOM ADDITIVE ON Cu LASER CHARACTERISTICS <b>V.A. Kelman</b> , E.A. Svitlichnyi, Yu.V. Zhmenyak, Yu.O. Shpenik, <b>O.I. Plekan</b>	141
<b>Th-24</b>	GENERALIZED SPACE-TRANSLATED DIRAC EQUATION AND ITS EQUIVALENT PAULI FORM FOR SUPERINTENSE LASER-ATOM INTERACTIONS <b>Madalina Boca</b> , Viorica Florescu and Mihai Gavrilă	142

<b>Th-25</b>	ATOMIC IONIZATION BY SUDDEN MOMENTUM TRASFER <b>D. G. Arbó</b> , K. Tókési, and J. E. Miraglia	143
<b>Th-26</b>	INTERACTION OF INTENSE SHORT LASER PULSES WITH POSITRONIUM <b>S. Borbély</b> , K. Tókési, D. G. Arbó, L. Nagy	144
<b>Th-27</b>	PHOTOABSORPTION AND PHOTOIONIZATION OF DIATOMIC MOLECULES <b>Irina Dumitriu</b> and Alejandro Saenz	145
<b>Th-28</b>	IONIZATION IN INTENSE LASER FIELD: INTENSITY-DEPENDENT ENHANCEMENTS AT INDUCED CHANNEL CLOSINGS <b>Mihai Dondera</b>	146
<b>Th-29</b>	COLD ATOMS PHOTOASSOCIATION WITH INTENSE LASER PULSES <b>Mihaela Vatasescu</b>	147
<b>Th-30</b>	PROPAGATION EFFECTS IN ATTOSECOND PULSE GENERATION <b>V. Tosa</b>	148
<b>Th-31</b>	GENERATION OF ULTRA-SHORT X-RAY PULSES IN CLUSTER SYSTEM DURING IONIZATION BY FEMTO-SECOND OPTICAL PULSE A. Glushkov, <b>O. Khetselius</b> and A. Ignatenko	149
<b>Th-32</b>	DISORDER EFFECTS IN REFLECTANCE SPECTRA OF COLLOIDAL PHOTONIC CRYSTALS E. Vințeler, C. Farcău, S. Aștilean	150
<b>Th-33</b>	INTERACTION OF LIGHT WITH METALLIC NANO HOLE ARRAYS <b>V. Canpean</b> and S. Astilean	151
<b>Th-34</b>	LUMINESCENCE PROPERTIES OF GOLD NANORODS <b>F. Toderas</b> , M. Iosin and S. Astilean	152
<b>Th-35</b>	PLASMON-ENHANCED FLUORESCENCE OF DYE MOLECULES <b>M. Iosin</b> , P.L. Baldeck and S. Astilean	153
<b>Th-36</b>	THE STUDY OF RAMAN ENHANCEMENT EFFICIENCY AS FUNCTION OF NANOPARTICLE SIZE AND SHAPE <b>Sanda C. Boca</b> , Cosmin Farcau, Simion Astilean	154
<b>Th-37</b>	TEM XRD AND DSC ANALYSIS OF Mn DOPED FINEMET M.Moneta, J.Balcerski, P.Uznański and P.Sovak	155
<b>Th-38</b>	SURFACE AND BULK PLASMON EXCITATIONS IN CARBON NANOTUBES. COMPARISON WITH THE HYDRODYNAMIC MODEL Mario Zapata Herrera and J. L. Gervasoni	156
<b>Th-39</b>	ATOMIC FORCE MICROSCOPY CHARACTERIZATION OF GOLD NANOCRYSTALS <b>R. Stiufiuc</b> , F. Toderas, G. Stiufiuc and S. Astilean	157

<b>Th-40</b>	INFRARED SPECTRA OF SMALL WATER CLUSTERS: RELEVANCE OF INDUCED POLARIZATION Titus Adrian Beu, Gabriel Cabau	158
<b>Th-41</b>	PROPERTIES OF POSITIVE AND NEGATIVE IONS IN ANTHRACENE DERIVATIVES: A THEORETICAL STUDY A.V. Kukhta, I.N.Kukhta, O.L. Neyra, E. Meza	159
<b>Th-42</b>	FORMATION OF LONG LIVED NEGATIVE IONS IN ANTHRACENE DERIVATIVES A.V. Kukhta, S.A. Pshenichnyuk, N.L. Asfandiarov	160
<b>Th-43</b>	INTERACTION OF LOW-ENERGY ELECTRONS WITH PHTHALOCYANINE AND PORPHIRINE MOLECULES IN THE GAS PHASE A.V. Kukhta, S.M. Kazakov	161
<b>Th-44</b>	SPECTROSCOPIC INVESTIGATIONS OF NEW METALLIC COMPLEXES WITH LEUCINE AS LIGAND Cs. Nagy, A. Marcu, A. Stanila, D. Cozma, D. Rusu and L. David	162
<b>Th-45</b>	STRUCTURAL INVESTIGATIONS OF SANDWICH-TYPE HETEROPOLYOXOMETALATE WITH DINUCLEAR VANADIUM CLUSTER O. Baban, I. Hauer, D. Rusu, M. Rusu, N. L. Mogonea and L. David	163
<b>Th-46</b>	SPECTROSCOPIC INVESTIGATION OF SOME $UO_2^{2+}$ - POLYOXOMETALATE COMPLEXES N. L. Mogonea, O. Baban, I. Hauer, D. Rusu, M. Rusu and L. David	164
<b>Th-47</b>	SURFACE MORPHOLOGY INFLUENCE ON D RETENTION IN BE FILMS PREPARED BY THERMIONIC VACUUM ARC METHOD A. Anghel, C. Porosnicu, M. Badulescu, I. Mustata, C. P. Lungu	165
<b>Th-48</b>	CHARACTERISATION OF A NEW PLASMA JET BASED ON ATOMIC AND MOLECULAR PROCESSES S. D. Anghel, A. Simon, A. I. Radu and I.J. Hidi	166
<b>Th-49</b>	ENERGY APPROACH TO CALCULATING ELECTRON-COLLISION STRENGTHS AND RATE COEFFICIENTS IN MULTICHARGED IONS PLASMA A. Glushkov, O. Khetselius, A. Loboda and E. Gurnitskaya	167
<b>Th-50</b>	RESONANCE AND MULTI-BODY PHENOMENA IN HEAVY IONS COLLISIONS A. Glushkov, O. Khetselius and A. Loboda and Yu. Dubrovskaya	168
<b>Th-51</b>	MICROORGANISM SENSITIVITY TO IONS AND FREE RADICALS DELIVERED BY PLASMA DISCHARGE Antonia Poiata, Iuliana Motrescu, Cristina Tuchilus, A. Nastuta, D. E. Creanga, G. Popa	169

<b>Th-52</b>	ON THE DYNAMIC OF PLASMA PLUME IN HIGH-FLUENCE LASER ABLATION C. Ursu, b, S. Gurlui, M. Ziskind, G. Popa and C. Focsa	170
<b>Th-53</b>	ON THE CARBON AND TUNGSTEN SPUTTERING YIELD IN A MAGNETRON DISCHARGE V. Tiron, S. Dobrea, C. Andrei and G. Popa	171
<b>Th-54</b>	DIAGNOSTICS AND ACTIVE SPECIES FORMATION IN AN ATMOSPHERIC PRESSURE HELIUM STERILIZATION PLASMA SOURCE Alpar Simon; Sorin Dan Anghel; Mihaela Papiu; Otilia Dinu	172
<b>Th-55</b>	STUDIES ABOUT THE ACRYLIC ACID PLASMA POLYMERS I. Topala, N. Dumitrascu, Gh. Popa	173
<b>Th-56</b>	STUDIES AND CALCULATION OF ENERGY FILTER PARAMETERS A.S. Agafonova, V.A. Surkov	174
<b>Th-57</b>	MASS SPECTROMETRIC STUDY OF A GLUCOSE MOLECULE A.N.Zavilopulo, L.G.Romanova, O.B.Shpenik, A.S.Agafonova	175
<b>Th-58</b>	MASS SPECTROMETRIC DETERMINATION OF RESIDUAL AMOUNTS OF PH <sub>3</sub> AND SO <sub>2</sub> F <sub>2</sub> IN FOOD A.N. Zavilopulo, V.A. Mamontov, L.G. Romanova, M.I. Mykyta	176
<b>Th-59</b>	MASS SPECTROMETRY OF ASCORBIC ACID A.N.Zavilopulo, A.S.Agafonova, L.G.Romanova, M.I.Mykyta	177
<b>Th-60</b>	PRESHOWER DETECTOR IMPLEMENTATION IN $\pi^+\pi^-$ HADRONIC ATOM BREAKUP STUDIES M. Pentia, D.E. Dumitriu, M. Gugiu, C. Ciocarlan, S. Constantinescu, and C. Caragheorgheopol	178
<b>Th-61</b>	COMPUTATIONAL CHEMISTRY ir SPECTRA SIMULATION OF DEUTERATED TRIGLYCIN SULFATE II FOR NEUTRON QUASIELASTIC INCOHERENT SCATTERING ON MICROCRYSTALS C.A. Simion, V. Tripăduș, A. Niculescu	179
<b>Th-62</b>	APLICATION OF COMPTON SCATTERING IN ORGANIC SCINTILLATORS FOR THE ENERGY CALIBRATION IN $\beta$ AND NEUTRON SPECTROSCOPY L. Daraban	180

**FUNDAMENTAL INFORMATION IN ATOMIC PHYSICS**  
**- Opening address -**

**Dénes BERÉNYI**

Institute of Nuclear Research of HAS, Debrecen, Hungary

It shall be shown that the atomic physics research is important not only from the point of view of the different applications but also from that of the fundamental information. After a short historical retrospect three more recent results in question will be treated in a bit more detailed, namely the quantum teleportation, the Bose-Einstein condensation and the recently observed left-right asymmetry in outer-shell photo-ionization.

**PLANETARY ORBITS IN ATOMIC PHYSICS**

**Karl-Ontjes Groeneveld**

Institut für Kernphysik, Johann-Wolfgang-Goethe Universität, Frankfurt am Main, Germany

## KINEMATICALLY COMPLETE EXPERIMENTS IN ATOMIC COLLISIONS

**M. Schulz<sup>1</sup>, R. Moshhammer<sup>2</sup>, A. Hasan<sup>1,3</sup>, D. Fischer<sup>2</sup>, M.F. Ciappina<sup>4</sup>, T. Kirchner<sup>5</sup>,  
N. Maydanyuk<sup>1</sup>, M. Dürr<sup>2</sup>, T. Ferger<sup>2</sup>, J.Ullrich<sup>2</sup>**

<sup>1</sup>Physics Dept., Missouri University of Science & Technology, Rolla, MO 65409, USA

<sup>2</sup>Max-Planck-Institut für Kernphysik, 69117 Heidelberg, Germany

<sup>3</sup>Dept. of Physics, UAE University, P.O. Box 17551, Al-Ain, Abu Dhabi, UAE

<sup>4</sup>Max-Planck-Institut für Physik Komplexer Systeme, 01187 Dresden, Germany

<sup>5</sup>Institut für Theoretische Physik, TU Clausthal, 38678 Clausthal-Zellerfeld, Germany

With the development of recoil-ion momentum spectroscopy [1] kinematically complete experiments on inelastic processes in ion-atom collisions have become feasible even for heavy fast projectiles. Such studies revealed that our understanding of even the most basic one-electron processes, such as single ionization, is not as complete as previously assumed [2,3]. Experimental work will be reviewed for various processes including single and double ionization and mutual ionization of both collision partners.

Furthermore, a novel technique to analyze four-body fragmentation processes will be presented.

In the case of single ionization fully differential cross sections (FDCS) were studied for a large variety of collision systems. Three-dimensional angular distributions of the ejected electrons for fully determined kinematics were analyzed. In all cases considerable discrepancies to theory were found. It appears that the problem in theory can always be traced to an incomplete description of the role of the interaction between the projectile and the residual target ion. Depending on the collision system this interaction manifests itself in a variety of features: for very fast collisions it leads to a strong filling of the minimum that in the first Born approximation (FBA) separates the well-known binary and recoil peaks from each other [2]. For highly charged ion impact it leads to a strong peak structure in the initial projectile beam direction [4]. Finally, for relatively slow collisions it can lead to a backward shift of the binary peak relative to the direction of the momentum transfer  $q$  from the projectile to the target atom [3], while theory predicts either no shift at all or a forward shift.

For the case of four-body fragmentation processes, like double ionization or mutual ionization of both collision partners, 4-particle Dalitz (4-D) plots present a powerful complementary method to FDCS of analyzing kinematically complete experiments [5]. The disadvantage compared to FDCS is that the degree of differentiability of the cross sections is lower. However, two very important advantages are that the spectra are plotted as a function of all four fragments simultaneously and that the integral of the spectrum represents the total cross section. As a result, correlations between all four particles are visible in a 4-D plot and yet the complete double ionization dynamics is contained in the spectrum without loss of any part of the total cross section. With this technique we were able to extract valuable information about the relative importance of different double ionization mechanisms [6].

[1] J. Ullrich et al., Rep. Prog. Phys. 66, 1463 (2003)

[2] M. Schulz et al., Nature 422, 48 (2003)

[3] N.V. Maydanyuk et al., Phys. Rev. Lett. 94, 243201 (2005)

[4] M. Schulz et al., J. Phys. B36, L311 (2003)

[5] M. Schulz et al., J. Phys. B40, 3091 (2007)

[6] M.F. Ciappina et al., submitted to Phys. Rev. A (2008)

## Relativistic, QED and nuclear effects in highly charged ions revealed by resonant electron-ion recombination in storage rings

Stefan Schippers

Institut für Atom- und Molekülphysik, Justus-Liebig-Universität Giessen, Germany  
email: Stefan.E.Schippers@iamp.physik.uni-giessen.de

Recently electron-ion merged-beams experiments at heavy ion storage rings have become sensitive to nuclear and higher-order QED effects. This is due to technological advances in electron-beam preparation and ion-beam cooling techniques. For example, the hyperfine splitting of dielectronic recombination (DR) recombination resonances has been observed [1] (figure 1) at the Heidelberg storage ring TSR utilizing an ultra-cold electron beam from a photo cathode. At the same time the resonance positions were determined with a precision that is sensitive to second order QED effects.

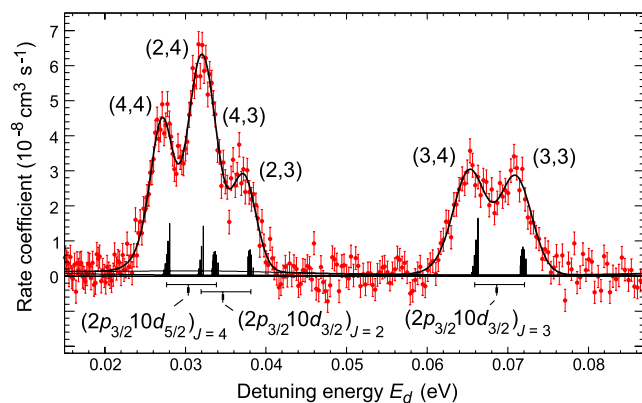


Figure 1: DR of  $\text{Sc}^{18+}$  at very low electron-ion collision energies [1]. Clearly, distinct peaks (labeled by the angular momenta  $(J, F)$  of the doubly excited intermediate states) arising from different hyperfine (HF) groups of resonances are observed. HF subcomponents are marked by stick diagrams.

Among other experimental results from the borderline between atomic and nuclear physics that will be presented and discussed are the measurement the hyperfine induced lifetime of the  $^{47}\text{Ti}^{18+}(1s^2 2s 2p^3 P_0)$  state [2] and isotope shifts of DR resonances that were recently measured [3] at the ESR storage ring of GSI.

### References

- [1] M. Lestinsky *et al.*, Phys. Rev. Lett. 100, 033001 (2008).
- [2] S. Schippers *et al.*, Phys. Rev. Lett. 98, 033001 (2007).
- [3] C. Brandau *et al.*, Phys. Rev. Lett. 100, 073201 (2008).



## FULLY DIFFERENTIAL EXPERIMENTS FOR ELECTRON IMPACT IONISATION OF SMALL ATOMS AND MOLECULES

**A. Lahmam-Bennani<sup>a,b</sup>, E. M. Staicu Casagrande<sup>a,b</sup> and A. Naja<sup>a,b</sup>**

<sup>a</sup> Université Paris-Sud 11, Laboratoire des Collisions Atomiques et Moléculaires (LCAM),  
Bât. 351, 91405 Orsay Cedex, France

<sup>b</sup> CNRS-LCAM (UMR 8625), Bât. 351, 91405 Orsay Cedex, France

The (e,2e) collisions are electron impact ionising processes where the two emerging electrons are fully analysed in energy and momentum and detected in coincidence. The corresponding triple differential cross section (TDCS) has been experimentally and theoretically studied for a wide variety of kinematics and geometries, symmetric or asymmetric, coplanar or non coplanar. See, for example, [1-3] for some reviews. A large body of the published works concerns the ionisation of helium. This has resulted in an increasing and encouraging agreement between theoretical predictions and experimental data for simple targets such as H and He, and has allowed for the exploration of the interaction dynamics in more and more detail.

However, the situation does not look as satisfactory for more complex, many-electron atomic targets (not to mention molecular targets) for which the agreement between experiment and theory deteriorates significantly. We will describe new coplanar (e,2e) results for ionisation of several rare gases (He, Ne, Ar) [4,5] as well as small molecules (H<sub>2</sub>, N<sub>2</sub>, CH<sub>4</sub>, ...) [6,7], under kinematics which have remained rather unexplored to date and characterised by large energy transfer and close to minimum momentum transfer from the projectile to the target. The experimental results are used as a sensitive test of a number of state-of-the-art available theoretical models for multi-electron atoms or for molecules. In the case of H<sub>2</sub>, based on a *direct* comparison between experimental results for He and H<sub>2</sub>, we observe [6] an oscillatory pattern which is attributed to the destructive or constructive interference effects due to the scattering from the two H-nuclei.

*Keywords:* (e,2e) ; TDCS; Electron impact ionisation ; Interference effects

### References

- [1] Ehrhardt H, Jung K, Knoth G and Schlemmer P 1986 Z. Phys. D: Atoms, Molecules and Clusters **1** 3-32
- [2] Lahmam-Bennani A 1991 J. Phys. B: At. Mol. Opt. Phys. **24** 2401
- [3] Weigold E and McCarthy I E 1999 in Electron Momentum Spectroscopy, Kluwer Academic/ Plenum Publishers, New York
- [4] Catoire F, Staicu Casagrande E M, Nekkab M, Dal Cappello C, Bartschat K and Lahmam-Bennani A 2006 J. Phys. B: At. Mol. Opt. Phys. **39** 2827-2838
- [5] Naja A, Staicu Casagrande E M, Lahmam-Bennani A, Stevenson M, Lohmann B, Dal Cappello C, Bartschat K, Kheifets A, Bray I and Fursa D V 2008 J. Phys. B: At. Mol. Opt. Phys. **41** in press
- [6] Staicu Casagrande E M, Naja A, Mezdari F, Lahmam-Bennani A, Bolognesi P, Joulakian B, Chuluunbaatar O, Al-Hagan O, Madison D H, Fursa D V and Bray I 2008 J. Phys. B: At. Mol. Opt. Phys. **41** 025204
- [7] Naja A, Staicu Casagrande E M, Lahmam-Bennani A, Nekkab M, Mezdari F, Joulakian B, Chuluunbaatar O and Madison D H J 2007 J. Phys. B: At. Mol. Opt. Phys. **40**, 3775-3783

**SPARC's FLAIR AT FAIR:  
NEW PERSPECTIVES FOR ATOMIC PHYSICS RESEARCH WITH HIGHLY  
CHARGED IONS AND ANTIPROTONS AT THE FUTURE FAIR FACILITY**

**A. Braeuning-Demian in behalf of SPARC and FLAIR collaborations**

GSI, Planckstrasse 1, 64291 Darmstadt, Germany

Atoms under 'extreme' conditions - high atomic charge states in high electrical fields and at very high or very low velocities - represent a still widely unexplored field of research. The atomic spectroscopy of highly charged relativistic ions and the study of the collision dynamics involving atoms, electrons and photons are seeking answers to questions connected to quantum electrodynamics, astrophysics, as well as to material and biological research. With the tremendously improved beam qualities at the future Facility for Antiproton and Ion Research (FAIR), experiments of highest precision and studies of rare processes using highly charged heavy ion beams can be performed. In addition, high yields of different unstable nuclei will be available for investigation of nuclear properties using atomic physics methods. This new facility will extend the energy range for studies involving highly charged heavy ions not only toward the high energy limit (10-20 GeV/u) but also at low energies, down to rest, via HITRAP installation.

The advent of high intensity antiproton beams will open a research field not yet present at GSI: physics with antiprotons. At the proposed Facility for Low-energy Antiproton and Ion Research (FLAIR) the low-energy limit of the physics with antiprotons will be exploited in atomic collisions, in nuclear and particle physics studies along with matter-antimatter symmetry studies.

Two collaborations, SPARC (Stored Particle Atomic Research Collaboration) and FLAIR (Low-energy Antiproton Physics) aim to take advantage of these new opportunities. This contribution will review the main atomic physics research topics proposed to be carried out at FAIR and the on going development of the proposed experiments.

## Interaction of charged particles with insulators

*Univ. Tokyo and RIKEN, Yasunori Yamazaki*

We have been studying the interaction of charged particles with insulating targets such as a multi-microcapillaries, a single tapered glass capillaries, and a pair of flat glass plates. Although insulating material had not been physicists' favorites because of their uncontrollable charge-up natures, recent intensive studies have revealed various interesting properties of charging and discharging phenomena of insulators.

First of all, a so-called guiding effect, which was discovered by N. Stolterfoht in 2002[1] for multi-microrcapillaries, is discussed. I will then extend the discussion for (1) single tapered capillaries[2], which showed not only a guiding effect but also a focusing effect, (2) pair of glass plates separated by 0.1mm or so [3]. It is expected that these phenomena are the result of self-organized charging and discharging of the insulator surfaces. A similar effect was also observed for a MeV ions transmitted through tapered glass capillaries [4], where multiple small-angle scattering would play a decisive role. Recently, we have succeeded to develop a single tapered glass capillary with a thin window at the top, which can be applied for a living cell surgery [5]. Further possible applications to other particles like muons, positrons and clusters will be discussed at the conference.

[1] N. Stolterfoht, J.-H. Bremer, V. Hoffmann, R. Hellhammer, D. Fink, A.Petrov, and B. Sulik, *Phys. Rev. Lett.* **88** (2002)133201.

[2] T. Ikeda, Y. Kanai, T. M. Kojima, Y. Iwai, T. Kambara, Y. Yamazaki, M. Hoshino, T. Nebiki, and T. Narusawa, *Appl. Phys. Lett.* **89**(2006) 163502.

[3] G.Pokhil, et al., private communications

[4] T. Nebiki et al., *J. Vac. Sci. Technol. A* 21 (2003) 1671.

[5] Y.Iwai et al., *Appl. Phys. Lett.* 92 (2007) 023509.

## MOLECULAR FRAGMENTATION ON SWIFT ION COLLISION

**John R. Sabin<sup>a</sup>, Remigio Cabrera Trujillo<sup>b</sup>, Yngve Öhrn<sup>a</sup>, Erik Deumens<sup>a</sup>,  
and Nikolaus Stolterfoht<sup>c</sup>**

<sup>a</sup>Quantum Theory Project, University of Florida, Gainesville, Florida 32611, USA

<sup>b</sup>Instituto de Ciencias Físicas, Universidad Autónoma de México, Cuernavaca, Morelos, 62210, México

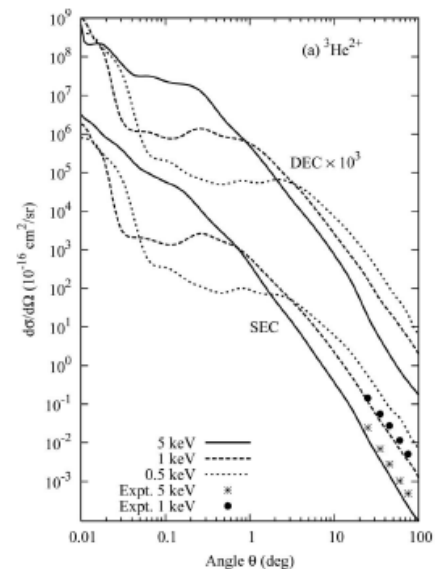
<sup>c</sup>Hahn-Meitner Institut, Glienickestraße 100, D-14109 Berlin, Germany

Impact of swift ions on molecules with collision energies of tens to hundreds of eV/amu frequently results of fragmentation of the target molecule into atoms, electrons, ions, and radicals of various sizes. The details of these processes give insight into such diverse subjects as radiation protection, tumor therapy, and initiation of explosion of energetic materials.

Over the past several years, we have applied Electron Nuclear Dynamics (END), a full quantum mechanical, fully coupled dynamics to the study of fragmentation of small molecules, ranging from H<sub>2</sub> to water to ethane, and, to proto-biological molecules such as formaldehyde. The calculations produce total cross sections, differential cross sections, charge exchange cross sections, fragmentation cross sections, and kinetic energy release probabilities.

In this contribution we will discuss molecular fragmentation of water initiated by swift <sup>3</sup>He<sup>+</sup> and <sup>3</sup>He<sup>2+</sup> ions and the information that can be gleaned from such calculations. Among the quantities discussed will be electron capture by the projectile in the collision of <sup>3</sup>He<sup>2+</sup> → H<sub>2</sub>O. The differential cross section for single electron capture (SEC) and double electron capture (DEC) as a function of scattering angle for such a collision are shown below [1] for projectile energies of 1, 3, and 5 keV/amu and compared to experiment [2].

Although there are no experiments reporting double electron capture, and the experiments for single electron capture are confined to large scattering angles, the results agree well with theory. These and other results from the calculations will be discussed.



### References

- [1] R. Cabrera-Trujillo, E. Deumens, Y. Öhrn, O. Quinet, J.R. Sabin, and N. Stolterfoht, Phys. Rev. A 75 (2007) 052702  
 [2] P. Sobocinski, Z.D. Pešić, R. Hellhammer, N. Stolterfoht, B. Sulik, S. Legenfre, and J.-Y. Chesnel, J. Phys. B 38 (2005) 2495.

## PHOTOEMISSION SPECTROSCOPY OF DNA BASE TAUTOMERS

**O. Plekan**<sup>\*a</sup>, **V. Feyer**<sup>a</sup>, **R. Richter**<sup>a</sup>, **M. Coreno**<sup>b</sup>, **M. de Simone**<sup>c</sup> and **K. C. Prince**<sup>a</sup>,  
**G. Vall-Iloera**<sup>d</sup>, **A. B. Trofimov**<sup>e</sup>, **I. L. Zaytseva**<sup>e</sup>, **E. V. Gromov**<sup>f</sup> and **J. Schirmer**<sup>f</sup>

<sup>\*</sup>Permanent address: Institute of Electron Physics, 88017 Uzhgorod, Ukraine

<sup>a</sup> Sincrotrone Trieste, in Area Science Park, I-34012 Basovizza (Trieste), Italy

<sup>b</sup> CNR-IMIP, Montelibretti (Rome), I-00016 Italy

<sup>c</sup> Laboratorio Nazionale TASC, INFN-CNR, 34012 Trieste, Italy

<sup>d</sup> Royal Institute of Technology, Department of Physics, 10691 Stockholm, Sweden

<sup>e</sup> Irkutsk State University, Karl Marx str. 1, 664003 Irkutsk, Russian Federation

<sup>f</sup> Theoretische Chemie, Physikalisch-Chemisches Institut,

Universität Heidelberg, Im Neuenheimer Feld 229, D-69120 Heidelberg, Germany

Nucleobases are fundamental building blocks of life, and their physical chemistry has been extensively studied both experimentally and theoretically, since the electronic properties of these molecules play an important role in biochemistry, biophysics, medical chemistry and nano-biotechnological applications. Gas Phase studies of these compounds provide an opportunity to examine the spectra of these molecules in the absence of solvation effects and thus obtain detailed and precise information.

An important characteristic of nucleobases is their tendency to form tautomers. Tautomers are organic compounds which are formed by migration of a hydrogen atom, accompanied by a switch of a single bond and neighboring double bond: these tautomers can cause genetic mutations by pairing incorrectly with complementary bases. For example, guanine (see Fig. 1) has the possibility of oxo  $\leftrightarrow$  hydroxo, amino  $\leftrightarrow$  imino, N1H  $\leftrightarrow$  N3H and N7H  $\leftrightarrow$  N9H prototropy and is therefore the nucleobase with the largest number of possible tautomeric forms.

Recently we have studied the electronic structure of adenine, guanine, cytosine, thymine and uracil in the gas phase by core level photoemission spectroscopy using synchrotron radiation. The XPS (X-ray Photoelectron Spectra) and NEXAFS (Near Edge X-ray Absorption Fine Structure) spectra at the C, N and O 1s edges have been measured and interpreted with the aid of polarization propagator ADC(2) and one-particle Green's function ADC(4) calculations [1]. In the core level photoemission spectra of adenine, thymine and uracil, tautomers have not been observed. For guanine and cytosine, different types of tautomers have been clearly identified, and their relative populations at the temperature of the experiment have been determined.

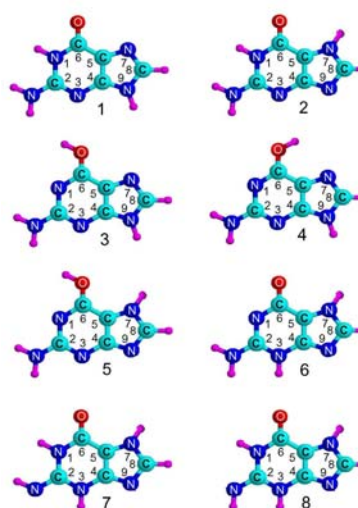


Fig. 1. Possible tautomeric forms of guanine.

**Keywords:** nucleobases, tautomers, X-ray photoemission spectroscopy.

### References

[1] O. Plekan, V. Feyer, R. Richter, M. Coreno, M. de Simone, K.C. Prince, A.B. Trofimov, E.V. Gromov, I. L. Zaytseva, J. Schirmer. Chem. Phys., in press, <http://dx.doi.org/10.1016/j.chemphys.2007.09.021>.

## INTERFERENCES IN COHERENT ELECTRON EMISSION FROM DIATOMIC MOLECULES

**J.A. Tanis**

Department of Physics, Western Michigan University, Kalamazoo, MI 49008, USA

In recent studies ionization of molecular hydrogen by fast ions has been shown to give rise to electron interference effects [1,2]. The interferences are manifested as oscillations in the velocity (or energy) distributions of the ejected electron spectra, and are analogous to the interference of light in Young's two-slit experiment with the slits replaced by the atomic centers of the molecule. While such interferences were predicted more than four decades ago [3], only recently was experimental evidence for these effects observed in collisions of 1-5 MeV/u  $H^+$  [4] and  $\sim 60$  MeV/u  $Kr^{33+}$  [1,2] ions with  $H_2$ . To reveal the relatively small oscillations superimposed on an exponentially decreasing "background" of continuum electrons, measured molecular yields are normalized to theoretical atomic cross sections. The resulting ratios exhibit a damped oscillatory behavior described by the function  $[1+\sin(kcd)/kcd]$  [5], where  $k$  is the outgoing electron momentum,  $c$  is a parameter representing the oscillation frequency, and  $d$  is the internuclear separation. The frequencies of the oscillatory structures are found to depend strongly on the electron observation angle [2,4] and to a lesser extent on the collision velocity [4]. Comparison with existing theories [5,6,7] shows good agreement for forward ejection angles but not for backward angles [8]. Additionally, secondary oscillations with  $\sim 2$ -3 times higher frequencies are observed superimposed on the primary oscillations [9]. These secondary structures have been attributed to scattering of the primary electron "wave" at the second atomic center resulting in interference with the original wave, an effect that has no analogy in Young's experiment.

More recently interference studies have focused on diatomic molecules other than  $H_2$ , including 1-5 MeV  $H^+ + N_2$  [10] and 30 MeV  $O^{5,8+} + O_2$  [11]. Ratios of experimental molecular  $N_2$  to theoretical atomic N cross sections for electron emission are found to exhibit nearly constant frequency sinusoidal oscillations for all electron observation angles and for the collision velocities studied. Furthermore, the oscillations do not appear damped over the range of the measurements. The results suggest suppression of primary Young-type interferences, in sharp contrast to observations for  $H_2$ , with the structures being instead secondary oscillations due to intramolecular scattering. Theoretical calculations predict suppression of the primary interferences but not to the extent observed in the measurements.

All of these various results will be reviewed, outstanding problems identified, and future directions indicated.

*Keywords:* electron interferences, coherent electron emission, secondary interferences, molecular ionization

### References

- [1] N. Stolterfoht *et al.*, Phys. Rev. Lett. **87** (2001) 023201.
- [2] N. Stolterfoht *et al.* Phys. Rev. A **67** (2003) 030702(R).
- [3] H. D. Cohen and U. Fano, Phys Rev. **150** (1966) 30.
- [4] S. Hossain *et al.*, Phys. Rev. A **72** (2005) 010701(R).
- [5] L. Nagy, L. Kocbach, K. Póra, and J.P. Hansen, J. Phys. B **35** (2002) L453.
- [6] M.E. Galassi *et al.*, Phys. Rev. A **66** (2002) 052705; and Phys. Rev. A **70** (2004) 032721.
- [7] L. Sarkadi, J. Phys. B **36** (2003) 2153.
- [8] J.A. Tanis *et al.*, Phys. Rev. A **74** (2006) 022707.
- [9] N. Stolterfoht *et al.*, Phys. Rev. A **69** (2004) 012701.
- [10] J.L. Baran *et al.*, J. Phys.: Conf. Ser. **58** (2007) 215.
- [11] M. Winkworth *et al.*, Abstracts, this conference.

## FAST OSCILLATING STRUCTURES IN ELECTRON SPECTRA FOLLOWING SLOW $\text{He}^{q+} + \text{He}$ COLLISIONS: SEARCH FOR ELECTRON INTERFERENCES

F. Frémont<sup>a</sup>, A. Hajaji<sup>a</sup>, A. Naja<sup>a</sup>, C. Leclercq<sup>a</sup>, J. Soret<sup>a</sup>, J. A. Tanis<sup>b</sup>, B. Sulik<sup>c</sup> and J.-Y. Chesnel<sup>a</sup>

<sup>a</sup>Centre de Recherche Ions Matériaux et Photonique (CIMAP), Unité Mixte CEA-CNRS-EnsiCaen-Université de Caen, 6 bd du Mal Juin, F-14050 Caen Cedex4, France

<sup>b</sup>Western Michigan University, Kalamazoo, MI 49008, USA

<sup>c</sup>Institute of Nuclear Research (ATOMKI), H-4001 Debrecen, Hungary

Since 2001, many works [1-6] have been devoted to the study of interferences resulting from the coherent emission of electrons from  $\text{H}_2$  following the impact of fast charged particles. These interference effects manifest themselves as oscillations in the electron spectra as a function of the ejected electron velocity [1-6]. Moreover, evidence for significantly higher frequency oscillations was reported in the electron emission spectra of  $\text{H}_2$  by fast  $\text{H}^+$  impact [6]. Although no conclusion was reached, an explanation, considered not likely for the relatively fast  $\text{H}^+ + \text{H}_2$  collisions of Ref. [6], involved coherent electron emission from the transient molecule formed by the passing ion with one (or both) of the target  $\text{H}_2$  centers. Within the framework of this hypothesis, such interference effects would also be expected in collisions of ions with *atomic* targets where the number of centers of the transient molecule is reduced to two. In a theoretical study of  $\text{H}^+ + \text{H}$  collisions at 20 keV [7], inclusion of the interferences between the target centered and projectile centered amplitudes led to results in good agreement with experimental differential cross sections. Thus, Ref. [7] shows that, even using an *atomic* target, the interferences resulting from coherent electron emission may be revealed.

In the present work [8], distributions of ejected electrons following collisions of slow  $\text{He}^+$  and  $\text{He}^{2+}$  ions and an *atomic* He target were measured for projectile energies of 20 and 40 keV, respectively. The electrons were detected at angles of  $30^\circ$  and  $90^\circ$  with respect to the incident beam direction. Superimposed on a continuous background originating from target ionization, small amplitude, high-frequency oscillations are revealed. The frequency of these oscillations is found to be nearly independent of the projectile charge and observation angle. In view of recent experiments and calculations, the origin of such oscillations is discussed. Processes such as autoionization following the production of highly excited states, Fermi-shuttle ionization, or coherent electron emission caused by interference between the target centered and projectile centered amplitudes, are considered.

*Keywords:* Ion-atom collision; Electron spectra; Fast oscillating structures; Autoionization; Fermi-shuttle ionization; Electron interference

### References

- [1] N. Stolterfoht *et al.*, Phys. Rev. Lett. **87** (2001) 023201.
- [2] M. E. Galassi, R. D. Rivarola, P. Fainstein and N. Stolterfoht, Phys. Rev. A **66** (2002) 052705.
- [3] L. Nagy, L. Kocbach, K. Poraund and J. P. Hansen, J. Phys. B **35** (2002) L453.
- [4] L. Sarkadi, J. Phys. B **36** (2003) 2153.
- [5] O. Kamalou *et al.*, Phys. Rev. A **71** (2005) 010702(R).
- [6] S. Hossain, A. L. Landers, N. Stolterfoht and J. A. Tanis, Phys. Rev. A **72** (2005) 010701(R).
- [7] J. F. Reading, J. Fu and M. J. Fitzpatrick, Phys. Rev. A **70** (2004) 032718.
- [8] F. Frémont *et al.*, Phys. Rev. A **72** (2005) 050704(R).

## YOUNG-TYPE INTERFERENCES USING SINGLE-ELECTRON SOURCES AND AN ATOMIC-SIZE TWO-CENTER INTERFEROMETER

**F. Frémont<sup>a</sup>, S. Suarez<sup>b</sup>, R. O. Barrachina<sup>b</sup>, A. Hajaji<sup>a</sup> and J.-Y. Chesnel<sup>a</sup>**

<sup>a</sup>Cimap, Unité Mixte Université de Caen Basse-Normandie-CEA-CNRS-EnsiCaen, 6 bd du Mal Juin, F-14050 Caen Cedex France

<sup>b</sup>Centro Atómico Bariloche and Instituto Balseiro (Comisión Nacional de Energía Atómica and Universidad Nacional de Cuyo), 8400 S. C. de Bariloche, Río Negro, Argentina

Recently, interferences caused by a single electron impacting on an independent double-center scatterer, which plays the role of an atomic-size double-slit system, were experimentally evidenced for the first time [1,2]. The electron originates from the autoionization of doubly excited  $2lnl'$  ( $n \geq 2$ ) configurations of He following a double charge exchange process by 30 keV  $\text{He}^{2+}$  ions impinging on  $\text{H}_2$  molecules. Well-defined oscillations were visible in the angular distribution of the electrons emitted towards the receding H protons. The presence of these oscillations was shown to be a clear demonstration that a single electron interferes with itself. The period of the oscillations was found to be  $\sim 17^\circ$ , in agreement with the predictions of the model developed recently [3].

In the present work, we discuss the dependence of the interference pattern with interference parameters. It is well known that, when light passes through two slits, the distance  $i$  between two maxima on a screen strongly depends on the light wavelength  $\lambda$  and on the distance  $d$  between the slits. Consequently, the angular period, defined by  $T \sim \lambda/d$ , varies also with these two parameters. Similarly, by modifying the electron wavelength and the distance between the protons, the interference pattern is expected to change. This can be easily done by changing the projectile velocity, or the projectile itself.

We performed a Young-type experiment using 8 keV  $\text{He}^{2+}$  and 105 keV  $\text{N}^{6+}$  projectile ions. In the case of  $\text{He}^{2+}$  ions, the period  $T$  is found to be practically the same as that found at 30 keV, within the uncertainties. However, the shape of the interference pattern changes strongly, since a phase shift of nearly  $\pi$  in the angular distribution of autoionizing electrons is observed. For  $\text{N}^{6+}$  projectile ions, no oscillation is found. We will show that all these results can be interpreted using the simple model developed previously [3].

*Keywords:* Young; electron interferences; autoionization.

### References

- [1] J.-Y. Chesnel, A. Hajaji, R. O. Barrachina and F. Frémont, Phys. Rev. Lett. **98** 100403 (2007)
- [2] F. Frémont, A. Hajaji, R. O. Barrachina and J.-Y. Chesnel, J. of Phys, Conference Series **88** 012020 (2007)
- [3] R. O. Barrachina and M. Zitnik, J. Phys. B **37** 3847 (2004)



## THE ROLE OF NUCLEAR DYNAMICS IN H<sub>2</sub> IONIZATION AND DISSOCIATION BY SYNCHROTRON RADIATION AND LASER PULSES

**Fernando Martín**

Departamento de Química, C-9, Universidad Autónoma de Madrid, 28049-Madrid, Spain

Molecular ionization is one of the most elementary processes that occur in the atmosphere and the interstellar space. Since in molecules the absorbed energy is shared between electronic and nuclear degrees of freedom, the remaining molecular ion can be left in an excited vibrational or dissociative state. This is at variance with atomic ionization where the energy is entirely absorbed by the electrons. In early pictures of molecular ionization, the nuclear motion was described in terms of the Franck-Condon approximation, in which electronic processes occurring at different positions of the nuclei are weighted by the overlap between the initial and final vibrational states. With the advent of kinematically complete experiments, in which the momenta of all charged particles is determined, this picture has been revealed to be incomplete.

In this lecture, the important role of nuclear dynamics in molecular ionization produced by synchrotron radiation and ultrashort pulses will be demonstrated using accurate ab initio theoretical calculations that account for all electronic and vibrational degrees of freedom. In particular, recent results for electron angular distributions from fixed-in-space molecules will be analyzed and compared with kinematically complete photoionization experiments [1-4]. The range of excess photon energies considered goes from a few to several hundreds of eV. Also, multiphoton ionization of molecules by ultrashort pulses will be discussed [5].

### References

- [1] W. Vanroose et al, *Science* **310**, 1787 (2005)
- [2] J. Fernández et al, *Phys. Rev. Lett.* **98**, 043005 (2007)
- [3] F. Martín et al, *Science* **315**, 630 (2007)
- [4] D. A. Horner et al, *Phys. Rev. Lett.* **98** 073001 (2007)
- [5] A. Palacios et al, *Phys. Rev. Lett.* **96**, 173201 (2006)

## ATOMIC AND MOLECULAR FRAGMENTATION DYNAMICS IN INTENSE LASER FIELDS

Robert Moshhammer

*Max-Planck-Institut für Kernphysik, Saupfercheckweg 1, 69117 Heidelberg, Germany*

The free-electron-laser FLASH at DESY in Hamburg provides fs light pulses in the VUV at unprecedented high photon intensities. It enables for the very first time the investigation of highly non-linear phenomena, i.e. the simultaneous interaction of few photons with atoms or molecules in a photon energy regime that was not accessible before. Thus, experimental benchmark data may be provided on fundamental processes guiding the development of few-photon – few-electron theories. Due to the “small” number of photons involved ab-initio theories have been developed and are at hand. It is expected that these new experiments will provide basic information on the dynamics of few-photon matter interactions.

Here we report on first differential experiments of few-photon multiple ionization of He, Ne and small molecules by intense FEL radiation using a Reaction Microscope. Measurements were performed at wavelengths of 44 nm (28.2 eV), 32 nm (38.7 eV) and 28 nm (44.9 eV) and estimated intensities in the range of  $10^{12} - 10^{14}$  W/cm<sup>2</sup>. Experimental results will be presented and discussed in terms of possible multiple ionization pathways due to the instantaneous or sequential absorption of several photons.

## DETAILED DESCRIPTION OF COLLISION DYNAMICS IN ATOMIC IONIZATION PROCESSES

**J. Fiol<sup>\*†</sup>, and R. O. Barrachina<sup>\*‡</sup>**

<sup>\*</sup>División Colisiones Atómicas, Centro Atómico Bariloche, S. C. de Bariloche, Argentina  
Consejo Nacional de Investigaciones Científicas y Técnicas (CONICET), Argentina

<sup>†</sup>E-mail: [fiol@cab.cnea.gov.ar](mailto:fiol@cab.cnea.gov.ar)      <sup>‡</sup>E-mail: [barra@cab.cnea.gov.ar](mailto:barra@cab.cnea.gov.ar)

Important efforts during the past decades have been directed to the theoretical and experimental determination of the total, single and double differential cross sections for atomic ionization by positron impact [1, 2, 3, 4]. On the contrary, while theoretical descriptions of triple differential cross sections for atomic ionization by positron impact have been obtained for almost two decades [5], their experimental counterpart have only recently become feasible [6, 7]. These novel experiments made possible detailed investigations of the collisions dynamics that differs considerably from that of heavy ions, being strongly affected by the interaction with the target nucleus [8, 9].

A decade ago, a differential study of the positron impact ionization of H<sub>2</sub> shown the occurrence of a capture-to-the-continuum (ECC) cusp [6]. This is a well-known phenomenon in ion-atom ionization collisions that had been predicted for positrons over a decade earlier [5]. These measurements, together with further coincidental measurement of the electron and the positron [7, 10] unveiled a very surprising result, an unexpected energy shift with respect to the matching velocity. This phenomenon had been unforeseen by quantum mechanical calculations [8, 11], even though a recent classical trajectory Monte Carlo (CTMC) calculation seems to corroborate the effect [9]. Since then, different explanations had been tried as for instance a competition from the Ps formation [10] or the annihilation channels [13].

In this communication, by studying the collision dynamics, we address the issue of the origin of the experimentally observed shift by means of classical and quantum-mechanical methods by studying the momentum distributions of the electron, positron and residual-ion. In particular, we determine if the cusp shift occurs during the collision, when all three particles are close to each other in the condensation region or as a result of the post-collision positron-electron interaction.

*Keywords:* Keyword; Keyword; Keyword

### References

- [1] M. Charlton Rep. Prog. Phys. 48 (1985) 737.
- [2] A. Kover, G. Laricchia, M. Charlton J. Phys. B: At. Mol. Phys. 27 (1994) 2409.
- [3] Á. Kövér, R. M. Finch, M. Charlton, G. Laricchia J. Phys. B: At. Mol. Phys. 30 (1997) L507.
- [4] D. R. Schultz, L. Meng, R. E. Olson J. Phys. B: At. Mol. Phys. 25 (1992) 4601.
- [5] M. Brauner, J. S. Briggs J. Phys. B: At. Mol. Phys. 19 (1986) L325.
- [6] Á. Kövér, G. Laricchia Phys. Rev. Lett. 80 (1998) 5309.
- [7] Á. Kövér, K. Paludan, G. Laricchia J. Phys. B: At. Mol. Phys. 34 (2001) L219.
- [8] J. Fiol, V. D. Rodríguez, R. O. Barrachina J. Phys. B: At. Mol. Phys. 34 (2001) 933.
- [9] J. Fiol, R. E. Olson J. Phys. B: At. Mol. Phys. 35 (2002) 1173.
- [10] C. Arcidiacono, Á. Kövér, G. Laricchia Phys. Rev. Lett. 95 (2005) 223202.
- [11] J. Berakdar Phys. Rev. Lett. 81 (1998) 1393.
- [12] V. D. Rodríguez, Y. D. Wang, C. D. Lin Phys. Rev. A 52 (1995) 9.
- [13] J. Fiol, R. O. Barrachina, Int. Workshop on LEP and Positronium Physics (Reading, 2007)

## MONTE CARLO SIMULATION OF ELECTRON INTERACTION WITH SOLIDS AND SURFACES

**Z.J. Ding<sup>a</sup>, Y.G. Li<sup>a</sup>, S.F. Mao<sup>a</sup>, R.G. Zeng<sup>a</sup>, H.M. Li<sup>b</sup> and Z.M. Zhang<sup>c</sup>**

<sup>a</sup>Hefei National Laboratory for Physical Sciences at Microscale and Department of Physics, University of Science and Technology of China, Hefei, Anhui 230026, China

<sup>b</sup>USTC-HP Laboratory of High Performance Computing, University of Science and Technology of China, Hefei, Anhui 230026, China

<sup>c</sup>Department of Astronomy and Applied Physics, University of Science and Technology of China, Hefei, Anhui 230026, China

Monte Carlo simulation method has been playing an important role in materials analysis by electron spectroscopies, electron microscopy, and electron probe microanalysis. An overview will be given on several aspects of its application to surface related electron spectroscopy and scanning electron microscopy. A Monte Carlo model with the use of bulk dielectric function and optical constants has reproduced systematically experimental backscattering background in the energy distribution of Auger electron spectroscopy for a number of elemental materials [1]. Furthermore, a simulation of reflection electron energy loss spectra for metals has been compared with experiments based on an improved electron inelastic scattering model by taking into account of surface excitation effect [2,3]. For study of the quasi-elastic electron scattering from an overlayer/substrate system, the energy shift, the Doppler broadening and especially the peak intensity ratio have been derived in a well agreement with experimental results [4]. Secondary electron generation inside the sample can also be properly modeled to acquire necessary information about secondary electron signals in a scanning electron microscope [5]. A Monte Carlo simulation code has been extended to consider complex sample geometries, thus, the structured and/or chemical inhomogeneous sample can be handled with a quite flexibility [6].

This work was partially supported by the National Natural Science Foundation of China (Grant Nos. 10025420, 10574121, 90406024), Chinese Academy of Sciences and Chinese Education Ministry.

Keywords: Monte Carlo; electron spectroscopy; surface

### References

- [1] Z.J. Ding, H.M. Li, K. Goto, Y.Z. Jiang, R. Shimizu, *J. Appl. Phys.* 96 (2004) 4598.
- [2] Z.J. Ding, H.M. Li, Q.R. Pu, Z.M. Zhang, R. Shimizu, *Phys. Rev. B* 66 (2002) 085411.
- [3] Z.J. Ding, K. Salma, H.M. Li, Z.M. Zhang, K. Tokesi, D. Varga, J. Toth, K. Goto, R. Shimizu, *Surf. Interface Anal.* 38 (2006) 657.
- [4] Y.G. Li, Z.M. Zhang, S.F. Mao, H.M. Li, Z.J. Ding, *Surf. Sci.* (submitted).
- [5] Z.J. Ding, R. Shimizu, *Scanning* 18 (1996) 92.
- [6] Z.J. Ding, H.M. Li, *Surf. Interface Anal.* 37 (2005) 912.

# ATOMIC DYNAMICS ON THE ATTOSECOND SCALE: PHOTONS AND CHARGED PARTICLES

**J. Burgdörfer**

Institute for Theoretical Physics, Vienna University of Technology, Wiedner  
Hauptstrasse 8-10, A-1040 Vienna, Austria, EU

Advances in ultrashort-pulse technology have made it possible to generate electromagnetic pulses with a duration as short as few hundred attoseconds approaching the classical orbital period of an atomic electron. Charged-particle collision at moderate collision energies also routinely provides electromagnetic field pulses on a comparable or even shorter time scale. It is therefore of interest to compare and to contrast the insight into the atom dynamics that can be gained from the interactions of atoms with these alternative sources of ultrashort electromagnetic pulses. The atomic response the two processes have in common is the formation of an electronic wavepacket. The talk will highlight similarities and differences between charged particles and photons generated wavepackets with the help of a few recent prototypical examples. They include time resolved formation and decay of resonances in doubly excited states [1, 2], path interferences effects in the energy and angular distributions of ionized electrons [3], and sequential and non-sequential double ionization of helium [4]. We also discuss recent extensions to attosecond-pulse interaction with surfaces [5, 6].

*Keywords:* attosecond pulses, photon, charged particle

## References

- [1] M. Wickenhauser, J Burgdörfer, F. Krausz, and M. Drescher, Phys. Rev. Lett. **94** (2005) 023002, J. Mod. Optics **53**, (2006) 247.
- [2] J Burgdörfer, and R. Morgenstern, Phys. Rev. A **38**, (1988) 5520.
- [3] D.G. Arbó, S. Yoshida, E. Persson, K. I. Dimitriou, and J Burgdörfer, Phys. Rev. Lett. **96** (2006) 143003, D.G. Arbó *et al.* Phys. Rev. A. (2008) submitted.
- [4] J. Feist, S. Nagele, R. Pazourek, E. Persson, B. I. Schneider, L. A. Collins, and J Burgdörfer, Phys. Rev. A. (2008) accepted.
- [5] A. L. Cavalieri, N. Müller, Th. Uphues, V. S. Yakovlev, A. Baltuka, B. Horvath, B. Schmidt, L. Blümel, R. Holzwarth, S. Hendel, M. Drescher, U. Kleineberg, P. M. Echenique, R. Kienberger, F. Krausz, and U. Heinzmann, Nature, **449** (2007) 1029.
- [6] C. Lemell *et al.* Phys. Rev. A. (2008) submitted.

# Atomic stabilization in superintense laser fields, then and now

Mihai Gavrilă

FOM Institute for Atomic and Molecular Physics,  
Amsterdam 1098 SJ, The Netherlands

We present an overview of atomic stabilization in superintense laser fields, a subject that has attracted considerable interest over the years. Results prior to 2002 have been discussed in a review by the author [1], and shall be referred to as the “then” part. Recent results, in the process of publication [2], will be referred to as the “now” part.

Two forms of atomic stabilization have been identified theoretically from the very beginning. The first one, “quasistationary (adiabatic) stabilization” (*QS*) refers to the limiting case of plane-wave monochromatic radiation. *QS* characterizes the fact that ionization rates, as calculated from single-state Floquet theory, decrease with the intensity at high values of the field. Predictions for *QS* from various forms of Floquet theory agree quantitatively, and high accuracy numerical results have been obtained for hydrogen. Predictions from non-Floquet theories are also considered.

The alternative form of stabilization, “dynamic stabilization” (*DS*) expresses the fact that the ionization probability  $P_{ion}$  at the end of a laser pulse of fixed shape and duration, does not approach 1 as the peak intensity is increased, but either starts decreasing with the intensity (possibly in an oscillatory manner), or levels off at a value smaller than 1. Extensive research has been done on 1D models, and, although full 3D Coulomb calculations have encountered severe numerical difficulties in the past, in recent years a rather complete and accurate mapping of *DS* could be made for hydrogen. We indicate the conceptual connection between *DS* and *QS*, based on the possibility of expanding wave packets in superpositions of Floquet states, known as “multistate Floquet theory”.

We next examine the inhibiting effects of relativity on stabilization. We consider results from the Schrödinger equation corrected for retardation, and the prospects of applying the Dirac equation. We mention the role of classical relativistic concepts in supplementing numerical computations.

The “then” part of stabilization has been limited almost exclusively to the high-frequency case, e.g., to  $\omega > 0.5$  au for H. The “now” part of the theory [2] has shown that stabilization is not necessarily a high-frequency phenomenon, but in fact can occur at any low frequency if the intensity is sufficiently high. This applies to both *QS* and *DS*, in 1D and 3D. Numerically, we illustrate this on a 1D model, for which we have calculated at low  $\omega$  comprehensive “Floquet maps” (i.e., the dependence of the quasienergies on the field magnitude), showing *QS*. By extending the  $P_{ion}$  calculations into this regime, we show the existence of *DS*.

1. M. Gavrilă, J. Phys. B **35**, R147 (2002).
2. M. Stroe, I. Simbotin and M. Gavrilă, submitted to PRA.

## X-RAY RESONANT RAMAN SCATTERING FROM NOBLE GAS ATOMS AND BEYOND

M. Žitnik, M. Kavčič, K. Bučar, A. Mihelič

J. Stefan Institute, Jamova 39, P.O.B. 3000, SI 1000, Ljubljana, Slovenia

Photoabsorption is one of the most useful spectroscopic techniques. Energy dependence of the 'missing' photon current after the light has passed through the target displays characteristic peaks due to discrete excitations of an inner-shell electron passing smoothly into the continuum. Positioning and shape of the corresponding continuum step is related to the atomic valence (XANES) and undulations above the threshold carry information about the kind and number of the nearest atomic neighbors (EXAFS). Superimposed are many weak structures, the fingerprints of electron multiple excitations and their respective thresholds (for example, [1]). There is an intrinsic limitation of the technique: spectral features reflect the natural width of the inner hole created by the photon absorption. Such final state broadening is present also in XPS spectra where the yield of ejected electrons is recorded as a function of their energy [2].

Complementary to these are the methods for observing channels along which the excited states release the energy, mostly by Auger decay (AES) or x-ray emission (XES). The available resolving power of spectrometers can be fully exploited in experiments where energy resolution is not limited by the lifetime of the hole - the resonant Raman effect. It follows from energy conservation that if for a given reaction the energies of all particles involved in the production of initial hole and decay are measured, so that the total experimental energy uncertainty is smaller than the natural width of the hole, the corresponding spectral lines display a substantial narrowing and reflect the experimental rather than the combined experimental plus inner hole broadening. Such a situation occurs most easily by the narrow band excitation of discrete states when observing Auger electrons (Auger resonant Raman effect) [3] or photons (x-ray resonant Raman scattering) [4] emitted in the fast decay of an atomic inner-hole. The energy positions, intensities, and line shapes in the RIXS spectrum depend on the precise energy and bandwidth of the incident x-ray beam in all the near ionization threshold region.

We will present the results obtained by our high resolution x-ray spectrometer [5] at XAFS@Elettra and ID26@ESRF synchrotron beamlines. We have studied single excitations converging to Xe  $L_3$ -edge and Ar  $K$ -edge. In Ar the RIXS signal was recorded in the region of doubly excited  $KM$  and  $KL$  states. Focusing excitation onto the sulfur  $K$ -edge region, we followed the evolution of  $K_\alpha$  and  $K_\beta$  lines emitted by  $SF_6$  and  $SO_2$  molecules. Finally, the advantages of the RIXS technique such as element selectivity, high penetrating power with selective energy deposition and high energy resolution, will be shown in case of a solid target.

*Keywords:* High resolution x-ray spectroscopy; Resonant inelastic x-ray scattering;

### References

- [1] I. Arčon et al, Phys. Rev. A 51 (1995) 147.
- [2] S. Svensson et al, Phys. Scr. 14 (1976) 141.
- [3] R. Camilloni et al, Phys. Rev. Lett. 77 (1996) 2646.
- [4] M. A. MacDonald et al, Phys. Rev. A 51 (1995) 3598.
- [5] M. Kavčič et al, Nucl. Instrum and Meth. B 222 (2004) 601.

## OVER-THE-BARRIER IONIZATION OF THE HYDROGEN ATOM BY INTENSE ULTRASHORT LASER PULSES

**S. Borbély<sup>a</sup>, K. Tőkési<sup>b</sup>, D. G. Arbó<sup>c</sup>, L. Nagy<sup>a</sup>**

<sup>a</sup>Babeş-Bolyai University, Faculty of Physics, str. Kogălniceanu nr. 1, 400084 Cluj-Napoca, Romania

<sup>b</sup>Institute of Nuclear Research of the Hungarian Academy of Sciences (ATOMKI), P. O. Box 51, H-4001 Debrecen, Hungary

<sup>c</sup>Institute for Astronomy and Space Physics, IAFE, Buenos Aires, Argentina

We present theoretical studies of the ionization of the hydrogen atom at the over-the-barrier regime. At these high intensities, the available theoretical models have deficiencies. One of the first models was the Volkov model, which gives acceptable results only for very high field intensities. An improved version of the Volkov model is the Coulomb-Volkov (CV) [1] approximation, where instead of the simple plane-waves for final state, CV wave functions are used. The pulse duration within the CV model is limited by the use of sudden approximation.

The classical trajectory Monte Carlo method (CTMC) is also a feasible approach at this high intensities and provides reasonable results [2]. The direct numerical solution of the time dependent Schrödinger equation (TDSE) gives the most reliable data [3], but it implies extensive numerical calculations. Recently we developed a so called momentum space strong field approximation (MSSFA) model [2], which overcomes the disadvantages of the previous models. It was found that the MSSFA model gives less accurate results than the Volkov and CV models only for the case of low momentum transfer. In this work, the MSSFA model was further improved by eliminating its shortcomings at low momentum transfer. Here we present and compare differential ionization probability distributions (see Fig. 1.) of the photo-electrons for various laser pulse parameters applying classical and quantum models.

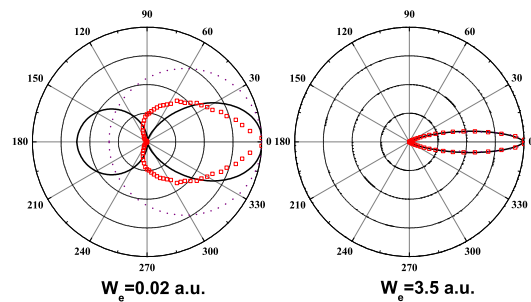


Fig. 1. Angular distribution of the photoelectrons for given ejection energies  $W_e$ . The time-dependent electric field along the  $\hat{z}$  direction in the time interval between 0 and  $\tau$  is defined as  $\vec{F}(t) = \hat{z}F_0 \cos[\omega(t - \tau/2)] \sin^2(\frac{\pi t}{\tau})$ , where  $E_0 = 1$  a.u.,  $\omega = 0.05$  a.u.,  $\tau = 5$  a.u. pulse parameters. Solid line: MSSFA. Dotted line: Volkov. Squares: CTMC.

*Keywords:* over-the-barrier ionization; intense, ultrashort laser pulses

### References

- [1] G. Duchateau et. al., J. Phys. B.: At. Mol. Opt. Phys. **33**, (2000) L571.
- [2] S. Borbély et. al., Phys. Rev. A **77** (2008) 033412.
- [3] D. G. Arbó et. al., Phys. Rev. A **77**, (2008) 013401.



## HIGHLY CHARGED ION-INDUCED NANOSTRUCTURES ON SURFACES

F. Aumayr

Institut f. Allgemeine Physik, TU Wien, A-1040 Vienna, Austria, EU

Controlled modifications of surface and bulk properties of materials by irradiation with ion beams is a widely used technique in applied fields like micro-electronics, biotechnology or photonics. In these applications high ion-fluences are used and the kinetic energy of the ions is controlled to induce the desired surface modification. With decreasing dimensions of devices, new experimental tools have to be developed. Recent work in this area has concentrated on substituting individual slow highly charged ions (HCI) for singly charged ion beams. Single HCI-impact induced surface modifications with only nanometer dimensions have recently been demonstrated [1-8]. During their recombination at a surface, slow HCI deposit a large amount of potential energy into a small and shallow surface region [9], which can lead to nano-sized surface defects. For example the formation of SiO<sub>2</sub> nano-dots on a hydrogen passivated silicon surface [6] and the creation of nano-diamonds on HOPG [5] due to the impact of individual slow HCI were reported.

Current research therefore attempts to control the production of material modifications on surfaces and thin films with well-defined size in the nanometer region by a variation of the HCI's potential energy. Within this talk we will review the current state of this field. In particular we will discuss the creation of nano-sized protrusions on insulating surfaces like CaF<sub>2</sub>(111) using slow highly charged ions [7]. This method holds the promise of forming regular structures on surfaces without inducing defects in deeper lying crystal layers. We find that only projectiles with a potential energy above a critical value are able to create hillocks [7]. Below this threshold no surface modifications are observed. This is similar to the track and hillock formation induced by swift heavy ions. We finally present a model for the conversion of potential energy stored in the projectiles into target lattice excitations (heat) and discuss possible applications [10].

**Keywords:** Highly charged ions, nanostructuring, ion - surface interaction

This work has been supported by Austrian FWF and was carried out within Association EURATOM-ÖAW. The irradiation experiments were performed at the distributed LEIF-Infrastructure at MPI Heidelberg Germany, supported by Transnational Access granted by the European Project RII3-026015, and at Forschungszentrum Dresden-Rossendorf through AIM (EU contract no. 025646).

### References

- [1] D. H. Schneider, et al., Rad.Eff.Def. in Solids 127 (1993) 113.
- [2] D. C. Parks, et al., Nucl.Instr.Meth. B 134 (1998) 46.
- [3] L. P. Ratliff, et al., Appl.Phys.Lett. 75 (1999) 590.
- [4] G. Hayderer, et al., Phys.Scripta T92 (2000) 156.
- [5] T. Meguro, et al., Appl.Phys.Lett. 79 (2001) 3866.
- [6] G. Borsoni et al. Solid-State Electr. 46 (2002) 1855.
- [7] A. S. El-Said, et al. Nucl.Instr.Meth. B 258 (2007) 167. arXiv.org cond-mat/0609246 (2006);
- [8] M. Tona et al. Surf. Sci. 601 (2007) 723
- [9] F. Aumayr, HP. Winter, Phil. Trans. R. Soc. Lond. A 362 (2004) 77.
- [10] C. Lemell, et al., Solid State Electron. 51 (2007) 1398

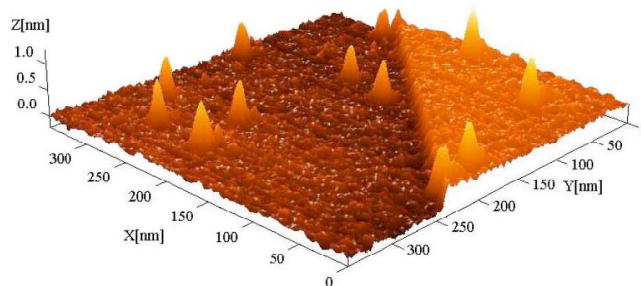


Fig. 1 Topographic contact mode AFM image of a CaF<sub>2</sub>(111) surface after irradiation with 0.5 keV/amu Xe<sup>33+</sup> ions showing hillock-like nanostructures.

SCALING LAWS FOR GUIDED TRANSMISSION OF HIGHLY-CHARGED IONS  
THROUGH NANOCAPILLARIES IN A PET POLYMER

N. Stolterfoht, R. Hellhammer, J. Bundesmann, and D. Fink

Hahn-Meitner-Institut Berlin GmbH, Glienickerstr. 100, D-14109 Berlin, Germany

Recent studies from our laboratory reported on transmission of  $\text{Ne}^{7+}$  ion through capillaries in insulating polyethylene terephthalate (PET) [1]. When the capillary axis is tilted with respect to the incident beam direction, the transmission of highly charged ions was found to occur with negligible electron capture so that a considerable fraction of ions is guided through the capillary in its incident charge state. The guiding phenomenon is understood in terms of incident ions depositing positive charges at the inner wall of the capillaries in a self-organizing process. Due to the increasing interest in this subject, several laboratories started investigations of capillary guiding in different insulating materials (cited e.g. in [2]).

In the present work guided transmission was investigated using a variety of ionic species, such as  $\text{Ne}^{7+}$ ,  $\text{Ne}^{9+}$ ,  $\text{Ar}^{9+}$ ,  $\text{Ar}^{13+}$ , and  $\text{Xe}^{25+}$  [3]. The incident energy was varied within the range of 3 - 40 keV. The fraction of transmitted ions was measured as a function of the capillary tilt angle. The results are used to evaluate the guiding angle, which is a measure of the guiding power specifying the ability of a material to guide ions. Moreover, the FWHM  $\sigma_t$  of the angular distribution of the transmitted ions was studied as a function of their energy and charge state.

Model calculations have shown [3] that the fraction of transmitted ions can be described as

$$f(\psi) = f_0 \exp\left(-\frac{\sin^2 \psi}{\sin^2 \psi_c}\right) = f_0 \exp\left(-\frac{E_p}{qU} \sin^2 \psi\right) \quad (1)$$

which defines the guiding angle  $\psi_c$  as the tilt angle  $\psi$  for which the intensity of the transmitted ions drops to  $1/e$ . Moreover,  $E_p$  and  $q$  are the projectile energy and charge. The quantity  $U$  is a free model parameter characterizing the potentials in the entrance region. For constant  $U$ , Eq. (1) predicts that  $\sin^2 \psi_c$  is proportional to  $E_p/q$ . In fact, Fig. 1(b) shows a nearly linear dependence, i.e., the quantity  $\sin^2 \psi_c$  can well be fitted by  $(E_p/q)^{1.3}$  apart from a constant (see solid curve). Similar results were found for the fitting of  $\sin^2 \sigma_t$  as depicted in Fig. 1(a).

In conclusion, the profile width and the guiding angle were found to follow the same scaling law and are fitted by the same function. It will be shown that this finding provides evidence that both angles are governed by the main charge patch deposited in the entrance region of the capillary.

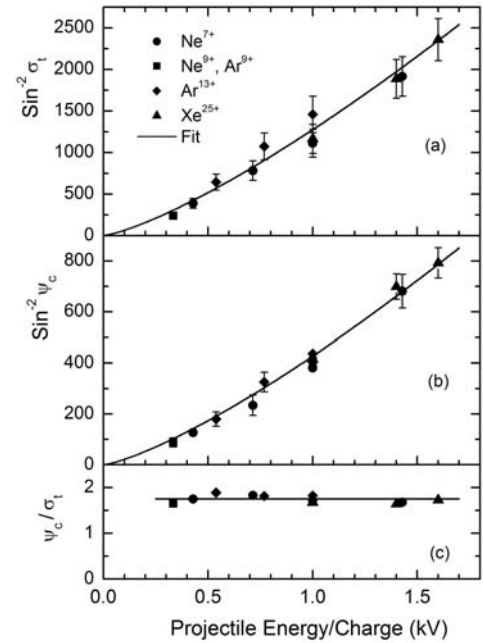


Fig. 1. Scaling laws for the FWHM  $\sigma_t$  (a) and the guiding angle  $\psi_c$  (b) in terms of the projectile energy to charge ratio.

## References

- [1] N. Stolterfoht, J. H. Bremer, V. Hoffmann, R. Hellhammer, D. Fink, A. Petrov, and B. Sulik, Phys. Rev. Lett., 88, 133201 (2002).
- [2] S. Das, B. S. Dassanayake, M. Winkworth, J. L. Baran, N. Stolterfoht, and J. A. Tanis, Phys. Rev. A, 76, 042716 (2007).
- [3] N. Stolterfoht, R. Hellhammer, J. Bundesmann, and D. Fink, Phys. Rev. A, 77, 1 (2008).

# TEMPORAL ASPECTS IN ATOMIC IONIZATIONS INITIATED BY ELECTRON OR PHOTON IMPACT

**F. Koike**

Physics Department, School of Medicine, Kitasato University, Sagami-hara, Kanagawa 228-8555 Japan

In the present report, we discuss temporal aspects in the processes of electron emissions from atoms after their electronic state excitations by electron or photon impact.

Firstly, we consider the time correlations between the atomic autoionization processes and atomic internal motions. Autoionization of photon-impact or particle-impact induced doubly or inner-shell excited atomic states may sometimes leaves multiplet states in residual ions. In atomic species with moderate atomic numbers, the multiplet nature is typically caused by spin-orbit interactions in ionic open-shell electrons[1][2]. In these systems, the open-shell undergoes precessions between different total angular momentum states of ions, and its cycle time gives us a good clock to measure the lifetime of the autoionizing states. In Fig. 1, we illustrate the features of time correlations for atomic autoionization processes as an example.

And further on, there is a class of ionization processes in which multiple electrons leave the atomic system. Due to a correlations among the escaping electrons, we sometimes observe the effects that are so called post-collision interactions. The post-collision interaction effects can be observed, in general, when we have multiple electron emissions at different instances, which constitute the time correlation effects of the atomic systems[3][4].

In this paper, we investigate the role of this type of atomic clocks in detail by tracing the time dependent state vector of the total system with the aid of accurate relativistic calculations of atomic structures and ionization dynamics[5][6].

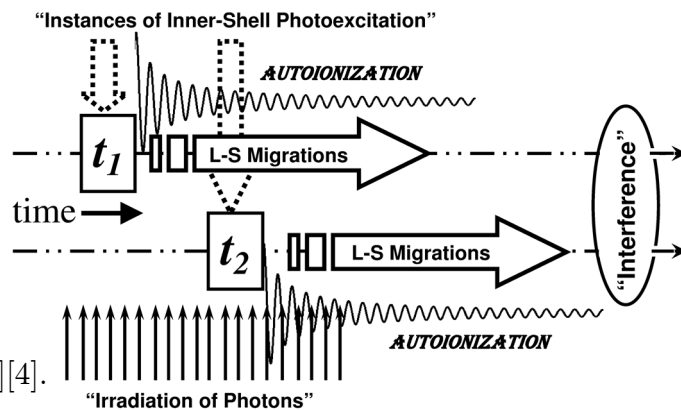


Fig. 1. Schematic Drawing of the Interference Features in Autoionization of Atoms with *LS* Multiplet Ion Cores

*Keywords:* Auger Effect; Autoionization; Post-Collision Interaction; MCDF

## References

- [1] M. Koide, et al, J. Phys. Soc. Jpn. **71** (2002) 1676.
- [2] M. Koide, F. Koike, Y. Azuma, and T. Nagata, J. Elec. Spec. Rel. Phenom. **144-147** (2005) 55.
- [3] P. Lablanquie, F. Penent, et al. Phys. Rev. Lett. **84** (2000) 47.
- [4] T. Hayaishi, T. Tanaka, et al. J. Phys. B: At. Mol. Opt. Phys. **32** (1999) 1507.
- [5] F. A. Parpia, C. F. Fischer, and I. P. Grant, Commpt. Phys. Commun. **94** (1996) 249.
- [6] S. Fritzsche, J. Elec. Spec. Rel. Phenom. **114-116** (2001) 1155.

**Dispersion relation and plasmon excitation in nanostructures by charged particles.**

Gervasoni J. L.<sup>1,2</sup>, Segui S.<sup>1</sup>, Arista N. R.<sup>2</sup>

Centro Atómico Bariloche, 8400 S. C. de Bariloche, Río Negro, Argentina

<sup>1</sup> Consejo Nacional de Investigaciones Científicas y Técnicas (CONICET).

<sup>2</sup> Comisión Nac. de Energía Atómica (CNEA) – Instituto Balseiro (Univ. Nac. de Cuyo).

One of the most remarkable feature of nanostructured materials is that their optical response due to plasmon excitation is very sensitive to their geometry and composition. The interaction of charged particles with the electron gas of the considered system is one of the most used methods to excite and study plasmons.

In this work we study the similarities and differences arising in these excitations due to the interaction of the charged particles with a variety of nanoscopic systems (capillaries, wires, tubules, spheres). In particular, we study resonance effects that appear for incident particles with given specific trajectories [1-6], an important aspect due to the increasing requirement of devices of reduced dimensions for their application in different areas.

1. Arista N. and Fuentes M. A., Arista N. R., PRB 63 (2001)165401
2. Gervasoni J. L. and Arista N. R., PRB 68 (2003)235302; Phys. Stat. Sol.(C) Vol.1, Issue S1, pp. S9-S12 (2004).
3. Segui S., Gervasoni J. L. and Arista N. R., NIMB B 233, 227-231 (2005).
4. J. L. Gervasoni, Surface and Interface Analysis 38, pp.583- 586 (2006).
5. J. L. Gervasoni, S. Segui and N. R. Arista, Radiation Effects and Defects in Solids, 162, pp.267-275 (2007).
6. S. Segui, J. L. Gervasoni and N. R. Arista, Surface Science 601, pp.4169-4174 (2007).

# Fragmentation processes

Colm T Whelan

Department of Physics, Old Dominion University, Norfolk, Virginia, 23529-0166

## Abstract

In this talk, I will describe the theory that has been developed to describe kinematically complete collision experiments. In such experiments, all the fragments from an atomic collision are detected in coincidence with their angles and energies resolved. The technique offers both the possibility of a direct determination of the target wave function and profound insights into the nature of few body interactions. What information you extract from such an experiment really depends on the kinematics you chose and the target you use. What is measured is the cross section, i.e. the ratio of the number of measured events corresponding to the final state fragments being detected at fixed position in space with well-defined energies per unit time per unit scatterer as compared to the incident flux. Technically, we are talking here about a multiply differential cross section as opposed to one where we have integrated over one or more of the fragment co-ordinates. Integrated cross sections can be crude things and you need the full power of a highly differential measurement to tease out the delicacies of the interactions. In the last few years, revolutionary advances in experimental techniques and spectacular increases in computer power have offered unique opportunities to develop a much more profound understanding of the atomic few body problem. I will pay particular attention to recent studies of inner shell ionization and processes with two active target electrons

## THE SOLVATED ELECTRON IN RECENT CLUSTER EXPERIMENTS

Udo Buck

Max-Planck-Institut für Dynamik und Selbstorganisation, Göttingen, Germany

Solvation effects play a crucial role in a number of fields in physics and chemistry. One of the most interesting features is the behavior of the excess electron in metal and acidic solutions of the hydrogen bonded networks of water and ammonia. Although the effect is known for many years, the details of its structure and properties have emerged as one of the outstanding problems in chemical physics. To elucidate the microscopic behavior of the underlying dynamics, the corresponding properties of clusters are investigated as function of their size. In these experiments the size selection is crucial and presents, in particular for neutral systems, a special challenge. Therefore many experiments have been carried out with negatively charged cluster anions. In this contribution three different experimental arrangements and their results will be presented which deal with size selected neutral clusters in the special configuration of the solvated electron. The excitation is caused in all cases by photons ranging from 0.4 to 6.4 eV

The measurement of the ionization potential after the excitation of Na doped ammonia clusters by photons in the range of 2-4 eV gave the surprising result that the extrapolation to the bulk limit does neither agree with the results of the metallic solutions in liquid ammonia nor with the results of negatively charged ammonia clusters. The differences are explained by the presence and the various distances of the counter ions from the solvated electron [1].

By means of a new double resonance scheme we extended the infrared spectroscopy of completely size selected hydrogen bonded clusters [2] to large Na doped water clusters. Here we observe the direct interaction of the H-atoms of the solvent molecules with the delocalized electron distribution [3, 4]. Again the results do not agree quantitatively with those obtained for water cluster anions.

Finally, the formation of solvent-separated ion pairs and their photoreactions are investigated in photodissociation experiments of HCl and HBr on the surface of large water clusters at 193 nm. The results for different isotope distributions are explained by the existence of the  $\text{H}_3\text{O}^+$  [5] radical which has been theoretically predicted to be another modification of the solvated electron.

Keywords: solvated electron, hydrogen bonded network, size selected neutral clusters

### References

- [1] C. Steinbach and U. Buck, *J. Chem. Phys.* 122 (2005) 134302.
- [2] U. Buck and F. Huisken, *Chem. Rev.* 100 (2000) 3863.
- [3] C. Steinbach and U. Buck, *J. Phys. Chem. A* 110 (2006) 3128.
- [4] U. Buck, I. Dauster, B. Gao, and Z. F. Liu, *J. Phys. Chem. A*, 111 (2007) 12355.
- [5] V. Poterya, M. Fárník, P. Slavicek, U. Buck, and V. V. Kresin, *J. Chem. Phys.* 126 (2007) 071101.

## INNER SHELL SPECTROSCOPY AND THE SHAPE OF BIOMOLECULES

V. Feyer<sup>a</sup>, O. Plekan<sup>\*a</sup>, R. Richter<sup>a</sup>, M. Coreno<sup>b</sup>, M. de Simone<sup>c</sup>, K. C. Prince<sup>a</sup>, and V. Carravetta<sup>d</sup>

<sup>a</sup> Sincrotrone Trieste, in Area Science Park, I-34012 Basovizza (Trieste), Italy,

<sup>\*</sup>Permanent address: Institute of Electron Physics, 88017 Uzhgorod, Ukraine,

<sup>b</sup> CNR-IMIP, Montelibretti (Rome), I-00016 Italy,

<sup>c</sup> Laboratorio Nazionale TASC, INFN-CNR, 34012 Trieste, Italy,

<sup>d</sup> CNR-Institute of Chemical Physical Processes, Via Moruzzi 1, 56124 Pisa, Italy.

Many biological macromolecules are characterized by flexible structures, which allow them to assume many different folded shapes. In proteins, the origin of this flexibility can be traced to the basic building blocks, amino acids: they generally have low resistance to rotational distortion, can assume several shapes (conformers) at ambient temperatures, and can form a variety of intramolecular hydrogen bonds. Most information about these gas phase (or matrix isolated) conformers has been obtained by microwave, vibrational and laser spectroscopic techniques. We are currently exploring the extent to which we can learn about the structure of free amino acids by means of core level spectroscopy.

Eight amino acids (glycine, methionine, proline, alanine, threonine, tyrosine, phenylalanine, tryptophan) have been investigated in the gas phase by core level photoemission and photoabsorption (NEXAFS) at the C, N and O 1s edges [1]. The interpretation of the spectra is supported by calculations of selected spectra, and the agreement between theory and experiment is very good. The spectra of glycine and phenylalanine are in agreement with published investigations but are better resolved [2, 3].

The carbon and oxygen 1s photoemission spectra of all compounds are easily assigned. The nitrogen core level spectra of proline, phenylalanine and tyrosine show two peaks. In tryptophan there is a second nitrogen atom in the indole ring, but even after subtraction of the contribution of this atom, there are two core level states present. In addition, the spectra of threonine and alanine show extra broadening compared with glycine. Calculations demonstrate that the extra peaks and broadening are due to the presence of conformers, but the electronic structure differences giving rise to the core level shifts are complex. In a phenomenological approach, we correlate the type of hydrogen bond (amino group acceptor or donor) with the core level binding energy. The hydrogen bonding is what determines the energy of each conformer.

In NEXAFS we see no spectroscopic evidence for different conformers, and calculations support the view that generally the differences are smaller than in photoemission. This appears to be due to a compensation mechanism, whereby both the core hole and unoccupied orbital energies shift by a similar amount between one conformer and another, so that the transition energy is similar for different conformers.

Our samples are in equilibrium at a well defined temperature, and core photoemission is a quantitative method. This allows us to acquire direct quantitative information about the populations of the conformers and thermodynamic quantities, which is more difficult with other spectroscopic methods.

### References

- [1] O. Plekan et al, Chem. Phys. Lett. **442** (2007) 429; O. Plekan et al, J. Electron Spectroscopy and Rel. Phenomena **155** (2007) 47; O. Plekan et al J. Phys. Chem. A **111** (2007) 10998; V. Feyer et al, to be published.
- [2] M. L. Gordon et al, J. Phys. Chem. A **107** (2003) 6144.
- [3] A. R. Slaughter and M. S. Banna, J. Phys. Chem. **92** (1988) 2165.

## INTERACTION OF HIGHLY CHARGED CLUSTERS WITH SURFACE

E.S. Parilis

California Institute of Technology, 200-36,  
Pasadena, CA, 91125, USA

The modern electrohydrodynamic spraying sources allow generating some beams of very large and highly charged clusters. Such clusters containing up to  $10^8$ - $10^9$  molecules have a mass up to  $10^9$ - $10^{10}$  amu and a diameter as large as  $10^3$  nm. The charge of the clusters could reach several  $10^3$  e, but with the charge-to-mass ratio not exceeding  $10^{-7}$  -  $10^{-6}$  e/amu. Due to large size, the Rayleigh condition is not violated and the clusters remain stable towards Coulomb explosion despite the large charge.

When accelerated with a voltage up to  $10^4$  V the clusters can acquire a kinetic energy of  $10^4$  KeV, but a very slow velocity, less than  $5 \cdot 10^4$  cm/sec, which corresponds to ca  $10^{-2}$  eV/atom. This velocity is well below the threshold of kinetic electron emission, so the impacts of slow highly charged clusters on solid surface cannot cause any electron emission of that kind. In the meantime the conditions are favorable for potential electron emission via Auger neutralization of the large positive charge.

It was shown that the impacts of even smaller water – glycerol clusters of  $10^6$ - $10^7$  amu charged up to  $+3 \cdot 10^2$  e eject from a metal surface around 120 electrons per cluster [1]. The potential emission under larger clusters with 10 times higher positive charge could emit from a surface more than 1000 el / cluster.

It is known that slow highly charged atomic ions, for instance  $Xe^{+44}$ , approaching a non-metal surface cause it sputtering, erosion, and create on it some craters and blisters via the mechanism of Coulomb explosion following a cascade Auger neutralization [2].

The same mechanism would create analogous features on a non-metal surface under impacts of slow large highly charged clusters.

Keywords: Clusters, Highly Charged Particles, Interaction with Surface.

### References

- [1] J.F.Mahoney, E.S.Parilis, J.Perel and S.A.Ruatta, NIMB B73 (1993) 29-34.
- [2] E.S.Parilis, Physica Scripta, T92 (2001)197-201.



**ATOMIC COLLISIONS INVOLVING ANTIMATTER****H.R.J.Walters<sup>a</sup>**<sup>a</sup>Department of Applied Mathematics, Queen's University, Belfast BT7 1NN, UK

In this talk I shall review theoretical developments in positron and positronium scattering by atoms. Most promising amongst these is the coupled pseudostate approach. This is able to include the main physical processes, and in particular ionization channels, in a coherent and consistent way. As a result, a complete picture of all the main processes can be obtained. Applications to positron scattering by atomic hydrogen, the alkali metals and helium will be shown. Positronium scattering is a much more difficult system to treat theoretically since now both the projectile and the target have internal structure. Here I shall highlight the role of target excitation, both real and virtual, and how resonances can be formed when the atom is capable of supporting a negative ion. Applications to positronium scattering by atomic hydrogen, helium, neon and argon will be shown.

*Keywords:* positron, positronium, pseudostates, resonances

## IONIZING COLLISIONS BY POSITRONS AND POSITRONIUM IMPACT

G. Laricchia<sup>a</sup>, S. Brawley<sup>a</sup>, D. Cooke<sup>a</sup>, Á. Kövér<sup>b</sup>, D.J. Murtagh<sup>a</sup> and A. Williams<sup>a</sup>

<sup>a</sup>Department of Physics and Astronomy, UCL (University College London), London WC1E 6BT, United Kingdom

<sup>b</sup>Institute of Nuclear Research, Debrecen, Hungary (ATOMKI)

Recent progress in the study of positron and positronium induced ionization is presented. The focus is on experimental techniques and results, which comprise both integral and differential cross-sections [e.g. 1-4]. Measurements for positronium formation and direct ionization by positron impact now include Ps formation in an excited state [5] and/or excitation of the residual ion [6]. First data, integral and differential, on the fragmentation of positronium in collision with helium and xenon [7] are also presented. Comparisons with theories and other projectiles are made where possible and future prospects are considered.

Keywords: positron, positronium, ionization, fragmentation, excitation

### References

- [1] G. Laricchia, S. Armitage, Á. Kövér and D.J. Murtagh *Advances in Atomic and Molecular Physics* vol. 56 (2008).
- [2] G. Laricchia, P.V. Reeth, M. Szluinska and J. Moxom (2002). *J. Phys. B: At., Mol. and Opt. Phys.* 35, 2525--2540.
- [3] C. Arcidiacono, A. Kövér and G. Laricchia (2005). Energy-sharing asymmetries in ionization by positron impact. *Phys. Rev. Lett.* 95, 223202--4.
- [4] S. Armitage, D.E. Leslie, A.J. Garner, and G. Laricchia, *Phys. Rev. Lett.* 89 (2002) 173402--4.
- [5] D. Murtagh et al (2008) in preparation.
- [6] D. Cooke et al (2008) in preparation.
- [7] S. Brawley et al (2008) in preparation.

## POSITRON IMPACT IONIZATION OF ATOMS AND MOLECULES

**R.I.Campeanu**

Department of Physics and Astronomy, York University, Toronto, Canada

Positron impact ionization of atoms and molecules has been studied both experimentally and theoretically. Most results were reported for hydrogen, rare gas atoms and diatomic molecules.

On the theoretical side the study of triple differential cross sections for positron impact ionization of H<sub>2</sub> and He required the use of a model representing the final state with 3 Coulomb wave functions [1].

In the study of integrated cross sections for hydrogen and rare gas atoms good agreement with the experiments are obtained with a model which represents the final state with only two Coulomb or distorted wave functions [2]. This agreement is surprisingly good even at very low impact energies [3].

In the case of diatomic molecules we employed a two-centre distorted-wave formalism. As in the case of atoms we obtained very good agreement with the experiments and our models containing in the final state only two distorted wave functions. However for the larger molecules our model seems to fail to reproduce the experimental data [4].

### References

- [1] A.Benedek, R.I.Campeanu, *Nuclear Instruments and Methods in Physics Research B*, Vol.266, pp.407-9 and 458-61, 2008, *Journal of Physics B*, Vol.40, pp.1589-96, 2007
- [2] R.I.Campeanu, R.P.McEachran and A.D.Stauffer, *Nuclear Instruments and Methods in Physics Research B*, Vol.192, pp.146-9, 2002, *Canadian Journal of Physics*, Vol.79, pp.1231-36, 2001
- [3] R.I.Campeanu, L.Nagy and A.D.Stauffer, "Near-Threshold Ionization of Atoms and Molecules by Positron Impact", *Canadian Journal of Physics*, Vol.81, pp.919-27, 2003
- [4] R.I.Campeanu, V. Chis, L. Nagy and A.D. Stauffer, *Physics Letters A*, A Vol.325, pp.66-69, 2004, Vol.344, pp.247-52, 2005, *Nuclear Instruments and Methods in Physics Research B*, Vol.221, pp.21-23, 2004, Vol.247, pp.58-60, 2006

## **Ionization of noble gas atoms in slow antiproton collisions**

H. Knudsen<sup>\*1</sup>, H.-P. E. Kristiansen<sup>1</sup>, S. P. Møller<sup>1</sup>, H.D. Thomsen<sup>1</sup>, U. Uggerhøj<sup>1</sup>, T. Ichioka<sup>2</sup>, R. W. McCollough<sup>3</sup>, C. A. Hunniford<sup>3</sup>, M. Charlton<sup>4</sup>, N. Kuroda<sup>5</sup>, Y. Nagata<sup>5</sup>, H. Imao<sup>6</sup>, H. A. Torii<sup>5</sup>, Y. Yamazaki<sup>5,6</sup>, H. H. Andersen<sup>7</sup>, K. Tökesi<sup>8</sup>

<sup>1</sup>*Department of Physics and astronomy, University of Aarhus, Denmark*

<sup>2</sup>*University of Barcelona, Spain*

<sup>3</sup>*Department of Physics, Queens University of Belfast, UK*

<sup>4</sup>*Department of Physics, University of Swansea, UK*

<sup>5</sup>*Institute of Physics, Komaba, University of Tokyo, Japan*

<sup>6</sup>*Atomic Physics Laboratory, RIKEN, (Saitama,) Japan*

<sup>7</sup>*Niels Bohr Institute, University of Copenhagen, Denmark*

<sup>8</sup>*ATOMKI, Debrecen, Hungary*

In order to improve our understanding of the physics of atomic collisions, accurate experimental data are needed which can be used as benchmarks for the development of advanced calculations of these dynamically developing many-body systems. One of the simplest processes in this field is the single ionization of helium by antiproton impact. Here, there is a strong many-body effect, namely the electron-electron correlation, but on the other hand there is no complication from electron transfer. Furthermore the projectile is heavy which means that it moves in a classical orbit and that we can investigate ionization in collisions where the projectile moves with a speed much slower than that of the target electrons. At CERN's LEAR we measured the total cross sections for single and multiple ionization of a multitude of targets for impact of antiprotons with velocities down to that of the outer electrons in the targets [1,2]. This in turn led to the development of more than a dozen advanced theories. These calculations coalesce at high projectile speed, but shown great spread at low projectile energies. In order to judge the validity of these models, we therefore need to measure ionization for impact of antiprotons of a few keV.

Using a new technique for the production of intense beams of very slow antiprotons [3] developed by the ASACUSA collaboration at CERN's AD facility, we have been able to obtain accurate cross sections for single ionization of helium and single and double ionization of argon down to impact energies of 3 keV [4]. In this talk, I will present the technique and the results and compare them to the theoretical calculations.

[1] L. H. Andersen, P. Hvelplund, H. Knudsen, S. P. Møller, J.O.P. Pedersen, S. Tang-Petersen, E. Uggerhøj, K. Elsener and E. Morenzoni *Phys Rev* **A41** 6536 (1990)

[2] P. Hvelplund, H. Knudsen, U. Mikkelsen, E. Morenzoni, S. p. Møller, E. Uggerhøj and T. Worm *J. Phys.* **B27** 925 (1994)

[3] N. Kuroda, H. A. Torii, K. Yoshiki Franzen, Z. Wang, S. Yoneda, M. Inoue, M. Hori, B. Juhasz, D. Horvath *Phys. Rev. Letters* **94** 023401 (2005)

[4] H. Knudsen, H.-P. E. Kristiansen, S. P. Møller, H.D. Thomsen, U. Uggerhøj, T. Ichioka, R. W. McCollough, C. A. Hunniford, M. Charlton, N. Kuroda, Y. Nagata, H. Imao, H. Torii, Y. Yamazaki, H. H. Andersen, K. Tökesi submitted to *Phys. Rev. Letters* (2008)

---

\* Corresponding author: [hk@phys.au.dk](mailto:hk@phys.au.dk)

## QED THEORY OF RADIATION EMISSION AND ABSORPTION LINES FOR ATOMS AND IONS IN A STRONG LASER FIELD

A. Glushkov<sup>a,b</sup>

<sup>a</sup>Institute for Spectroscopy of Russian Academy of Sciences (ISAN), Troitsk, 142090,  
Russia

<sup>b</sup>Odessa University, P.O.Box 24a, Odessa-9, Ukraine

A consistent QED approach [1], [2] is applied to studying the interaction of the atoms and ions of plasma with an intense electromagnetic (laser) field. Method bases on description of atom in a field by the  $k$ - photon emission and absorption lines. The lines are described by the QED moments of different orders, which can be calculated with the use of the Gell-Mann and Low S-matrix adiabatic formalism ( $T=0$ ). In relativistic version the Gell-Mann and Low formulae expresses an imaginary part of the energy shift  $ImE$  through the QED scattering matrix, including interaction of atom with electromagnetic field and field of the photon vacuum. We present QED S-matrix energy formalism ( $T \neq 0$ ) for calculation of the spectral lines shape in dense plasma. For any atomic level we calculate  $ImE(w)$  as function of the laser pulse central frequency  $w$ (resonant curve). We calculate the moments for resonance, connected with concrete atomic a-p transition (a,p-discrete levels;  $k$  photons is absorbed). To calculate the moments we need to get the expansion of  $E$  into the perturbation theory series. Numerical modelling carried out for H- and Ar-like plasma. QED approach to description of radiation atomic lines for atoms and ions in plasma is generalized on a case of the confined atomic systems, including a case of the Debye approximation.

*Keywords:* Radiation; Laser; Atom

### References

- [1] A. Glushkov, L.N. Ivanov, Phys. Lett. A 170 (1992) 33; Preprint ISAN N AS-3, Moscow-Troitsk (1992).
- [2] A. Glushkov et al, Int.Journ. Quant. Chem. 99 (2004) 889; 104 (2005) 512; J.Phys.CS 11 (2005) 188; 35 (2006) 425.

## X-RAY SPECTROSCOPY OF HIGHLY-CHARGED HEAVY IONS AT FAIR

A. Gumberidze

for the SPARC collaboration

Laboratoire Kastler Brossel, Universit P. et M. Curie, Paris, France

The new international accelerator Facility for Antiproton and Ion Research (FAIR) at GSI has key features that offer a range of new opportunities in atomic physics and related fields [1]. The proposed facility will provide the highest intensities of relativistic beams of both stable and unstable heavy nuclei, in combination with the strongest possible electromagnetic fields, thus allowing to extend atomic spectroscopy virtually up to the limits of atomic matter. In the current contribution, an overview of the x-ray spectroscopy program within the atomic physics research collaboration SPARC (Stored Particle Atomic Research Collaboration), at the FAIR facility will be given. These activities comprise, among others, the investigation of relativistic collision dynamics, electron correlation in the presence of strong fields, the test of Quantum Electrodynamics in extremely strong electromagnetic fields, the use of atomic physics techniques for the determination of properties of stable and unstable nuclei, and ideas to test the predictions of fundamental theories besides Quantum Electrodynamics [2]. The state of the art x-ray spectroscopy will be of key importance for realization of these challenging goals. The world-wide unique experimental conditions and opportunities offered by the future FAIR facility will be combined with advanced x-ray detection devices (i.e. large-area, segmented solid-state detectors, high-resolution crystal spectrometers, calorimetric detectors etc).

*Keywords:* FAIR; SPARC; X-ray Spectroscopy

### References

- [1] W.F. Henning et al, Internal Accelerator Facility for Beams of Ions and Antiprotons, GSI, Darmstadt, 2001, <http://www.gsi.de/GSI-Future/cdr/>.
- [2] Documents related to the SPARC collaboration, Letter of Intent, Technical Proposal , Definition of Working Groups and Working Packages can be found at: <http://www.gsi.de/sparc>.

## ULTRA-COLD ELECTRON TARGET FOR RECOMBINATION EXPERIMENTS AT THE NEW EXPERIMENTAL STORAGE RING, NESR

**Christopher Kozhuharov**

for the Electron Target Working Group of SPARC

GSI Darmstadt, Germany

The new experimental storage ring, NESR, will provide both intense beams of highly-charged stable nuclei up to bare uranium as well as beams of exotic radioactive nuclei from the super fragment separator, SFRS. Within the SPARC Collaboration, we are planning to furnish the NESR with an ultra-cold electron target. It will be operated independently from beam cooling tasks and will be optimized with respect to high resolution and sensitivity for future experiments on photo recombination. The two main objectives of these are: (i) precise studies of ionic structures with an emphasis on QED-Effects and (ii) studies of the nuclear properties—such as isotope shift—with atomic physics methods. The first case will focus on H-like and/or on few-electron high-Z ions, such as Li-like ones. Pioneering experiments have been performed at ESR in Darmstadt and at TSR in Heidelberg [1,2,3]. Envisaged are experiments on QED effects in overlapping resonances in H-like uranium [4]. The second physics case will focus on Li and Be-like chains of heavy isotopes; both stable as well as long-lived ones ( $> 10$  sec). The potential of this method has been investigated in a first pilot experiment studying the isotopic shift of Li-like  $^{142}\text{Nd}^{57+}$  versus  $^{150}\text{Nd}^{57+}$ . As depicted in Fig. 1 the data show a clearly pronounced shift of the DR resonances studied [5].

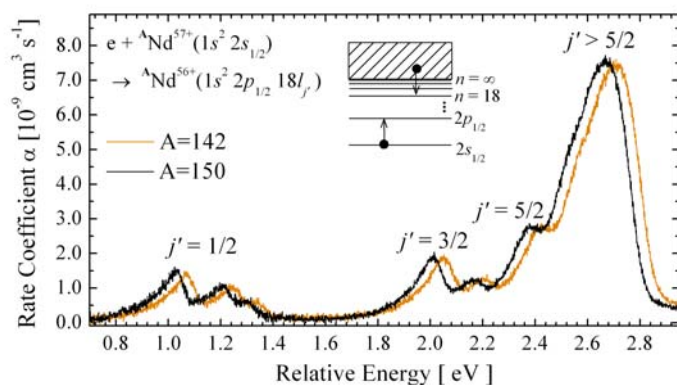


Figure 1:  
Dielectronic recombination of the Li-like neodymium isotopes  $^{142}\text{Nd}^{57+}$  (black line) and  $^{150}\text{Nd}^{57+}$  (grey line) in the energy range of the  $1s^2 2p_{1/2} 18l_j$  resonance groups. Background contributions from non-resonant radiative recombination and from capture in the residual gas have been subtracted. The labels indicate the individual fine structure components  $j'$  of the  $n = 18$  Rydberg electron.

The anticipated low electron temperature in the new target and the stability of the ion energy due to the separate dedicated ion cooling will lead to an energy resolution of at least an order of magnitude better than the ESR one. This narrow response will improve by the same factor the signal to background ratio and will lead to an excellent performance in measuring the position, the area and the line shape of DR resonances. The good energy resolution will be achieved by adiabatic expansion and adiabatic acceleration of the electron beam. Further details of the technical concept will be presented as well.

### References

- [1] C. Brandau, C. Kozhuharov, A. Müller, W. Shi, S. Schippers et al. Phys. Rev. Lett. **91** (2003) 073202
- [2] D. Bernhard, C. Brandau, Z. Harman, C. Kozhuharov, A. Müller, W. Scheid et al. to be published
- [3] Stefan Schippers, contribution to this Conference
- [4] A.V. Nefiodov, L.N. Labzovsky, D.L. Moores, Phys. Rev. **A60** (1999) 2069
- [5] C. Brandau, C. Kozhuharov, Z. Harman, A. Müller, S. Schippers et al. Phys. Rev. Lett. **100** (2008) 0703201

**Recent theoretical progress in studying  
x-ray emission from highly-charged, heavy ions**

**A. Surzhykov<sup>a</sup>, S. Fritzsche<sup>b,c</sup> and Th. Stöhlker<sup>a,b</sup>**

<sup>a</sup>Physikalisches Institut, Universität Heidelberg, D-69120 Heidelberg, Germany

<sup>b</sup>Gesellschaft für Schwerionenforschung (GSI), D-64291 Darmstadt, Germany

<sup>c</sup>Max-Planck-Institut für Kernphysik, Postfach 103980, D-69029 Heidelberg, Germany

The photon emission from highly-charged, heavy ions has been in the focus of intense experimental studies at the GSI facility for many years. While these studies have already revealed unique knowledge about the electron-electron and electron-photon interaction in the presence of strong fields [1], there are further challenges to be faced in forthcoming years. For instance, the angular and polarization properties of characteristic x-rays following relativistic ion-atom collisions are to be explored in detail within the framework of the SPARC collaboration [2]. In this contribution, we summarize the recent advances in the theoretical description of the photon emission from relativistic, high- $Z$  ions [3, 4]. Special attention will be paid to the  $K\alpha$  transitions in the helium-like uranium  $U^{90+}$  ions produced by means of *radiative* (RR) as well as *dielectronic* (DR) recombination. The results obtained for such capture processes will be also compared with the theoretical predictions for the characteristic radiation following *Coulomb excitation* of initially two-electron projectiles [5].

*Keywords:* characteristic radiation; relativistic and many-body effects; energetic ion-atom collisions

#### References

- [1] S. Fritzsche, P. Indelicato, Th. Stöhlker, J. Phys. B: At. Mol. Opt. Phys. 38 (2005) S707-S726.
- [2] Th. Stöhlker *et al.*, Nuclear Instruments and Methods in Physics Research B 261 (2007) 234-238.
- [3] A. Surzhykov, U. D. Jentschura, Th. Stöhlker, S. Fritzsche, Phys. Rev. A 74 (2006) 052710.
- [4] S. Fritzsche, A. Surzhykov, U. D. Jentschura, Th. Stöhlker, J. Phys.: Conf. Ser. 88 (2007) 012018.
- [5] A. Surzhykov, U. D. Jentschura, Th. Stöhlker, S. Fritzsche, Phys. Rev. A (2008) in press.



## HIGH POWER LASERS AND X-RAY LASERS FOR EXPERIMENTS WITHIN SPARC COLLABORATION

D. Ursescu<sup>a</sup>

<sup>a</sup>Lasers Department, Atomistilor 409, Magurele, National Institute for Lasers, Plasma and Radiation Physics, Romania

Within SPARC collaboration, the experiments connected to lasers cover a broad range. An overview of these experiments will be made. Further, few examples will illustrate recent progress at GSI in laser spectroscopy with infrared lasers [1] and with X-ray lasers [2] and also preliminary experiments related to ions in intense laser fields in an electron beam ion trap (EBIT) [3]. The long term road map for ultrashort and ultra intense laser developments at INFLPR, relevant to SPARC experiments, will also be presented.

*Keywords:* SPARC; lasers

### References

- [1] R. Sanchez, W. Nortershauser, G. Ewald, D. Albers, J. Behr, P. Bricault, B. A. Bushaw, A. Dax, J. Dilling, M. Dombisky, G. W. F. Drake, S. Gotte, R. Kirchner, H.-J. Kluge, Th. Kuhl, J. Lassen, C. D. P. Levy, M. R. Pearson, E. J. Prime, V. Ryjgov, A. Wojtaszek, Z.-C. Yan, and C. Zimmermann, Phys. Rev. Lett. 96 (2006) 033002
- [2] T. Kuehl, D. Ursescu, V. Bagnoud, D. Javorkova, O. Rosmej, K. Cassou, S. Kazamias, A. Klisnick, D. Ros, P. Nickles, B. Zielbauer, J. Dunn, P. Neumayer, G. Pert, Lasers and Particle Beams 25(1) (2007) 93-97.
- [3] D. Schneider, J. McDonald, B. Zielbauer, D. Ursescu, U. Spillmann, Th. Stoehlker, T. Kuehl, T. Schenkel, G. Andler, E. Lindroth, and R. Schuch, Nuclear Instruments and Methods in Physics Research B 261 (2007) 239243

## Reaction Microscopes in heavy-ion storage rings - results and prospects

D. Fischer

Max-Planck-Institut für Kernphysik, Saupfercheckweg 1, 69 117 Heidelberg, Germany

Reaction Microscopes become a standard tool to investigate the dynamics of atomic and molecular break-up processes [1]. With this technique kinematically complete data sets can be obtained by the momentum resolved and coincident detection of all charged fragments of an atom or molecule produced in single collisions with electrons, ions, single photons, or in strong laser fields. Recently a Reaction Microscope has been operated for the first time in a heavy-ion storage ring, the ESR at GSI in Darmstadt (Germany). The ESR provides excellent experimental conditions w.r.t intensity and emittance of the ion beam and thus, in combination with a Reaction Microscope, represents the ideal tool to obtain highly differential information on fundamental HCI-atom collision processes.

The results of first experiments on target ionization and charge transfer in collisions of highly charged projectiles ranging from 13 AMeV  $U^{92+}$  to 400 AMeV  $Ni^{28+}$  with He, Ne, and Ar targets will be presented. Future experiments are planned to study e.g. radiative and non-radiative charge transfer reactions where also photons are detected in coincidence. Furthermore, simultaneous ionization of target and projectile shall be investigated to obtain insight into the dynamics of collision induced electron emission from HCIs.

### References

[1] J. Ullrich, et al., Rep. Prog. Phys. **66** (2003), 1463

## T->V, R ENERGY EXCHANGE FOR INELASTIC COLLISIONS OF COLD MOLECULES IN THE SYSTEM CsBr + CsBr

V.M. Azriel, L.Yu. Rusin

Institute of Energy Problems of Chemical Physics RAS,  
Leninski prospect 38, Bldg.2, Moscow 119334, Russia

Dynamics of the conversion of translational energy into internal energy of the molecules in the system CsBr + CsBr has been investigated by classical trajectory technique for based initial vibrational and rotational states of both molecules ( $V=0$  and  $J=0$ ). It was found that relative efficiencies of T->V and T->R energy exchange depend significantly on collision energy. At  $E_{rel}=0,2$  eV (see figures 1,a and 1,b) the final distribution of vibrational energy of molecules is characterized by higher temperature in comparison with distribution of rotational energy. At increase  $E_{rel}$  up to 1,0 eV, on the contrary, distribution of rotational energy has higher temperature (figures 1,c and 1,d).

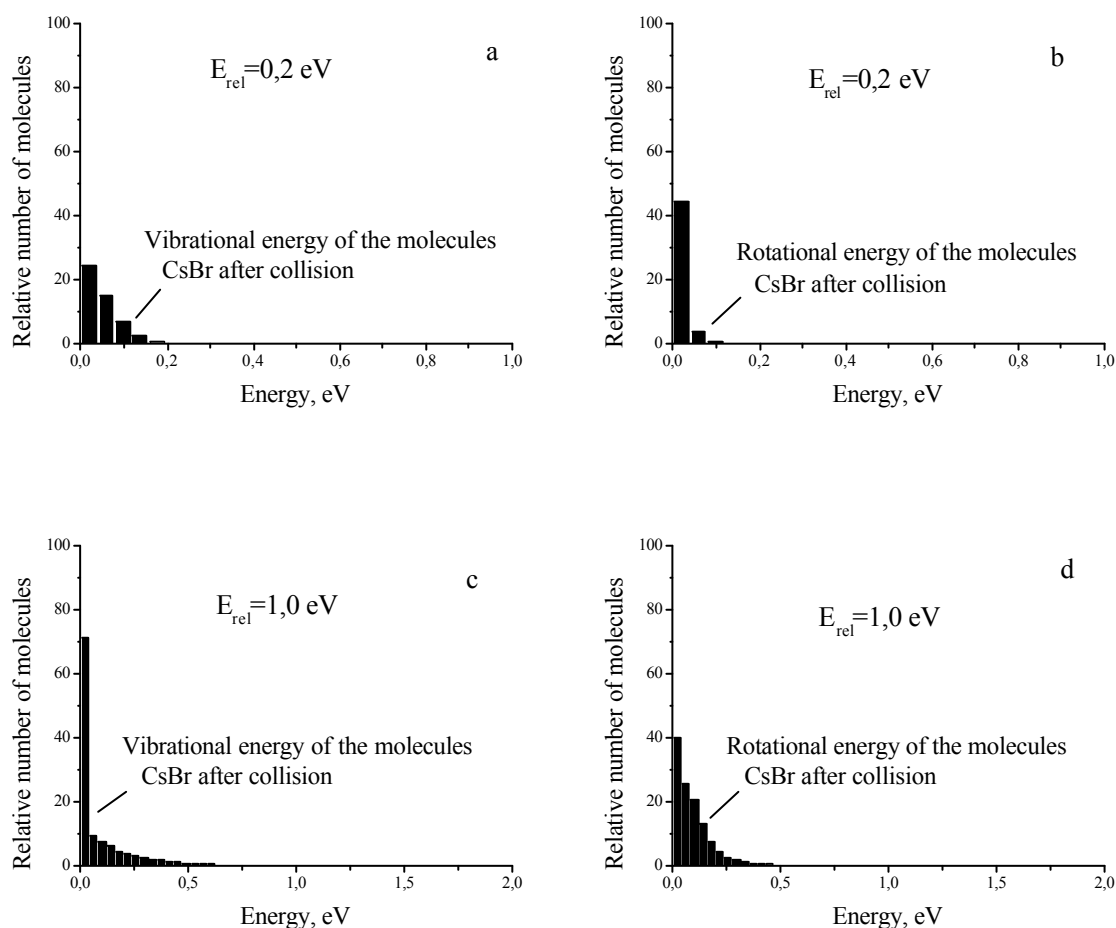


Fig. 1. Histograms of distributions of vibrational (a, c) and rotational (b, d) energies of the molecules CsBr after collision at  $E_{rel}=0,2$  eV (a, b) and  $E_{rel}=1,0$  eV (c, d).

## IONIZATION OF METASTABLE THALLIUM ATOMS

**I.I. Shafranyosh, V.I. Marushka, R.O. Fedorko,  
T.A. Snegurskaya, V. Perehanets**

Uzhgorod National University, Department of Physics,  
54 Voloshyn str., Uzhgorod 88000, Ukraine

The processes of electron-impact ionization of atoms from the metastable states play an important role in technological and natural plasmas due to the large effective ionization cross sections and low energy thresholds. At the same time the data on the regularities of the processes of ionization from the metastable states are available only for a limited number of elements, which is due to the experimental difficulties of such investigations.

Here we report on the results of experiments on the metastable Tl atom ionization by electrons. Tl atom provides a unique possibility of experimental studies of ionization processes from the initial states differing by the total momentum only. The ground-state term of Tl atom is the doublet one with the  $6s^26p^2P_{3/2}$  i  $6s^26p^2P_{1/2}$  components. In natural conditions, Tl atom is in the  $6s^26p^2P_{1/2}$ -state, while the  $6s^26p^2P_{3/2}$ -state is metastable (with excitation energy 0.966 eV).

Our studies were carried out in the conditions of electron and atomic beams crossed at the right angle. A five-electrode electron gun was used as the electron beam source. Electron beam current was 1–2  $\mu\text{A}$  at the energy spread of  $\Delta E_{1/2} \approx 0.3$  eB (FWHM). Energy scale was calibrated with respect to the ground-state Tl atom ionization threshold with the accuracy  $\pm 0.15$  eB. Electron gun was placed in the longitudinal magnetic field with the  $1.2 \cdot 10^{-2}$  Tl induction that prevented scattered electrons to reach the probe. Ion detecting system operated in the analog mode. The beam of metastable Tl atoms was produced using the discharge technique. Metastable atom concentration was determined by a single-mirror method according to the self-absorption of the spectral lines and amounted to  $4 \cdot 10^9 \text{ cm}^{-3}$  for the metastable  $6s^26p^2P_{3/2}$  and  $6 \cdot 10^{10} \text{ cm}^{-3}$  for the ground-state  $6s^26p^2P_{1/2}$  Tl atoms. An atomic beam divergence angle was  $\sim 8.7 \cdot 10^{-2}$  rad. Experimental layout and technique are described in detail in our previous paper [1].

Completeness of the positive ion collection was provided by the ion collector with an axial electrode (probe) held at the negative potential. It has been found that at  $-25$  V potential the ion current at the probe was saturated.

As a result of experimental studies, the absolute value of the total ionization cross section for the metastable Tl atoms was determined to be  $\sim 3.5 \cdot 10^{-15} \text{ cm}^2$  at the incident electron energy 12 eV (i.e. at the point of optimal signal to noise ratio). The total ionization cross section for the ground-state atoms at the same energy is  $\sim 0.25 \cdot 10^{-15} \text{ cm}^2$ . The relative uncertainty in determining the cross section values did not exceed 60%. Thus, at the 12 eV electron energy the ionization cross section for the metastable  $6s^26p^2P_{3/2}$ -state appeared to be 14 times larger than that for the ground  $6s^26p^2P_{1/2}$ -state.

*Keywords: Thallium Atom; Ionization; Metastable State; Cross Section.*

### References

- [1]. I.I. Shafranyosh, M.O. Margitich, J. Phys. B. 33 (2000) 905

# EXTRACTING INTERACTION PARAMETERS FROM NEAR THRESHOLD EXPERIMENTS

P. A. Macri<sup>a</sup> and R. O. Barrachina<sup>b</sup>

<sup>a</sup>Departamento de Física, FCEyN, Universidad Nacional de Mar del Plata, Deán Funes 3350, 7600 Mar del Plata, Argentina

<sup>b</sup>Centro Atómico Bariloche and Instituto Balseiro, R8402AGP S. C. de Bariloche, Río Negro, Argentina

We analyze and compare different methods to extract, from experiments, scattering parameters such as polarizability, scattering length and effective range. For example, different generalizations of O'Malley et al.'s modified effective range theory [1], such as Fabrikant's approach [2] or the multi channel theory of Watanabe and Greene [3] have been extensively used in the literature to fit the experimental data of electrons or positrons interacting with atoms and molecules.

In a previous work [4], we showed that near-threshold cross sections can be understood considering two factors: i) the Wigner threshold law and ii) the Jost function for the interaction between those two particles which move with low relative energy after the reaction. Specifically, all what is needed to know by forehand is the behavior of the potential tail. The method allows to determine a characteristic distance  $R$  where the asymptotic behavior starts to be effective. Once  $R$  is determined, all scattering parameters are determined through the corresponding  $\ell$ -wave Jost function. In this communication, we demonstrate that this approach shows a significant improvement over other methods on a much broader range of energies. We discuss the applicability of this method for extracting information on low-energy electron or positron interactions with atoms and molecules. For example in Fig 1. we show a fit using the present approach to highly accurate ab-initio computations of Refs. [5] and [6] for elastic proton-Positronium collisions. Our fit succeeds to explain the cross section in a broad energy domain and allows us to obtain a scattering length for the proton-Positronium interaction of  $a_0 = 15.9$  au in fully agreement with the ab-initio computations.

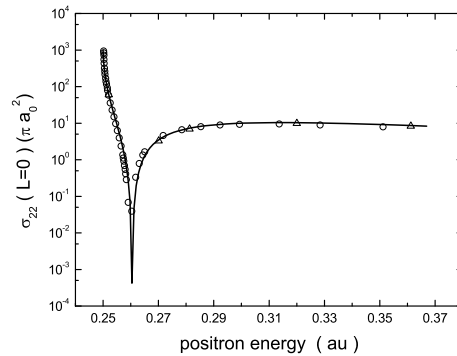


Fig. 1. S-wave cross-section  $\sigma_{22}$  for elastic positronium-proton scattering. Triangles, computation of [5]; circles, [6]; full line, present fit.

*Keywords:* low energy collisions; scattering length; effective range

## References

- [1] T. F. O'Malley, L. Spruch and L. Rosenberg, J. Math. Phys. 2 (1961) 491.
- [2] I. I. Fabrikant, Opt. Spectrosc. (USSR) 53 (1982) 131.
- [3] S. Watanabe and C. H. Greene, Phys. Rev. A 22 (1980) 158
- [4] P. A. Macri and R. O. Barrachina, Phys. Rev. A 65 (2002) 062718.
- [5] T. T. Gien, Phys. Rev. A 56 (1997) 1332.
- [6] J. W. Humberston et al J. Phys. B 30 (1997) 2477.

# LOW-ENERGY ELECTRON SCATTERING FROM CALCIUM

**S. Gedeon and V. Lazur**

Department of Theoretical Physics, Uzhgorod National University, 88000, Ukraine

The  $B$ -spline  $R$ -matrix method (BSR) [1] is used to investigate the integrated cross sections (ICS) of elastic electron scattering from neutral calcium in the ultra-low energy range from threshold to 0.5 eV. The close-coupling expansion includes 39 bound states of neutral calcium, covering all states from the ground state to  $4s8s\ ^1S$  (see details in [2]).

Fig. 1 compares the total and partial electron-impact cross sections from Ca in the ultra-low energy region, calculated in two different  $R$ -matrix approaches: the present BSR method and  $R$ -matrix with pseudostates method (RMPS) [4]. As seen from Fig. 1, basic difference between the cross sections in two  $R$ -matrix approaches comes mainly from the dominated  $^2P^o$  partial wave. In the same time, partial cross sections for the  $^2S^e$  and  $^2D^e$  partial waves in these two methods practically coincide. Fig. 1 also shows the comparison of total BSR39 and RMPS cross sections with experimental data of Romaniuk *et al* [3].

Fig. 2 compares the  $^2S^e$ ,  $^2P^o$  and  $^2D^e$  partial eigen-phases of electron-impact scattering from Ca at low energies region between most recent calculations: BSR39 (the present calculation), RMPS [4] and method of static-exchange formalism [5]. Again, the largest discrepancy between different method was found for  $^2P^o$  partial wave.

*Keywords:* Cross Section; Electron-impact; Calcium

## References

- [1] O. Zatsarinny, *Comput. Phys. Commun.*, **174** (2006) 273.
- [2] O. Zatsarinny et al., *Phys. Rev. A*, **74** (2006) 052708.
- [3] N.I. Romanyuk, O.B. Shpenik, I.P. Zapesochnyi. *Pis'ma Zh. Eksp. Teor. Fiz.* **32**, (1980) 472 [*JETP Lett.* **32** (1980) 452].
- [4] K. Bartschat and H.R. Sadeghpour. *J. Phys. B.* **36** (2003) L9.
- [5] J. Yuan, Zh. Zhang. *Phys. Rev. A* **42** (1990) 5363.

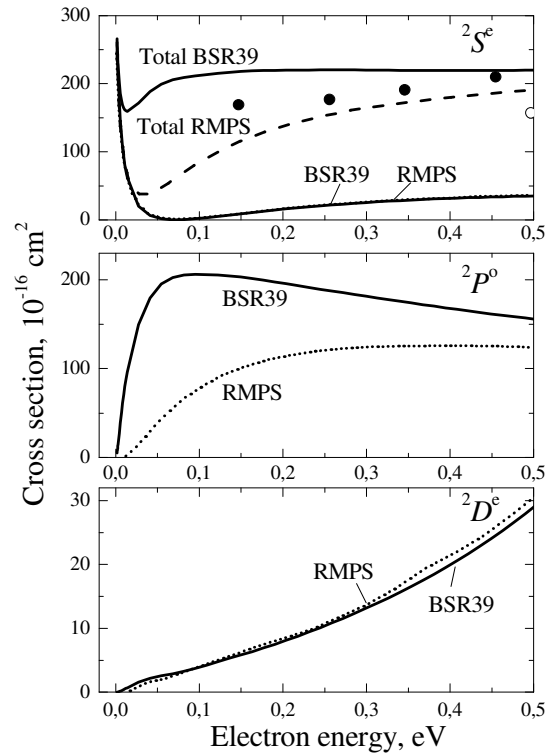


Fig. 1. The total and partial electron-impact cross sections from Ca: (●) – experiment [3]; (—) – BSR39; (---) – RMPS [4].

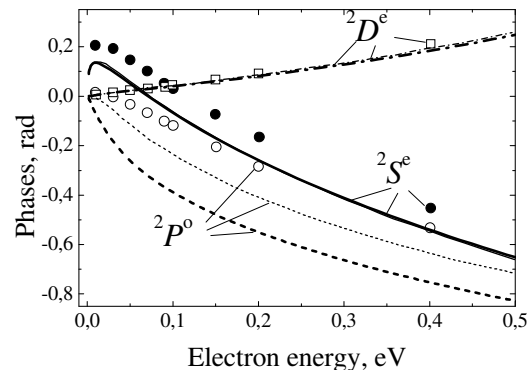


Fig. 2. The  $^2S^e$ ,  $^2P^o$  and  $^2D^e$  partial phases for electron-impact scattering from Ca: bold lines – BSR39; thin lines – RMPS [4]; („●”, „○”, „□”) – static-exchange calculation [5].

## Angular distribution of x-ray satellites following the dielectronic recombination of high-Z ions

**S. Fritzsche<sup>a,b</sup>, N. M. Kabachnik<sup>a,c</sup>, A. Surzhykov<sup>d</sup> and Th. Stöhlker<sup>a,d</sup>**

<sup>a</sup> Gesellschaft für Schwerionenforschung (GSI), D-64291 Darmstadt, Germany

<sup>b</sup> Max-Planck-Institut für Kernphysik, D-69029 Heidelberg, Germany

<sup>c</sup> Institute for Nuclear Physics, Moscow State University, Moscow 119991, Russia

<sup>d</sup> Physikalisches Institut, Universität Heidelberg, D-69120 Heidelberg, Germany

The angular distribution of the x-ray satellites, following the dielectronic recombination of high-Z hydrogen-like and lithium-like ions, is considered in the framework of the density matrix theory. Emphasis has been placed especially on the influence of higher multipoles in the coupling of the radiation field to the x-ray emission of the doubly-excited ions. A strong interference effect is shown between the electric-dipole (E1) and magnetic-quadrupole (M2) contributions that increases rapidly with the charge of the ions. Results are shown for the  $1s \rightarrow (2lj)(2l'j')$  dielectronic recombination of initially hydrogen-like ions and the angular distribution of their subsequent x-ray photon emission into the  $1s2s$   $J = 0, 1$  and  $1s2p$   $J = 0, 1, 2$  fine-structure levels. Moreover, first computations have been carried out for the doubly excited states of (finally) berullium-like projectiles. The theoretical results are compared also with experiment as far as data are available. These investigations extent a number of previous theoretical and experimental case studies on *relativistic* collisions of highly-charged ions with electrons and various gas targets [1, 2].

*Keywords:* characteristic radiation; dielectronic recombination; relativistic ion-electron collisions

### References

- [1] S. Fritzsche, P. Indelicato, Th. Stöhlker, J. Phys. B: At. Mol. Opt. Phys. 38 (2005) S707.
- [2] A. Surzhykov, S. Fritzsche, A. Gumberidze and T. Stöhlker, PRL 88 (2002) 153001.

## RESONANT AUGER DECAY OF AR 2p HOLE INDUCED BY ELECTRON IMPACT

M. Žitnik<sup>a</sup>, M. Kavčič<sup>a</sup>, K. Bučar<sup>a</sup>, B. Paripás<sup>b</sup>, B. Palásthy<sup>b</sup>, K. Tőkési<sup>c</sup>

<sup>a</sup>J. Stefan Institute, Jamova 39, P.O.B. 3000, SI 1000, Ljubljana, Slovenia

<sup>b</sup>Dept. of Physics, University of Miskolc, 3515 Miskolc-Egyetemváros, Hungary

<sup>c</sup>Institute of Nuclear Research of the Hungarian Academy of Science (ATOMKI),  
H-4001 Debrecen, P.O. Box 51, Hungary

The kinetic energy region of L-MM transitions in Ar extends from 200-214 eV and was studied extensively in the past by coincidence and noncoincidence techniques as well as by electron, photon and ion impact experiments ([1] and ref. therein). Up to 207 eV, one finds the 'normal' Auger lines, multiplets  $^1S_0$ ,  $^1D_2$  and  $^3P_{0,1,2}$  which originate from Auger decay of an ion:  $Ar^+ [L_{2,3}] \longrightarrow Ar^{2+} [M_{2,3}M_{2,3}] + e$  and appear as soon as the energy deposited in the atom exceeds 248.628 eV ( $L_3$  hole) and 250.776 eV ( $L_2$  hole) [2]. A series of singly excited atomic states  $[2p_{3/2,1/2}]nl$ , where  $l$  is restricted to  $s$  and  $d$  in the dipole (photon impact) approximation, approach the corresponding thresholds from below. In decay of these atomic states the so-called resonant Auger electrons are released with energies lying mainly in the upper part of the  $L - MM$  kinetic energy region and after the decay, argon is usually left in one of the singly excited final ionic states  $[3p^2]n'l'$ .

A considerable amount of studies using high resolution spectroscopy was done in the realm of photo-induced resonant Auger transitions [3] and final valence satellite states build on a double  $3p$  hole in argon [4]. Fully isolated resonant Auger spectra were measured for  $[2p_{3/2}]4s$ ,  $3d$ ,  $4d$ ,  $5d$  and  $[2p_{1/2}]4s$  resonances and the results were compared to the calculated decay probabilities. However, systematic studies of electron impact induced Auger resonant spectra are not reported so far. Since the resonant lines appear only in a narrow range of the electron energy loss, in the non-coincidence experiment they are obscured by the much stronger normal Auger lines (or by the signal from the cascade Auger or double L-hole Auger decay) and the lines which originate from different resonances may overlap between themselves. Clearly, an (e,2e) measurement is needed to measure the Auger spectrum of the selected resonance and, since the signal is weak, a highly efficient coincidence detection of both electrons is required [5]. Another interesting aspect unavoidably present in photon or electron impact experiments of this kind, is a possibility of interferences. In this work, we present our recent results related to the electron impact induced resonant Auger emission of argon  $2p$  hole.

*Keywords:* (e,2e) experiment; Argon; Resonant Auger emission.

### References

- [1] K. Bučar, M. Žitnik, Rad. Phys. Chem. 76 (2007) 487.
- [2] G.C. King, M. Tronc, F.H. Read and R.C. Bradford, J. Phys. B10 (1977) 2479.
- [3] J.A. de Gouw, J. van Eck, A.C. Peters, J. van der Weg and H.G.M. Heideman, J. Phys. B28 (1995) 2127.
- [4] A. Kikas A., S.J. Osborne, A. Ausmees, S. Svensson, O.-P. Sairanen and S. Aksela, J. Electron Spectrosc. Relat. Phenom. 77 (1996) 241.
- [5] B. Paripás and B. Palásthy, Rad. Phys. Chem. 76 (2007) 565.



# PROPERTIES OF AUGER ELECTRONS FOLLOWING EXCITATION OF POLARIZED ATOMS BY POLARIZED ELECTRONS

A. Kupliauskienė, V. Tutlys

Institute of Theoretical Physics and Astronomy of Vilnius University, A. Goštauto 12,  
LT-01108 Vilnius, Lithuania

Auger decay following excitation of atoms by electrons is a powerful tool for the investigation of matter and interactions. The excited atom can 'remember' the direction of polarization of the incident electron or photon and the following Auger electron may have a nonisotropic angular distribution [1]. In two-step approximation, the general expression of the differential cross section describing the polarization and angular distribution of Auger electrons following the excitation of polarized atoms  $A(\alpha_0 J_0 M_0)$  by polarized electrons  $e^-(\mathbf{p}_1 m_1)$  can be written in the form of the expansion over the multipoles of the non registered intermediate state of an excited atom  $A(\alpha_1 J_1 M_1)$  by using the method proposed in [2] as follows:

$$\frac{d^2\sigma(\alpha_0 J_0 M_0 \mathbf{p}_1 m_1 \rightarrow \alpha_1 J_1 \mathbf{p}_2 m_2 \rightarrow \alpha_2 J_2 M_2 \mathbf{p}_2 m_2 \mathbf{p}_A m_A)}{d\Omega_e d\Omega_A} =$$

$$= \sum_{K_1 N_1} \frac{d\sigma_{K_1 N_1}^{\text{ex}}(\alpha_0 J_0 M_0 \mathbf{p}_1 m_1 \rightarrow \alpha_1 J_1 \mathbf{p}_2 m_2)}{d\Omega_e} \frac{dW_{K_1 N_1}^r(\alpha_1 J_1 \rightarrow \alpha_2 J_2 M_2 \mathbf{p}_A m_A)}{d\Omega_A}.$$

The expressions for the first and second terms are presented in [3] and [4], respectively.

The general expression represents the most general case of the cross section describing the polarization of all particles participating in the two-step process and angular distributions as well as angular correlations of scattered and Auger electrons in the final state. These general expressions can be used to derive more simple expressions applicable for the specific experimental conditions with less number of polarization states specified. Some special cases suitable for the specific conditions are studied as more simple cases of the general expression. These cases are: the angular distribution of Auger electrons following excitation of non polarized atoms by non polarized electrons, angular correlations between Auger and scattered electrons following excitation of non polarized atoms by non polarized electrons, magnetic dichroism in the angular distribution and the total cross section of Auger electrons following excitation of polarized atoms by non polarized electrons. For other experimental conditions, the expressions can be easily obtained by using the general expression derived in the present work as well.

*Keywords:* Electron-impact excitation of atoms; Angular distributions; Polarization; Auger electrons

## References

- [1] B. Cleff, W. Mehlhorn, J. Phys. B 7 (1974) 593.
- [2] A. Kupliauskienė, Lithuanian J. Phys. 44 (2004) 17.
- [3] A. Kupliauskienė, Physica Scripta 75 (2007) 524.
- [4] A. Kupliauskienė, V. Tutlys, Physica Scripta 67 (2003) 290.

# FLUORESCENCE OF POLARIZED ATOMS EXCITED BY POLARIZED ELECTRONS

A. Kupliauskienė

Institute of Theoretical Physics and Astronomy of Vilnius University, A.Goštauto 12,  
LT-01108 Vilnius, Lithuania

The radiation is an important source of the information about the processes taking part in laboratory and astrophysical plasmas. The excitation of atoms by electrons is one of the most important processes following which the fluorescence radiation is emitted. The process of the radiation with the wave vector  $\mathbf{k}_{01}$  and polarization unit vector  $\hat{\epsilon}_q$  emitted following the excitation of polarized atom  $A(\alpha_0 J_0 M_0)$  by polarized electron  $\mathbf{p}_1 m_1$  can be written as follows:

$$A(\alpha_0 J_0 M_0) + e(\mathbf{p}_1 m_1) \rightarrow A^*(\alpha_1 J_1 M_1) + e(\mathbf{p}_2 m_2) \rightarrow A(\alpha_2 J_2 M_2) + e(\mathbf{p}_2 m_2) + h\nu(\hat{\epsilon}_q \mathbf{k}_{01}).$$

In two-step approximation, the general expression of the differential cross section describing fluorescence radiation following the excitation of polarized atoms by polarized electrons can be written in the form of the expansion over the multipoles of the non registered intermediate state of an excited atom  $A(\alpha_1 J_1 M_1)$  by using the method proposed in [1] as follows:

$$\begin{aligned} & \frac{d^2\sigma(\alpha_0 J_0 M_0 \mathbf{p}_1 m_1 \rightarrow \alpha_1 J_1 \mathbf{p}_2 m_2 \rightarrow \alpha_2 J_2 M_2 \hat{\epsilon}_q \mathbf{k}_{01})}{d\Omega_e d\Omega_f} = \\ & = \sum_{K_1 N_1} \frac{d\sigma_{K_1 N_1}^{\text{ex}}(\alpha_0 J_0 M_0 \mathbf{p}_1 m_1 \rightarrow \alpha_1 J_1 \mathbf{p}_2 m_2)}{d\Omega_e} \frac{dW_{K_1 N_1}^r(\alpha_1 J_1 \rightarrow \alpha_2 J_2 M_2 \hat{\epsilon}_q \mathbf{k}_{01})}{d\Omega_f}. \end{aligned}$$

The expressions for the first and second terms are presented in [2] and [3], respectively.

The general expression is suitable to describe the polarization state as well as the angular distributions of all particles taking part in the process in both initial and final states. A number of more simple expressions suitable for the specific experimental conditions are derived as special cases of the general one. In the case of the excitation of non polarized atoms by non polarized electrons, the cross section describing the angular distribution of fluorescence radiation as well as the angular correlations between the scattered electrons and fluorescence photons are obtained. In the case of the excitation of polarized atoms by non polarized electrons, the expression describing the magnetic dichroism in the angular distribution of fluorescence radiation as well as in the total cross section are also derived. The alignment parameters of excited Na and K atoms and polarization degree of radiation from the lowest autoionizing states  $np^5(n+1)s^2 \ ^2P_{3/2}$  following the excitation of non polarized Na and K atoms by non polarized electrons are calculated. The calculated in DW approximation alignment parameters for the K atoms excited to the state  $3p^5 4s^2 \ ^2P_{3/2}$  by electrons are in good agreement with experimental data in the case of projectile electron energies greater than 50 eV.

*Keywords:* Electron-impact excitation of atoms; Angular distributions; Fluorescence

## References

- [1] A. Kupliauskienė, Lithuanian J. Phys. 44 (2004) 17.
- [2] A. Kupliauskienė, Physica Scripta 75 (2007) 524.
- [3] A. Kupliauskienė, Nucl. Instrum. Methods B 235 (2005) 252.

## MODELLING ELECTRON KINETICS IN BF<sub>3</sub>

O. Šašić<sup>1,2</sup>, Z. Raspopović<sup>1</sup>, Ž. Nikitović<sup>1</sup>, V. Stojanović<sup>1</sup> and Z. Lj. Petrović<sup>1</sup>

<sup>1</sup> Institute of Physics, POB 68, 11080 Belgrade, Serbia

<sup>2</sup> Faculty of Transport and Traffic Engineering, University of Belgrade, Belgrade, Serbia

In this paper we used the available data [1] for electron impact scattering cross sections for electrons in BF<sub>3</sub> to calculate the transport coefficients for electrons. Monte Carlo simulation was used to perform calculations calculating transport coefficients as well as rate coefficients in DC electric fields, crossed electric and magnetic DC fields and RF fields.

Cross section sets were compiled and tested against the swarm data and transport coefficients were calculated and measured for DC and RF fields [2]. We have also tested how transport coefficients are affected by the presence of radicals such as F or the molecule F<sub>2</sub>.

Calculations were performed by using our Monte Carlo technique for electron (and also ion and fast neutral) transport involving either time integration method or null collision method. Both approaches have been verified on basic swarm benchmarks [3, 4].

Our Monte Carlo simulation is initiated by 500000 electrons with the initial Maxwellian electron energy distribution function with mean energy of 1eV. Gas number density was  $3.54 \cdot 10^{22} \text{ m}^{-3}$  and phase between electric and magnetic field was  $\pi/2$ .

The presently derived set of data provides a basis for a complete plasma model implantation by using BF<sub>3</sub> containing plasmas. Such data are the foundation for development of computer aided design of plasma devices and should include: electron scattering cross sections, DC electron transport data for  $E$  and  $ExB$  fields, ion-molecule reactions and excited state collision data.

*Keywords:* BF<sub>3</sub>, transport coefficients,  $E$ ,  $ExB$  fields.

### References

- [1] S. Biagi, unpublished (2005).
- [2] O. Šašić, Z. Lj. Petrović, Z. Raspopović, L. Godet and S. Radovanov, *58th Annual Gaseous Electronics Conference*, October 16-20, 2005, San Jose, California, p.28, *Bul. Am. Phys. Soc.* 50 (7) (2005) 28 UH2 4.
- [3] Z. Raspopović, S. Sakadžić, Z. Lj. Petrović and T. Makabe, *J. Phys. D* **33** (2000) 1298.
- [4] Z. Lj. Petrović and V. D. Stojanović, *J. Vac. Sci. Technol A* **16** (1998) 329.

# STUDY OF THE ELECTRON-ELECTRON CORRELATION VIA OBSERVING THE TWO-ELECTRON CUSP

L. Sarkadi and A. Orbán

Institute of Nuclear Research of the Hungarian Academy of Sciences (ATOMKI),  
H-4001, Debrecen, Hungary

In this report we present experimental data for electron-electron correlation in atomic collisions, investigating the process of the two-electron emission with velocity vectors equal to that of the projectile. By observing the two-electron cusp the study of the threshold phenomenon for two-electron break-up is possible. It is a particularly interesting question whether the outgoing charged projectile can attract the two repulsing electrons so strongly that the two-electron cusp is formed. If it is so, a further question arises: Are the two electrons correlated as it is predicted by the Wannier theory [1]?

In our experiment, carried out at the 1.5 MV VdG accelerator of ATOMKI, the two-electron continuum states were populated in 100 keV  $\text{He}^0 + \text{He}$  collisions following the mutual ionization of the target and projectile. The process was identified in a triple coincidence measurement by the simultaneous detection of the two ejected electrons and the outgoing charge-state analyzed projectile. The energies of the electrons were determined with our new time-of-flight (TOF) electron spectrometer [2].

In Fig. 1a we present the contour plot of our measured fourfold differential cross section (FDCS). For a comparison, in Fig. 1b we display the corresponding data for *uncorrelated* electron pair emission. These latter data were synthesized artificially, generating the energies of the electron pairs by two independent double coincidence experiments. Fig. 1a clearly shows the correlation between the energies of the two electrons. In order to see whether our data reflect the  $180^\circ$  angular correlation of the electrons predicted by the Wannier theory, we carried out a Monte Carlo simulation. In the simulation we supposed that the two electrons are emitted isotropically with  $180^\circ$  angular correlation, and we took into account the detection conditions of the electrons (acceptance angles), the time resolution and the finite size of the beam and target. The results of the simulation show similar behavior of the energy sharing between the electrons as our measurement. The strong energy correlation observed in the experiment can be explained by an angular correlation of  $180^\circ$  in the projectile-centered reference system: The correlation between the low- and high-energy emission in the laboratory system corresponds to that between backward and forward emission in the projectile frame.

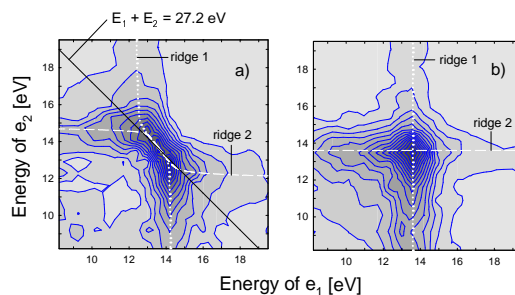


Fig. 1. Contour plots of FDCS as a function of the electron energies obtained at  $0^\circ$  in 100 keV  $\text{He}^0 + \text{He}$  collisions. Part (a): Measured FDCS. Part (b): Uncorrelated electron emission.

*Keywords:* electron correlation; electron cusp; Wannier threshold theory

## References

- [1] G. H. Wannier, Phys. Rev. 90 (1953) 817.
- [2] L. Sarkadi and A. Orbán, Meas. Sci. Technol. 17 (2006) 84-90.

# POST-COLLISION INTERACTION AFTER ELECTRON IMPACT MEASURED BY (e,2e) COINCIDENCE TECHNIQUE

B. Paripás and B. Palásthy

Department of Physics, University of Miskolc, 3515 Miskolc-Egyetemváros, Hungary

Auger electron lineshapes after electron impact inner shell ionization of argon is studied by (e,2e) coincidence technique. Emitted Auger electrons are detected in coincidence with the ionizing high energy scattered electrons. The energy of the PCI inducer low energy ejected electron is calculated from energy conservation. Regarding that the very low energy electrons can cause a significant PCI effect, the cases when the scattered electron takes nearly the whole excess energy were studied.

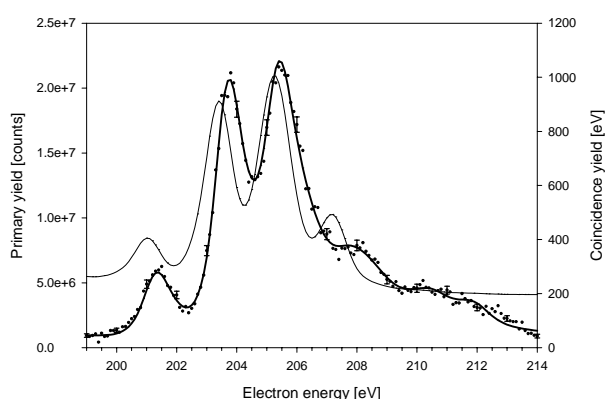


Fig. 1. The Auger electron spectrum of Ar measured in coincidence with 250 eV scattered electrons at 500 eV primary electron energy

Our previous measurements were made at 500 eV primary energy. In this case the excess energies above the ionization potentials of the  $L_3$  and  $L_2$  inner shells are 251.4 eV and 249.2 eV, respectively. At 250 eV coincidence condition (i.e. the detected scattered electrons have 250 eV energy) the PCI inducer electrons ejected from the  $L_3$  and  $L_2$  shells have 1.4 eV and -0.8 eV nominal kinetic energy, respectively. (The  $\approx 1.2$  eV energy spread (HWHM) of the analyzer system makes still possible their detection.) We found [1] good

agreement between the calculated and the experimental results, except for the near threshold intensities of the Auger peaks originating from the  $L_2$  ( $2p_{1/2}$ ) inner shell ionic state. This discrepancy is caused by the  $2p_{1/2} \rightarrow 3d$  and  $2p_{1/2} \rightarrow 4d$  inner shell excitations which produce lines (resonant Auger lines) close to the triplet diagram line at about 207 eV.

We started a more sophisticated study at lower primary energy (350 eV) where better energy resolution can be achieved. Here the excess energies (101.4 eV and 99.2 eV for the two subshells) result approximately the half energy spread of the analyzer system. Due to this we can avoid the appearance of the resonant Auger lines in the coincidence spectrum even in the vicinity of the threshold. Without these disturbing lines the effect of PCI can be more precisely evaluated.

*Keywords:* (e,2e) experiment, Argon, PCI

## References

- [1] B. Paripás, B. Palásthy, G. Vitéz and Z. Berényi, J. Phys. B: At. Mol. Phys. 41 (2008) 035201.

## INTERPLAY OF INITIAL AND FINAL STATES FOR $(e, 3e)$ AND $(\gamma, 2e)$ PROCESSES ON HELIUM

**L.U. Ancarani<sup>a</sup>, G. Gasaneo<sup>b</sup>, F.D. Colavecchia<sup>c</sup> and C. Dal Cappello<sup>a</sup>**

<sup>a</sup>Laboratoire de Physique Moléculaire et des Collisions,  
Université Paul Verlaine - Metz, 57078 Metz, France

<sup>b</sup>Departamento de Física, Universidad Nacional del Sur and CONICET,  
8000 Bahía Blanca, Buenos Aires, Argentina

<sup>c</sup>Centro Atómico Bariloche and CONICET, 8400 S. C. de Bariloche, Río Negro,  
Argentina

The theoretical study of the double ionization of helium by electron impact ( $(e, 3e)$  experiments) allows one to gain information on correlated systems [1]. Since no exact wave function is known for either the scattering or the bound states, approximate wave functions are used, and  $(e, 3e)$  cross sections on helium obtained with different theoretical description of the initial and final states are not in agreement with each other. Moreover, when these are compared with absolute experimental data, a rather confusing picture emerges; this is the subject of many recent studies (as discussed and summarized in [2]). It has been mentioned throughout the literature (see, e.g., [3]) that a balanced description of the initial and final two-electron states may play a key role in reproducing experimental  $(e, 3e)$  data. This issue is investigated here with a systematic study of double ionization cross sections of helium, by both electron and photon impact.

For  $(e, 3e)$  processes, calculated differential cross sections can be compared with the high energy absolute experimental data [4]. The two electrons ejected in the final channel at equal energy (10 eV) are modeled here with the "pure" C3 (or BBK) wave function [5]. For the initial channel we consider different sets of double bound wave functions with only angular correlation or with both angular and radial correlation. The comparison with the measurements allows us to see which of them are balanced when describing  $(e, 3e)$  processes. Moreover, the photon impact  $(\gamma, 2e)$  cross sections calculated in different gauges and with the same set of initial and final channel wave functions, indicate whether the wave functions are really "balanced" or not.

Our study of the  $(\gamma, 2e)$  gauge discrepancies shows that the agreement with absolute  $(e, 3e)$  experimental data at 10+10 eV ejected energy obtained with simple initial states is fortuitous and can hardly be attributed to a balanced description with respect to the final state. This result is further confirmed by an investigation of the ejected energy dependence. Moreover, it seems that the approximate C3 wave function is not suitable to describe sufficiently well the double continuum of two electron ejected at 10 eV.

Finally, new theoretical studies and experimental data are clearly needed to help understanding the interplay of initial and final states in double ionization processes.

*Keywords:*  $(e, 3e)$ ;  $(\gamma, 2e)$ ; correlation

### References

- [1] J. Berakdar, A. Lahmam-Bennani and C. Dal Cappello Phys. Rep. **374** (2003) 91
- [2] L.U. Ancarani, G. Gasaneo, F.D. Colavecchia and C. Dal Cappello, submitted to Phys. Rev. A
- [3] J. H. Macek and S. Jones, Rad. Phys. and Chem. **75** (2006) 2206
- [4] A. Lahmam-Bennani *et al.*, Phys. Rev. A **59** (1999) 3548
- [5] C. R. Garibotti and J. E. Miraglia, Phys. Rev. A **21** (1980) 572; M. Brauner, J. Briggs and H. Klar, J. Phys. B **22** (1989) 2265

## NEAR-THRESHOLD EXCITATION OF THE RESONANCE $\lambda$ 158.6 nm LINE IN ELECTRON-INDIUM ION COLLISIONS

A. Gomonai, A. Imre, E. Ovcharenko, Yu. Hutyach

Institute of Electron Physics, Ukrainian National Academy of Sciences,  
21 Universitetska str., 88017 Uzhgorod, Ukraine

A deeper understanding of the physics of resonance processes taking place in complex multi-electron ions requires precise experimental studies, the results of which have applied significance and stimulate the further development of theoretical calculation methods as well.

Here we report on the observations of the resonance phenomena in the electron-impact excitation of the  $\lambda$  158.6 nm resonance line ( $5s5p\ ^1P^{\circ}_1 \rightarrow 5s^2\ ^1S_0$ ) in single-charged indium ion. The experiment was carried out by a photon spectroscopy method using a crossed electron and ion beam technique, which allows the detailed studies to be performed with the energy resolution  $\Delta E_{1/2} \sim 0.4$  eV. The specific features of the experimental technique for studying the processes occurring at the inelastic slow electron collisions with indium ions are described in details in [1].

Precise studies of near-threshold area of the energy dependence of effective electron excitation cross section for the  $\lambda$  158.6 nm resonance line reveal distinct resonance features both below and above the excitation threshold (see Fig.1). The analysis of the data with electron configurations and energy positions of indium atom autoionizing states (AIS) [2,3] being taken into account has shown that the features below the threshold are mainly due to the radiative decay of the  $5s5p(^1P^{\circ}_1)nl$  AIS into the bound  $5s^2(^1S_0)nl$  levels of indium atom in the dielectronic recombination process.

As seen from Fig.1, the process of radiative decay of AIS, which is commonly neglected in theoretical calculations, results in deformation of the ascendant area of the energy dependence of the effective excitation cross section at the threshold and in the decrease of its value close to the threshold.

A complicated electron structure of indium ion leads to the fact that the structural features above the excitation threshold of the  $5s5p\ ^1P^{\circ}_1$  level result from a combination of multi-step processes due to the cascade transitions from the ionic levels and from the averaged contribution of multiple series of mixed atomic AIS.

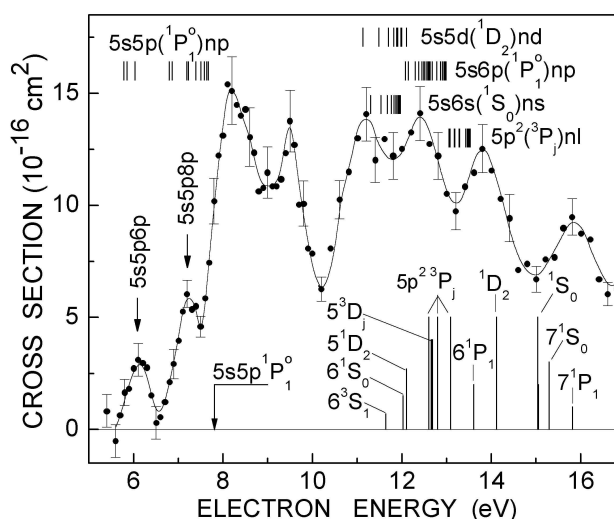


Fig. 1. Energy dependence of the near-threshold electron-impact excitation cross section for  $\text{In}^+$  resonance line

As seen from Fig.1, the process of radiative decay of AIS, which is commonly neglected in theoretical calculations, results in deformation of the ascendant area of the energy dependence of the effective excitation cross section at the threshold and in the decrease of its value close to the threshold.

A complicated electron structure of indium ion leads to the fact that the structural features above the excitation threshold of the  $5s5p\ ^1P^{\circ}_1$  level result from a combination of multi-step processes due to the cascade transitions from the ionic levels and from the averaged contribution of multiple series of mixed atomic AIS.

*Keywords:* Electron; Indium Ion; Excitation; Dielectronic Recombination; Autoionizing States

### References

- [1] A.Gomonai, E.Ovcharenko, A.Imre, Yu.Hutyach, Nucl. Instr. and Meth. in Phys. Res. **B** 233 (2005) 250 – 254.
- [2] M.Aslam Baig, Ishaq Ahmed, J.P.Connerade, J. Phys. B: At. Mol. Opt. Phys. **21** (1988) 35 – 46.
- [3] D Kilbane, J-P Mosnier, E T Kennedy, J T Costello, P van Kampen, J. Phys. B: At. Mol. Opt. Phys. **39** (2006) 773–782.

## MECHANISM INVESTIGATION IN COLLISION OF CLOSED ELECTRON SHELL ATOMIC PARTICLES

**R.Lomsadze, M. Gochitashvili, B.Lomsadze, N.Tsiskarishvili, O.Taboridze.**

Tbilisi State University, Department of Exact and Natural Sciences, Georgia.

In the present work absolute cross sections for charge exchange, ionization, stripping and excitation have been measured for  $K^+$  ions colliding with He and Ne atoms at laboratory energies of 0.7 – 10 keV. The experimental techniques include condenser plate methods, angle- and energy-dependent collection of product ions, energy-loss and optical spectroscopy. The experimental data and the rules of constructing the correlation diagram are used to discuss the detailed mechanisms in these collisions. It is shown that in each case the charge exchange is caused by capture of an electrons to the ground state of the atom. In  $K^+$  He collisions, corresponding quasimolecular terms are populated through  $^1\Sigma - ^1\Sigma$  transitions in nonadiabatic regions. An interaction of inelastic channels gives rise structural features on the energy dependence of the cross sections. The contributions made by the various processes to the total cross sections of an electron emission in these collisions are estimated. It was found that the ionization mechanism involves the filling of quasimolecular autoionization terms, which decay in the stage in which the quasimolecule exists. The stripping in  $K^+$  - He collisions occurs by a mechanism involving transition of a diabatic term into the continuum. The increase of the excitation probability of inelastic channels at the energy loss spectrum, with increasing the angle of scattering incident ions is revealed. Anomalously small and significantly large value of the excitation cross section for the potassium atom and ion respectively, a structural peculiarity for the excitation function of resonance helium atomic line are explained.

Keywords: charge exchange, ionization, excitation.



## INNER-SHELL PHOTODETACHMENT OF IRON AND RUTHENIUM NEGATIVE IONS

I. Dumitriu<sup>a</sup>, René C. Bilodeau<sup>a,b</sup>, T. Gorczyca<sup>a</sup>, G. Ackerman<sup>a</sup>, C. W. Walter<sup>c</sup>,  
N. D. Gibson<sup>c</sup>, A. Aguilar<sup>b</sup>, Z. Pesic<sup>a,b</sup>, D. Rolles<sup>a,b</sup>, and N. Berrah<sup>a</sup>

<sup>a</sup>*Department of Physics, Western Michigan University, Kalamazoo, Michigan 49008, USA*

<sup>b</sup>*Lawrence Berkeley National Laboratory, Advanced Light Source, Berkeley, California 94720*

<sup>c</sup>*Department of Physics and Astrophysics, Denison University, Granville, OH 43023, USA*

Transition metals are of interest for their catalytic properties and participation of d-orbital electrons in the bonding properties [1]. The analysis of transition metals is of wide application in oceanography, cosmochemistry, and geology.

Iron is one of the most abundant terrestrial elements with an important position in technology. Its fundamental physics is interesting but hard to describe due to a large number of possible terms resulting from the approximately half-open 3d-shell [2]. Ruthenium is of interest in that some of its complexes efficiently convert solar energy into chemical energy by photoinduced electron transfer [3].

The first inner-shell photodetachment studies in Fe<sup>-</sup> and Ru<sup>-</sup> conducted using the Ion Photon Beamline (IPB) on ALS beamline 10.0.1 at Lawrence Berkeley National Laboratory will be presented. The negative ions extracted from the SNICS ion source are mass selected and merged collinearly with the photon beam. Inner-shell photodetachment and subsequent Auger decay [4] produce positive ions which are detected as a function of photon energy over a range of 48 to 72 eV. Excitations from p-electrons to open d-shells were carried out in both Fe<sup>-</sup> and Ru<sup>-</sup>. Two shapes resonances were observed in Fe<sup>-</sup> and no clear resonance was observed in Ru<sup>-</sup>. The absolute cross-section for the production of Fe<sup>+</sup> and Ru<sup>+</sup> will also be presented.

Keywords: atomic negative ions; inner-shell; photodetachment

### References

- [1] For recent reviews, see for example: M. Martins *et al.*, J. Phys. B **39** (2006) R79; T. Andersen Phys. Rep. **394** (2004) 157; J.C.Rienstra-Kiracofe *et al.*, Chem.Rev. **102** (2002) 231.
- [2] B. W. Whitfield, R. Wehlitz, and M. Martins, Rad. Phys. Chem. **70** (2004) 3; K. A. Berrington, C. Balance, J. Phys. B **34** (2001) 2697; S. N. Nahar, A. Pradhan, Astron. Astrophys. **119** (1996) 509.
- [3] G. Sprintschink, H. Sprintschink, P. Kirsch, and D. G. Whitten, J. Am. Chem. Soc. **98** (1976) 2337.
- [4] H. Kjeldsen, *et al.*, J.Phys.B **39** (2006) R325; H. Kjeldsen, *et al.*, J.Phys.B **34** (2001) L353 ; A.M.Covington *et al.*, J.Phys.B **34** (2001) L735; N.Berrah *et al.*, Phys.Rev.Lett **87** (2001) 253002.

## GENERALIZED OSCILATOR STRENGTHS FOR ELECTRON SCATTERING BY In ATOM AT SMALL ANGLES

**M. S. Rabasović<sup>a</sup>, S. D. Tošić<sup>a</sup>, V. Pejčev<sup>a,b</sup>, D. Šević<sup>a</sup>, D. M. Filipović<sup>a,c</sup> and  
B. P. Marinković<sup>a</sup>**

<sup>a</sup>Laboratory for Atomic Collision Processes, P. O. Box 68, 11080 Belgrade, Institute of  
Physics, Serbia

<sup>b</sup>Faculty of Natural Sciences, Radoja Domanovića 12, Kragujevac, University of Kragujevac,  
Serbia

<sup>c</sup>Faculty of Physics, P.O. Box 368, 11001 Belgrade, University of Belgrade, Serbia

We present results of measurements of generalized oscillator strengths (GOS) for the  $^2P_{1/2} - ^2S_{1/2}$  resonant transition of indium atom. Absolute values of GOS for the  $^2S_{1/2}$  state of the indium atom are shown in Fig. 1 as a function of  $K^2$  together with forward scattering function (FSF) for indium. The normalization has been achieved through displacing each data set of experimental GOS down until its  $\theta=0^\circ$  point intersect the FSF( $K^2$ ) curve. We have used the (FSF) method introduced by Avodina et al. [1].

In this experiment we employed an electron spectrometer in crossed electron-atom beam arrangement. The experimental set-up consists of an oven, electron monochromator and analyzer situated in high-vacuum chamber. Indium vapor beam was produced by heating the oven crucible containing In metal (99,9% purity). Working temperature was approximately 1300 K and the metal-vapor pressure was about 10 Pa (0.07 Torr). For this experiment we made modifications on the design of the oven in order to achieve higher temperatures. External overheating was avoided by additional water cooling. These measurements were carried out for scattered electrons that had lost 3.025 eV ( $6s^2S_{1/2}$  state) at each 2 degrees from  $-10^\circ$  to  $+10^\circ$ . The angular scale was corrected for zero position. Then, angular dependencies of the scattering signal were multiplied by effective path length correction factors to get relative differential cross sections (DCS). We have applied the correction factors of Brinkman and Trajmar [4], modified for our experimental conditions.

Keywords: Generalized Oscillator Strengths, Differential Cross Sections.

### References

- [1] N. B. Avodina, Z.Felfli, A. Msezane, J. Phys. B: At. Mol. Opt. Phys. **30** (1997) 2591.
- [2] S. Milisavljević, M. S. Rabasović, D. Šević, V. Pejčev, D. M. Filipović, Lalita Sharma, Rajesh Srivastava, A. D. Stauffer and B. P. Marinković, Phys. Rev. A **75** (2007) 052713.
- [3] B. P. Marinković, V. Pejčev, D. M. Filipović, D. Šević, S. Milisavljević, and B. Predojević, Radiat. Phys. Chem. **76** (2007)455.
- [4] R. T. Brinkman and S. Trajmar, J. Phys. E,Sci Instrum. **14** (1981) 245.

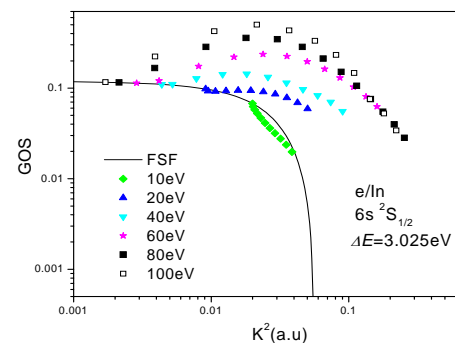


Fig 1. Generalized oscillator strengths for the  $6s^2S_{1/2}$  state of indium atom at 10, 20, 40, 60, 80 and 100eV impact energies.

## ELASTIC ELECTRON SCATTERING BY SILVER ATOMS

**S. D. Tošić<sup>a</sup>, V. I. Kelemen<sup>d</sup>, D. Šević<sup>a</sup>, V. Pejčev<sup>b</sup>, D. M. Filipović<sup>c</sup>,  
E. Yu. Remeta<sup>d</sup> and B. P. Marinković<sup>a</sup>**

<sup>a</sup>Laboratory for Atomic Collision Processes, Pregrevica 118, 11080 Belgrade, Institute of Physics, Serbia

<sup>b</sup>Faculty of Natural Sciences, Radoja Domanovića 12, 34000 Kragujevac, University of Kragujevac, Serbia

<sup>c</sup>Faculty of Physics, P. O. Box 368, 11001 Belgrade, University of Belgrade, Serbia

<sup>d</sup>Institute of Electron Physics, Universitetska 21, 88017 Uzhgorod, Ukraine

Elastic electron scattering by silver atom has been investigated both experimentally and theoretically. Differential cross sections (DCSs) have been obtained in the intermediate impact electron energy range from 10 to 100 eV. The experimental method used to determine DCS is based on crossed beam technique where effusive atomic beam is perpendicularly crossed by monochromatic electron beam [1]. The well collimated effusive Ag vapour beam has been produced by heating oven crucible containing silver atoms by two resistive bifilar heaters. The elastically scattered electron intensities are detected as a function of scattering angle ranging from  $10^\circ$  to  $150^\circ$  and then converted to relative DCSs using the effective path length correction factors [2] determined for the present experimental conditions. The overall system energy resolution was 140 meV and the angular resolution was estimated to be  $1.5^\circ$ .

Corresponding theoretical results were obtained using the complex optical potential (OP) with the inclusion of spin-orbit interaction. The real part of this potential consists of static, local exchange, polarization and spin-orbit potentials [3]. The imaginary part of OP takes into account the absorption effects [4]. We have obtained DCSs values using two different approaches, i.e. calculations with (*SEPASo*-approximation) and without (*SEPSo*-approximation) absorption [3,4].

In Fig.1 our relative experimental DCS results at 100 eV impact electron energy are normalized at scattering angle of  $40^\circ$  to the present *SEPASo* calculations and presented with DCSs calculated using both *SEPASo*- and *SEPSo*-approximations. Other details as well as DCS results at 10, 20, 40, 60 and 80 eV will be presented at the conference.

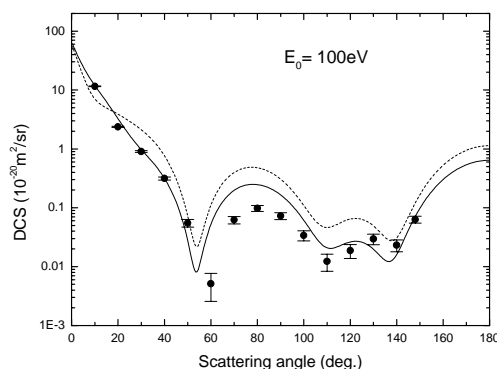


Fig. 1. Differential cross sections for the elastic electron scattering by silver atom at 100 eV incident electron energy: ●, experiment; —, *SEPASo*- approximation; - - - - - , *SEPSo*-approximation.

**Keywords:** Differential cross sections; Elastic scattering; Silver

### References

- [1] S. D. Tošić, M. S. Rabasović, D. Šević, V. Pejčev, D. M. Filipović, Lalita Sharma, A. N. Tripathi, Rajesh Srivastava, B. P. Marinković, Phys. Rev. **A77** (2008) 012725.
- [2] R. T. Brinkmann, S. Trajmar, J. Phys. **E 14** (1981) 245.
- [3] V. I. Kelemen, M. M. Dovhanych, E. Yu Remeta, J. Phys. B: At. Mol. Opt. Phys. **41** (2008) 035204.
- [4] A. R. Milosavljević, V. I. Kelemen, D. M. Filipović, S. M. Kazakov, V. Pejčev, D. Šević, B. P. Marinković, J. Phys. B: At. Mol. Opt. Phys. **38** (2005) 2195.

## ELASTIC ELECTRON SCATTERING BY Zn, Cd AND Hg ATOMS IN THE OPTICAL POTENTIAL APPROACH

V. Kelemen, M. Dovhanych and E. Remeta

Institute of Electron Physics, 21 Universitetska str, Uzhgorod, Ukraine

In the optical potential approach [1] the influence of two different parameter-free polarization potentials Vp1 [2] and Vp2 [3] on the values of differential (DCS) and integral elastic cross sections is investigated for electron scattering by Zn, Cd and Hg atoms. The results of calculations are compared with the experimental and theoretical data. In figures these cross sections are presented. For Cd atom the relative experimental data from [6] are normalized at scattering angle of 20° to present DCSs calculated with potential Vp1.

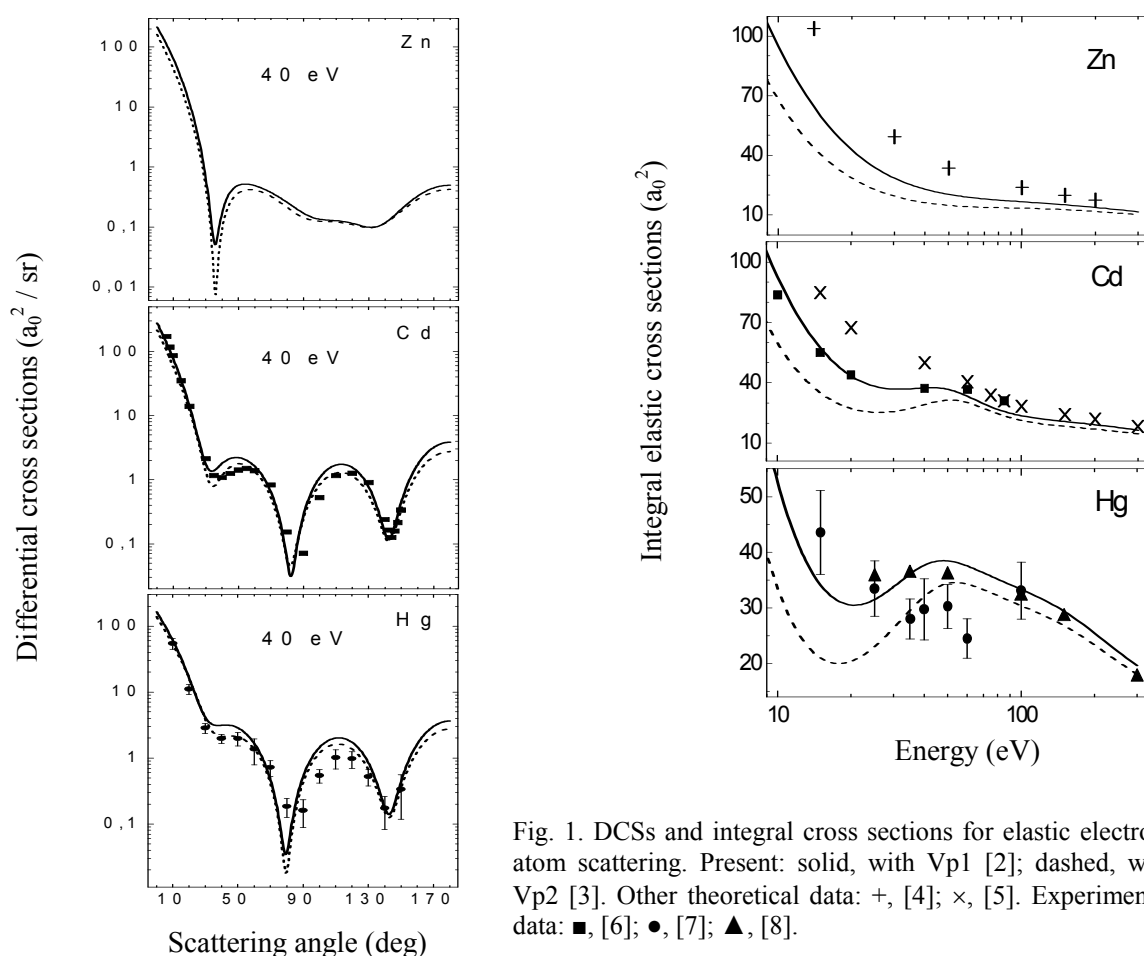


Fig. 1. DCSs and integral cross sections for elastic electron-atom scattering. Present: solid, with Vp1 [2]; dashed, with Vp2 [3]. Other theoretical data: +, [4]; ×, [5]. Experimental data: ■, [6]; ●, [7]; ▲, [8].

*Keywords:* Cross section; optical potential; electron scattering

### References

- [1] V. Kelemen, E. Remeta, E. Sabad, *J. Phys. B* **28** (1995) 1527.
- [2] J. O'Connell, N. Lane, *Phys. Rev.* **A27** (1983) 1893.
- [3] N. Padial, D. Norcross, *Phys. Rev.* **A29** (1984) 1742.
- [4] P. Kumar, A. Jain, A. Tripathi, S. Nahar, *Phys. Rev.* **A49** (1994) 899.
- [5] S. Nahar, *Phys. Rev.* **A43** (1991) 2223.
- [6] B. Marinković, V. Pejčev, D. Filipović, L. Vušković, *J. Phys. B* **24** (1991) 1817.
- [7] R. Panajotović, V. Pejčev, M. Konstantinović, D. Filipović, B. Marinković, *J. Phys. B* **26** (1993) 1005.
- [8] G. Holtkamp, K. Jost, F. Peitzmann, J. Kessler, *J. Phys. B* **20** (1987) 4543.

## COLLISIONS IN TERMS OF QUANTUM TRAJECTORIES

M. Acuña<sup>†</sup>, and J. Fiol<sup>\*‡</sup>

División Colisiones Atómicas, Centro Atómico Bariloche, S. C. de Bariloche, Argentina

<sup>\*</sup> Consejo Nacional de Investigaciones Científicas y Técnicas (CONICET), Argentina.<sup>†</sup>E-mail: *acunam@ib.cnea.gov.ar*      <sup>‡</sup>E-mail: *fiol@cab.cnea.gov.ar*

Recently there have been renewed interest in the resolution of Quantum-Mechanical problems by means of the so-called “Quantum Trajectories Method” (QTM) [1, 2, 3]. This approach, based in Bohm’s formulation of Quantum Mechanics [4, 5], describe the quantum dynamics in term of pseudo-particles that evolve obeying equations similar to those of Classical-Mechanics. While this treatment in terms of trajectories represents a full solution of the Time-Dependent-Schrödinger Equation (TDSE), the main drawback is due to the strong coupling among trajectories and the unstability of some of the resulting equations [3]. However, its scalability characteristics, through parallel implementations and Monte Carlo methods, make the quantum trajectory approach a promising field for the investigation of many-particle collision processes.

In this communication we present some benchmark calculations of ion-atom collision models employing several level of approximations to the quantum trajectory method. In particular, we implemented and systematically investigated a method suggested a few years ago to circumvent the problems arising from the strong coupling among the trajectories [6]. The resulting equations, derived from rewriting the de Broglie-Bohm equations, uncouple the quantum trajectories, allowing us to solve each of them individually. Each trajectory becomes the solution of a system of infinite coupled differential equations that can be solved at different levels of approximation.

*Keywords:* Quantum Mechanics; Bohm; Quantum Trayectory; Ion-Atom Collisions

**References**

- [1] C. L. Lopreore, R. E. Wyatt Phys. Rev. Lett. 82 (1999) 5190.
- [2] C. J. Trahan, K. Hughes, R. E. Wyatt J. Chem. Phys. 118 (2003) 9911.
- [3] R. E. Wyatt Quantum Dynamics with Trajectories vol. 28 of *Interdisciplinary Applied Mathematics* Springer (2005).
- [4] L. de Broglie C. R. Acad. Sci. Paris 184 (1927) 273.
- [5] D. Bohm Phys. Rev. 85 (1952) 166.
- [6] J. Liu, N. Makri J. Phys. Chem. A 108 (2004) 5408.

## THEORETICAL AND EXPERIMENTAL INVESTIGATIONS OF ELECTRON EMISSION DURING WATER IONIZATION BY LIGHT ION IMPACT

**C. Champion, H. Lekadir and C. Dal Cappello**

*Laboratoire de Physique Moléculaire et des Collisions, ICPMB (FR2843),  
Institut de Physique, Université Paul Verlaine-Metz, 1 Boulevard Arago,  
57078 Metz Cedex 3, France*

Ionization of atoms and molecules by fast charged particles is of prime importance in a large number of areas including plasma physics, radiation physics and the study of penetration of charged particles through matter. It has also been shown that experimental and theoretical data about the ionization of biological systems are needed in fundamental studies of charged particle interaction in biological matter (and more precisely in heavy-ion cancer therapy [1]). Moreover with the more and more regular use of ionizing radiations in medicine, it is today necessary to appraise the biological consequences of radiological examinations particularly to know, with the highest degree of accuracy, the energy deposits induced by all the radiations commonly used in radiotherapy and even in medical imaging (light and heavy ions, electrons and positrons, X-rays and  $\gamma$ -rays).

To describe the track-structure of a charged particle in the biological matter and then to quantify the full spectra of molecular damage radio-induced, Monte Carlo simulation is the preferential method. This latter consists in simulating, interaction after interaction, the history of each ionizing particle created during the irradiation of the biological matter. In this kind of study, all the projectile-target interactions are modelled by means of a large set of multi-differential and total cross sections to describe the complete kinematics of the collisions.

We present in this work both doubly, singly differential and total cross sections for the direct ionization of water vapour by light ions (protons, alpha particles and Carbon ions). An ab-initio calculation has been made by using the first Born approximation and an accurate molecular wave function proposed by Moccia [2]. The results of this model are compared to experimental data and to results obtained via semi-empirical models and a good agreement is generally observed [3, 4].

### References

- [1] T. Nakano *et al.*, *Cancer J. Sci. Am.* **5** (1999) 369.
- [2] R. Moccia, *J. Chem. Phys.* **40** (1964) 2186.
- [3] O. Boudrioua *et al.*, *Phys. Rev. A.* **75** (2007) 022720.
- [4] C. Champion *et al.*, *Phys. Rev. A.* **75** (2007) 032724.

# ELECTRONIC RELATIVISTIC EFFECT IN BINARY-ENCOUNTER APPROXIMATION FOR ION-ATOM COLLISIONS

Takeshi Mukoyama

Kansai Gaidai University,  
16-1 Nakamiya-Higashinocho, Hirakata, Osaka, 573-1001, Japan

The classical binary-encounter collision theory has been successfully applied to inner-shell ionization processes in ion-atom collisions. It is well known that the calculated ionization cross section is quite sensitive to the choice of assumed electron momentum distribution in the target atom.

In most theoretical calculations, the nonrelativistic electron momentum distributions have been obtained as the Fourier transform of the hydrogenic wave functions or the atomic wave functions with the Hartree-Fock-Roothaan model (HFR). The latter method is especially useful for this purpose, because realistic electron wave functions in the atom can be expressed in terms of Slater-type of orbitals (STO's) and their Fourier transforms can be given analytically.

Since all these calculations are nonrelativistic, it is interesting to study the electronic relativistic effect by the use of relativistic wave functions in the BEA. However, there has been reported only one theoretical calculations with the relativistic electron momentum distribution in the BEA. Kumar et al. [1] calculated the K- and L-shell ionization cross sections for proton and  $\text{He}^+$  impact on Au by the use of the electron momentum distributions based on the relativistic HFR (RHFR) model [2].

In the present work, we use the Dirac-Fock program [3] to obtain the relativistic atomic wave functions numerically and these wave functions are fitted to the sum of STO's by the use of the genetic algorithm [4]. The analytical expressions for relativistic electron momentum wave functions are obtained by means of the Fourier-Bessel transformation [2]. The inner-shell ionization cross sections are calculated with the expressions of Vriens in the BEA using the electron momentum distributions obtained above. The results are compared with the BEA cross sections with the nonrelativistic hydrogenic and the HFR models, the relativistic hydrogenic model and with the experimental data. The electronic relativistic effect in the BEA is discussed.

*Keywords:* Binary-Encounter Approximation; Electronic relativistic effect; Dirac-Fock method

## References

- [1] A. Kumar, S. N. and B. N. Roy, *Pramana – J. Phys.* 34 (1990) 447.
- [2] T. Mukoyama and T. Kagawa, *J. Phys. B: At. Mol. Phys.* 16 (1983) 1875.
- [3] J. P. Desclaux, *Comput. Phys. Commun.* 9 (1975) 31.
- [4] D. A. Goldberg, *Algorithms in Search of Optimization and Machine Learning*, Addison-Wesley, Reading, MA (1989).
- [5] L. Vriens, *Proc. Roy. Phys.* 90 (1967) 935.

## INNER-SHELL IONIZATION IN ION-ATOM COLLISIONS AT MeV/u ENERGIES

M.M. Gugu, C. Ciortea, A. Enulescu, I. Piticu, D.E. Dumitriu,  
D. Fluerașu, A.C. Scafes, M.C. Pentia, C. Ciocarlan, and M.D. Pena

Department of Nuclear Physics - Tandem,  
“Horia Hulubei” National Institute of Physics and Nuclear Engineering (NIPNE),  
Atomistilor St. 407, P.O.Box MG-6 Magurele, 077125 Bucharest, Romania

Energetic atomic collisions, produced by light and heavy ions for a large domain of energies and collision systems, lead to inner-shell ionization and deexcitation processes.

The purpose of this work was to examine some characteristic features associated with the K and L-vacancy production in light ion-atom collisions, like inner-shell perturbation [1], intra-shell coupling [2] and multiple ionization effects (see e.g. [3]). The experiments have been performed at the Van de Graaff tandem accelerator of NIPNE, Bucharest, at rather low projectile energies, in the range of 0.5 – 2.5 MeV/u, where these effects are important.

For two collision systems,  $^{16}\text{O} + \text{Ag}$  and  $^{32}\text{S} + \text{Pt}$ , by using measured integral X-ray yields, the K- and L-shell ionization cross sections have been determined. The induced changes in the fluorescence yields and relative decay widths by the multiple ionization of the outer shells were considered for computation of inner-shell vacancy production cross sections. Mean ionization probabilities per electron of the outer shells have been estimated. Comparison of the experimental data with some model calculations will be presented.

*Keywords:* inner-shell ionization, X-ray yields

### References

- [1] W. Brandt and G. Lapicki, Phys. Rev. A 23 (1981) 1717
- [2] L. Sarkadi and T. Mukoyama, J. Phys. B 14 (1981) L255
- [3] C. Ciortea, I. Piticu, D. Fluerașu, D.E. Dumitriu, A. Enulescu, M.M. Gugu, A.T. Radu, and L.C. Penescu, Nucl. Instrum. Methods Phys. Res. B 235 (2005) 342



# A SETUP FOR ELECTRON-ION COLLISIONS STUDIES EMPLOYING HIGH-RESOLUTION ELECTRON SPECTROSCOPY

**K. Holste<sup>a</sup>, S. Schippers<sup>a</sup>, A. Müller<sup>a</sup> and S. Ricz<sup>b</sup>**

<sup>a</sup>Institute for Atomic and Molecular Physics, Giessen, Germany

<sup>b</sup>Institute of Nuclear Research of the Hungarian Academy of Sciences, Debrecen, Hungary

Experimental investigations of electron-ion collisions are challenging since the particle densities that can be obtained in charged particle beams are orders of magnitude lower than those available in e.g. neutral gas jets or solid targets. Nevertheless, the reaction cross-sections of electron-ion interaction are routinely measured nowadays with applying of crossed and merged beams arrangements [1]. In these experiments the high directionality of the ion beam is employed for the efficient detection of the heavy reaction products.

An experimental arrangement is worked out for the high-resolution spectroscopy of the energy and angular distribution of emitted electrons from electron-ion collisions. To this end a crossed electron-ion beams experiment has been built in Giessen at the Institute of Atomic and Molecular Physics [2]. The main part of the experimental setup is the ESA-22G electrostatic electron spectrometer that was developed at the Institute of Nuclear Research of the Hungarian Academy of Sciences (Debrecen, Hungary [3, 4]). The electrons that emerge from the crossed-beams interaction volume are focussed by a spherical mirror condenser with  $2\pi$ -detection geometry ( $\sim 1\%$  solid angle) to the ring shape entrance slit of the second stage. In the second stage their energy is determined by a cylindrical mirror analyzer with variable energy resolution. The energy and angular distributions of the electrons are simultaneously recorded with a position sensitive micro-channelplate detector.

First results for elastic scattering of electrons from  $\text{Cs}^+$  ions have already been obtained and will be presented (Fig. 1). In the future we will concentrate on electrons that arise from indirect pathways of electron-impact ionization and that are fingerprints of many-electron phenomena in electron-ion collision processes [5].

*Keywords:* electron spectroscopy; electron-atom collision; electron-ion-collision

## References

- [1] A. Müller, Adv. in Atomic, Molecular and Optical Physics, **55**, 293-417 (2008)
- [2] K. Holste, Diploma Thesis (Giessen, 2006)
- [3] D. Varga et al., Nucl. Instrum. Methods A **313**, 163 (1992).
- [4] S. Ricz et al., Phys. Rev. A **65**, 042707 (2002).
- [5] A. Müller, Nucl. Instrum. Methods B **233**, 141 (2005).

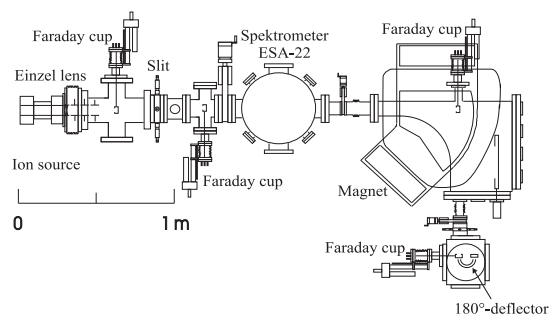


Fig. 1. Crossed-beams experiment at the IAMP

**PULSE HEIGHT DISTRIBUTION MEASUREMENTS  
ON POLYCRYSTALLINE CVD-DIAMOND  
WITH HEAVY IONS AT ENERGIES OF 11 MeV/u AND 50 MeV/u**

A. Braeuning – Demian<sup>a</sup>, D. Fluerasu<sup>b</sup>, D. Dumitriu<sup>b</sup>

<sup>a</sup>GSI, Planckstrasse 1, 64291 Darmstadt, Germany

<sup>b</sup>IFIN-HH, Atomistilor 407, 077125 Bucharest-Magurele, Romania

The detection of highly charged heavy ions in atomic physics experiments at intermediate energies in the range of few MeV/u to 100 MeV/u is still a challenging task. Due to the reduced range of such ions in matter, a windowless detection device is needed for position sensitive detection of the ions which will be mostly stopped in the detector. The high amount of energy deposited in the detector paired with high beam intensities creates extreme working conditions which request a fast, radiation hard detection device.

An impressive amount of work performed in the last decade demonstrated that diamond offers new possibilities for fast, radiation hard detection devices for charged particles, photons and neutrons. The main characteristics such as the high electron hole mobility, high band gap and in particular the radiation hardness, recommend it for detector fabrication [1]. The polycrystalline CVD material available today in large size and at affordable price could be a good candidate. However, it was shown that due to the particular structure of the material, the detection devices present a relative non stability during the operation. This instability is clearly correlated to the existence of deep traps in the material, which need to be filled, in order to improve the detection properties.

For the particular case of heavy ions stopped in the detector bulk, an additional effect shows up: internal polarization [2] induced by the large amount of charge created inside the detector by the stopped ions. This charge will counterbalance the bias field applied on the detector and the result is a reduction of the signal on the detector electrodes.

The aim of the present study is to investigate in what extent the polycrystalline diamond is a suitable material for high efficiency, high count rate, position sensitive detector for highly charged heavy ions in the energy range mentioned above.

For this, measurements of pulse height distribution were performed at UNILAC and SIS accelerators at GSI-Darmstadt, using very heavy projectiles as Xe, Pb and U at 11.4 MeV/u and 50 MeV/u on polycrystalline CVD samples with different thicknesses. The measurements show a strong dependence of the detector response, at these energies, on the material quality and thickness. In contrary, the value of the bias voltage seems to have a smaller importance.

The results obtained indicate that the bulk polarization occurs and its influence on the detection efficiency can be observed and estimated. However this material still remains a competitive candidate for the detection of highly charged ions in hard radiation conditions.

*Keywords:* highly charged ions detection; polycrystalline diamond; polarization

#### References

- [1] W. Adam, E. Berdermann, P. Bergonzo, W. Boer et al. Eur. Phys. Journal C 33 (2004) 1014
- [2] M. Marinelli, E. Milani, A. Paolett, A. Tucciaronea G. Verona Rinati, M. Angelone, M. Pillon, Nucl. Instr. Meth. Phys. Res.A 476 (2002) 701

## PRODUCTION OF MOLECULAR HYDROGEN IONS FROM C<sub>2</sub>H<sub>4</sub> AND C<sub>2</sub>H<sub>6</sub> UNDER ELECTRON CAPTURE AND LOSS COLLISIONS OF 2MeV Si IONS

**Akio Itoh<sup>a,b</sup>, Takahiro Yamada<sup>a</sup>, Tomoya Mizuno<sup>a</sup>, Hidetsugu Tsuchida<sup>b</sup>**

<sup>a</sup>Department of Nuclear Engineering, Kyoto University, Kyoto 606-8501, Japan

<sup>b</sup>Quantum Science and Engineering, Kyoto University, Kyoto 606-8501, Japan

Collision-induced molecular fragmentation by energetic charged particles has attracted considerable attention in various research fields ranging from physics to radiation biomedicine. Although a number of investigations have been carried out using sophisticated coincidence techniques, the formation mechanism of specific molecular ions such as molecular hydrogen is still less understood so far. In this work, we investigate the formation mechanism of molecular hydrogen ions from hydrocarbon molecules (C<sub>2</sub>H<sub>4</sub>, C<sub>2</sub>H<sub>6</sub>) bombarded by 2 MeV Si<sup>2+</sup> ions. This is because such collision systems are thought to be important for the production of hydrogen molecules in some planets like the satellite Titan of the Saturn, where hydrocarbon molecules are known as the atmospheric constituents of the satellite.

Measurements of fragment molecular ions were performed by means of a time of flight coincidence method. A series of experimental data were taken under charge-changing conditions of electron capture and loss of projectile ions detected with a solid state detector. Fragment ions were detected two-dimensionally with a delay-line type

position sensitive detector. One example of such two-dimensional spectra is demonstrated in Fig.1 obtained for an ethane gas target under a single electron capture collision. It is found that molecular hydrogen ions are produced only when the C-C bond stays unbroken, and otherwise only atomic hydrogen is produced. Also we find that the production of H<sub>3</sub><sup>+</sup> always accompanies the residual ions like C<sub>2</sub>H<sub>3</sub><sup>+</sup> or C<sub>2</sub>H<sub>2</sub><sup>+</sup>. These results implies that the formation of molecular hydrogen ions is promoted only in soft (distant) collisions where an inelastic energy deposition into a target molecule is small and, consequently, the internal excitation energy is also small. In violent (close) collisions where the internal excitation energy is large enough leading to coulomb explosion or highly amount of evaporation of hydrogen atoms, the formation of molecular hydrogen ions may be strongly reduced.

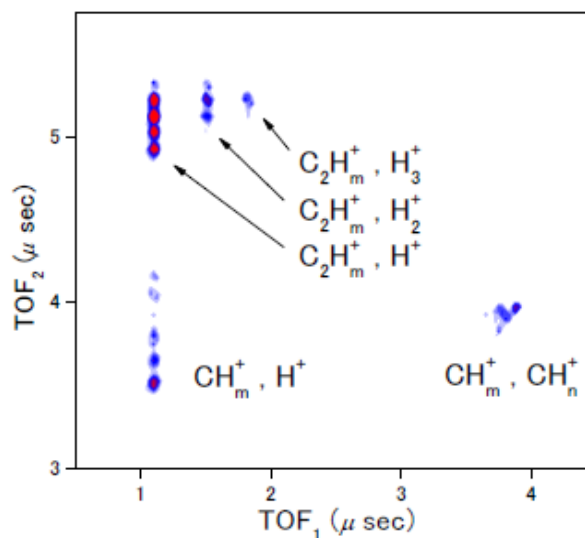


Fig. 1. 2D-correlation spectra from C<sub>2</sub>H<sub>6</sub>

### References

- [1] T. Mizuno, T. Majima, H. Tsuchida, Y. Nakai and A. Itoh, J. of Phys: Conference Series, 58 (2007) 173.

## DIFFERENTIAL CROSS SECTIONS FOR ELECTRON-IMPACT SCATTERING ON BORON

**L. Bandurina<sup>a</sup>, V. Gedeon<sup>b</sup>**

<sup>a</sup>Institute of Electron Physics, Uzhgorod, 88026, Ukraine

<sup>b</sup>Department of Theoretical Physics, Uzhgorod National University, 88000, Ukraine

We will present an extensive *B*-spline *R*-matrix (BSR) [1] calculation of the electron-impact scattering from neutral boron. The close-coupling expansion includes 8 first bound states of neutral boron and 20 pseudostates (see Table 1).

Table 1. Energies of the first 8 terms of B I and 20 pseudostates relative to the  $2s^22p^2P^0$  ground state.

No	States	Energy,	Energy,	Diffe-
		eV	eV	
		BSR28	NIST [2]	eV
1	$2s^22p^2P^0$	0.0000	0.0013	0.0013
2	$2s2p^2^4P$	3.5452	3.5803	0.0352
3	$2s^23s^2S$	4.9859	4.9643	-0.0216
4	$2s2p^2^2D$	5.9358	5.9335	-0.0022
5	$2s^23p^2P^0$	6.0140	6.0273	0.0132
6	$2s^23d^2D$	6.7217	6.7903	0.0686
7	$2s2p^2^2S$	7.8678	7.8805	0.0128
8	$2s^26d^2D$	8.3592	7.9158	-0.4434
9	$2s2p^2^2P$	9.0446	8.9924	-0.0521
10	$2s2p3p^2Da$	10.9474	10.8559	-0.0915
11	$2s2p3d^2D^0$	11.1127	11.5677	0.4550
12	$2s2p3p^2P$	11.6179	10.7696	-0.8483
13	$2p^3^4S^0$	12.0324	12.0393	0.0070
14	$2p^3^2D^0$	12.7290	12.3736	-0.3554
15	$2p^3^2P^0$	14.8666	13.7808	-1.0858
16	$2s2p3p^2S$	15.7284		
17	$2s25d^2D$	16.1692		
18	$2s2p3p^2Db$	16.3402		
19	$2p^27d^2Pa$	22.1128		
20	$2p^23s^2S$	23.4600		
21	$2p^27d^2Pb$	23.9232		
22	$2p^23p^2P^0$	24.5191		
23	$2s2p7d^2D^0$	24.5734		
24	$2p^23d^2D$	25.6681		
25	$2s7p^2^2S$	26.2965		
26	$2s2p3d^2P^0a$	27.7505		
27	$2s2p3d^2P^0b$	29.0855		
28	$2s7d^2^2S$	36.0046		

As example, Fig. 1 and 2 show the differential cross sections for transitions from the  $2s^22p^2P^0$  ground state of boron.

**Keywords:** Cross Section; Electron-impact; Boron

### References

- [1] O. Zatsarinny, *Comput. Phys. Commun.*, **174** (2006) 273.  
 [2] NIST Atomic Spectra Database, <http://physics.nist.gov>.

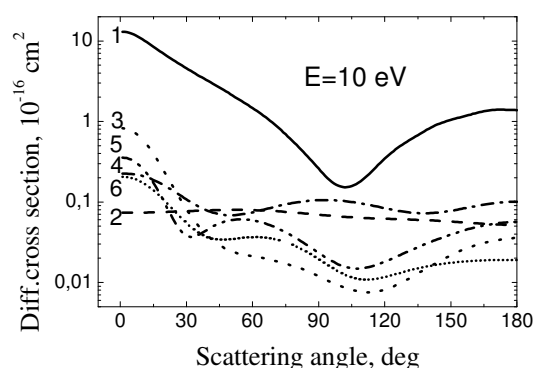


Fig. 1. Angle-differential cross sections for transitions with  $2s^22p^2P^0$  ground state of boron: 1 – elastic scattering; 2-6 – excitation of  $2s2p^2^4P$ ,  $2s^23s^2S$ ,  $2s2p^2^2D$ ,  $2s^23p^2P^0$  and  $2s^23d^2D$  states, respectively.

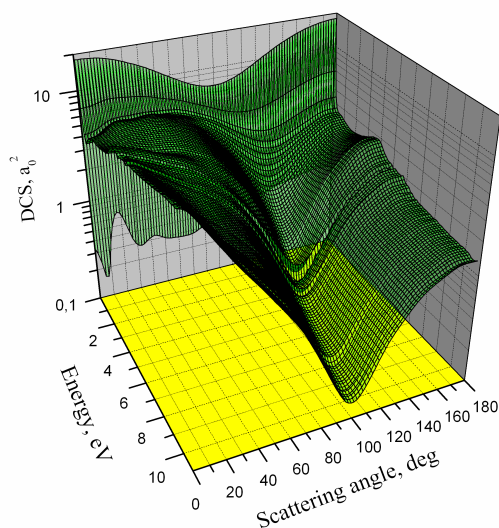


Fig. 2. Angle-differential cross sections for elastic electron scattering from B atoms.

# IMPACT PARAMETER METHOD CALCULATIONS FOR FULLY DIFFERENTIAL IONIZATION CROSS SECTIONS

**F. Járαι-Szabó<sup>a</sup> and L. Nagy<sup>a</sup>**

<sup>a</sup>Faculty of Physics, RO-400084 Cluj-Napoca, str. Kogalniceanu 1, Babeş-Bolyai University, Romania

Detailed information about collision processes may be obtained by studying fully differential cross sections. Previously, based on the semiclassical impact parameter method, a theoretical model has been constructed to calculate fully differential cross sections for single ionization of helium by impact with fast  $C^{6+}$  ions [1]. Based on the semi-empirical version of the model good agreement with the experiment has been achieved in the scattering plane, while in the perpendicular plane a structure similar to that observed experimentally was obtained. The impact parameter values have been selected based on the experimental data available in scattering plane.

In this work a method is presented for calculating impact parameter values corresponding to different momentum transfer values. The method will be used to improve the fully differential cross section calculations with the semiclassical impact parameter method. By the use of the transverse momentum balance [2] it can be proved that higher impact parameters have to be used in the case of a binary peak than of a recoil peak. Instead of the previously tried Rutherford scattering formula, the projectile scattering angle will be calculated as a classical potential scattering problem [3] in the field of the target helium system. The method is tested calculating fully differential cross sections for single ionization of helium produced by fast  $C^{6+}$  ion.

*Keywords:* Fully differential cross sections; Scattering angle; Ionization

## References

- [1] F. Járαι-Szabó, L. Nagy, J. Phys. B: At. Mol. Opt. Phys. 40 (2007) 4259.
- [2] Ullrich J, Moshhammer R, Dörner R, Jagutzki O, Mergel V, Schmidt-Böcking H and Spielberger L, J. Phys. B: At. Mol. Opt. Phys. 30 (1997) 2917.
- [3] Roger G. Newton, Scattering Theory of Waves and Particles, Second edition, Mineola, New York (2002) ISBN 0-486-42535-5.

## CROSS SECTIONS AND TRANSPORT PROPERTIES OF F<sup>-</sup> IONS IN Ar, Kr AND Xe

**J.V. Jovanović<sup>a,b</sup>, Z.Lj. Petrović<sup>a</sup> and V. Stojanović<sup>a</sup>**

<sup>a</sup>Institute of Physics, P.O.B. 68, Zemun, Belgrade, Serbia

<sup>b</sup>Faculty of Mechanical Engineering, Kraljice Marije 16, Belgrade, Serbia

The aim of the current work is to determine with relatively high accuracy the elastic momentum-transfer cross sections of F<sup>-</sup> ions in collisions with noble gases Ar, Kr and Xe. We have applied a simple form of Momentum Transfer Theory (MTT) [1] based on elastic collisions as the first step in order to develop negative fluorine ion/Ar, Kr, Xe elastic momentum transfer cross sections based on the available data for reduced mobilities [2, 3] at 300 K as a function of  $E/N$ .

In our procedure MTT is used only as the initial step to make adjustments and thus save a lot of computation time. However, our final results have been all obtained by exact Monte Carlo (MC) technique that has been well tested and documented. In order to make proper calculations for thermal energies, we allowed the momentum transfer cross sections to converge towards Langevin's cross section. In the case of F<sup>-</sup>/Ar, the momentum transfer cross section is supplemented by detachment cross section [4] that was used from the threshold around 7 eV up to 200 eV (Fig.1).

The unfolded cross sections were validated or further improved by assuring a good agreement between our Monte Carlo (MC) calculated transport data and the available experimental results for reduced mobility and longitudinal diffusion. We have also calculated the net rates of elastic scattering and detachment.

The data are produced with an aim to provide plasma modellers with cross section data and transport coefficients.

*Keywords:* Cross sections; Transport properties; Kinetic and transport theory of gases

### References

- [1] R. E. Robson, *Introductory Transport Theory for Charged Particles in Gases*, World Scientific Publishing, Singapore, 2006.
- [2] H. W. Ellis, E. W. McDaniel, D. L. Albritton, L. A. Viehland, S. L. Lin and E. A. Mason, *At. Data Nucl. Data Tables* **22** (1978) 179.
- [3] L. A. Viehland, C.C. Kirkpatrick, *Chem. Phys.* **202** (1996) 285.
- [4] M.S. Huq, L.D. Doverspike, R.L. Champion, V.A. Esaulov, *J. Phys. B: At. Mol. Phys.* **15** (1982) 951.

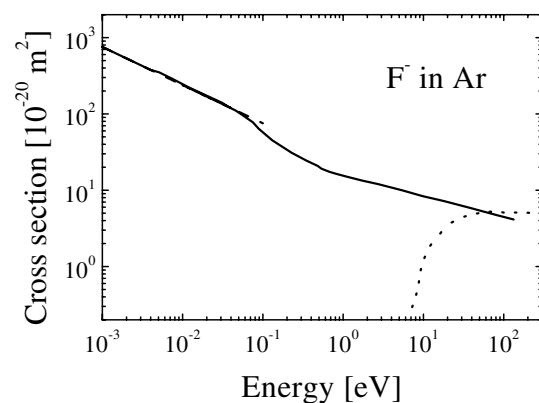


Fig. 1. Cross sections for F<sup>-</sup> in Ar. Solid line: momentum transfer cross section; dashed line: Langevin cross section; dotted line, detachment cross section from reference [4].

## **Z<sub>2</sub> structure of the stopping power for electron beams**

Hasan Gümüş, Önder Kabadayi<sup>1</sup>

Department of Physics, Faculty of Sciences and Arts, Ondokuz Mayıs University

55139 Samsun-Turkey

<sup>1</sup>Department of Physics, Faculty of Sciences and Arts, Giresun University

28100 Giresun-Turkey

### **Abstract:**

The target atomic number ( $Z_2$ ) dependence of the collision stopping power for electron beams have been investigated for the purpose of determining primary mechanisms in stopping of electrons in elemental matter. The stopping powers of target elements with atomic numbers  $Z_2=1$  to 92 for the electrons have been evaluated on the basis of Gümüş method. The variation of the stopping power depending on energy of electrons and type of target has been studied to obtain the elements with the strongest stopping force for electron beams. A strong  $Z_2$  oscillation in the collision stopping power has been observed whereas the mass collision stopping powers are found to be decreasing with increasing atomic number of the target. It is also found that electrons mainly slowing down depending on the atomic density of target and initial energy of electrons.

PACS: 34.50Bw; 61.80Fe

*Key Words:* Collision stopping power,  $Z_2$  oscillation, Electron

---

<sup>1</sup> Corresponding author. Tel.: +90 454 2162520

Email: onderkabadayi@gmail.com

## DESIGN, SIMULATION AND CONSTRUCTION OF MULTI-FIELD LINEAR TIME-OF-FLIGHT MASS SPECTROMETERS

Erengil Z<sup>b</sup>, Kaymak N<sup>a</sup>, Yildirim M<sup>a</sup>, Sise O<sup>b</sup>, Dogan M<sup>b</sup> and Kilic HS<sup>a</sup>

<sup>a</sup>Department of Physics, Science and Arts Faculty, Selcuk University, Turkey

<sup>b</sup>Department of Physics, Science and Arts Faculty, Afyon Kocatepe University, Turkey

Linear time-of-flight mass spectrometer (TOFMS) is one of the most versatile mass spectroscopic area growing quite fastly and has undergone many changes and expansions. It is well known that flight-time error resulting from the finite width of the ion packets along the axis of the flight tube is commonly minimized by incorporating the two-field acceleration geometry and space-focusing principles. Improvements to the Wiley-McLaren space focusing have been proposed by a number of authors [1,2]. These articles make reference to providing higher order corrections to Wiley-McLaren spatial focusing and in many cases the resolution is improved considerably. This result has important implications for the design of mass spectrometers.

In this work we present the results of ion trajectory calculations optimizing the performance of multi-field TOFMS under the aspects of space and mass resolution, using the ray-tracing simulation program SIMION 8.0 [3]. A brief account of the TOFMS theory is given together with optimum dimensions and voltages which provide space focusing. Space focusing conditions of two-, three- and four-field linear TOFMS have been analyzed in detail, in order to investigate the characteristics of the TOFMS and determine the most desirable configuration. The capabilities and limitations of these instruments are discussed by means of numerical examples. The effect on the time-width of a peak in the mass spectrum and on the resolution was demonstrated.

The simulations presented here have to be checked experimentally and the issue about the space and mass resolution for multi-field linear TOFMS also has to be investigated in practice. For this purpose, we have constructed a new four-field TOFMS and its ion optics which is contained in a non-magnetic stainless steel vacuum chamber pumped by a turbomolecular pump. A vacuum chamber has been constructed at the machine shop in Afyonkarahisar, Turkey. The spectrometer is built of four acceleration regions and a grounded flight tube. The experimental system is almost completed and will be used in coupling to a sophisticated optical parametric oscillator system (OPO, output wavelength region is over 420-2500 nm), pumped by a high power Nd:YAG (Surelite III) laser at 10 Hz repetition rate with pulse energy of nearly 900 mJ at 3064 nm. The simulated data will be compared to the experimental results using our multi-field linear TOFMS in the near future.

Keywords: Time-of-flight mass spectrometer, simulation of ion motion, space focusing, mass resolution, SIMION.

### References

- [1] U. Even and B. Dick, Rev. Sci. Instrum. 71 (2000) 4415-4420.
- [2] D. P. Seecombe and T. J. Reddish, Rev. Sci. Instrum. 72 (2001) 1330-1338.
- [3] SIMION 3D v8.0, Scientific Instrument Services Inc. www.simion.com.

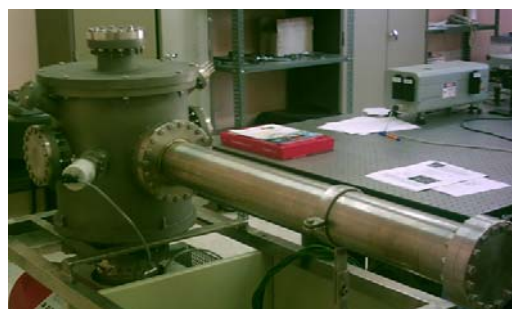


Fig. 1. The instrument design which worked in simulations, and was constructed and will be used in subsequent experiments.



## MONTE CARLO CALCULATIONS OF THE SECONDARY ELECTRON EMISSION INDUCED BY IONS

A. Nina, M. Radmilović-Radjenović, V. Stojanović and Z. Lj. Petrović

Center for Experimental Physics, Pregrevica 118, POB 68, 11080 Zemun, Belgrade, Institute of Physics, Serbia

Electrons released at the cathode travel the whole distance to the anode and produce more ionization than electrons created en route. Ions are produced by electron-impact ionization and most of these ions are accelerated into the cathode sheath, causing secondary electrons to be emitted. These secondary electrons enter the trapping region and cause sufficient ionization to maintain the discharge. For this reason, the onset of breakdown is determined by  $\gamma$ -effects at the cathode. The secondary electron emission from a surface under the action of an ion is described by the coefficient quantifying the number of secondary electrons produced at the cathode per ion usually known as the electron yield per ion and denoted by  $\gamma_i$ .

In this paper, we present our Monte Carlo simulation results for the yield of secondary electrons as a function of  $E/N$  in argon Ar with dirty metal cathode [1] and nitrogen  $N_2$  with molybdenum cathode. In our calculations the number of the initial electrons emitted from the was 10000, while their initial energy was 1 eV.

In Fig. 1, we have shown that the yields  $\gamma_i$  obtained from the realistic energy distribution of ions for each  $E/N$  based on given dependencies of yields on energy of ions. A good agreement for argon indicates that effective energy in beam model of Phelps [1] adequately represents the ion energy distribution.

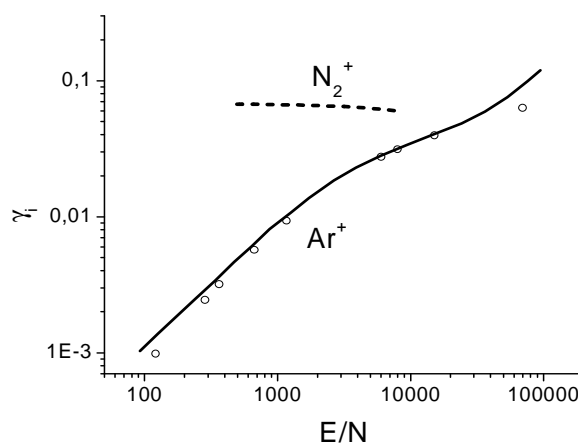


**Fig. 1** Dependence of the yield of secondary electrons on the reduced electric field

Monte Carlo code will be used to analyze the secondary electron emission processes due to impact of other particles such as photons, metastables and fast neutrals and in other gasses.

[1] A. Phelps and Z.Lj. Petrović, 1999 *Plasma Sources Sci. Technol.* **8** 21

[2] A. Phelps, L. Pitchford, C Pedoussat and Z Donko, 1999 *Plasma Sources Sci. Technol.* **8** B1

[3] P. Mahadevan, G. Magnuson, J. Layton and C. Carlston, 1965 *Physical Review* **140** A 1407

## MEASUREMENTS AND ANALYSIS OF SECONDARY ELECTRON YIELDS IN TOWNSEND DARK DISCHARGES

G. Malović, D. Marić , S. Živanov, M. Radmilović- Radjenović and Z.Lj. Petrović

<sup>1</sup> *Institute of Physics, POB 68, 11080 Belgrade, Serbia*

Accurate determination of the secondary electron yield needed for plasma modeling requires inclusion of the width of non-hydrodynamic region usually known as delay or equilibration distance in the analysis of the breakdown data. This paper contains the experimental results as well as the detailed theoretical simulation studies of the influence of the delay distance on the effective secondary electron yield and the breakdown mechanism. Our work was motivated by the fact that published results for the secondary electron yields from ion beam experiments and gas discharges are systematically in serious disagreement requiring revision of Townsend's theory. The emphasis was made on the experimental results in order to illustrate a wide range of applications of measurements of spatial profiles of emission, which may be used as a principal source for obtaining the cross sections, as much as they provide the basis for understanding the kinetics of breakdown, secondary electron yields and non-equilibrium conditions close to the electrodes. Beside measurements that were carried out, exact model of gas breakdown at low currents was also developed. The model was based on Monte Carlo simulation of electron that allowed us to consider how non-hydrodynamic transport close to electrodes affects the breakdown. The presented results have great significance for many discharge applications such as glow discharge lamps, gas-filled switches, gas insulation and lasers.

Keywords: breakdown, secondary electron yields, argon, hydrogen.

## **ENERGY-BAND STRUCTURE AND INELASTIC SCATTERING EFFECTS IN THE LOW-ENERGY ABSORBED CURRENT AND SECONDARY-ELECTRON EMISSION SPECTROSCOPIES**

**O.F. Panchenko and L.K. Panchenko**

A.A. Galkin Donetsk Institute of Physics & Engineering, 72 Rozy Luxemburg Str.,  
83114 Donetsk, Ukraine

The low-energy secondary-electron spectroscopy (based on the study of phenomena accompanying the process of interaction between the flow of slow-moving primary electrons and crystal surface) which does not destroy the sample is one of the methods to control surface roughness. In this case the observed experimental spectra of truly secondary electrons (SEES) and spectra of absorbed current (ACS) show the totality of phenomena taking place both in the volume and near-surface layer of the crystal. The fine structure of those spectra is determined by the energy dispersion of unoccupied high-level electronic states (above the vacuum level) to which the electrons are scattered or from where they are emitted. The present study deals with the development of the above-mentioned methods basing on the bulk energy-band structure (BES) of crystals. As before, (see, e.g. [1-4]) during the calculation of SEES and ACS the electron scattering with a preset momentum at the crystal was considered within the approximation, when the probability of scattering was proportional to a number of finite states at a given energy level with a preset direction of quasi-momentum. The energy dependence of the band energy level broadening, the electron-electron and electron-plasmon contributions to the distribution function of highly non-equilibrium charge carriers (obtained from the solution of the kinetic (Boltzmann-type) integral transport equations describing the cascade process of the inelastic scattering of the primary electron flow [5]), the isotropic component of current from the electrons scattered on the surface were taken into consideration. In addition, it was a success for us to rather satisfactorily explain the main structure in spectra of a number of crystals. The extrema in the SEES and ACS reflect the energy position of the critical points (the band edges or boundaries and the points of extreme curvature of the dispersion branches) in the unoccupied BES. And there occurs a possibility for the experimental study of the electron dispersion in the region of energies much higher than the vacuum level (thus adding to the traditionally used data of the photoemission, inverse photoemission and optical spectroscopy). The method being developed enables one to distinguish between the volume effects in SEES and ACS from the surface ones which are to be investigated separately [6, 7].

Keywords: low-energy electrons, inelastic scattering, energy-band structure, unoccupied electronic states

### **References**

- [1] O.F. Panchenko, L.K. Panchenko, *Phys. Lett. A* 192 (1994) 289.
- [2] O.F. Panchenko, L.K. Panchenko, *Solid State Commun.* 89 (1994) 849.
- [3] O.F. Panchenko, L.K. Panchenko, *Solid State Commun.* 101 (1997) 483.
- [4] O.F. Panchenko, L.K. Panchenko, J.A. Schaefer, *Surf. Sci.* 507-510 (2002) 192.
- [5] O.F. Panchenko, L.K. Panchenko, *Radiation Phys. Chem.* 75 (2006) 1711.
- [6] O.F. Panchenko, *Surf. Sci.* 482-485 (2001) 723.
- [7] O.F. Panchenko, L.K. Panchenko, *Vacuum* 81 (2007) 766.

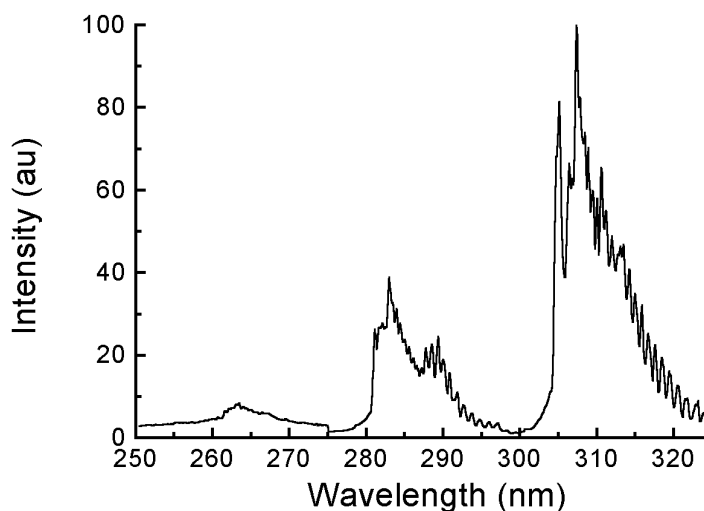
## WATER VAPOUR UV DISCHARGE SOURCE

**V.A. Kelman, A.A. Heneral, Yu.V. Zhmenyak, Yu.O. Shpenik, O.I. Plekan**

Department of Quantum Electronics, Universitetska str., 21, Uzhhorod, Institute of Electron Physics, 88017, Ukraine

Not only coherent, but often noncoherent discharge sources of UV radiation have important applications. Among the last type of sources well known are excimer lamps typically having gaseous mixture filling. Having an advantage as mercury-free lamps, nevertheless they contain halogen molecules in gaseous phase (typically HCl, HBr etc.). Actually pure UV source seems to be the water discharge lamp.

In this work for the first time we studied spectral parameters of high voltage pulse-periodical discharge in water vapour. Discharge was excited in quartz tube (length 40 cm, inner diameter 15 mm). Current pulses (frequency 10 kHz) were formed by full discharge of storage capacitor (1650 pF) through the tube and thyatron TGI1-2000/35. Time integrated emission spectra in the range 250 – 325 nm was registered using grating grid monochromator MDR-6 and photomultiplier FEU-106 type.



The obtained spectra at the estimated water vapour pressure of about 0.1 mm Hg is presented on the Figure. The measured relative spectral sensitivity of the registration apparatus was taken into account.

Three different parts of registered spectra are easily identified [1]. Part I (250 – 275 nm) is attributed to B – A electronic transition of hydroxyl OH molecule. This part is excited less intensively than another two as required discharge electrons of much higher energy. Parts II (275 – 300 nm) and III (300 – 325 nm) of the spectra are attributed to the A – X electronic transition of OH molecule. In these parts the most intensive is the band, connecting with vibrational transition (1-0) 283 nm and the band connecting with (0-0) 309 nm vibrational transition. No another radiating species of water molecule H<sub>2</sub>O destruction products were identified.

Time dependence of the intensity of 309 nm band was measured using oscilloscope technique. It clearly indicate that the emission pulse fully coincides with the current pulse and electron impact processes define the properties of water discharge UV source.

The average power of emitted radiation in spectral range 250 – 325 nm was estimated to be 1.5 W and efficacy about 0.2 %. It may be noted that when the ordinary water H<sub>2</sub>O in tube is replaced by the hard water D<sub>2</sub>O, the output power is increased of approximately by twice.

*Keywords:* Water vapour, longitudinal high-voltage discharge, OH specie, UV emission.

### References

[1] A.A. Radzig, B.M. Smirnov. Handbook on atomic and molecular physic. Moscow. Atomizdat (1980).

## JONES EFFECT ON LI AND NA ATOMS

**V.V. Chernushkin<sup>a</sup>, V.D. Ovsianikov<sup>a</sup>**

<sup>a</sup> Theoretical Physics Department , Voronezh State University, Voronezh, 394006. Russia  
E-mail: [albert@phys.vsu.ryu](mailto:albert@phys.vsu.ryu)

Magnetolectric birefringence, which was predicted by Jones [1] and first observed in liquids [2], may also become a useful tool for the high-precision spectroscopy of atomic systems [3]. In the case of resonance with an excited D-level, the dipole-forbidden bilinear Jones effect on a medium of free atoms in their ground S-states may become significantly stronger than the dipole-allowed Kerr and Cotton-Mouton effects [4], quadratic respectively in electric and in magnetic field. In this paper we present an account for the influence on the Jones amplitude of the resonant-level fine structure.

The Jones effect is determined by the bilinear in the static fields amplitude of the Rayleigh scattering of a monochromatic wave, which for the frequency  $\omega = E_{n'D_J} - E_{nS_{1/2}} - \varepsilon_J$  in resonance ( $|\varepsilon_J| \ll \omega$ ) with the D-level doublet substates of the total momentum  $J = 3/2, 5/2$ , may be written as (taking into account only the terms with the second-order resonance singularities):

$$U = AQ_D \left( \frac{7}{(\varepsilon_{3/2})^2} + \frac{47}{(\varepsilon_{5/2})^2} - \frac{4}{\varepsilon_{3/2}\varepsilon_{5/2}} \right) [\varphi_0 + \varphi_1]$$

where the constant factor  $A = F^2 F_0 B / 1500$  is proportional to the product of the square laser field  $F^2$ , static electric field  $F_0$  and magnetic field  $B$ . For atoms with the singlet structure of levels, the resonance detuning  $\varepsilon_{3/2} = \varepsilon_{5/2} \equiv \varepsilon$  and the double-resonance fractions in parentheses combine into  $50/\varepsilon^2$  [4]. The polarization-dependent factors are

$$\begin{aligned} \varphi_0 &= (\mathbf{e}_0 \cdot [\mathbf{n} \times \mathbf{e}_B]); \\ \varphi_1 &= \text{Re} \left\{ (\mathbf{e}_0 \cdot \mathbf{e}) (\mathbf{e}^* \cdot [\mathbf{n} \times \mathbf{e}_B]) \right\}, \end{aligned}$$

where  $\mathbf{e}_B$  and  $\mathbf{e}_0$  are the unit vectors of the magnetic and electric fields,  $\mathbf{e}$  and  $\mathbf{n}$  are the unit polarization and wave vectors of the laser wave. In addition to birefringence, the imaginary part of the detuning  $\varepsilon_J = \Delta_J + i\Gamma_J/2$ , which equals to the resonance level width  $\Gamma_J$ , may cause the dichroism effects. The factor  $Q$  is a product of the radial matrix elements for the first-order quadrupole and second-order dipole radiation transition between the ground  $nS_{1/2}$  and resonance  $n'D_J$ .

The Jones birefringence appears, when  $\mathbf{e}_0 = \mathbf{e}_B$ , being directly proportional to the difference  $\Delta U_D^{(J)} = U_D^{(+)} - U_D^{(-)}$  between the amplitude  $U$  for  $\mathbf{e} = \mathbf{e}^{(+)}$  and  $\mathbf{e} = \mathbf{e}^{(-)}$ , where  $\mathbf{e}^{(\pm)} = (\mathbf{e}_0 \pm [\mathbf{n} \times \mathbf{e}_0]) / \sqrt{2}$ . Similar effects in atoms with singlet structure of levels, which correspond to  $\varepsilon_{3/2} = \varepsilon_{5/2}$ , were discussed in [4].

### References

- [1] R. C. Jones, J. Opt. Soc. Am. 38, 671 (1948).
- [2] T. Roth and G. L. J. A. Rikken, Phys. Rev. Lett. 85, 4478 (2000).
- [3] D. Budker and J. E. Stalnaker, Phys. Rev. Lett. 91, 263901 (2003).
- [4] P. V. Mironova, V. V. Tchernouchkine, V. D. Ovsianikov, J. Phys. B, 39, 4999 (2006).

## ON RYDBERG SERIES OF AUTOIONIZING RESONANCES

**V. Stancalie**

Department of Lasers, Atomistilor 409, Magurele, National Institute for Laser, Plasma and  
Radiation Physics, 077125 Romania

This work describes progress in understanding the role of Laser Induced Degenerate State (LIDS) phenomenon [1] on resonances obtained by using lasers. The effect of one-photon transition, that couples the autoionizing state to the degenerate continuum state via the stimulated emission and subsequent absorption of a photon, on the resonance profile is studied as function of the laser field intensity. This type of process, implicitly included in the R-matrix Floquet [2] calculation, contributes, to some degree, to the overall behaviour of the resonance profiles. In the present case the LIDS phenomenon plays the most dominant role and it is investigated.

For the purposes of our work, the process under investigation is the electron scattering by Li-like ions in their ground state ( $1s^2 2s$  ( $^2S^e$ )) followed by electron capture in a doubly excited  $1s^2 2pns$  ( $^1P^0$ ) state. This state can decay by radiative transition to other excited state ( $1s^2 2sns$  ( $^1S^e$ )), or can autoionize. For highly ionized ions in an isoelectronic sequence the autoionization probabilities are approximately independent of  $Z$  but radiative probabilities are proportional to  $Z^4$  (for transition involving a change of the principal quantum number). Radiative decay therefore becomes more important as  $Z$  increases.

The present work refers to  $Al^{10+}$  and  $C^{3+}$ , as an example. The excited Rydberg state ( $1s^2 2sns$  ( $^1S$ )) and the doubly excited Rydberg state ( $1s^2 2pns$  ( $^1P^0$ )) of these ions, are studied throughout the resonant Rydberg series in a region where the autoionization and radiative rates are comparable in size. To this aim, it is analyzed the situation when two excited Rydberg states are resonantly coupled by an intense, monochromatic, monomode, linearly polarized laser field.

It has been demonstrated [3, 4] that the motion, of the trajectories in the complex plane, shows different features for these coupled states. More interesting is the critical region where a crossing (or an avoiding crossing) of trajectories occurs. For certain values of field intensity and frequency, the two quasi-energies become equal, giving rise to LIDS. Following our model, if the equivalent intensity of the spontaneous emission is less than the LIDS intensity, then the two widths are converging towards each other into the region where perturbation theory will not be used. We will make use of previously reported results to investigate the role of LIDS to the overall behaviour of the resonance profile.

The description generalizes the non-radiative coupling matrix element of the autoionizing state to the continuum, so as to include an explicit intensity dependence. The model considers an approximation to the K matrix, in particular keeping only the lowest-order term in an expansion of K in powers of atom-field Hamiltonian.

Keywords: atoms in laser field, laser-induced continuum structures, laser-induced degenerate states

### References

- [1] O. Latinne et al., Phys. Rev. Lett. 74(1995)46-49.
- [2] P.G. Burke, P. Francken, C.J. Joichain, J. Phys. B: At. Mol. Opt. Phys. 24 (1991) 761-790.
- [3] V. Stancalie, Physics of Plasmas 12 (2005) 043301.
- [4] V. Stancalie, Physics of Plasmas 12 (2005) 100705.

## THERMAL IONIZATION OF CS RYDBERG STATES

**Glukhov I. L. and Ovsianikov V. D.**

Department of Physics, 394006 Voronezh, University Square 1,  
Voronezh State University, Russia

Blackbody radiation (BBR) is a ubiquitous perturbing factor for Rydberg states at normal temperatures. Having a wide energy spectrum, BBR photons stimulate upward and downward transitions and ionization, depopulating Rydberg states within small fractions of a second. In addition, the ionization distorts configurations of trapping fields.

The BBR-induced ionization of cesium s-, p-, d- Rydberg states was investigated theoretically. We used wavefunctions of the Fues' model potential [1] for calculating matrix elements of bound-free dipole transitions. Obtained results are in a good agreement with the latest available theoretical and experimental data [2].

To present the results of our calculations in a compact and simply executable form, we have addressed to our previously reported three-term approximation, earlier applied to helium [3] for the thermal ionization rate  $P_n$  (in inverse seconds):

$$P_n = \frac{a_0 + a_1x + a_2x^2}{\tilde{\nu}^4[\exp(x) - 1]}; \quad (1)$$

$$\tilde{\nu} = \frac{\nu}{100}, \quad \nu = \frac{1}{\sqrt{-2E_{nl}^{\text{exp}}}}, \quad x = \frac{E_{nl}^{\text{exp}}}{kT} = \frac{0.1579}{(y\tilde{\nu})^2}, \quad y = \sqrt{\frac{T}{100}},$$

where  $E_{nl}^{\text{exp}}$  is an experimentally known ionization potential of the Rydberg state,  $T$  is the temperature in Kelvins. Smoothly dependent on temperature, coefficients  $a_i$  were fitted on the basis of the data for states with  $n=8-45$  and  $x < 1.6$  ( $x < 1.05$  for s-states). To extend applicability range for our three-terms formula (1), we propose the following approximation,

$$a_i = \sum_{k=0}^2 b_{ik}y^{-k}, \quad i = 0, 1, 2. \quad (2)$$

The nine fitted once for all coefficients  $b_i$  allow for a fast and accurate calculation of ionization rates not only for states within interpolation range with maximal 1% deviation (fig. 1), but also give right values for higher states with deviation, less than 17%, for  $n=100$  Rydberg states.

Besides a good accuracy for the range of the main interest  $T=100-1000$  K, equation(2) provides correct extrapolation for  $a_i$ -coefficients to higher temperatures, so that the deviation of ionization rate (1) from directly calculated results does not exceed 26% at 10000 K for all states with  $n \leq 100$ .

*Keywords:* blackbody radiation; ionization; Rydberg atom

### References

- [1] Manakov N.L., Ovsianikov V.D., Rapoport L.P, Physics Reports 141 (1986) 319.
- [2] Beterov I.I., Tretyakov D.B., Ryabtsev I.I., Ekers A., Bezuglov N. N., JETP to be published (2008).
- [3] Glukhov I.L., Ovsianikov V.D., Proc. of SPIE Vol. 6726 (2007) 67261F.

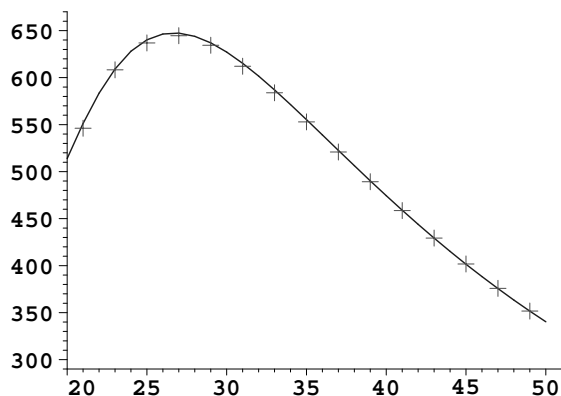


Fig. 1. Approximate (solid curve) and exact (crosses) ionization rate for p-states at 300 K

**THE ELECTRONIC g-FACTOR OF HYDROGEN-LIKE IONS  
AS TEST OF BOUND-STATE QUANTUM ELECTRODYNAMICS**

**G. Werth, K. Blaum, B. Schabinger, S. Sturm**

Johannes Gutenberg University, D-55099, Mainz (Germany)

The g-factor of the single electron bound in hydrogen-like ions serves as test of bound-state quantum electrodynamics (BS-QED) calculations [1]. Experiments have been performed on  $C^{5+}$  [2] and  $O^{7+}$  [3] to an accuracy of a few ppb. They confirm the validity of the calculations and represent a stringent test of BS-QED. The experiments use single ions confined under nearly ideal conditions for virtually unlimited time in a Penning trap. The ions motional frequencies are measured by induced image currents in the trap electrodes with high precision for calibration of the superimposed magnetic field. Induced spin flips are monitored by coupling of the spin motion to the orbital trajectories in a slightly inhomogeneous magnetic field. Assuming the validity of the BS-QED calculations a new value for the electron mass can be derived from the measured g-factor. Experiments are in progress to measure the g-factor in H-like  $^{19}Ca^+$  which will increase the accuracy of the BS-QED test.

*Keywords:* g-factor, Quantum electrodynamics, Ion traps

**References**

- [1] V.A. Yerokhin, et al., Phys. Rev. Lett. 89, 143001 (2002)
- [2] H. Häffner et al., Phys. Rev. Lett. 85, 5308 (2000)
- [3] J. Verdú, et al., Phys. Rev. Lett. 92, 093002 (2004)
- [4] M. Vogel et al., Nucl. Instr. Meth. B 235, 7 (2005)



## QED APPROACH TO THE PHOTON-PLASMON TRANSITIONS AND DIAGNOSTICS OF THE SPACE PLASMA TURBULENCE

A. Glushkov<sup>a,b</sup>, O. Khetselius<sup>b</sup> and A. Svinarenko<sup>b</sup>

<sup>a</sup>Institute for Spectroscopy of Russian Academy of Sciences (ISAN), Troitsk, 142090,  
Russia

<sup>b</sup>Odessa University, P.O.Box 24a, Odessa-9, 65009, Ukraine

Energy approach in QED theory is developed and applied to modelling photon-plasmon transitions with emission of photon and Langmuir quanta in space and astrophysical plasma. It is well known that the positronium  $Ps$  is an exotic hydrogen isotope with ground state binding energy of  $E = 6.8$  eV. The hyperfine structure states of  $Ps$  differ in spin  $S$ , life time  $t$  and mode of annihilation. The ortho- $Ps$  atom has a metastable state  $2s1$  and probability of two-photon radiation transition from this state into  $1s1$  state  $0.0018s^{-1}$ . In the space plasma there is the competition process of destruction of the metastable level - the photon-plasmon transition  $2s - 1s$  with emission of photon and Langmuir quanta. We carried out calculation of the probability of the photon-plasmon transition in the  $Ps$ . The approach represents the decay probability as an imaginary part of energy shift  $dE$ , which is defined by S-scattering matrix. Standard S-matrix calculation with using an expression for tensor of dielectric permeability of the isotropic plasma and dispersion relationships for transverse and Langmuir waves allows getting the corresponding probability  $P(ph - pl)$ . Numerical value of  $P(ph - pl)$  is  $5.2 \cdot 10^6 U(1/s)$ , where  $U$  is density of the Langmuir waves energy. Our value is correlated with others:  $P(ph - pl) = 6 \cdot 10^6 U(1/s)$ . Comparison of obtained probability with lifetime  $t$  ( $3 \gamma$ ) allows getting the condition of predominance of photon-plasmon transition over three-photon annihilation. The considered transition may control the population of  $2s$  level and search of the long-lived  $Ps$  state can be used for diagnostics of the plasma turbulence.

*Keywords:* Photon-plasmon; Space; Plasma

### References

- [1] A. Glushkov, L.N. Ivanov, Phys. Lett. A 170 (1992) 33; Preprint ISAN N AS-4, Moscow-Troitsk (1994).
- [2] A. Glushkov et al, Int.Journ. Quant. Chem. 99 (2004) 936; 104 (2005) 562; Europ.Phys. Journ. (2008); Low Energy Antiproton Phys. 796 (2006) 211.

**QUANTUM DYNAMICS OF THE RESONANT LEVELS FOR ATOMIC  
AND NUCLEAR ENSEMBLES IN A LASER PULSE: OPTICAL  
BI-STABILITY EFFECT AND NUCLEAR QUANTUM OPTICS**

**O. Khetselius**<sup>a</sup>

<sup>a</sup>Odessa University, P.O.Box 24a, Odessa-9, 65009, Ukraine

Present paper has for an object (i) to carry out numerical quantum computation of a temporal dynamics of populations differences at the resonant levels of atoms in a large-density medium in a non-rectangular form laser pulse and (ii) to determine possibilities that features of the effect of internal optical bi-stability at the adiabatically slow modification of effective field intensity appear in the sought dynamics. It is known that the dipole-dipole interaction of atoms in dense resonant mediums causes the internal optical bi-stability at the adiabatically slow modification of radiation intensity. The experimental discovery of bistable co-operative luminescence in some matters, in crystal of  $Cs_3Y_2Br_9Yb_3+$  particularly, showed that an ensemble of resonant atoms with high density can manifest the effect of optical bi-stability in the field of strong laser emission. The Z-shaped effect is actually caused by the first-type phase transfer. On basis of the modified Bloch equations, we simulate numerically a temporal dynamics of populations differences at the resonant levels of atoms in the field of pulse with the non-rectangular  $ch$  form. Furthermore, we compare our outcomes with the similar results, where there are considered the interaction between the ensemble of high-density atoms and the rectangularly- and sinusoidally-shaped pulses. The modified Bloch equations describe the interaction of resonance radiation with the ensemble of two-layer atoms taking into account the dipole-dipole interaction of atoms [1]. A fundamental aspect lies in the advanced possibility that features of the effect of internal optical bi-stability at the adiabatically slow modification of effective field intensity for pulse of  $ch$  form, in contrast to the pulses of rectangular form, appear in the temporal dynamics of populations' differences at the resonant levels of atoms. Modelling nuclear ensembles in a super strong laser field provides opening the field of nuclear quantum optics [2].

*Keywords:* Radiation; Laser; Atom

**References**

- [1] O. Khetselius, Photoelectronics 17 (2008) 37; A. Glushkov, O. Khetselius et al, Recent Advances in Theory of Phys. and Chem. Systems (Springer) 15 (2006) 285;
- [2] T.J. Burvenich, J. Evers, C.H. Keitel, Phys. Rev. Lett. 96 (2007) 142051; A. Glushkov, S. Malinovskaya, O. Khetselius, Europ. Phys. Journ. (2008). A. Glushkov, O. Khetselius et al, Recent Advances in Theory of Phys. and Chem. Systems (Springer) (2008);

# RELATIVISTIC CALCULATING THE HYPERFINE STRUCTURE PARAMETERS IN THE HEAVY-ELEMENTS AND LASER SEPARATION OF ISOTOPES AND NUCLEAR ISOMERS

O. Khetselius<sup>a</sup>

<sup>a</sup>Odessa University, P.O.Box 24a, Odessa-9, 65009, Ukraine

Relativistic calculation of the spectra hyperfine structure parameters for heavy elements is carried out. Calculation scheme is based on gauge-invariant QED perturbation theory with using the optimized one-quasiparticle representation at first in the theory of the hyperfine structure for relativistic atomic systems [1], [2]. Within the new method it is carried out calculating the energies and constants of the hyperfine structure for valent states of cesium  $^{133}\text{Cs}$ , Cs-like ion Ba, isotopes of  $^{201}\text{Hg}$ ,  $^{223}\text{Ra}$ ,  $^{252}\text{Cf}$  are defined. The contribution due to inter electron correlations to the hyperfine structure constants is about 120-1200 MHz for different states, contribution due to the finite size of a nucleus and radiative contribution is till 2 dozens MHz. Obtained data for hyperfine structure parameters are used in further in laser photoionization detecting the isotopes in a beam and the buffer gas for systematic studying the short-lived isotopes and nuclear isomers. We propose a new approach to construction of the optimal schemes of the laser photoionization method for further applying to problem of the nuclear reactions products detecting. It's studied the reaction of spontaneous  $^{252}\text{Cf}$  isotope fission on non-symmetric fragments, one of that is the cesium nucleus. The corresponding experiment on detecting the reactions products is as follows [1]. The heavy fragment of the Cf nucleus fission created in the ionized track 106 electrons which are collected on the collector during 2 mks. The collector is charged negatively 40mks later after nuclear decay and 10mks before the laser pulse action. The photo electrons, arisen due to the selective two-stepped photoionization are drafted into the proportional counter for their detecting. Usually a resonant excitation of Cs is realized by the dye laser pulse, the spectrum of which includes the wavelengths of two transitions  $6S_{1/2}-7P_{3/2}$  (4555Å) and  $6S_{1/2}-7P_{1/2}$  (4593Å). This pulse also realizes non-resonant photoionization of the Cs excited atoms. The disadvantages of the standard scheme are connected with non-optimality of laser photoionization one, effects of impact lines broadening due to the using the buffer gas, the isotopic shift and hyperfine structure masking etc. We proposed new laser photoionization scheme, which is based on a selective resonance excitation of the Cs atoms by laser radiation into states near ionization boundary and further autoionization decay of excited states under action of external electric field [2]. The corresponding optimal parameters of laser and electric fields, atomic transitions, states, decay parameters etc are presented.

*Keywords:* Radiation; Laser; Atom

## References

- [1] A. Glushkov, O. Khetselius et al, Nucl.Phys. A 734 (2004) e21; J.Phys. CS 35 (2006) 425; A. Glushkov, O. Khetselius et al, Recent Advances in Theory of Phys. and Chem. Systems (Springer) 15 (2006) 285;
- [2] O. Khetselius, Photoelectr. 16 (2007) 101; A. Glushkov, O. Khetselius et al, Recent Advances in Theory of Phys. and Chem. Systems (Springer) (2008);

## GENERATION OF X-RAY RADIATION AT THE INTERACTION OF CHARGE PARTICLES WITH DIELECTRICS

**V.P. Petukhov**

D.V. Scobeltsin Institute of Nuclear Physics, MSU, 119991 Moscow, Russia

The transmission of ions through dielectric capillaries has attracted considerable attention during recent years [1], [2] and [3]. As a result of experimental and theoretical studies performed, it was demonstrated that high transmission coefficient ions through a dielectric channel is explained by electrification of channel walls in the course of ions motion, followed by self-organization of a beam – wall charge system, i.e. a charge is generated, at which there are no more collisions of ions with the wall and no more changes in the charge distribution. In this work we investigate some properties of the characteristic X-rays induced by protons and electrons at the interaction of charge particles with dielectrics. The measurements of the X-rays are importance for an understanding of the mechanism transporting charge particles through glass capillaries.

It was measured Si-K rays excited by 100 keV protons impeding on the quartz plate. It is measured that the quartz emits three orders of magnitude stronger Si-K<sub>α</sub> rays than silicon samples. After the proton beam was turned off the X-ray detector was still counting radiation coming from the target. That is the residual activity has been observed in quartz sample. We have measured the yield of the enhancement X-rays and the duration of the residual emission as a function of the beam current, the pressure in the chamber and the angle of grazing. The results of the measurements indicate that the enhancement emission from the insulators is related with electrical charge-up and discharge on the bulk and on the surface of the target due to incident protons.

We also investigate the transmission of electrons with the energy from 1 keV to 30 keV through glass tube, poly-capillaries and tapered glass capillary. The experiment was conducted using chamber designed for electron and X-Ray spectroscopy measurements. Glass poly-capillaries were fabricated by M.A. Kumakhov, Institute for Roentgen Optics.

The main results of these measurements are: The transmission coefficient of electrons depends on the size of capillary and decreases with the increase of incident electron beam current. The transmission coefficient of electrons decreases with the increase of time of measurement and after that the curve flattens. Electron energy at the exit of glass tube differs by several percent from energy of incident electrons, i.e. the most part of electrons moves without collisions with the wall of the tube. From the X-ray spectrum at the exit of the glass tube follows that the part of the electrons ionizes the atoms of the wall during collision with the walls. The results of the measurements indicate that the transporting of the electrons through the glass capillary is related with electrical charge-up on the surface of the dielectric due to incident electrons.

Keywords: Proton, Electron, X-ray, Capillary, Dielectric

### References

- [1] S. Ninomiya, Y. Yamazaki, F. Koike, et. al, Phys. Rev. Lett. 78 (1997) 4557.
- [2] N. Stolterfoht, J.-H. Bremer, V. Hoffmann, et al, Phys.Rev.Lett. 88 (2002). 133201-1 – 4.
- [3] K A Vokhmyanina, L A Zhilyakov, A V Kostanovsky, et. al, Phys. A: Math. Gen. **39** (2006) 4775–4779

This work has been supported by INTAS Grant No. № 06-100012-8972

## ELECTRON-IMPACT EXCITATION OF Yb RESONANCE LINE

O.B. Shpenik, M.M. Erdevdy, J.E. Kontros

*Institute of Electron Physics, Ukr. Nat. Acad. Sci., 21 Universitetska str., 88017 Uzhgorod, Ukraine*

Studies of rare-earth atom excitation by electron impact, in particular, optical excitation functions (OEFs) is of specific interest by a number of reasons, including applied ones, i.e. creation of lasers using the above metal vapors as working media. Of particular interest is ytterbium atom, though the number of papers dedicated to relevant problems is quite scarce. This is primarily due to the complexity of the Yb atom spectrum, weak intensity of spectral lines and high temperature required to produce necessary concentration of atoms. One may mention two quite extensive studies on the studies of electron-impact excitation of Yb atom [1,2]. First of them deals with measurements of OEFs for 36 spectral transitions in Yb atom and ion. Electron energy spread of exciting electrons in both experiments was 0.8–1.2 eV. Therefore measured OEFs demonstrated quite smooth behavior with no distinct features.

Here we report on the results of Yb atom excitation by monoenergetic electrons near the threshold. Excitation of atoms was carried out in the gas-filled cell at the incident electron current of 100 nA (the energy spread being 50 meV (FWHM)) provided by a hypocycloidal electron monochromator [3]. The optical emission was separated by a diffraction monochromator and detected using a photomultiplier. An automated setup and measuring technique are described in [4]. Figure 1 shows the measured OEF for the Yb 398.8 nm ( $4f^{14}6s^2\ ^1S_0-4f^{14}6s6p\ ^1P_1^o$ ) resonance spectral line with the 50 meV energy step. As seen, this excitation function reveals several structural features at the energies 3.4, 3.9, 4.5, 5.5, 7.1, 8.1, 8.9 and 9.7 eV.

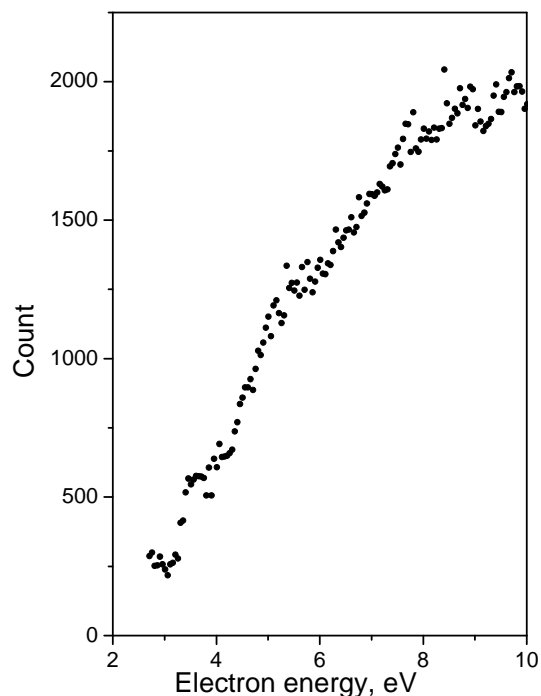


Fig. 1. The OEF of the  $\lambda_{398,8}$  nm resonance spectral line

Keywords: electron, atom, excitation.

This work was supported in part by the CRDF grant No. UKC2-2832-UZ-06.

### References

- [1] L.L. Shimon, N.V. Golovchak et al. *Opt.Spectr.* 50 (6) (1981) 1037.
- [2] P.V. Johnson, Y. Li et al. *J.Phys.B.* 31 (13) (1998) 3027.
- [3] O.B. Shpenik, N.M. Erdevdy et al. *Instrum.Exper.Tech.* 41 (1) (1998) 97.
- [4] O.B. Shpenik, N.M. Erdevdy et al. *Ukr.Phys.Journ.* 50 (4) (2005) 341.

## LOW-ENERGY ELECTRON SPECTROSCOPY OF Bi FILMS

O.B. Shpenik, T.Yu. Popik, R.O. Ortikov

Department of Ion Processes, Institute of Electron Physics, Ukr. Nat. Acad. Sci.,  
Universytetska Str. 21, Uzhgorod, Ukraine

Bismuth is well known as a typical representative of semimetals, its electronic properties being intermediate between those of metals and semiconductors. The electron energy structure of bismuth, responsible for its extraordinary properties, has been studied mostly by UPS and XPS techniques for both single crystals and films, sputtered on various substrates. However, the energy distribution of the density of bulk and surface electron states over the entire Brillouin zone for Bi has not been unambiguously determined yet. Besides, the processes of excitation of these states by slow electrons practically have not been investigated.

Here we report on the studies of the processes of elastic and inelastic scattering of slow (0-5 eV) monoenergetic electrons by Bi films, sputtered on a mirror surface of Si (100) and a rough ground surface of sapphire  $\text{Al}_2\text{O}_3$  (0001) in order to determine the energy distribution of surface and bulk electron states of Bi and the specific features of distribution of these states by slow electrons.

The experiments were performed on a high-vacuum ( $P \sim 10^{-7}$  Pa) automated setup, based on a hypocycloidal electron spectrometer (HES). The HES enables an electron beam to be formed and analyzed within the energy range 0–10 eV with a full width at half-maximum of ~20-50 meV. A typical feature of the HES is the possibility of detecting both elastically and inelastically scattered electrons within a small (1-3°) solid angle with a centre at the primary electron beam incidence point. A detailed description of the experimental setup and the measurement technique is given in [1].

Experiments of two types were performed: studies of energy dependences of elastically backscattered electron intensity and energy loss spectra at different excitation energies within the range 0–5 eV.

The intensity of electrons, elastically backscattered by the bismuth films under investigation within the range 0-5 eV is shown to decrease sharply with the incident electron energy increase.

The energy loss spectra are also characterized by a sharp decrease of the backscattered electron intensity with the excitation energy increase. Besides, the backscattered electron intensity also decreases with the energy loss increase. In the loss spectra, obtained for the films under investigation at different incident electron energies, distinct features are revealed, most likely determined by the excitation of bulk, surface, and/or resonance states of Bi. Existence of these states in this energy range was revealed earlier from UPS and XPS studies [2,3].

Further investigation with an improved energy resolution of the electron spectrometer and various type of the Bi films modification will enable the energy positions of the features observed to be determined more precisely and assigned to the excitation of certain electron transitions.

*Keywords:* Bismuth; Electron energy structure; Low-energy electron scattering

### References

- [1] O.B.Shpenik, N.M.Erdevdy, N.M.Romanyuk, T.Yu.Popik, A.N.Zavilopulo, Instr. Exp. Tech. 41(1998) 97.
- [2] R. Ast Christian, H. Hechst. Phys. Rev. B, 2002, 66, 125103.
- [3] A. Tanaka, M. Hatana, K. Takahashi, H. Sasaki, S. Suruki, S.Sato. Phys.Rev.B, 1999, 59, 1786.

## ON SURFACE ELEMENTARY PROCESSES AND POLYMER SURFACE MODIFICATIONS INDUCED BY DOUBLE PULSED DBD

**A. S. Chiper, A. V. Nastuta , G. B Rusu and G. Popa**

Plasma Physics Department, Al. I. Cuza University, 700506 Iasi, Romania

Plasma treatment is an efficient method used for improved wettability of the polymer surface and for surface roughness increasing. This is possible because plasma parameters as particle density, collision frequency, mean energy of the particles, presence of chemical active species will cause a large variety of elementary processes both within the plasma volume and on the plasma-polymer interface. In this way by controlling the plasma parameters might control the magnitude of the treatment effects on the polymer surface as etching, functionalization or crosslinking.

Function on the research purposes, the plasma can be generated in different gases, range of pressures or discharge geometries. The present experimental set-up consists of a plane-parallel geometry of dielectric barrier discharge (DBD) system, which presents a second current pulse with inverse polarity induced at the decreasing applied voltage flank in addition to the main current pulse. This kind of discharge is also named double DBD. The dielectric barriers were placed both on ground electrode and high voltage electrode. The experiments were made at room temperature, in helium with nitrogen gas mixture, without preliminary vacuum pumping.

The surface modifications of polymer (polyethylene terephthalate and polyethylene) samples were pointed out by two complementary methods: the contact angle method and Atomic Force Microscopy (AFM) technique. The plasma parameters (metastables density and current density) were analyzed by tunable diode laser absorption spectrometry technique (TDLAS) and electrical diagnosis. So, using the TDLAS technique has been proven that the highest density of oxygen metastables was located near cathode. Consequently, based on the fact that metastable atoms are very important for surface modifications [1] it results that an efficient plasma treatment of polymer surface will be obtained if the polymer samples are placed on the ground electrode.

The influence of the voltage pulse parameters as: width, raising and falling rate, amplitude and frequency on the secondary discharge formation was studied and correlated with polymer surface modifications. The most interesting result refers to the influence of the falling rate of the age pulse on the polymer surface modifications. Te pulsed DBD plasma treatment is improved when the discharge is driven by a voltage pulses with very fast falling flank.

Key words: symmetric dielectric barrier discharge, double DBD, surface treatment

### References

- [1] G. Placinta, F. Arefi-Khonsari, M. Gheorghiu, J. Amouroux, G. Popa,, J. Appl. Polym. Sci. (1997) 1367.

## MONOATOMIC DEEP NANOSTRUCTURES ON ALKALI HALIDE SURFACES INDUCED BY HIGHLY CHARGED IONS

**S. Facsko, R. Heller, R. Wilhelm, Z. Pešić and W. Möller**

Institute of Ion Beam Physics and Materials Research, Forschungszentrum Dresden-  
Rossendorf e.V., P.O. Box 510119, 01314 Dresden, Germany

Highly charged ions release a large amount of potential energy when interacting with solid surfaces [1]. Each ion can carry up to several tens of keV of potential energy which is deposited into a small surface area of a few nm<sup>2</sup> on an fs time scale. It has been found that up to 80% of this energy is retained into the surface [2]. Thus the electronic system is highly excited and the subsequent relaxation can induce structural, morphological, or chemical modifications in the topmost layers of the solid, especially in insulators and layered materials. Depending on the material hillock structures, e.g. on CaF<sub>2</sub> [3], and modifications in the electronic system, e.g. on HOPG, were observed [4].

We present atomic force microscopy (AFM) investigations of crystalline alkali halide surfaces after irradiation with slow, highly charged Xe ions. The Xe ions with charge state up to 35+ are extracted from a room temperature electron beam ion trap (EBIT) and decelerated to a kinetic energy of 40 keV. The alkali halide crystals were cleaved and shortly annealed in the vacuum chamber prior to irradiation. For high enough charge states each ion produces a mono atomic deep pit with a diameter of 15 - 50 nm (depending on charge state) on the atomically flat surface. Figure 1 shows an AFM image of a KBr(001) surface irradiated at a fluence of  $1 \times 10^{10}$  cm<sup>-2</sup> with Xe<sup>34+</sup> ions. The pits result from the simultaneous desorption of up to 3000 atoms from the first atomic layer. The desorption of such a high amount of material can not be induced by kinetic sputtering, which dominates in this kinetic energy regime, but is induced by the excitation due to the potential energy. The pit volume and therewith the sputtering yield exhibits a linear dependence on the potential energy. However, the kinetic energy also plays an important role. Evidence is presented that complex defect centers, i.e. several self-trapped excitons in a small volume, induced by the highly charged ions are responsible for the formation of the pit structures.

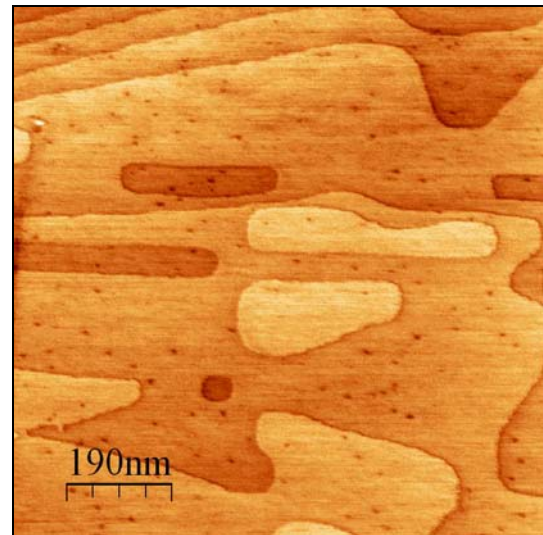


Fig. 1. AFM image of a KBr(001) surface irradiated with highly charged Xe<sup>34+</sup> ions and a fluence of  $1 \times 10^{10}$  cm<sup>-2</sup>.

**Keywords:** Highly Charged Ions; Potential Sputtering; Alkali Halides

### References

- [1] J. Burgdörfer, P. Lerner, F.W. Meyer, Phys. Rev. A (1991) 5674.
- [2] D. Kost, S. Facsko, W. Möller, R. Hellhammer, N. Stolterfoht, Phys. Rev. Lett. 98 (2007) 225503.
- [3] A. S. El-Said et al., Nucl. Instrum. Meth. B 256 (2007) 346.
- [4] I. C. Gebeshuber, S. Cernusca, F. Aumayr, H. P. Winter, Int. J. Mass Spectrom. 229 (2003) 27.



# TRANSMISSION OF 4.5 keV Ar<sup>9+</sup> IONS THROUGH A SINGLE MACROSCOPIC GLASS-CAPILLARY

R. J. Bereczky<sup>a</sup>, G. Kowarik<sup>b</sup>, F. Aumayr<sup>b</sup> and K. Tökési<sup>a</sup>

<sup>a</sup>Institute of Nuclear Research of the Hungarian Academy of Sciences, Debrecen, Hungary

<sup>b</sup>Institute für Allgemeine Physik, Technische Universität Wien, Austria

Investigations of the interactions of highly charged ions (HCI) with internal surfaces recently became available due to the advances in the fabrication of nano-, micro-, and macrocapillaries. The first measurements were performed using metallic microcapillaries and the obtained experimental data were in good agreement with theoretical predictions. Then investigations of HCIs and insulating nanocapillaries became available. In contrast to the case of metallic capillaries guiding of the charged particles through nanocapillaries tilted by large angles with respect to the direction of the incident beam was discovered [1]. However, the slow HCI projectiles were not only able to simply pass through the tilted capillaries, but they unexpectedly did so by keeping their initial charge state as a consequence of a self-organized charge-up inside the capillary.

Since the experiments so far have used thin insulating foils with randomly distributed capillaries (produced by swift heavy ion bombardment) or ordered arrays of regular nanocapillaries, collective effects due to the presence of neighboring capillaries must be also taken into account for an accurate simulation of the ion trajectories. These collective effects make a full theoretical description of the interaction between charged particles and insulator capillary walls rather difficult.

To obtain an easier situation for comparison with simulation, we have investigated the transmission of 4.5 keV Ar<sup>9+</sup> ions through a single, cylindrical-shaped glass capillary of macroscopic dimensions (0.17 mm diameter and 11 mm length) produced in ATOMKI. The measurements were carried out using HCI beams produced by the 14.5 GHz Electron Cyclotron Resonance Ion Source in Vienna. The glass capillary was positioned in an UHV chamber with a pressure of better than 10<sup>-8</sup> mbar. The beam was collimated by an aperture to a diameter of 3 mm and an opening angle of +/- 1.5° and the transmitted projectiles were recorded by a position sensitive channelplate detector [2]. As a result we found that a electric guiding field can also build-up inside such a macroscopic capillary and that slow HCIs can be transmitted in wide range of the tilt angles (see Fig. 1.) in a similar manner than for the case of nano-capillaries.

The work was supported by the “Stiftung Aktion Österreich-Ungarn” grant no. 67öu3, the Hungarian National Office for Research and Technology, the grant “Bolyai” from the Hungarian Academy of Sciences, as well as Austrian FWF (P17449).

*Keywords:* capillaries, highly charged ion, ion guiding

## References

- [1] N. Stolterfoht *et al.*, Phys. Rev. Lett. **88** (2002) 133201.
- [2] M. Fürsätz *et al.*, J. Phys. Conf. Proc. of HCI **58** (2007) 319.

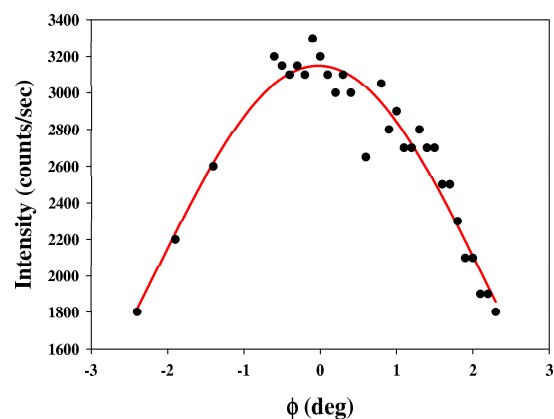


Fig. 1. Angular distribution of 4.5 keV Ar<sup>9+</sup> projectiles passing through a single glass macrocapillary. The solid line is a Gaussian fit of the measured data.

## MCP IMAGES OF IONS TRANSMITTED THROUGH ION GUIDING ALUMINA CAPILLARIES

**Z. Juhász<sup>a</sup>, B. Sulik<sup>a</sup>, Gy. Víkor<sup>b</sup>, S. Biri<sup>a</sup>, I. Iván<sup>a</sup>, K. Tókési<sup>a</sup>, E. Takács<sup>b</sup>, S. Mátéfi-Tempfli<sup>c</sup>, M. Mátéfi-Tempfli<sup>c</sup>, L. Piraux<sup>c</sup>, J. Pálinkás<sup>b</sup>**

<sup>a</sup>Institute of Nuclear Research (ATOMKI), Bem tér, 18/c, H-4026 Debrecen, Hungary

<sup>b</sup>Dep. of Exp. Physics, University of Debrecen, Egyetem tér 1, H-4032 Debrecen, Hungary

<sup>c</sup>Unité de Physico-Chimie et de Physique des Matériaux, Université Catholique de Louvain (UCL), Place Croix du Sud, 1, B-1348 Louvain-la-Neuve, Belgium

Insulating nanocapillaries have attracted considerable attention since the discovery of capillary guiding [1]. Recent experiments have shown that slow charged projectiles (highly charged ions) are guided through nanocapillaries avoiding collisions with the capillary walls. Collecting experimental data with different kind of materials is of great importance for the understanding of this self-organizing phenomenon.

In the present study we measured the two-dimensional angular distribution of 3-6 keV  $\text{Ne}^{6+}$  ions transmitted through  $\text{Al}_2\text{O}_3$  capillaries with diameters of a few 100 nm. The ions were detected by a position sensitive MCP detector.

We observed the guiding phenomenon as in our earlier one-dimensional experiments [2], i.e. ions left the capillaries in directions close to the capillary axes.

We performed charge state analysis by applying electric fields in front of the detector to separate the different charge states. We found that all the transmitted ions are in their initial charge state. However we observed significant neutral emission from the samples, even at large tilt angles of the capillaries. Earlier similar observations were found for polymer capillaries [3], where the neutral emission was explained by the neutralization of Ne ions. The fact that no ions with lower charge state than the initial were detected suggests that the neutral particles are UV photons instead of neutralized Ne ions. The MCP is UV sensitive, and UV photons can be created in electron capture processes, when the ions get close contact with the capillary walls.

### *Acknowledgments*

This work was supported by the Hungarian National Science Foundation OTKA (Grant No's: T046905 and PD050000), and in part by the Belgian Science Policy through the Interuniversity Attraction Pole Program IAP (P5/1/1).

### **References**

- [1] N. Stolterfoht et al., Phys. Rev. Lett. **88** (2002) 133201-1.
- [2] S. Mátéfi-Tempfli et al., Nanotechnology **17** (2006) 3915.
- [3] Y. Kanai et al., Nucl. Instr. and Meth. in Phys. Res. B **258** (2007) 155–158.

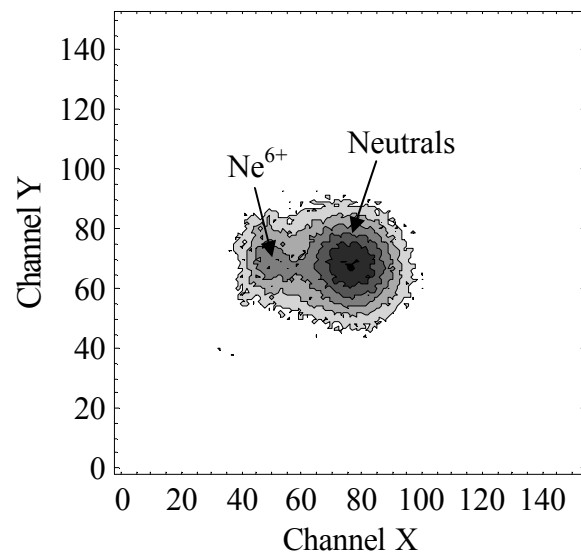


Fig. 1. 2-D image of transmitted  $\text{Ne}^{6+}$  ions through an  $\text{Al}_2\text{O}_3$  capillary sample. The sample was tilted by  $10^\circ$ . Different charge states are separated by an electric field. Ions in their initial charge states and neutrals (most likely to be photons, see text) were observed.

## INTERPLAY OF COULOMB EXPLOSION AND BINARY PROCESSES IN FRAGMENTATION OF MOLECULES BY HIGHLY CHARGED ION IMPACT

**Z. Juhász<sup>a</sup>, J.-Y. Chesnel<sup>b</sup>, F. Frémont<sup>b</sup>, A. Hajaji<sup>b</sup>, B. Sulik<sup>a</sup>**

<sup>a</sup>Institute of Nuclear Research (ATOMKI), Bem tér, 18/c, H-4026 Debrecen, Hungary

<sup>b</sup>CIRIL Unité Mixte CEA-CNRS-EnsiCaen-Université de Caen Basse-Normandie, F-14050Caen Cedex 04, France

Studying fragmentation processes of biologically relevant molecules due to highly charged ion impact is important to understand radiation damage in biological tissues. Non-coincident ion spectroscopy is a fast and rather sensitive method to study the double differential energy spectra of the charged molecule fragments. Energy spectra reveal the most important fragmentation patterns [1].

In the present work, we study anisotropies in fragment distribution due to electron transfer processes leading to the explosion of small molecules. The experiments have been performed at the ARIBE facility at GANIL, Caen (France). Fragmentations of H<sub>2</sub>O, C<sub>6</sub>H<sub>6</sub> and CH<sub>4</sub> molecules, which represent different levels of symmetry, have been studied by 30-60 keV N<sup>6+</sup> ion impact. Sample spectra of the charged fragments taken at different observation angles (with respect to the incident beam direction) are shown for C<sub>6</sub>H<sub>6</sub> in Figure 1.

At energy of ~2.5 eV, a structure dominates, originating mainly from heavy fragments. At energies larger than ~4 eV, the structures can be attributed to the lighter molecular fragments, in a large part, to protons, following the Coulomb explosion of multiply charged C<sub>6</sub>H<sub>6</sub> after the electron-capture process. Nearly the same applies for the other molecules.

For fragment energies larger than 20 eV, significant anisotropies are found in the angular distributions. This is the region, where a high degree of multiple ionization by electron transfer is likely, leading to large kinetic energy values of the multiply charged fragment ions. The anisotropies are increasing with decreasing collision energies. High degree of ionization corresponds to small impact parameters, which implicate the role of binary processes in fragmentation in accordance with the observed angular and energy dependences.

In contrast with C<sub>6</sub>H<sub>6</sub>, the angular distributions for H<sub>2</sub>O present significant anisotropy in the wide energy range from 2 to 100 eV. Some experiments have been performed with O<sup>7+</sup> and show clearly different fragmentation patterns. These observations are yet to be explained.

### Acknowledgement

This experiment was performed at the distributed LEIF-Infrastructure at ARIBE, GANIL, France, supported by Transnational Access granted by the European Project HPRI-CT-2005-026015. The work was supported by the Hungarian National Science Foundation OTKA (Grant No's: T046905 and PD050000).

### References

- [1] P. Sobocinski, Z. D. Pešić, R. Hellhammer, D. Klein, B. Sulik, J.-Y. Chesnel and N. Stolterfoht, J. Phys. B **39** (2006) 927.

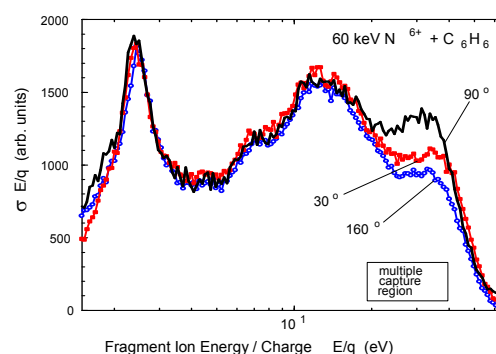


Fig. 1. Energy spectra of light and heavy fragments in collisions of 60 keV N<sup>6+</sup> and C<sub>6</sub>H<sub>6</sub>.

## THERMALLY INDUCED FRAGMENTATION OF NEUTRAL AND CHARGED C<sub>60</sub>

Titus Adrian Beu, Lóránd Horváth, Ioan Ghişoiu

*University "Babeş-Bolyai", Faculty of Physics, Cluj-Napoca 400084, Romania*

We investigated the radiation induced fragmentation of C<sub>60</sub> fullerene using tight-binding molecular dynamics and the parameterization scheme of Papaconstantopoulos et al. Fragment size distribution was averaged on a random set of initial configurations for excitation energies in the range of 50-1000 eV and with different initial ionizations, between 0e and 18e.

Excitation energy was introduced instantaneously in the system. We have considered integer total charges of the initial fullerene, but throughout the fragmentation process the charge distribution over different fragments was allowed to be fractional, with a view to mimicking the *average* charges of the fragments in typical experiments.

We focus on fragment size distributions, especially in the transition region from low energies (where asymmetrical dissociation occurs) to high energies (where an exponential decay in fragment size distribution of small fragments is observed).

We also investigated the effect of ionization on fragment size distribution and especially on the energy range where phase transition occurs.

With low excitation energy the fragmentation process occurs through sequential C<sub>2</sub> evaporation and therefore a U-shape fragment size distribution is formed. For high excitation energies predominantly multifragmentation occurs and a power law dependence of small size fragments is observed. For low energies however, the fragment distributions are not peaked at  $n=1$  but at higher values. With the increase of the excitation energy the peak moves at  $n=1$  and no fragments with  $n > 30$  appear.

The different ionizations included in our simulations seemed to decrease the energy necessary for phase transition. We calculated the charge for which no excitation energy is needed in order for the fragmentation process to occur.

The results are compared with experimental fragment size distribution spectra involving C<sub>60</sub> fragmentation, carried out with time of flight mass spectrometers. We analyzed the fragment size distribution with respect to energy, as well as the relative number of fragmented trajectories (phase transition) with respect to excitation energy and charge.

## FRAGMENTATION OF GLYCINE MOLECULE BY LOW-ENERGY ELECTRONS

V.S. Vukstich, A.I. Imre, A.V. Snegursky

Institute of Electron Physics, Ukr.Nat.Acad.Sci., 21 Universitetska str., 88017 Uzhgorod, Ukraine

It is well-established fact that interaction of ionizing radiation with live tissue results in irreversible effects at the genetic level. The mechanisms of cell material degradation include both direct action of high-energy ionizing radiation and indirect processes related to the chemical structure transformations under the influence of low-energy secondary electrons produced resulted from the incident ionizing radiation. The latter are capable of damaging the building blocks of nucleic acids, amino acids and DNA bases, leading, in particular, to single- and double-strand breaks, dissociative ionization etc.

Here we report on the first results of studies on fragmentation of the glycine molecule in its collisions with low-energy monoenergetic electrons. We have applied the crossed-beam technique with subsequent mass separation of collision products using the magnetic mass spectrometer to select the ions produced in the above reaction. The details of the apparatus and experimental technique will be presented at the conference.

The main problem here is related to the fact that the molecules of biological relevance, which glycine belongs to, undergo strong fragmentation due both to the effects of low-energy electron impact and thermal degradation in the process of molecular beam formation. It is essential, therefore, to trace the production of initial molecule fragments in the above processes. We tried to distinguish these two competing mechanism by measuring the yields of ionized fragments of the initial molecule in different conditions of formation of the molecular beam.

Figure 1 shows the mass spectrum of glycine molecule obtained at the 66 eV ionization energy and  $T = 80^\circ\text{C}$  temperature demonstrating the principal fragments of the initial molecule produced by electron impact. These results confirm the data of, e.g., Jochims et al [2] on the production of glycine molecule fragments. It is clearly seen that the main product of this process is the  $\text{CH}_4\text{N}^+$  ( $m=30$  a.m.u.) fragment, the peak intensity of which exceeds considerably those of other fragments. This fragment results, most probably, from simple bond rupture of the parent molecular ion accompanied by a loss of the  $\text{CHO}_2$  group. Figure 2 presents the temperature dependence of the above ion yield at the incident electron energy of 66 eV. This dependence has a distinct exponential shape showing a substantial rise in fragmentation above  $70^\circ\text{C}$  and proving the fact that thermal degradation plays an important role in the production of primary molecule fragments.

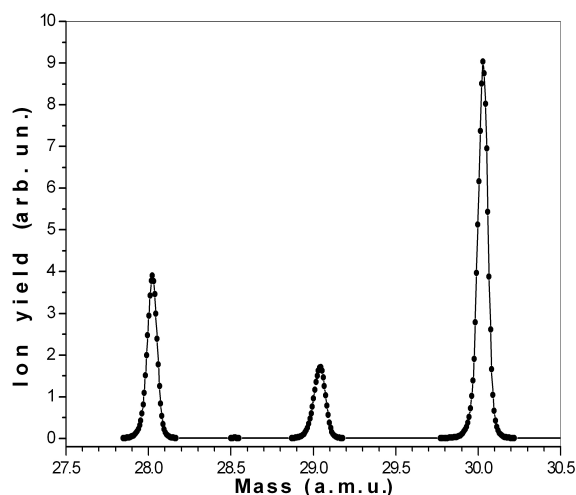


Fig. 1. Mass spectrum of glycine molecule

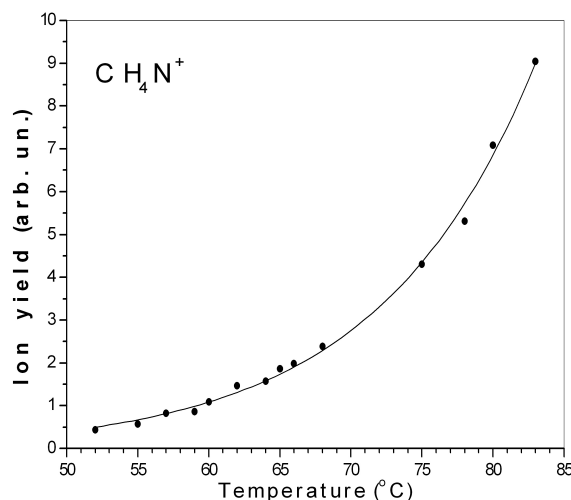


Fig. 2.  $\text{CH}_4\text{N}^+$  ( $m=30$ ) yield as a function of temperature

This work was supported in part by the CRDF grant No. UKC2-2832-UZ-06.

**Keywords:** Biomolecule; Fragmentation; Mass Spectrum.

### References

- [1]. H.-W. Jochims *et al*, Chem.Phys. **298** (2004) 279

# ABOVE-THRESHOLD IONIZATION OF CALCIUM BY LINEARLY AND CIRCULARLY POLARIZED LASER PULSES

G. Buica

Institute for Space Sciences, P.O. Box MG-23, Ro 77125, Bucharest-Măgurele, Romania

Multiphoton ionization (MPI) and above-threshold ionization (ATI) represent well-studied processes [1, 2]. Above-threshold ionization is a process in which atoms absorb more than the minimum number of photons required to be ionized, the photoelectron energy spectrum (PES) consisting of a series of peaks that are equally separated by the photon energy.

The aim of this work is to extend our previous investigations for Mg [3, 4, 5] to a more complex two-valence-electron atom such as Ca: We theoretically study MPI and ATI of Ca in a linearly/circularly polarized femtosecond laser pulse. For this purpose we employ a nonperturbative method in order to solve the time-dependent Schrödinger equation on an atomic basis of discretized states. Atomic structure calculations are performed using frozen-core Hartree-Fock [6] and also model potential approaches and the results are compared. We investigate the dynamics of the ionization process for different laser pulse durations and temporal profiles.

We report theoretical results for multiphoton ionization of Ca, in its ground state  $4s^2\ ^1S$ , by the second and third harmonic of a Ti-Sapphire laser field. The photoelectron energy spectrum and the ionization yield calculated as a function of the laser peak intensity are studied at the end of the laser pulse. The relative dense electronic structure of the Ca atom and the core-valence correlation might add new features in the PES, depending on laser intensity and pulse duration. We expect that the ATI photoelectron energy spectrum may exhibit intermediate peaks that are due to ionization from the bound excited states of the Ca atom. Moreover the main ATI peaks from the photoelectron energy spectra could exhibit substructures that are also due to the rich electronic structure of the Ca atom.

*Keywords:* Above-threshold ionization; Laser; Calcium

## References

- [1] K. Burnett, V. C. Reed, and P.L. Knight, *J. Phys. B* **26** (1993) 561.
- [2] L. F. DiMauro and P. Agostini, *Adv. At. Mol. Opt. Phys.* **35** (1995) 79.
- [3] T. Nakajima and G. Buica, *Phys. Rev. A* **74** (2006) 023411.
- [4] G. Buica and T. Nakajima, *J Quant Spectrosc Rad. Transfer* **109** (2008) 107.
- [5] L.A.A. Nikolopoulos, G. Buica-Zloh, and P. Lambropoulos, *Eur. Phys. J. D* **26** (2003) 245.
- [6] T.N. Chang *Many-body theory of Atomic Structure and Photoionization*, (World Scientific, Singapore) (1993) 213.

# ANGULAR MOMENTUM IN ATOMIC IONIZATION BY SHORT LASER PULSES: MULTIPHOTON VERSUS SEMICLASSICAL TUNNELING MODEL

D. G. Arbó <sup>a</sup>, K. I. Dimitriou <sup>b</sup>, E. Persson <sup>c</sup>, and J. Burgdörfer <sup>c</sup>

<sup>a</sup> Institute for Astronomy and Space Physics, IAFE, CC67, SUC. 28 (1428) Buenos Aires, Argentina

<sup>b</sup> Physics Department, National Technical University, Athens, Greece

<sup>c</sup> Institute for Theoretical Physics, Vienna University of Technology, Vienna, Austria

In atomic ionization by few-cycle laser pulses doubly-differential momentum distributions near threshold exhibit a radial nodal structure that results from peaked partial wave distribution near a particular angular momentum [1]. Recently, two different mechanisms were proposed to understand the populations of the different partial waves: (i) A biased random walk model assuming stochastic uncorrelated multi-photon processes [2], and (ii) a quasiclassical tunneling ionization process [1] calculated using classical-trajectory Monte-Carlo [3] simulations which incorporate tunneling through the potential barrier (CTMC-T). We compare these two models to results of momentum distribution of emitted electrons by solving the time dependent Schrödinger Equation (TDSE) and analyze near-threshold structures for different atomic species of the target.

It can be observed in Fig. 1 that both random walk multiphoton and quasiclassical tunneling model can predict the first moment of the TDSE distribution. However, in a Poissonian random walk model a broad distribution is observed at variance with both the TDSE and the quasiclassical CTMC-T results. For Keldysh parameters below or close to one, the narrow angular momentum distribution near threshold is the result of a tunneling process at variance with a broad Poissonian distribution resulting from a multiphoton random walk. We also find that the dominant angular momentum near threshold depends strongly on the laser frequency and peak field but not on the atomic species. This relation is reminiscent of generalized Ramsauer-Townsend diffraction oscillations [1]. As in the case of electron-ion scattering theory [4], it results from the existence of interfering paths under the influence of two competing forces: the atomic Coulomb potential and the electric field of the laser.

Work supported by Conicet (Argentina) and by SFB 016 ADLIS and project P15025-N08 FWF (Austria).

**Keywords:** Tunneling photoionization; Short-laser pulse; Angular momentum.

## References

- [1] D. G. Arbó *et al.*, Phys. Rev. Lett. **96**, 143003 (2006).
- [2] Z. Chen *et al.*, Phys. Rev. A **74**, 053405 (2006).
- [3] K. I. Dimitriou *et al.*, Phys. Rev. A **70**, 061404(R) (2004).
- [4] J. Burgdörfer, C. Reinhold, J. Sternberg, and J. Wang, Phys. Rev. A **51**, 1248 (1995).

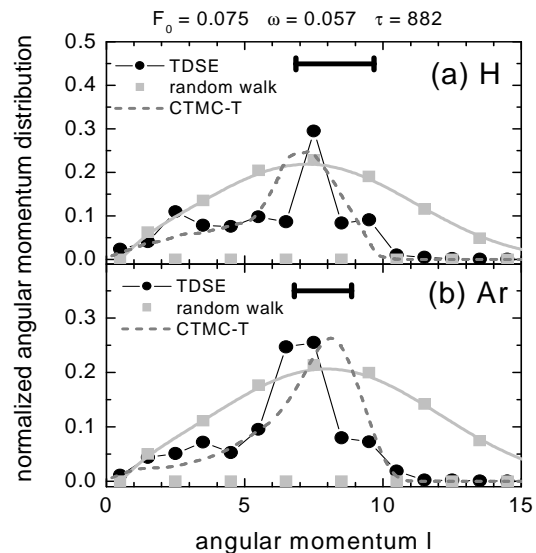


**Fig. 1:** Angular momentum distribution for the first ATI peak for (a) H and (b) Ar. Dots correspond to TDSE calculations, squares to the multiphoton model (connecting lines are only meant to guide the eye). The dashed line shows the quasiclassical distribution (CTMC-T). Horizontal bars correspond to the semiclassical prediction [2]

## POLARISATION EFFECTS IN EXCITATION OF STRONG PERTURBED ATOMIC STATES

**Bondar I.I., Suran V.V.**

Physical Department of Uzhgorod National University, Voloshin str.54, 88000 Uzhgorod,  
Ukraine

We studied experimentally the two-photon excitation of  $5d7s^3D_2$  state of  $Ba$  atom strongly perturbed in result of ac-Stark effect realisation. The perturbation of this state was fulfilled by influence of YAG-laser radiation. For excitation of this state we used the tunable dye laser radiation. The investigations were performed by the resonant ionization spectroscopy method. We measured the  $Ba^+$  ions yield caused by the ionization of  $Ba$  atoms through the two-photon resonance with perturbed  $5d7s^3D_2$  state in cases when the electric vectors of both used radiations were parallel and orthogonal. The results of our investigations are presents in figure.

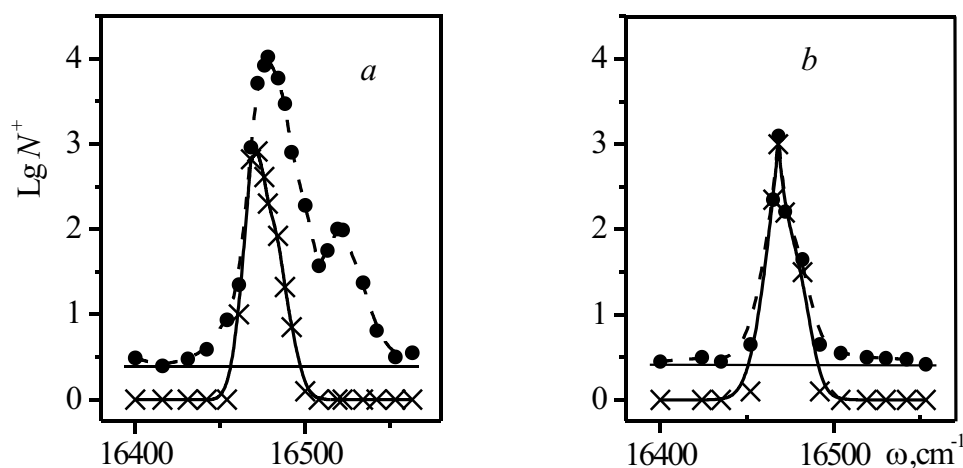


Fig. Dependences of the yield of  $Ba^+$  ions ( $N^+$ ) on the dye laser frequency  $\omega$ , measured under the conditions when the dye laser radiation acted on  $Ba$  atoms independently (crosses and solid lines) and simultaneously with the YAG laser radiation (circles and dashed lines). The average yield of  $Ba^+$  ions formed under the action of only YAG laser radiation is shown by solid horizontal lines. The electric vectors of the dye and YAG laser radiations are (a) parallel and (b) perpendicular to each other.

As follows from these figures the yield of  $Ba^+$  ions at simultaneous influence of both (YAG- and dye-lasers) radiations with parallel orientation of their electric vectors is large than its yield in case of influence only dye-lasers radiation. Note, that the resonant structure at influence only of dye-lasers radiation is caused by ionization of  $Ba$  atoms trough resonant with unperturbed  $5d7s^3D_2$  state. The resonant maximum in  $Ba^+$  ions yield at  $16520 \text{ cm}^{-1}$  is caused by increasing of probability of perturbed  $5d7s^3D_2$  state ionization in result of one-photon resonance with autoionising  $5d4f [3/2]^0_1$  state. In case of orthogonal orientation of electric vectors the  $Ba^+$  ions yield is the same as at influence only dye-lasers radiation. From these results follows that the excitation of perturbed state  $5d7s^3D_2$  is realised only in case, when the electric vectors of perturbed and excited radiations have the same orientations.

*Keywords:* Multiphoton excitation; Perturbation of atomic spectra; ac-Stark effect.



## OBSERVATION OF NEW TYPE RESONANT MAXIMA AT FORMATION OF DOUBLY CHARGED IONS UPON MULTIPHOTON IONIZATION OF BARIUM ATOMS BY LINEARLY AND CIRCULARLY POLARIZED RADIATION

**Suran V.V. and Bondar' I.I.**

Department of Physics, Voloshin str. 54, Uzhgorod 88000, Uzhgorod National University, Ukraine

Beginning with studies [1], in which the formation of doubly charged ions upon multiphoton ionization of atoms was discovered, the mechanism of their formation is extensively investigated. Our studies of formation of  $Ba^+$  and  $Ba^{2+}$  ions allow us to make the following conclusions: (i) in the majority of cases, the resonance maxima in the yields of the  $Ba^+$  and  $Ba^{2+}$  ions appear at different frequencies of the laser radiation; (ii) the resonance maxima in the yield of  $Ba^{2+}$  ions have widths from 5 to 40  $cm^{-1}$  and amplitudes from one to four orders of magnitude; (iii) some resonance maxima in the dependences  $N^{2+}(\omega)$  are observed for both linear and circular polarizations of the laser radiation, while other maxima exist only in the case of linear or circular (*unusual maxima*) polarization.

Comparing the transitions in the spectrum of  $Ba^+$  ions that correspond to the frequencies  $\omega_t$  and the maxima appearing at different polarizations of radiation, we can divide the maxima into the following five types:

(A)- The resonance maxima appear for linear and circular polarizations of radiation and the resonance transitions in the spectrum of  $Ba^+$  ions at the corresponding frequencies  $\omega_t$  are allowed for these two polarizations. These resonance maxima can be uniquely identified with the resonance transitions in the spectrum of  $Ba^+$  ions at the corresponding frequencies  $\omega_t$  because these transitions are allowed by the selection rules both for linear and circular polarizations. This fact unambiguously proves the realization of the cascade mechanism of formation of  $Ba^{2+}$  ions in the vicinity of the frequencies  $\omega_t$  corresponding to the localization of resonance maxima in the dependences  $N^{2+}(\omega)$ .

(B)- The resonance maxima appear only for linear polarization of radiation and the resonance transitions in the spectrum of  $Ba^+$  ions at the corresponding frequencies  $\omega_t$  are allowed only for this polarization.

(C)- The resonance maxima appear only for linear polarization of radiation, but the resonance transitions in the spectrum of  $Ba^+$  ions at the corresponding frequencies  $\omega_t$  are allowed for both linear and circular polarizations of radiation.

The B and C types maxima also point to the cascade mechanism of formation  $Ba^{2+}$  ions near frequencies  $\omega$ . The some part maxima (type D) are observed both for linear and circular, or only linear polarization and cannot be identified with the resonance transitions in the spectrum of Ba atoms and  $Ba^+$  ions.

(E)- The resonance maxima appear only for circular polarizations of radiation and cannot be identified with the resonance transitions in the spectrum of Ba atoms and  $Ba^+$  ions. These facts proves the realization of the non-cascade mechanism of formation of  $Ba^{2+}$  ions in the vicinity of the frequencies  $\omega$  corresponding to the localization of the above considered resonance maxima in the dependences  $N^{2+}(\omega)$ .

*Keywords:* multiphoton ionization; doubly charged ions; cascade mechanism; two electron mechanism

### References

- [1] Suran V. V. and Zapesochnyi I. P., Sov. Tech. Phys. Lett. **1** (1975) 420.

# MULTIPHOTON IONIZATION OF ATOMS WITH SHORT INTENSE LASER PULSES CLOSE TO RESONANCE CONDITIONS

V. D. Rodríguez<sup>a</sup>, D. G. Arbó<sup>b</sup> and P. A. Macri<sup>c</sup>

<sup>a</sup>Departamento de Física, FCEyN, Universidad de Buenos Aires, 1428 Buenos Aires, Argentina

<sup>b</sup>Institute for Astronomy and Space Physics, Buenos Aires, Argentina

<sup>c</sup>Departamento de Física, Universidad Nacional de Mar del Plata, Mar del Plata, Argentina

In this work, we study Hydrogen ionization by a few cycle laser pulse when the laser frequency is close to the first excitation level ( $2p_0$ ) resonance. With this aim, we compare results of time dependent Schrödinger equation simulations (TDSE) [1] with three simple theoretical approaches based on Coulomb-Volkov (CV) wave functions. In the first one, called previously ( $CV2^-$ ) the final state time-dependent wave function is approximated by the CV wave function for the continuum of the electron in the field of the nucleus and the laser pulse. This approximation has an excellent agreement with TDSE computations as long as the laser frequency is greater than atom ionization energy [2]. For lower frequencies, an improved theory called  $MCV2^-$  was developed, which takes into account the pathways through intermediate bound states [3] in the First Born Approximation. However, close to resonance this latter approximation overestimate the ionization probabilities. An improvement is achieved by using the close coupling method that accounts transitions between bound states in more accurate form although neglecting the coupling with the continuum states. The method called close-coupling  $CV2^-$  ( $CC-CV2^-$ ) reproduces fairly well the total ionization probabilities. This can be appreciated in Fig. 1, where H(1s) total ionization probability by a 30 cycle and  $F = 0.02$  au amplitude laser pulse as a function of the laser frequency near the  $1s - 2p$  resonance energy  $\omega_0 = 0.375$  au. We can observe that  $CV2^-$  results do not show any enhancements around the resonance. On the other hand  $MCV2^-$  display such a behavior but overestimate by a factor two the ionization probabilities. Finally the new  $CC-CV2^-$  approximation is able to describe both qualitative and quantitative the TDSE results.

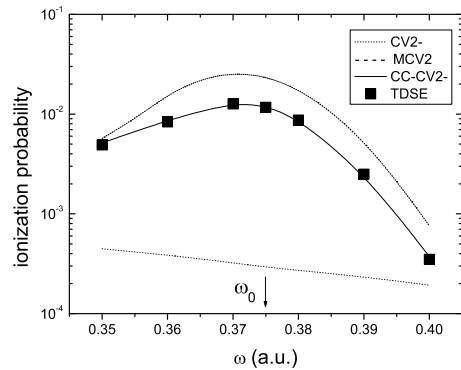


Fig. 1. H(1s) total ionization probabilities as a function of the laser frequency. Symbols, TDSE; full line,  $CC-CV2^-$  results; dashed line,  $MCV2^-$ ; dotted line,  $CV2^-$ .

*Keywords:* Short laser pulses; multiphoton ionization

## References

- [1] D. G. Arbó *et al*, Phys. Rev. Lett. **96** (2006) 143003.
- [2] G. Duchateau, E. Cormier and R. Gayet, Phys. Rev. A **66** (2002) 023412; P. A. Macri, J. E. Miraglia, and M. S. Gravielle, J. Opt. Soc. Am. B **20** (2003) 1801.
- [3] V.D. Rodríguez, E. Cormier and R. Gayet, Phys. Rev. A **69** (2004) 053402.

## NON-INVASIVE MARKERS MEASUREMENTS

**M.Culea<sup>a</sup>, O. Cozar<sup>a</sup>, E. Culea<sup>b</sup>**

<sup>a</sup>“Babes-Bolyai” University, Str. M. Kogalniceanu, Nr. 1, Cluj-Napoca, 400084, Romania

<sup>b</sup>Technical University of Cluj-Napoca, 400020 Cluj-Napoca, Romania

Organic biomarkers exhaled or present in urine of healthy and patients suffering of diabetes or other diseases were measured by using non-invasive sampling and analysis with gas chromatography-mass spectrometry (GC-MS). Acetone was measured by using halothane as internal standard. The methods were validated for quantitative determination by studying the parameters of linearity, precision, accuracy, limit of detection. Comparative results for some VOCs in urine or breath by different methods are presented.

Keywords: Diabetes, GC-MS, diagnosis

### References

- [1] C. Deng, N. Li, X. Wang, X. Zhang, J. Zeng, Rapid Commun Mass Spectrom.; 19 (2005), 647-6453.
- [2] M. Phillips, R.N. Cataneo, T. Cheema, J. Greenberg, Clin Chim Acta.; 344 (2004), 189-194.
- [3] R. J Delfino, H. Gong, W.S. Linn, Y. Hu, E.D. Pellizzari, J Expo Anal Environ Epidemiol.; 13 (2003):348-363

## RESIDUAL CHARACTERIZATION OF SOME PESTICIDES IN WINE

**M. Culea<sup>a</sup>, C. Lehene<sup>a</sup>, O. Cozar<sup>a</sup>**

<sup>a</sup>“Babes-Bolyai” University, Str. M. Kogalniceanu, Nr. 1, Cluj-Napoca, 400084, Romania

A method for the determination of some pesticide residues in wine samples was developed using solid-phase microextraction (SPME) and gas chromatography-mass spectrometry (GC-MS). The procedure needs the dilution as sample pre-treatment and is simple, fast and solvent-free. Some fungicides and insecticides were quantified. The reproducibility of the measurements was found acceptable, RSDs below 20%. Detection limits of 20 µg/L were good for the maximum admissible concentration for these compounds in wine.

The analytical method was applied to the determination of these compounds in Jidvei wine samples from the market.

Keywords: GC/MS; SPME, pesticides

## CHARACTERIZATION OF SOME PLANT EXTRACTS BY GC-MS

**A. Iordache<sup>a</sup>, M. Culea<sup>b</sup>, O. Cozar<sup>a</sup>**

<sup>a</sup>“Babes-Bolyai” University, Str. M. Kogalniceanu, Nr. 1, Cluj-Napoca, 400084, Romania

Recovery study by using different extraction methods is presented for a synthetic mixture of some compounds found in plants. The extraction was compared at the same variables in the optimization process: amount of samples, extracting solvent volume, extraction temperature, extraction time.

A liquid –liquid extraction method (LLE) was compared with two different solid-phase extraction method (SPE), a microwave one (MWE) and ultrasonic extraction one (USE). Good recovery values for a standard mixture were obtained. Precision of extraction methods gave relative standard deviation lower than 3%. The extracts were analyzed by GC and GC/MS. A HP-1 capillary column, 30m x 0.32 mm, 0.25µm film thick-ness, in a temperature program from 50<sup>0</sup>C, kept 2 minutes, then increased to 250<sup>0</sup>C, with a rate of 8<sup>0</sup>C per minute was used. Good recovery values, between 90-99% were obtained for all the extraction methods studied.

The study was applied for fingerprint chromatograms to characterize the flavors extracted from herb plants of different sources.

Keywords: GC/MS; LLE, SPE

**STATISTICAL STUDY OF DATA FOR CIRRHOSIS DIAGNOSIS BY GC/MS****C. Mesaros<sup>a</sup>, M. Culea<sup>a</sup>, O. Cozar<sup>a</sup>**<sup>a</sup>“Babes-Bolyai” University, Str. M. Kogalniceanu, Nr. 1, Cluj-Napoca, 400084, Romania

Two different methods have been used to study the pharmacokinetic data for cirrhosis diagnosis. Gas chromatographic-mass spectrometry (GC/MS) is one of the best methods used for measuring drugs. Applications are very important for purity control, pharmacokinetic studies, metabolic studies, clinical applications but also for treatment and diagnosis [1-3]. Due to the high sensitivity needed, the selected ion monitoring (SIM) mode was used in caffeine test measurements and isotopic dilution by adding known amounts of <sup>15</sup>N-theophylline as internal standard. A single dose of 4 mg/kg p.o. of caffeine was followed by blood concentrations measurements at two points, 1h and 9 h. Caffeine clearance, measured in patients with cirrhosis and chronic hepatitis, was reduced and half live time was increased in children with liver disease as compared with control.

Keywords: Cirrhosis, Caffeine test, GC-MS

**References**

- [1]. M. Culea, D.L. Hachey, Rapid Commun. Mass Spectrom., 9, (1995) 655- 659.
- [2]. M. Culea, P. Panta., M. Nanulescu, N. Palibroda, O. Cozar, I. Vintilă, Balcanic Physics Letters, 5, (1997) 1861-1864.
- [3].M. Culea, N. Palibroda, P. Panta Chereches, M. Nanulescu, Chromatographia, 53, (2001) S387- S390.

## Laser spectroscopic studies of collisional dynamics in antiprotonic helium

M. Hori

Laser spectroscopy division, Max-Planck-Institut für Quantenoptik,  
Hans-Kopfermann-Strasse 1, D-85748 Garching, Germany

Antiprotonic helium ( $\bar{p}\text{He}^+$ ) atoms are three-body Coulomb systems consisting of a helium nucleus, antiproton, and electron. The antiproton occupies a Rydberg state with high principal ( $n \sim 38$ ) and angular momentum ( $\ell \sim n - 1$ ) quantum numbers. We describe systematic experimental studies of various atomic collision processes associated with this atom carried out at CERN [1], namely:

- *Formation:* the  $\bar{p}\text{He}^+$  atom is formed when an antiproton is captured by a helium atom via the process  $\bar{p} + \text{He} \rightarrow \bar{p}\text{He}^+ + e^-$ . By laser spectroscopy we measured the distribution  $(n, \ell)$  of the states where this occurs [2, 3, 4, 5].
- *Collisional deexcitation:* some  $\bar{p}\text{He}^+$  states are rapidly destroyed by collisions with other helium atoms, whereas others retain microsecond-scale lifetimes at very high collision rates.
- *Internal Auger emission:* some  $\bar{p}\text{He}^+$  states have a large coupling to the electronic continuum, which causes the electron to be emitted via external Auger decay within several picoseconds to a few nanoseconds. We found that the Auger rates for some states are strongly enhanced by a coupling to an electronically excited  $\bar{p}\text{He}^+$  state [6].
- *Antiprotonic helium ion and collisional Stark effects:* After the Auger emission, a  $\bar{p}\text{He}^{2+}$  ion is produced. We measured the lifetime of these ions against annihilation of the antiproton via collisional Stark effects [7].

*Keywords:* antiprotonic helium; exotic atoms; collisional quenching

### References

- [1] M. Hori, A. Dax, J. Eades, K. Gomikawa, R.S. Hayano, N. Ono, W. Pirkl, E. Widmann, H.A. Torii, B. Juhász, D. Barna, D. Horvath, Phys. Rev. Lett. 96 (2006) 243401.
- [2] M. Hori, J. Eades, R.S. Hayano, T. Ishikawa, J. Sakaguchi, T. Tasaki, E. Widmann, H. Yamaguchi, H.A. Torii, B. Juhász, D. Horvath, T. Yamazaki, Phys. Rev. Lett. 89 (2002) 093401.
- [3] J.S. Cohen, Rep. Prog. Phys. 67 (2004) 1769.
- [4] J. Revai, N. Shevchenko, Eur. Phys. J. D 37 (2006) 83.
- [5] K. Tokesi, B. Juhász, J. Burgdorfer J. Phys. B 38 (2005) S401.
- [6] H. Yamaguchi, R.S. Hayano, T. Ishikawa, J. Sakaguchi, E. Widmann, J. Eades, M. Hori, H.A. Torii, B. Juhász, D. Horvath, T. Yamazaki, Phys. Rev. A 70 (2004) 012501.
- [7] M. Hori, J. Eades, R.S. Hayano, W. Pirkl, E. Widmann, H. Yamaguchi, H.A. Torii, B. Juhász, D. Horvath, K. Suzuki, T. Yamazaki, Phys. Rev. Lett. 94 (2005) 063401.

**INTERACTION OF POSITRONIUM ATOMS WITH PARAMAGNETIC  
MOLECULES MEASURED BY PERTURBED ANGULAR DISTRIBUTION IN  
3 - GAMMA ANNIHILATION DECAY**

E.A. Ivanov<sup>a</sup>, I. Vata<sup>a</sup>, S.Toderian<sup>a</sup>, D. Dudu<sup>a</sup>, I.Rusen<sup>a</sup> and S. Nitisor<sup>a</sup>

<sup>a</sup>National Institute for Nuclear Physics an Engineering –Horia Hulubei, Bucharest

Positronium, the simplest atomic structure, constituted by an electron and a positron, in the triplet state ( $S=1$ ) decays by three gamma annihilation having a life time of 142 ns in vacuum. The Positronium annihilation is affected by the magnetic field because in magnetic field the  $M=0$  states of ortho-Positronium is mixed with  $M=0$  states of para-Positronium atoms in a coherent state called ortho-like Positronium. The mixing fraction of the two  $M=0$  states, depend on the magnetic field intensity and has as effect a "quantum beat" of the angular time distribution of gamma annihilation decay. This effect was predicted by V.G. Baryshevski [1].

The Time Differential Perturbed Angular Distribution (TDPAD) method in connection with long-lived Positron Life-Time Spectroscopy (PLTS) have been used to observe "quantum beat" spin oscillations of positronium atom in an external magnetic field. PAD spectra for  $3\gamma$  decay of Positronium show the oscillations in an external magnetic field.

The annihilation characteristics are not influenced by Positronium interaction with Argon, Nitrogen, Hydrogen.

The Positronium depolarization and de coherence effects due to the Oxygen molecules paramagnetism were observed.

Our results are encouraging in developing a new method for investigating magnetic field at atomic scale.

Keywords: Positronium, quantum beats, polarization, coherence, paramagnetic molecules

Reference

[1] Positronium Spin Rotation and Time Oscillation of the Normal to the Three-Photon Positronium Decay Plane in Magnetic Field. V.G. Baryshevski phys.stat.sol.(b),124, 619 (1984)



## NEGATIVE DIFFERENTIAL CONDUCTIVITY OF POSITRONS IN GASES

A. Banković<sup>1</sup>, Z.Lj. Petrović<sup>1</sup>, G. Malović<sup>1</sup>, J.P. Marler<sup>2</sup> and R. E. Robson<sup>3</sup>

<sup>1</sup> Institute of Physics, POB 68, 11080 Belgrade, Serbia

<sup>2</sup> University of Aarhus, Aarhus Denmark

<sup>3</sup> CAMS, RSPHysSE, Australian National University, Canberra 2600, Australia

A new series of calculations of positron transport properties was carried out recently [1,2] based on current experimental cross section data and an improved understanding of the non-conservative transport for electrons [3,4]. It was found that positrons show a specific form of negative differential conductivity due to positronium (Ps) formation which while being a similar non-conservative process to electron attachment has a magnitude several orders higher. Thus it was found that *bulk* drift velocity  $W_B$  (the velocity of the center of the swarm) has negative differential conductivity (NDC) even when the *flux* drift velocity  $w_F$  (mean velocity) does not show any signs that conditions favourable to NDC are met in that particular gas. The relationship between the two drift velocities may be shown through the following equation [3]:

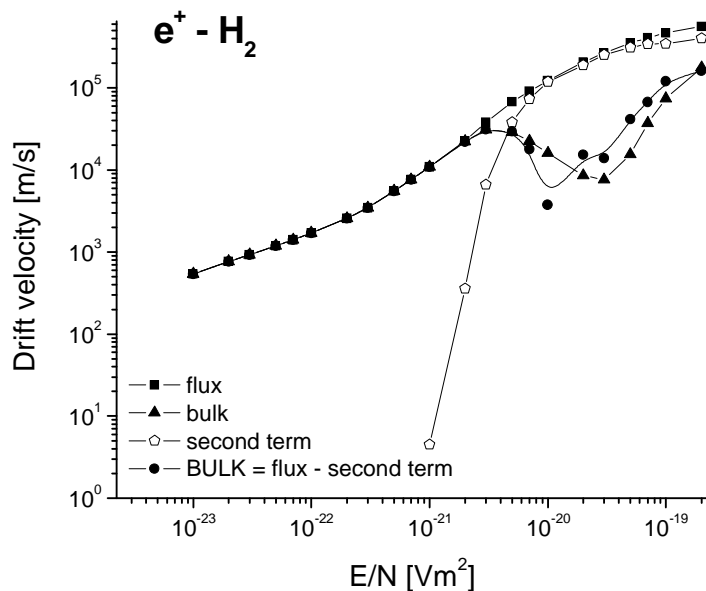


Figure 1. Calculation of the drift velocities for positrons in hydrogen [5] based on Monte Carlo Simulations and on eq. (1).

The relationship between the two drift velocities may be shown through the following equation [3]:

$$W_B = w_F - \frac{2\varepsilon d\alpha_{PS}}{3e dE} \quad (1)$$

where  $\alpha_{PS}$  is the Ps formation rate coefficient,  $\varepsilon$  is the mean energy and  $E$  is the electric field.

In this paper we perform calculations based on eq. (1), on momentum transfer theory and on conditions from [4].

Keywords: positrons, argon, hydrogen, transport coefficients, Monte Carlo.

### References

- [1] M. Šuvakov, Z. Lj. Petrović, J. P. Marler, S. Buckman, R.E. Robson and G. Malović, New.J. Phys. (2008) submitted.
- [2] A. Banković J. P. Marler M. Šuvakov, G. Malović, Z. Lj. Petrović Nucl. Inst. Methods B 266 (2008) 462.
- [3] R. Robson, J. Chem. Phys. 85, 4486 (1986)
- [4] S. B. Vrhovac and Z.Lj.Petrović, Phys. Rev. E 53, (1996) 4012.
- [5] A. Banković J. P. Marler M. Šuvakov, G. Malović (2008) unpublished.

## Annihilation of protonium by charged particle impact

A. Igarashi<sup>a</sup> and L. Gulyás<sup>b</sup>

<sup>a</sup> Department of Applied Physics, Faculty of Engineering, University of Miyazaki, Miyazaki 889-2192, Japan

<sup>b</sup>Institute of Nuclear Research of the Hungarian Academy of Sciences (ATOMKI), H-4001 Debrecen, P O Box 51, Hungary

The protonium ( $Pn = p\bar{p}$ ), the bound state of a proton and an antiproton, receives particular interest both from experimental and theoretical points of view [1]. Its formation is most effective in the low-energy collision between  $\bar{p}$  and atomic or molecular hydrogen, where the antiproton the heavy “electron” substitute the electron, thereby the Pn comes into existence. The energy matching condition results  $Pn(n\ell)$  in quantum states where  $n$  and  $\ell$ , the principal and angular quantum numbers, take large values ( $n = 30 - 60$  and  $\ell \gg 1$ ) [2].

States of Pn with large  $n$  and  $\ell$  quantum numbers are stable against the  $p\bar{p}$  annihilation, however, surrounding electric field or collision with charged projectile by inducing  $\ell$  mixing may affect this stability, as the annihilation is very fast for the s states [3]. The s states are those compounds of the  $p$  and  $\bar{p}$  system where the particles approach each other so close that they effectively experience the strong interaction.

In this work we analyze the mechanism of annihilation of Pn induced by charged particle impact within the frame of close-coupling treatment. Figure present the annihilation cross sections versus the total angular momentum of the system ( $J$ ) for Pn, initially in  $40p$  state, in collision with electron projectile. These calculations reveal that the energy dependence of the annihilation cross sections and the decay mechanisms differ considerably for each initial state of  $Pn(n\ell)$ . Scaling of cross sections are also discussed.

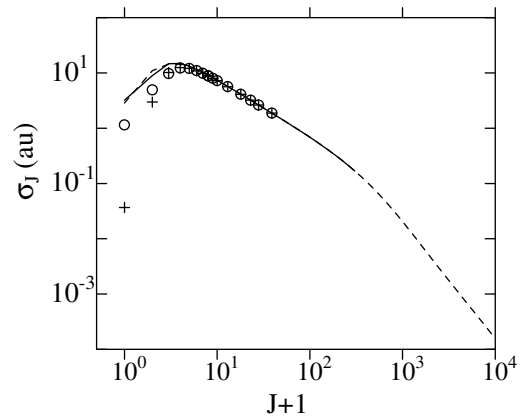


Fig. 1. Partial-wave cross sections for electron-impact annihilation of Pn in full quantal (solid line and circles) and in the corresponding semi-classical (dashed line and crosses) calculation for the  $40p$  initial states at  $E_c = 0.13$  center of mass collision energy.

*Keywords:* annihilation; protonium

### References

- [1] E. Klempt, F. Brandamante, A. Martin and J.-M. Richard, Phys. Rep. **368** (2002) 119
- [2] X. M. Tong, T. Shirahama, K. Hino and N. Toshima, Phys. Rev. A **75** (2007) 052711
- [3] K. Sakimoto, J. Phys. B: At. Mol. Opt. Phys **38**, (2005) 3447

## INFORMATION ABOUT TS-1 AND TS-2 DOUBLE IONIZATION MECHANISMS FOR POSITRON AND ELECTRON IMPACT IONIZATION OF ARGON\*

**R.D. DuBois, J. Gavin, O. G. de Lucio**

Department of Physics, Missouri University of Science and Technology, Rolla, MO USA

As explained by McGuire[1] many years ago, at intermediate energies removal of two, or more, electrons from an atom can occur via two channels. One channel consists of the projectile interacting independently with and transferring energy to each of the electron, leading to their ejection. This has become to known as the TS-2 mechanism which has an amplitude which scales as  $(Z/v)^n$ , where  $Z$  and  $v$  are the charge and velocity of the projectile and  $n$  is the number of electrons removed. The other channel, known as the TS-1 mechanism, results from the projectile interacting with only one of the electrons which, as it is being ejected, interacts with the second (or more) electrons, leading to their ejection also. The amplitude for this process scales as  $Z/v$ . The cross section for double ionization is obtained by summing these amplitudes and squaring. This results in a TS-1 term which scales as  $(Z/v)^2$ , a TS-2 term which scales as  $(Z/v)^4$ , and a cross (or interference) term which scales as  $(Z/v)^3$ . Note that for negative particle impact, e.g., electrons or antiprotons, the cross term is positive while for positive particle impact, e.g., positrons or protons, the cross term is negative. Also note that because of the velocity dependences, at high impact energies the TS-1 term eventually dominates whereas at low impact energies the TS-2 term can dominate. Many experimental studies were performed using a variety of projectiles and targets to investigate which mechanism was important. However, little is known about how these two mechanisms contribute and interfere when both are active.

A method being used in our lab to shed some light on this subject is to measure the angular dependences of the electron emission resulting from single, double, and triple ionization of argon by positron and electron impact. Data are obtained for electron and positron impact under identical conditions and ratios of multiple to single ionization are measured. Comparisons then allow us to extract information about how each of the three terms discussed above contribute to the angular emission of electrons.

To date, data have been collected for 200, 500, and 1000 eV impact. This covers situations where the TS-2 term should dominate, where both terms should be comparable in magnitude, and where the TS-1 term should dominate. However, in all cases, both terms are active and will interfere. These data will be presented and discussed

\* work supported by the National Science Foundation

Keywords: ionization, positron, electron

### References

[1] J. McGuire, Phys. Rev. Lett. 49 (1982) 1153.

## IONIZATION OF MOLECULES BY POSITRON AND ELECTRON IMPACT

I. Tóth<sup>a</sup>, R. I. Campeanu<sup>b</sup>, V. Chiş<sup>a</sup> and L. Nagy<sup>a</sup>

<sup>a</sup>Faculty of Physics, Kogălniceanu 1, 40084 Cluj, Babeş-Bolyai University, Romania

<sup>b</sup>Department of Physics and Astronomy, 4700 Keele Street Toronto, York University, Canada

In our work we compare theoretical cross sections for the ionization of several molecules by positron and electron impact. Previously we have performed calculations for the positron impact ionization of the H<sub>2</sub> [1], N<sub>2</sub> [2], O<sub>2</sub> [3], CO [4], CO<sub>2</sub> [4] and CH<sub>4</sub> [5] molecules. Recently, we have extended our research to the ionization of molecules by electron impact, employing the method used in the case of positron projectiles, adapted to the case of electron impact ionization. This adaptation implies not only the change in the sign of the projectile charge, but one should take into account the exchange interaction too.

For both projectiles, the calculations were based on the simple CPE (Coulomb plus plane waves with full energy range) and the DWBA (Distorted Wave Born Approximation) methods [6]. In both cases, the ground state of the target molecule was approximated by Gaussian-type wavefunctions. The distorted waves were determined by solving the radial Schrödinger equation in the field of the spherically averaged potential, created by the nuclei and the electrons of the target. In the case of electron projectiles direct and total (direct plus exchange) cross sections were calculated. For energies lower than 200 eV, we found that the direct ionization cross sections are higher for electron impact ionization than for positron impact ionization. By taking into account both the direct and exchange processes, the cross sections were diminished, and we generally obtained lower values in the case of electron induced ionization. In both cases (positron and electron projectiles) the calculated distorted-wave cross sections were in better agreement with the experimental data, than the CPE cross sections, especially in the case of the smaller diatomic molecules.

We may conclude that in the case of both projectiles, the use of correct distorted waves is important to calculate reliable cross sections. As expected, we have generally obtained higher cross sections for positron projectiles compared to the electron impact ionization case, where both the direct and exchange processes were taken into account in order to obtain accurate cross sections.

*Keywords:* ionization; distorted waves; exchange interaction

### References

- [1] R. I. Campeanu, V. Chiş, L. Nagy, A. D. Stauffer, Phys. Lett. A **310**, (2003) 445
- [2] R. I. Campeanu, V. Chiş, L. Nagy, A. D. Stauffer, Nucl. Instrum. Methods B **221**, (2004) 21
- [3] R. I. Campeanu, V. Chiş, L. Nagy, A. D. Stauffer, Phys. Lett. A **325**, (2004) 66
- [4] R. I. Campeanu, V. Chiş, L. Nagy, A. D. Stauffer, Phys. Lett. A **344**, (2005) 247
- [5] R. I. Campeanu, V. Chiş, L. Nagy, A. D. Stauffer, Nucl. Instrum. Methods B **247**, (2006) 58
- [6] I. Tóth, R. I. Campeanu, V. Chiş, L. Nagy, Phys. Lett. A **360**, (2006) 131

## CROSS SECTION OF POSITIVE IONS PRODUCTION IN ELECTRON COLLISION WITH ADENINE MOLECULES

M.I. Sukhoviya, V.V. Stecovych., M.I. Shafranyosh, O.V. Pavlyuchok, L.L. Shimon,  
I.I. Shafranyosh

**Department of Physics, Uzhgorod National University, Uzhgorod 88000, Ukraine**

A high-energy particle penetrating in a solid generates a large number of secondary electrons, predominantly with small energies. According to the existing notions [1], such low-energy electrons mostly account for destructive changes in biological structures on a molecular level, their main targets being genetic macromolecules. The results of our previous experiments [2,3] showed that the electron impact on heterocyclic fragments of such macromolecules induces various physical processes, including excitation, ionization, dissociative excitation, and dissociative ionization.

Reliable data on the ionization cross sections of molecules can be obtained only in high-precision physical experiments, in which the influence of the ambient medium is reduced practically to zero. This approach has been implemented in our investigation using modern equipment and the method of crossed molecular and electron beams. This study was stimulated by the fact that no such experiments have been reported so far.

Production of positive ions of adenine molecules (nucleic acid base) has been studied using a crossed electron and molecular beam technique. The method developed by the authors enabled the molecular beam intensity to be measured and the electron dependences and the absolute values of the total cross sections of production of positive adenine ions to be determined. A five-electrode electron gun with a thoriated tungsten cathode was used as an electron beam source. Electron gun temperature was about 410K providing gun parameter stability during operation. Electrons having passed the interaction region were trapped by a Faraday cup kept at the positive potential. Measurements were carried out at the  $10^{-7}$ – $10^{-6}$  A electron beam current and the  $\Delta E_{1/2} \sim 0.3$  eV (FWHM) energy spread. Electron gun was immersed into the longitudinal magnetic field (induction  $B = 1.2 \cdot 10^2$  Tl). An electron energy scale was calibrated with respect to the resonance peak of the  $SF_6^-$  ion production, the position of which determined the zero point of the energy scale.

Using the technique developed by the authors, the absolute cross sections of the positive adenine ions formation have been determined within the 0–200 eV incident electron energy ranges. It has been found that the maximal positive ion production cross section is observed at 90 eV and reaches  $2.8 \cdot 10^{-15}$  cm<sup>2</sup>. Value of the ionization cross section obtained by us has a sense of the total cross section, i.e. it includes ion production cross sections for both initial molecules and its fragments. The mass spectra of adenine have been obtained. Formation of the primary molecular positive ion dominates.

### References

- [1] C.Sonntag, *The Chemical Basis for Radiation Biology* (Taylor&Francis, London, 1987).
- [2] M.I. Sukhoviya and I.I.Shafranyosh, *Elementary Processes in Collisions of Atomic and Molecular Particles* (ChGU, Cheboksary, 1987), pp. 121-124 [in Russian].
- [3] M.I. Sukhoviya, V.N. Slavik, I.I. Shafranyosh, *et al.*, *Biopolim. Kletka* 7 (6), 77 (1991).

## IONIZATION OF GUANINE MOLECULES BY ELECTRON IMPACT NEAR THRESHOLD

A.N. Zaviopulo, O.B. Shpenik, A.S. Agafonova

Institute of Electron Physics, Ukr. Nat. Acad. Sci., 21 Universitetska str.,  
Uzhgorod 88017, Ukraine, *E-mail*: [an@zvl.iep.uzhgorod.ua](mailto:an@zvl.iep.uzhgorod.ua)

In the recent years the studies of biomolecules by traditional techniques of physics of electron collisions have been attracting a considerable interest. The present paper is devoted to the investigation of the specific features of guanine molecule fragmentation process under an electron impact, accompanied by the formation of ionized reaction products.

The experimental setup, used for the studies of partial cross-sections of dissociative ionization of molecules by electron impact, is described in detail in our earlier papers (See, e. g., [1]). Therefore, here we mention only its basic elements. The setup is based on a monopole mass spectrometer with an electron ionizer and a multichannel molecular source of effusive type. The product ions of the dissociative ionization reaction, separated by the analyser field, were detected by a channel electron multiplier. The ionizing electron energy scanning and data storage were performed by a computer with an intentionally developed software for measurements in the cycling mode of multichannel counting with data storage depending on the signal magnitude.

The duration of one measurement cycle was chosen in such a way that the amount of pulses of the useful signal in the maximum of the cross-section dependence on energy be not less than 104. In short, the measurement technique consisted in the following. First the guanine molecule mass spectrum was measured at the ionizing electron energy of 40 and 70 eV, then for each fragment the dissociative ionization function was measured. The mass scale was calibrated, using Ar, Kr, and Xe, and appearance potentials for different groups of fragment ions were determined, using a special method of processing of the threshold part of the cross-section by polynomial fit [2]. From the threshold dependences, the fragment appearance potentials were determined. It was also important to study the intensities of the fragment ions of the initial molecule versus temperature. The temperature range was 323–478 K. The measurements were reduced to the mass spectra measurements at different temperatures at  $E_{ion}=50$  eV (Fig.1). From the temperature dependences, the evolution of the fragment formation could be traced as well as the effect of temperature on the dissociative ionization.

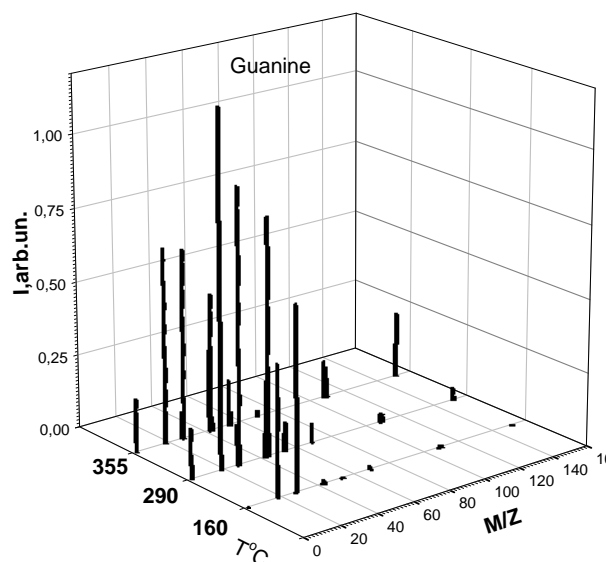


Fig.1 Mass spectra of the guanine molecules

This work was supported in part by the CRDF Grant # UKC-2832-UZ-06.

1. A.N.Zaviopulo, O.B.Shpenik, V.A Surkov *Anal.Chim.Acta* 573-74,(2006),427-431
2. T.Fiegele, et.al *J.Phys.B: Atom. Mol. Opt. Phys.* 33, P4263-4269.(2000)

## IONIZATION AND DISSOCIATIVE IONIZATION OF A POPOP MOLECULE

L.G.Romanova, A.N.Zavilopulo, A.S.Agafonova,  
O.B.Shpenik, M.I.Mykyta

Institute of Electron Physics, Ukr. Nat. Acad. Sci., 21 Universitetska str.,  
Uzhgorod 88017, Ukraine, *E-mail*: [an@zvl.iep.uzhgorod.ua](mailto:an@zvl.iep.uzhgorod.ua)

Electron-impact single and dissociative ionization of 1,4-bi(5-phenyloxazolyl) benzene (POPOP), an organic luminophore with a large Stokes shift, is studied. This material is promising for its application as a component of laser active media, liquid and plastic scintillators, luminescent concentrators of solar energy [1]. A detailed description of the setup, based on a monopole mass spectrometer MX-7304A, is given in [2]. Measurements were performed at different temperatures (420–500 K) and ionizing electron energies. Paths of fragmentation of the molecule under study are proposed, based on the presence of a common system of conjugated  $\pi$ -electrons and heteroatoms in the POPOP molecules what enables one to determine the most probable sites of charge localization at the formation of a molecular ion [3]. From the experimentally measured dependences of the ionization cross-section on the ionizing electron energy thresholds of appearance are determined for the fragments of the investigated molecule with the highest relative intensities in the mass spectrum. Contrary to the mass spectrum, presented in the NIST database, we have registered a fragment with  $m/z = 144$   $[\text{C}_9\text{H}_6\text{ON}]^+$ , which is complementary to the fragment with  $m/z = 220$   $[\text{C}_{15}\text{H}_{10}\text{ON}]^+$  (present in the NIST mass spectrum), and determined the threshold of its appearance ( $E_{ap} = 9.51$  eV).

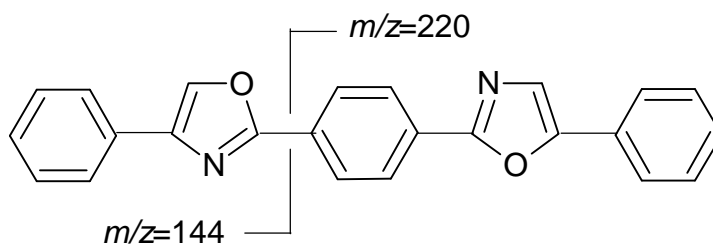


Fig.1. Breaking of a C–C bond in the POPOP molecule, resulting in the formation of the fragments with  $m/z$  220 and 144

The work was carried out in the framework of the agreement No. F014/309-2007 of DFFD of the Ministry of Education and Science of Ukraine.

*Keywords*: POPOP; mass spectrum; fragment ions

### References

1. Doroshenko A.O., Kirichenko A.V., Mitina V.G., Ponomarev O.A. Spectral properties and dynamics of the excited state structural relaxation of the ortho analogs of POPOP - effective abnormally large Stokes shift luminophores.// Journ. Photochem. Photobiol. A: Chem.– 1996.– v. 94, # 1.– p. 15-26.
2. A.N.Zavilopulo, O.B.Shpenik, V.A Surkov Anal.Chim.Acta 573-74, (2006), 427-431
3. I.G.Zenkevich, B.V.Ioffe, Interpretation of mass spectra of organic compounds (Khimiya, Leningrad, 1986).

## RADIATIVE CHARACTERISTICS OF POPOP MOLECULES AT LOW-ENERGY ELECTRON-IMPACT EXCITATION

M.M. Erdevdy, O.B. Shpenik, J.E. Kontros

*Institute of Electron Physics, Ukr. Nat. Acad. Sci., 21 Universitetska str., 88017 Uzhgorod, Ukraine*

Organic luminescent compounds are of particular interest due to a possibility of their use as laser-active media. Laser generation of that kind was reached for the first time using the 1,4-di[2-(5-phenyloxazolyl)]-benzene (POPOP) vapors [1]. Quite large number of papers is dedicated to the studies of spectral and luminescent properties of the above compounds during their optical excitation. However, the number of works on their gas-phase excitation by monoenergetic electrons is extremely limited.

Here we report on the results of the POPOP molecule excitation by slow electrons. Excitation was carried out using the gas-filled cell at the incident electron current of 300 nA (the energy spread being 150 meV (FWHM)) provided by a hypocycloidal electron monochromator [2]. The optical emission was separated by a diffraction monochromator and detected using a photomultiplier. An

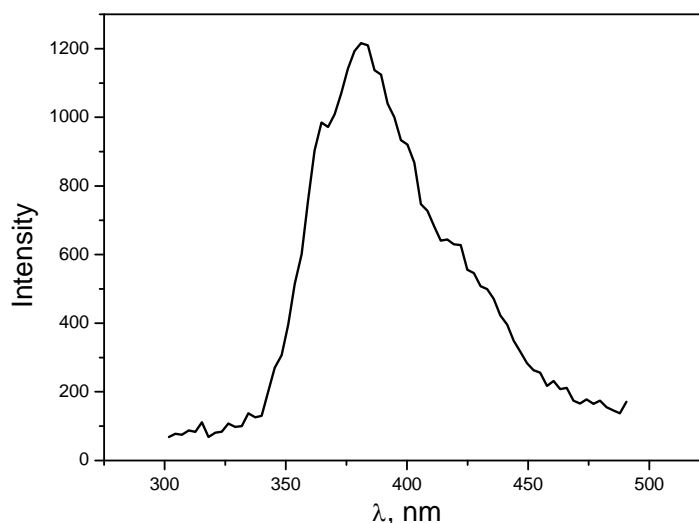


Fig. 1. The emission spectrum of the POPOP molecule

automated setup and measuring technique are described in [3]. Figure 1 shows the emission spectrum of the POPOP molecule measured at the 10 eV incident electron energy. The emission bands are observed in the 300–500 nm region with the maximum at 381 nm. We have also measured the optical excitation functions (OEFs) at the maximum and at the edges of the emission spectrum. The excitation thresholds for the above OEFs were measured. The energy position of the features revealed in the OEFs allow one to state that the observed emission spectrum is due to  $S_0-S_1$  and  $S_0-T_1$  transitions of the  $\pi-\pi^*$  type.

Keywords: electron, molecule, excitation.

This work was supported in part by the CRDF grant No. UKC2-2832-UZ-06.

### References

- [1] N.A. Borisevich, V.A. Tolkachev. *Uzp.Fiz.Nauk.* 138 (4) (1982) 545.
- [2] O.B. Shpenik, N.M. Erdevdy et al. *Instrum.Exper.Tech.* 41 (1) (1998) 97.
- [3] N.M. Erdevdy, O.B. Shpenik et al. *Opt.Spectr.* 95 (4) (2003) 529.



# ELECTRON SPECTROSCOPY OF POPOP MOLECULES

I.V.Chernyshova, J.E.Kontros, O.B.Shpenik

Institute of Electron Physics, Ukr. Nat. Acad. Sci., 21 Universitetska str.,  
Uzhgorod 88017, Ukraine, E-mail: [an@zvl.iep.uzhgorod](mailto:an@zvl.iep.uzhgorod)

With the development of laser and thin-film technologies, accurate data regarding the structure of organic molecules with high quantum efficiency are required. One of such molecules is POPOP. The data on the structure of its molecule have been mostly obtained from experiments with photon beams. Additional information can be obtained from the studies with monoenergetic electron beams.

Here we report on the results of studies of constant residual electron energy spectra (threshold spectra) in POPOP molecular vapour.

The threshold spectra were measured using a hypocycloidal spectrometer with a resolution not worse than 0.2 eV, earlier described in [1]. The spectra were detected at an angle close to  $0^\circ$  with respect to the incident electron beam. The target was formed in a vapour cell ( $P \approx 10^{-3}$  Torr).

Contrary to the optical absorption spectra, in the threshold spectrum of POPOP the bands, related to the  $S_0-T_1$  transition and a transition of a higher-energy triplet state, are observed (See Fig.1). At the excitation with electrons of sufficiently high energy, transitions up to  $S_0-S_5$  were registered in the range up to 8 eV. The ratio of intensities of the band maxima at  $E=0$  eV and at 3.86, 4.6, 7.33 eV is 630:1.0:0.37:0.29. The probability of direct electronic excitation of lower triplet states (at 2.5 eV and 4.6 eV) is seen to be very low. Even near the process threshold it is lower than the probability of excitation of  $\pi\pi^*$  type lower singlet states (at 3.86, 5.6, and 7.33 eV). Note that the observed maximum at 9.8 eV corresponds to an overexcited state. Our results agrees with [2] very well.

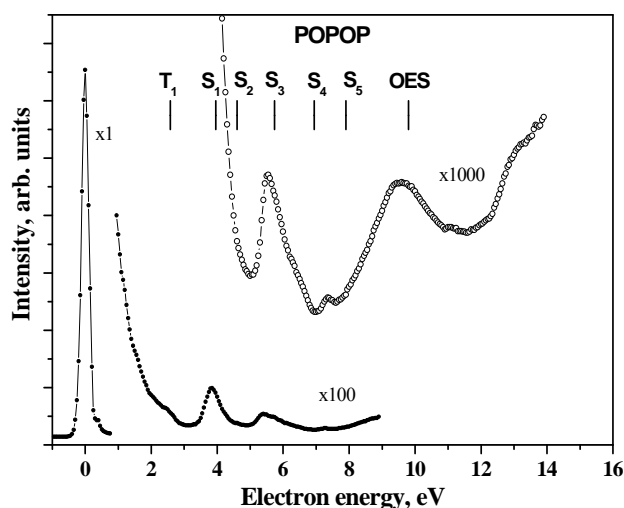


Fig.1 POPOP molecule excitation threshold spectrum  
( $E_r=0.1$ eV)

The work was carried out in the framework of the agreement № F014/309-2007 of DFFD of the Ministry of Education and Science of Ukraine.

*Keywords: POPOP, electron, molecule, excitation*

## References:

- [1] N.I.Romanyuk, O.B.Shpenik, I.A.Mandy, F.F.Papp, I.V.Chernyshova Tech. Phys. **38** (1993) 599.  
[2] N.A.Borisevich, S.M.Kazakov, A.V.Kukhta, D.V.Murtaazaliev, O.B.Khristoforov J.Appl.Spectrosc. 69 (2002) 166.

## ELECTRON-IMPACT IONIZATION OF GLUCOSE AND VITAMIN C

**J.E.Kontros, I.V.Chernyshova, O.B.Shpenik**

Institute of Electron Physics, Ukr. Nat. Acad. Sci., 21 Universitetska str.  
Uzhgorod 88017, Ukraine

The mechanisms of destruction of living cells by ionizing radiation can be studied in collisions of biomolecules with slow electrons. Glucose and vitamin C belong to the group of organic compounds playing an important role in the vital functions of living organisms. Therefore the comprehensive study of these organic compounds is actual.

In this work, the results of investigations of electron-impact ionization cross sections (formation of positive and negative ions) of glucose and vitamin C are presented. Experiments were performed using a modernized hypocycloidal spectrometer with energy resolution not exceeding 0.2 eV [1]. The target was formed using a vapor-filled cell ( $P \sim 10^{-3}$  Torr).

Below the first ionization potential (<11 eV) the main mechanism of interaction is the process of dissociative attachment of electron with formation of an anion in the final state. So, for the vitamin C the largest contribution to the cross-section is given by  $O^-$ ,  $H^-$  and  $OH^-$  anions. This is supported by investigations of [2].

In Fig.1 the total electron-molecule ionization cross-section for vitamin C in the energy region from the threshold up to 34 eV is presented. The appearance energy value for the positive vitamin C molecular is equal  $E=10.8$  eV. Detailed analysis of the measured ionization curves allows the number of weak features related to the appearance of fragment ions of the investigated molecule to be found.

This work was supported in part by the CRDF Grant# UKC-2832-UZ-06.

*Keywords: biomolecule, electron, ionization*

### References:

- [1] N.I.Romanyuk, O.B.Shpenik, I.A.Mandy, F.F.Papp, I.V.Chernyshova. Tech. Phys. **38** (1993) 599 (in Russian).  
[2] H. Abdoul-Carime, E. Illenberger, Chem. Phys. Lett. **390** (2004) 481.

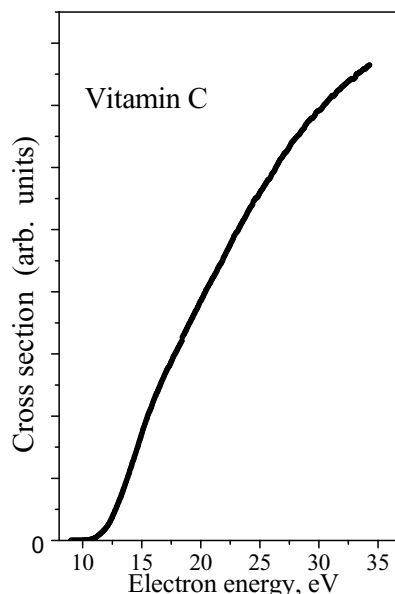


Fig. 1. The total electron-impact ionization cross-section for vitamin C molecule.

## THEORETICAL CROSS SECTIONS FOR IONIZING PROCESSES OF DNA BASES IMPACTED BY $H^+$ , $He^{2+}$ AND $C^{6+}$ IONS: A CLASSICAL MONTE CARLO APPROACH

**C. Champion, H. Lekadir, I. Abbas and J. Hanssen.**

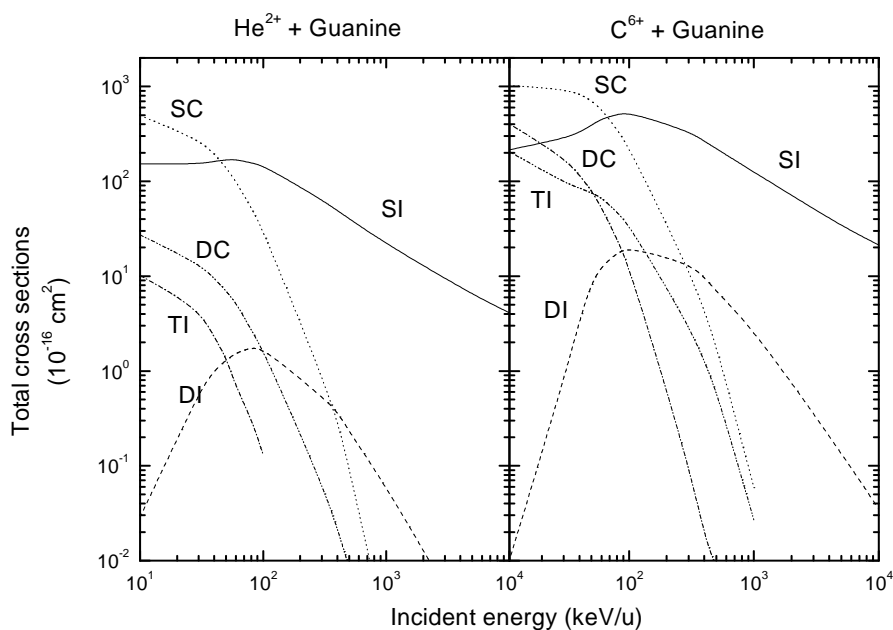
*Université Paul Verlaine Metz, Laboratoire de Physique Moléculaire et des Collisions  
ICPMB (FR CNRS 2843), Institut de Physique, 1 Bd Arago, 57078 Metz, Cedex3, France.*

Radiobiological effects like cellular death and chromosome aberration induction are now well documented and clearly highlight the absolute necessity to describe at the finest scale (atomic scale) the underlying physics of irradiations.

In this work, we present total and singly differential cross sections for multiple ionizing processes of biological systems (Adenine, Cytosine, Guanine, Thymine and Uracil) impacted by protons,  $\alpha$ -particles and Carbon ions in the 10 keV/u -10 MeV/u energy range.

To do that, we used a Classical Trajectory Monte Carlo (CTMC) method, initially developed by Zarour *et al.* [1] for multiple electron transfer in slow collisions of highly charged ions with atoms, and more recently adapted by Abbas *et al.* [2] for studying the water ionization induced by proton and  $\alpha$ -particle impact. In this kind of approach, all the particles are described in a classical way by assuming that the target electrons are treated as virtual particles whose creation is linked to the potential energy induced by the other particles (classical over-barrier (COB) approach).

The obtained results clearly exhibit the importance of the multiple processes with in particular single and double capture (SC and DC, respectively) which become the most preponderant processes in the low-energy range. Moreover, we observed that the different nucleobases provided very similar results in terms of total cross sections, for all the processes investigated here.



### References

- [1] B. Zarour *et al.*, *Nucl. Instrum. Meth.* **B 205** 610 (2003).
- [2] I. Abbas *et al.*, *Phys. Med. Biol.* **53** N41-N51 (2008).

## THE EFFECT OF INTERNAL STATE OF DIATOMIC MOLECULES ON THE DYNAMICS OF ENERGY EXCHANGE

V.M. Azriel, L.Yu. Rusin

Institute of Energy Problems of Chemical Physics RAS,  
Leninski prospect 38, Bldg.2, Moscow 119334, Russia

Quasiclassical trajectory calculations of inelastic collisions of two molecules CsBr have been fulfilled for the case when one molecule before collision obtained zero internal energy. Initial vibrational and rotational states of the second molecule are characterized by equilibrium distributions corresponding to temperature 1000K everyone separately or both together. Also collisions of two "cold" molecules ( $V=0$  and  $J=0$ ) are considered. Calculations show, that at absence of rotational energy for both partners of collision the conversion of translational energy into internal degrees of freedom of molecules proceeds more effectively, that is confirmed by histograms of distribution of kinetic energy of molecules after collision represented on figures 1(a) and 1(c). In both cases the most probable value of kinetic energy is less than collision energy and besides in all trajectories kinetic energy does not exceed collision energy. The presence of initial rotational excitation of one of colliding molecules reduces efficiency of energy transfer (see figures 1(b) and 1(d)). At the same time the vibrational energy does not change dynamics of energy transfer.

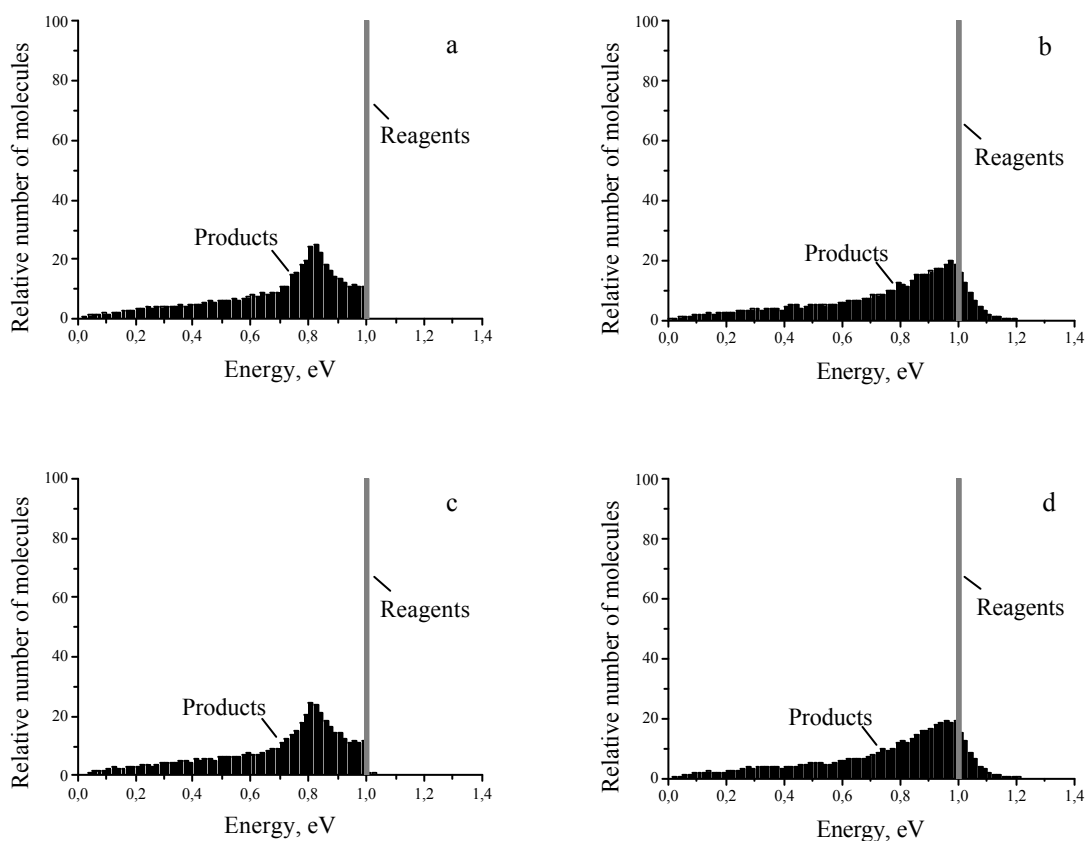


Fig. 1. Distributions of kinetic energy of molecules in the end of a trajectory at collision energy 1,0 eV and zero initial internal energy of both molecules (a), and also at corresponding to temperature 1000K equilibrium initial distributions of rotational (b), vibrational (c) and both components of internal energy (d) of one of colliding molecules.

# OFF-SHELL CONTINUUM-DISTORTED-WAVE THEORY FOR POSITRONIUM FORMATION FROM NOBLE GAS ATOMS

P. A. Macri<sup>a</sup> and R. O. Barrachina<sup>b</sup>

<sup>a</sup>Departamento de Física, FCEyN, Universidad Nacional de Mar del Plata, Deán Funes 3350, 7600 Mar del Plata, Argentina

<sup>b</sup>Centro Atómico Bariloche and Instituto Balseiro, R8402AGP S. C. de Bariloche, Río Negro, Argentina

The formation of positronium in collisions of positrons with noble gas atoms is studied by means of a modified eikonal final state - continuum distorted wave (EFS-CDW) approximation. We observe that an independent electron model extension of the EFS-CDW to many electrons atoms overestimates several times the total cross sections around its maximum. For the case of highly charged ions colliding with atoms, it was shown [1] that an accurate representation of both asymptotic and intermediate states is necessary for a consistent theory of electron capture. For this reason, in this work we explore an alternative model for the scattering amplitude where off-shell distortion effects are taken into account.

In Fig. 1, we compare our results for the total cross sections (TCS) for Ne atoms, with recent experiments measured on absolute units by Laricchia *et al.* [2] and by Marler *et al.* [3]. As the experiments did not discriminate between different final Ps bound states, we have multiplied our theoretical calculations of electronic capture into the  $1s$  state of Ps by a factor 1.202 in order to estimate the capture to excited states. We can see that the EFS-CDW approximation, without including the off-shell distortion, largely overestimates the TCS. On the other hand, we can observe the important effect introduced by the off-shell corrections. They reduce drastically the EFS-CDW estimations at low energies and give a milder effect at higher energies. Even though the present off-shell effect seems to overcorrect the EFS-CDW calculations in the proximity of the maximum of the TCS, for intermediate and large energies it provides a better overall agreement with experiments than higher order perturbation theories.

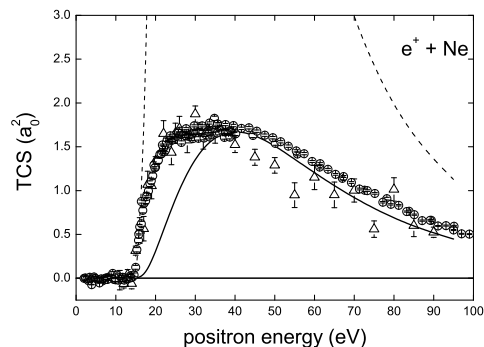


Fig. 1. TCS for Positronium formation in collisions of positrons against Ne atoms. The EFS-CDW theory with (Full line) and without (dashed line) off-shell distortions, is compared with experimental data by Laricchia *et al.* [2] (circles) and Marler *et al.* [3] (triangles).

*Keywords:* Ps formation; off-shell effects

## References

- [1] J. H. Macek and K. Taulbjerg, Phys Rev. A 39 (1989) 6064.
- [2] G. Laricchia, P. V. Reeth, M. Sz. uinska, and J. Moxom, J. Phys. B **35**, 2525 (2002).
- [3] J. P. Marler, J. P. Sullivan and C. M. Surko, Phys. Rev. A **71**, 022701 (2005).

**YOUNG-TYPE INTERFERENCE WITH SINGLE ELECTRONS IN THE  
AUTOIONIZATION OF ATOMS BY THE IMPACT OF MOLECULES:  
AN INDEPENDENT MEASUREMENT IN THE BACKWARD  
DIRECTION**

**S. Suárez<sup>a</sup>, D. Fregenal<sup>a</sup>, G. Bernardi<sup>a</sup>, P. Focke<sup>a</sup>, F. Frémont<sup>b</sup>, J.-Y.  
Chesnel<sup>b</sup>, A. Hajaji<sup>b</sup> and R. O. Barrachina<sup>a</sup>**

<sup>a</sup>Centro Atómico Bariloche and Instituto Balseiro , R8402AGP S. C. de Bariloche, Río Negro, Argentina.

<sup>b</sup>Centre de Recherche sur les Ions, les Matériaux et la Photonique (CIMAP), CEA-CNRS-EnsiCaen-Université de Caen, 6 bd du Mal Juin, F-14050 Caen Cedex 04, France.

In a recent article [1] we provided an unprecedented experimental evidence of a single electron interfering with itself in a set-up that was analogous to an atomic-size double-slit apparatus [2]. In that version of the famous gedanken experiment proposed by Feynman in 1963 [3] to illustrate the wave-like nature of matter, the electron originates from the autoionization of a doubly-excited helium atom following a double capture process in a 30 keV He<sup>2+</sup> + H<sub>2</sub> collision. The autoionizing He atom plays the role of a single-electron source, that is independent of the two-center target interferometer. In that experiment, performed at GANIL (Grand Accélérateur National d'Ions Lourds), in Caen (France), at least three distinctive oscillations were observed in the angular distribution of the electron emission cross section, in a range from 95 to 160 degrees. Here, we report the first results of an independent measurement performed at the Cockroft–Walton accelerator of the Centro Atómico Bariloche, with 40 keV He<sup>2+</sup> projectiles. The electron emission was observed from 155 to 180 degrees, overlapping with the previous experiment in a small region of angles and extending its range all the way to the backward direction. The H<sub>2</sub> gas target was provided by a needle of 0.3 mm bore located at the focus of the cylindrical mirror electron spectrometer [4] to reduce partially the extended gas target effect and increase the counting rate. The results are consistent with the oscillations observed with the Caen equipment. The prominent increase of the electron intensity at 180 degrees, despite of no corrections due to gas target extension, can be ascribed to a backward Glory effect [5, 6].

*Keywords:* Young interference; Autoionization; Atom-molecule collision

### References

- [1] J.-Y. Chesnel, A. Hajaji, R. O. Barrachina, F. Frémont, Phys. Rev. Lett. 98 (2007) 100403.
- [2] R. O. Barrachina and M. Zitnik, J. Phys. B 37 (2004) 3847.
- [3] R. Feynman, R. B. Leighton, and M. Sands, The Feynman Lecture on Physics (Addison-Wesley, Reading, MA, 1963), Vol. 3, Chap. 37.
- [4] G. Bernardi, S. Suárez, D. Fregenal, P. Focke and W. Meckbach, Rev. Sci. Instrum. 67 (1996) 1761.
- [5] J. K. Swenson et al., Phys. Rev. Lett. 63 (1989) 35.
- [6] R. O. Barrachina and J. H. Macek, J. Phys. B 22 (1989) 2151.

# MOLECULAR ORIENTATION INFLUENCE ON THE INTERFERENCE PATTERN

**K. Póra, L. Nagy**

Faculty of Physics, Babeş–Bolyai University, Kogălniceanu 1, Cluj-Napoca 400084, Romania

Interference effects in the double differential cross sections for ionization of hydrogen molecule by fast charged particles have been described theoretically by our group [1] using the semiclassical approximation. In order to emphasize the interference effects the cross section ratio of the hydrogen molecule and two hydrogen atoms is represented as a function of the ejected electron velocity. This ratio shows an oscillating pattern. In our previous study we examined the interference pattern after integration over all possible orientations of the molecular axis.

We have also calculated the double differential cross section in case of the ionization of the hydrogen molecule by 13.7 MeV/u  $C^{6+}$  projectile. We have chosen this projectile because there are already theoretical calculations [2] available. The cross sections for different molecular orientations with our simple model gives similar results as in paper [2].

The present work studies the influence of molecular axis orientation on the oscillation pattern observed in the cross section ratios as a function of ejected electron velocity. In Fig. 1. we present the influence of molecular axis orientation on the cross section ratio at forward electron ejection. As one may observe, at parallel orientation of the hydrogen molecule respective to the incident projectile direction, the cross section is less than one, and for several electron velocities the ratio is almost zero, which means, that at these electron velocities the interference is destructive. At perpendicular orientation of the hydrogen molecule the ratio is greater than one, so at this orientation the interference is always constructive.

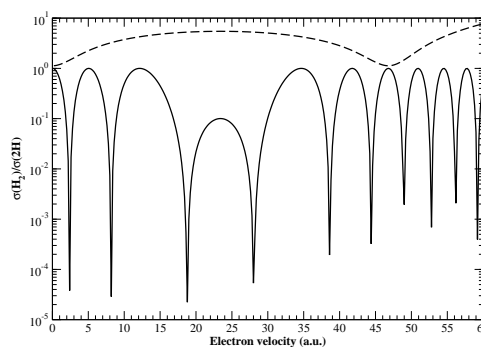


Fig. 1. Cross section ratios at parallel (solid line) and perpendicular (dashed line) orientation of the hydrogen molecule respective to the incident projectile direction, as a function of ejected electron velocities, at forward electron ejection and zero azimuthal angle of the molecular axis.

*Keywords:* Interference effects; Ionization; Hydrogen molecule

## References

- [1] L. Nagy, L. Kocbach, K. Póra, J. P. Hansen, J. Phys. B: At. Mol. Opt. Phys. 35 (2002) L453.
- [2] G. Laurent, P. D. Fainstein, M. E. Galassi, R. D. Rivarola, L. Adoui and A. Cassimi, J. Phys. B: At. Mol. Opt. Phys. 35 (2002) L495.

## INTERFERENCES IN ELECTRON EMISSION FROM O<sub>2</sub> BY 30 MeV O<sup>9+</sup> IMPACT

**M. Winkworth<sup>a</sup>, P. D. Fainstein<sup>b</sup>, M. E. Galassi<sup>c</sup>, J. Baran<sup>a</sup>, B.S. Dassanayake<sup>a</sup>,  
S. Das<sup>a</sup>, T. Elkafrawy<sup>a</sup>, D. Cassidy<sup>a</sup>, A. Kayani<sup>a</sup> and J.A. Tanis<sup>a</sup>**

<sup>a</sup>Department of Physics, Western Michigan University, Kalamazoo, MI 49008, USA

<sup>b</sup>CNEA, Centro Atómico Bariloche, Bariloche, Argentina

<sup>c</sup>Instituto de Física de Rosario (CONICET-UNR), Rosario, Argentina

In recent years there has been much interest in the study of interference phenomena associated with electron emission from H<sub>2</sub> colliding with fast ions [1,2]. Among them, H<sub>2</sub> collisions with 1-5-MeV H<sup>+</sup> revealed primary Young-type interferences due to coherent emission from the identical atomic centers as well as secondary interferences caused by intramolecular scattering [2]. The primary interferences showed a strong dependence on the electron observation angle, while the higher frequency secondary structures did not. More recently, interferences for 1-5-MeV H<sup>+</sup> + N<sub>2</sub> revealed apparently only secondary oscillations [3]. The present work extends the experimental studies to 30 MeV O<sup>5,8+</sup> impact with O<sub>2</sub>.

The 30 MeV O<sup>9+</sup> ion beam was obtained using the tandem Van de Graaff accelerator at Western Michigan University. After collimation, the ion beam was directed into the scattering chamber onto an O<sub>2</sub> target supplied by a gas jet with a flow rate set to maintain single collision conditions. The energy of electrons emitted from the target were analyzed with a parallel-plate analyzer equipped with a channel electron multiplier for angles of 30°, 60° and 90° with respect to the incident beam and ejected electron energies of 15 - 400 eV.

The measured molecular cross sections were divided by theoretical molecular O<sub>2</sub> cross sections calculated using one-center wave functions. Plotted as a function of the outgoing electron velocity, the resulting ratios were fit with the sinusoidal function  $f(k)$  shown in the Fig. 1. The oscillatory structures are suggestive of secondary interferences as evidenced by their independence on the observation angle and the fact that the oscillations do not appear to be damped with increasing electron velocity, similar to the structures observed for H<sup>+</sup> + N<sub>2</sub> [3]. No evidence for primary interferences is seen, as was also the case for N<sub>2</sub>. On the contrary, the oscillation interval for O<sub>2</sub> is  $\Delta k \sim 4$  a.u., while for N<sub>2</sub> a value of  $\Delta k \sim 2$  a.u. was found. Results for O<sup>8+</sup> + O<sub>2</sub> were similar to those for O<sup>5+</sup> and also gave  $\Delta k \sim 4$  a.u. The reason for the difference in  $\Delta k$  for O<sub>2</sub> and N<sub>2</sub> is presently being explored and may be due to the higher projectile charge and lower collision velocity in the case of 30 MeV O<sup>5,8+</sup> + O<sub>2</sub>, compared to 1-5 MeV H<sup>+</sup> + N<sub>2</sub> [3], resulting in a perturbation strength  $Z/v \sim 1$ .

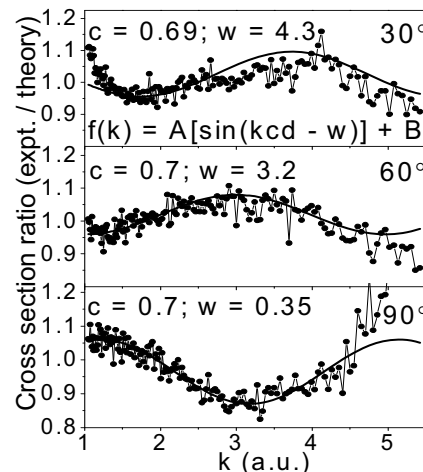


Fig. 1 Experimental to theoretical O<sub>2</sub> cross section ratios for 30 MeV O<sup>5+</sup> + O<sub>2</sub> plotted as a function of ejected electron velocity.

*Keywords:* electron interferences, coherent electron emission, molecular ionization

### References

- [1] N. Stolterfoht *et al.*, Phys. Rev. Lett. **87** (2001) 023201.
- [2] J.A. Tanis and S. Hossain, Nucl. Instrum. Meth. Res. B **261** (2007) 226.
- [3] J.L. Baran *et al.*, J. Phys.: Conf. Ser. **58** (2007) 215.



## ELECTRON TRANSPORT COEFFICIENTS IN N<sub>2</sub>O IN RF FIELDS

O. Šašić<sup>a,b</sup>, S. Dupljanin<sup>a,c</sup>, S. Dujko<sup>a</sup> and Z. Lj. Petrović<sup>a</sup>

<sup>a</sup> Laboratory for Gaseous Electronics, Institute of Physics, POB 68 11080 Belgrade, Serbia,

<sup>b</sup> Faculty for Traffic and Transport Engineering, University of Belgrade, Serbia

<sup>c</sup> Physics Department, Faculty of Natural Sciences, University of Banja Luka, Bosnia and Herzegovina

Due to importance in many biological processes, the role in infrared absorption in the Earth atmosphere and numerous applications in medicine and technology, electron interactions with N<sub>2</sub>O molecule have been the subject of many studies. To our knowledge, however, the electron kinetic in case of time dependent external field hasn't been investigated. In this paper we present calculated swarm data (e.g. electron mean energies, drift velocities and diffusion coefficients) for electrons in N<sub>2</sub>O as well as rate coefficients for individual processes in case of time varying crossed electric and magnetic fields. These data are interesting in particular for fundamental understanding of processes leading to RF plasma maintenance and they are also the necessary input data in modeling RF discharges.

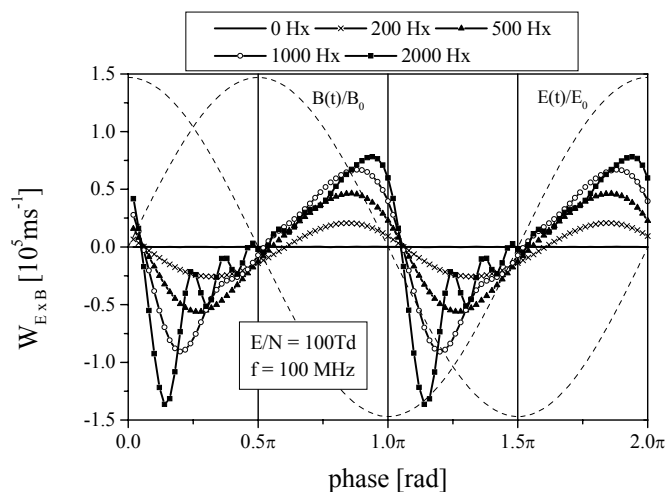


Fig. 1. Dependence of drift velocity ( $E \times B$  direction) on phase for  $E/N=100$  Td,  $f=100$  MHz and for different magnitudes of reduced magnetic field.

Cross section set for N<sub>2</sub>O was the compilation of the most reliable data from the literature improved by a standard swarm procedure and tested against new experimental data [1].

The calculation was made by using a well-tested Monte Carlo simulation code which was been described in details elsewhere [2,3]. In our simulations we followed the spatiotemporal evolution of each electron through time steps, in free space without any boundaries, in order to represent correctly the motion of electrons in RF fields. We have covered both purely electric and also ExB fields that are time

dependent with a phase between the two of  $\pi/2$ . It should be noted that all electron scattering was assumed to be isotropic. A behavior of transport coefficients under the influence of the magnitude and the frequency of the fields was studied separately revealing a number of complex features in the time dependence, most notably anomalous diffusion.

**Keywords:** N<sub>2</sub>O, transport coefficients, RF fields

[1] E. Basurto, J.L. Hernández-Avila, A.M.Juárez, J.de Urquijo, S. Dupljanin, O. Šašić, Z. Lj. Petrović, 28<sup>th</sup> ICPiG, July15-20 2007, Prague, Czech Republic, p.227

[2] Z. Lj. Petrović, Z.M. Raspopović, S. Dujko, and T. Makabe, Appl. Surf. Sci. **192**,(2002) 1-25

[3] S. Dujko, Z. M Raspopović, Z. Lj. Petrović, J. Phys. D: Appl. Phys. **38**, (2005)2952-2966

[4] K. Maeda., T. Makabe, N. Nakano, S. Bzenić. and Z. Lj. Petrović Z.Lj. Phys. Rev. E **55** (1997)5901

## FIELD-INDUCED ENHANCEMENTS OF DIELECTRONIC RECOMBINATION IN Na -LIKE S AND Na-LIKE Ar

**I. Orban<sup>a</sup>, S. Böhm<sup>a</sup>, S. Trotsenko<sup>b</sup>, and R. Schuch<sup>a</sup>**

<sup>a</sup> Department of Atomic Physics, S - 10691 Stockholm , Stockholm University, Sweden

<sup>b</sup> Gesellschaft für Schwerionenforschung, D - 64291 Darmstadt, Germany

Dielectronic recombination (DR) is a two step process in which an electron and an ion recombine, first creating a doubly excited state. To finalize DR, this intermediate state then decays radiatively below the ionization level of the recombined ion. DR in the presence of external electric fields (DRF) can show enhancement effects as first suggested by LaGattuta et al. [1] and experimentally verified by Muller et al. [2] in a crossed-beam experiment. Later, DRF was intensively studied for Li-like ions [3, 4], in storage ring experiments. We present preliminary results of the first DRF measurements for astrophysically abundant Na-like ions, performed at a storage ring.

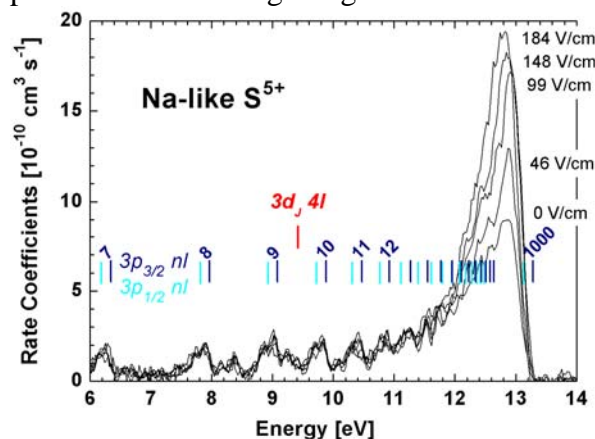


Fig. 1. Recombination spectra of Na-like S.

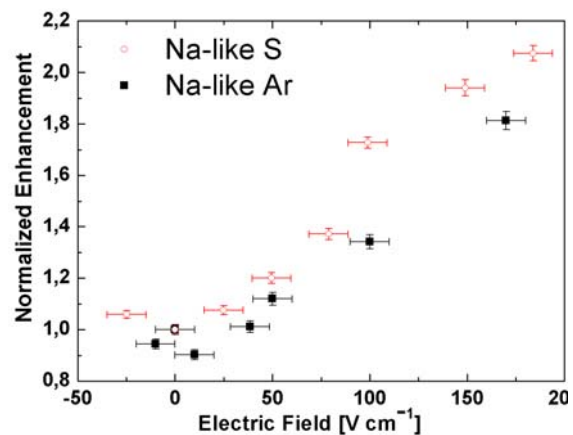


Fig. 2. Normalized enhancement coefficients.

Recombination spectra of Na-like S<sup>5+</sup> and Na-like Ar<sup>7+</sup>, in the presence of motional electric fields ranging between 0 and 185 Vcm<sup>-1</sup>, were measured at the CRYRING storage ring. In the electron cooler section of the storage ring, an electron beam was merged with the circulating ions over a distance of 80 cm. A motional electric field was created in the interaction region by inducing an angle between the 30 mT magnetic field guiding the electrons and the ion trajectory. Recombined ions were separated from the circulating beam in the first dipole magnet after the electron cooler. Field ionization at this dipole magnet hindered detection of ions recombined into states with principal quantum number  $n > 23$ .

The recorded spectra (fig. 1) were integrated over the range affected by the external electric fields and the results were normalized to the 0 field case. An enhancement increasing with the electric field was observed for both ions, with enhancement factors of over 2 and 1.8, in case of Na-like S and Na-like Ar, respectively. Saturation is not reached yet, as seen from the shape of the enhancement vs. electric field (see figure 2), even higher enhancements are to be expected at stronger fields. These enhancements can have important effects on various astrophysical and laboratory plasma properties, where external electric or magnetic fields are present, e.g. in magnetically confined fusion plasma.

### References

- [1] K. LaGattuta *et al.* Phys. Rev. Lett. **51** (1983) 558.
- [2] A. Müller *et al.* Phys. Rev. Lett. **56** (1986) 127.
- [3] T. Bartsch *et al.* Phys. Rev. Lett. **79** (1997) 2233.
- [4] S. Böhm *et al.* Phys. Rev. A **65** (2002) 052728.

## PHOTOIONIZATION OF $\text{Li}^+$ ION ABOVE THE EXCITED ION FORMATION THRESHOLD

T. Zajac<sup>a</sup>, A. Opachko<sup>b</sup> and V. Simulik<sup>c</sup>

<sup>a</sup>Department of Electronic Systems, 13 Kapitulna Str., Uzhgorod, Uzhgorod National University, Ukraine

<sup>b</sup>Transcarpathian Regional Center of Scientific and Technical Creative Work of the Pupil's Youth, 1 Buditeliv Str., Ukraine

<sup>c</sup>Institute of Electron Physics, 21 Universitetska str, Uzhgorod, National Academy of Sciences, Ukraine

In the problem of photoionization of  $\text{Li}^+$  ion above the excited ion formation threshold the positions of the lowest  $^1\text{P}$  autoionizing states (AIS) are calculated. The method of interacting configurations in complex number representation is used. The possibility of the application of this method to the problem of ionization of ions by photons, electrons and other particles is proved. The positions of the  $\text{Li}^+$  ion AIS, converging to the  $N=3$  threshold, are obtained. The multi-parametric Tweed's function is used in calculating the ground state of the ion.

The method of interacting configurations in complex number representation (MICCNR) was formulated in [1-4], where the procedure of calculation for the problem of ionization of atoms by photons and electrons was developed. Further, the calculations of the positions and total widths of AIS, converging to the  $N=3$  threshold of helium atom, were done in [1-4]. It is shown that the following approximations may be used within the framework of MICCNR:

1) the method of interacting configurations in real number representation is the approximation related to neglecting the complex terms  $i\gamma_{nm}(E)$  in the  $W_{nm}(E) = E_n \delta_{nm} + F_{nm}(E) - i\gamma_{nm}(E)$  matrix, see in [2];

2) the diagonalizing approximation in real number representation is related to neglecting the sum of all non-diagonal terms  $F_{nm}(E) - i\gamma_{nm}(E)$  in the  $W_{nm}(E)$  matrix;

3) the diagonalizing approximation with the account of the transitions outside the energy surface (or the diagonalizing approximation in complex number representation) is related to neglecting the term  $F_{nm}(E)$  during calculation.

№	E, eV
1	174,1
2	174,9
3	175,2
4	175,5
5	175,7
6	176,1
7	176,5
8	176,9
9	177,3
10	177,7
11	178,1
12	178,3
13	178,5
14	178,7
15	178,9

**Table 1.** Positions of the lowest AIS, converging to the  $N=3$  threshold, in the problem of photoionization of  $\text{Li}^+$  (MICCNR)

*Keywords:* Photoionization, excited ions, interacting configurations.

### References

- [1] S. Burkov, S. Strakhova, T. Zajac, J. Phys. B **23** (1990) 3677.
- [2] S. Burkov, T. Zajac, S. Strakhova, Opt. Spectr. (in Russ.) **63** (1988) 17.
- [3] S. Burkov, N.Letyaev, S. Strakhova, T. Zajac, XV ICPEAC (1987) 216.
- [4] S. Burkov, N.Letyaev, S. Strakhova, T. Zajac, J. Phys. B **21** (1988) 1995.

## STUDY OF LEFT-RIGHT ASYMMETRY IN PHOTOIONIZATION

T. Ricsóka<sup>a</sup>, S. Ricz<sup>a</sup>, Á. Kövér<sup>a</sup>, K. Holste<sup>b</sup>, A. A. Borovyk Jr.<sup>b</sup>, D. Varga<sup>a</sup>,  
S. Schippers<sup>b</sup> and A. Müller<sup>b</sup>

<sup>a</sup>Institute of Nuclear Research of Hung. Acad. Sci., H-4026 Debrecen, Hungary

<sup>b</sup>Institute for Atomic and Molecular Physics, Justus-Liebig University, D-35392  
Giessen, Germany

In the last years we observed a left-right asymmetry in the double differential cross sections of the outer  $s$ -shell photoelectrons ionized by linearly polarized synchrotron radiation. In order to verify our previous observation [1] a series of measurements were carried out at the beam line BW3 of the DORIS-III storage ring (Hamburg, Germany). The left-right asymmetry parameters were determined for He  $1s$ , Ne  $2s$ , Ar  $3s$  and Xe  $5s$  shells. The emitted electrons were analyzed with a newly built ESA-22 type ([2]) electron spectrometer of the Institute for Atomic and Molecular Physics (Giessen, Germany).

Figure 1. shows the comparison between our previous (solid circles) [1] and present (open circles) experimental left-right asymmetry parameters as well as the calculated one (dashed line and right hand scale). The theoretical estimation is based on the parity violation by the weak interaction between atomic nucleons and electrons (Standard Model) [1]. The experimental data sets do not increase with increasing nuclear mass and are in a good agreement with each other. This behaviour and the order of magnitude of the measured effect do not agree with the theoretical predictions. The present measurements confirm strongly our statement from Ref. [1] that the observed left-right asymmetry cannot originate from the weak interaction. The present non-zero asymmetry parameters suggest the breakdown of space inversion symmetry in photoionization and refute the interpretation of this breakdown with a few cycle VUV photon package. The present observation together with our previous one [1] strongly indicates that the left-right asymmetry is a result of a real physical process and cannot be interpreted as an instrumental effect.

We thank the staff of DORIS-III of HASYLAB for assistance during the measurements. This work was supported by the National Scientific Research Foundation and the National Office for Research and Technology of Hungary (NKTH-OTKA, Grant No. K67719).

*Keywords:* Photoionization; Electron spectroscopy

## References

- [1] S. Ricz, T. Ricsóka, Á. Kövér, D. Varga, M. Huttula, S. Urpelainen, H. Aksela and S. Aksela, *New J. Phys.* **9** (2007) 274.
- [2] S. Ricz, Á. Kövér, M. Jurvansuu, D. Varga, J. Molnár, and S. Aksela, *Phys. Rev. A* **65** (2002) 042707.

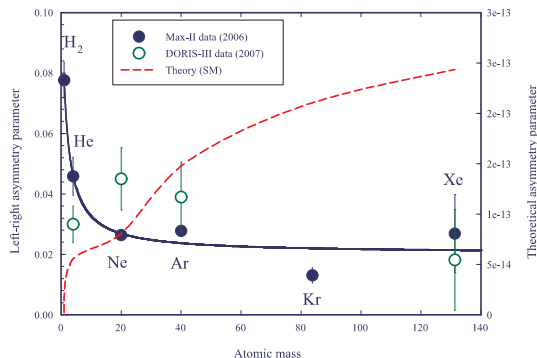


Fig. 1. The experimental and theoretical  $s$ -shell left-right asymmetry parameters as a function of the atomic mass. The solid line is drawn to guide the eye.

## THE INFLUENCE OF Zn ATOM ADDITIVE ON Cu LASER CHARACTERISTICS

**V.A. Kelman, E.A. Svitlichnyi, Yu.V. Zhmenyak, Yu.O. Shpenik, O.I. Plekan**

Department of Quantum Electronics, Universitetska str., 21, Uzhhorod, Institute of Electron Physics, 88017, Ukraine

Copper vapour laser (CVL) is known mostly due to large average and pulse output power, high pulse repetition frequency and efficacy. Therefore CVL has a wide sphere of various practical applications. In spite of CVL is known more than 40 years, still large number of investigations are carried out, having aim to improve it's output characteristics. In most of these investigations the influence of metal atom additive is studied. Among these additives the most known are Cs atom (energy acceptor) and Ag atom (energy donor). They promote to depopulation of lower or additional population of upper laser level.

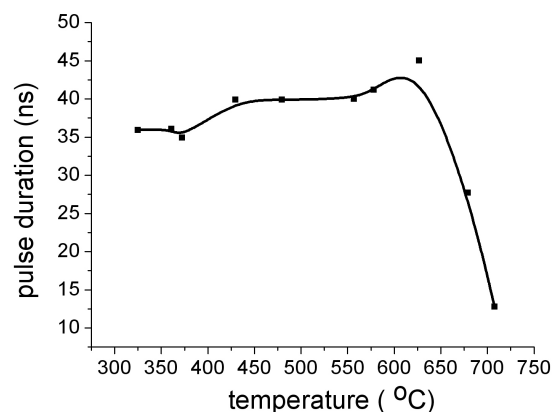
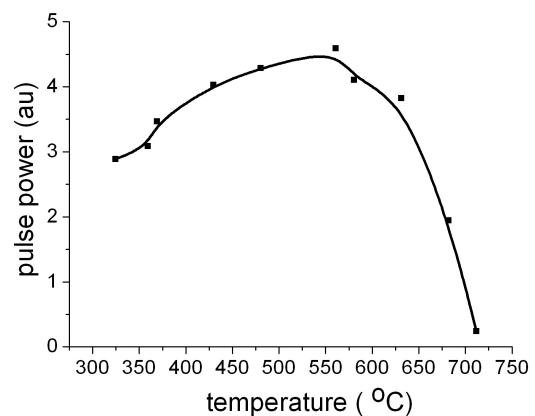
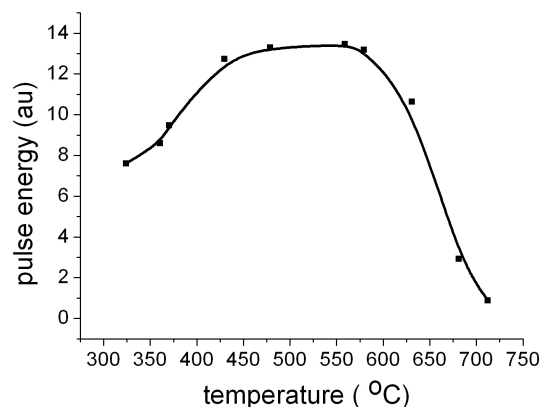
In this paper we report on experimental examination of Zn atom admixture influence on CVL output parameters. This additive can't be attributed to any of pointed classes. The modification of CVL using Zn additive firstly was reported in [1]. It was established pulse broadening by 220% and the peak power increasing by 180%. This drastically improvement was attributed both to depopulating of lower laser level due to resonance absorption of Zn resonant emission 213.9 nm and enhancing the upper laser level via cascading simultaneously. Ne-CuBr-Zn laser system was used. Here we used Ne-Cu-Zn system.

Two-section discharge tube was elaborated. Zn vapour was produced by heating container with Zn pieces placed between sections. Some results are demonstrated on the Figure as container temperature dependencies of pulse power, pulse width and pulse energy. So, in "pure" Cu vapour laser Zn atom additive also can improve output parameters. This improvement is not so large as in CuBr laser. At container temperature over 600 °C all output parameters diminished. The influence mechanism is now in process of detailed study.

*Keywords:* Copper vapour laser, output characteristics zink additive, absorption of resonant emission.

### References

[1] K. Fuji, K. Uno, F. Tawada, T. Hishida, M. Nishizawa, M. Suzuki, K. Oouchi. Appl. Phys. Lett. 80 (2002) 1859.



## Generalized space-translated Dirac equation and its equivalent Pauli form for superintense laser-atom interactions

Madalina Boca<sup>a</sup>, Viorica Florescu<sup>a</sup> and Mihai Gavrilă<sup>b</sup>

<sup>a</sup>Centre for Advanced Quantum Physics, University of Bucharest, Bucharest-Magurele, MG11, 077125, Romania

<sup>b</sup>FOM Institute for Atomic and Molecular Physics, Amsterdam, 1098 SJ, The Netherlands

We obtain the relativistic generalization of the space-translation transformation for the Dirac equation with a unidirectional laser pulse in terms of Volkov spinors. We show that a solution of the transformed equation, containing initially low-momenta  $p$  ( $p/mc \ll 1$ ), will maintain this property at all times, no matter how intense the field. As a consequence, the transformed equation splits at all times into two independent Pauli equations, one describing the evolution of electronic, the other of positronic wave packets. With spin neglected, these Pauli equations reduce to Schrödinger equations containing generalized potentials that are liable to extreme time-dependent distortion. The electron equation contains information that is equivalent to that of the original Dirac equation and covers all laser-atom interactions for frequencies  $\omega \ll mc^2$  and light ions ( $\alpha Z \ll 1$ ).

*Keywords:* Dirac equation, laser pulses, space-translation transformation

## ATOMIC IONIZATION BY SUDDEN MOMENTUM TRANSFER

**D. G. Arbó<sup>a</sup>, K. Tókési<sup>b</sup>, and J. E. Miraglia<sup>a,c</sup>**

<sup>a</sup> Institute for Astronomy and Space Physics, IAFE, CC67, SUC. 28 (1428) Buenos Aires, Argentina

<sup>b</sup> Institute of Nuclear Research of the Hungarian Academy of Science, Debrecen, Hungary

<sup>c</sup> Department of Physics, FCEN, University of Buenos Aires, Argentina

The Coulomb-Volkov approximation (CVA) is a time-dependent distorted-wave theory [1-4] which allows us to include the effect of the remaining core into the final state at the same approximation level as it can be performed for the case of the external field.

In this work we present a theoretical study of the electron distributions ejected from hydrogen atoms as a result of the ionization by a sudden momentum transfer (i.e., electric field:  $F(t) = -\Delta p \delta(t) \hat{z}$ ). We apply the CVA and the classical trajectory Monte Carlo (CTMC) [5] method to determine the doubly-differential electron momentum distribution and the final angular momentum. We show that the CVA reproduces the exact solution of the time dependent Schrödinger equation in the limit of zero pulse duration but with finite momentum transfer. Results are also compared with the values obtained by the strong-field approximation (SFA). It is noted that quantum and classical dynamics of the atomic electron suffering a kick are identical; nevertheless pronounced differences arise from the subsequent electron-nucleus interaction for small momentum transfers. These increased when the momentum transfer decreases, where the classical total ionization probabilities are smaller than the quantum one.

As an example, the 2D momentum distributions of the electron yield ionized by a kick with strength  $\Delta p = 2.5$  is shown in Fig. 1. Quantum mechanics brings in one lobe in the forward direction [Fig. 1a] which can be very accurately reproduced by CTMC [Fig. 1b]. Comparing these results to the SFA ones [Fig. 1c] two essentially effects due to the effect of the attractive Coulomb field can be noticed: (i) the center of the full quantum and classical distributions are slightly shifted towards the origin with respect to the SFA (the center is situated exactly at  $k_z = \Delta p$ , and (ii) the full quantum and classical momentum distributions are weakly distorted near the origin ( $k=0$ ).

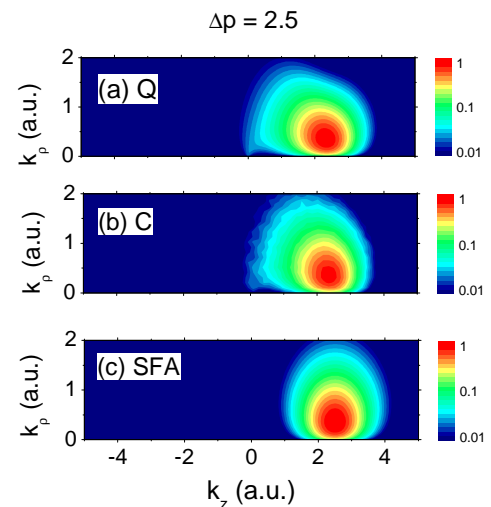


**Fig. 1:** 2D-momentum distributions of emitted electrons from H at the momentum transfer  $\Delta p = 2.5$  a.u. (a) Quantum, (b) Classical, and (c) SFA.

This work was supported by Conicet (Argentina) and the Argentina-Hungary collaboration HU/PA05-EIII/007.

*Keywords:* Coulomb-Volkov Approximation; Strong-Field Approximation; Sudden-Momentum Transfer

### References

- [1] F.H.M. Faisal and Schlegel, J. Phys. B **38** (2005) L223.
- [2] D. B. Milosevic, G. G. Paulus, D. Bauer, and W. Becker, J. Phys. B **39** (2006) R203.
- [3] P.A. Macri, *et al.*, J. Opt. Soc. Am. B **20** (2003) 1801.
- [4] D.G. Arbó *et al.*, Phys. Rev. A **77** (2008) 013401.
- [5] C. O. Reinhold and J. Burgdörfer, J. Phys. B **26** (1993) 3101.

# INTERACTION OF INTENSE SHORT LASER PULSES WITH POSITRONIUM

S. Borbély<sup>a</sup>, K. Tókési<sup>b</sup>, D. G. Arbó<sup>c</sup>, L. Nagy<sup>a</sup>,

<sup>a</sup>Babeş-Bolyai University, Faculty of Physics, str. Kogălniceanu nr. 1, 400084  
Cluj-Napoca, Romania

<sup>b</sup>Institute of Nuclear Research of the Hungarian Academy of Sciences, (ATOMKI),  
H-4001 Debrecen, P.O.Box 51, Hungary

<sup>c</sup>Institute for Astronomy and Space Physics, IAFE, Buenos Aires, Argentina

The ionization of the positronium by intense ultrashort laser pulses is studied theoretically. Calculations were performed applying quantum and classical approaches [1, 2]. The classical calculations were done within the framework of the classical trajectory Monte-Carlo (CTMC) method, where Newton's classical nonrelativistic equations of motion are solved numerically, when an external sine-square enveloped electromagnetic field is included.

In the quantum mechanical treatment we apply the strong field approximation to the direct solution of the time dependent Schrödinger equation (TDSE). We present the energy (see Fig. 1.) and angular distributions of the ionization probabilities of the photoelectrons for various laser parameters. We found that, while for the case of low electron energies larger discrepancies can be observed between the theories in the double differential ionization probabilities, at high electron energies the agreement is excellent.

This work was supported by the Romanian Academy of Sciences (grant No. 35/2007), the Romanian National Plan for Research (PN II) under contract No. ID 539, the Hungarian National Office for Research and Technology, the grant "Bolyai" from the Hungarian Academy of Sciences, and the Hungarian Scientific Research Found OTKA (K72172).

*Keywords:* positronium, short laser pulses, ionization

## References

- [1] D. G. Arbó et. al., Phys. Rev. A **77**, (2008) 013401.  
[2] S. Borbély et. al., Phys. Rev. A **77** (2008) 033412.

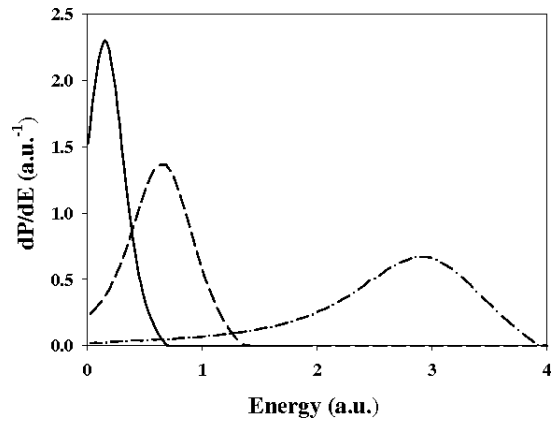


Fig. 1. Differential ionization probabilities of positronium obtained by CTMC method as function of the electron energy at various laser fields. The time-dependent electric field along the  $\hat{z}$  direction in the time interval between 0 and  $\tau$  is defined as  $\vec{F}(t) = \hat{z}F_0 \cos[\omega t - \omega\tau/2] \sin^2(\frac{\pi t}{\tau})$ . Solid line:  $F_0 = 1$ ,  $\omega = 0.05$ ,  $\tau = 3$ , Dashed line:  $F_0 = 1$ ,  $\omega = 0.05$ ,  $\tau = 5$ , Dashed-dotted line:  $F_0 = 1$ ,  $\omega = 0.05$ ,  $\tau = 10$ .



# PHOTOABSORPTION AND PHOTOIONIZATION OF DIATOMIC MOLECULES

**Irina Dumitriu<sup>a</sup> and Alejandro Saenz<sup>a</sup>**

<sup>a</sup> Institut für Physik, AG Moderne Optik, Hausvogteiplatz 5-7, D-10117 Berlin, Humboldt-Universität zu Berlin, Germany

The  $\text{HeH}^+$  molecular ion has been of interest for astrophysics, for the tritium neutrino mass experiments, and in itself as a model system for a long time. Currently it is drawing special attention due to the new FEL experiment performed at DESY, in Hamburg [1].

Theoretical data for the photoabsorption cross section of  $\text{HeH}^+$  exist so far only for the parallel orientation of the molecular axis with respect to the field [2]. Motivated by the Hamburg experiment, calculations for both parallel and perpendicular orientations have been performed and will be presented here together with an analysis of the two dissociation channels  $\text{He} + \text{H}^+$  (measured in the experiment) and  $\text{He}^+ + \text{H}$ . Since the experimental value is assumed to be obtained from a mixture of vibrational states, this aspect has also been analyzed and it will be shown and commented.

The method used for calculating the photodissociation cross sections is the one from [3]. Nuclear motion is solved in the adiabatic potential curves by expanding the nuclear wavefunction in  $B$  splines times spherical harmonics.

The same method is used for the calculation of the photoionization cross sections of the three lightest alkali dimer cations  $\text{Li}_2^+$ ,  $\text{Na}_2^+$  and  $\text{LiNa}^+$ . The motivation for this study is that although plenty of data exist for the bound states of these three molecules, no *ab initio* data were available for their photoionization spectra. The cross sections were calculated for the equilibrium internuclear distances of the three alkali dimer cations using a model potential to describe the core electrons and two different methods for obtaining the final spectra: the time-independent perturbative method from [3] and a time-dependent non-perturbative one (more details in [4]).

*Keywords:* photodissociation; photoionization; alkalis; diatomic molecules

## References

- [1] H. B. Pedersen, S. Altevogt, B. Jorodon-Thaden, O. Heber, M. L. Rappaport, D. Schwalm, J. Ullrich, D. Zajfman, R. Treusch, N. Guerassimova, M. Martins, J.-T. Hoeft, M. Wellhöfer, A. Wolf, *Phys. Rev. Lett.* 98 (2007) 223202.
- [2] Alejandro Saenz, *Phys. Rev. A.* 67 (2003) 033409.
- [3] Yulian V. Vanne, Alejandro Saenz, *J. Phys. B: At. Mol. Phys.* 37 (2004) 4101.
- [4] Irina Dumitriu, Yulian V. Vanne, Manohar Awasthi, Alejandro Saenz, *J. Phys. B: At. Mol. Phys.* 40 (2007) 1821.

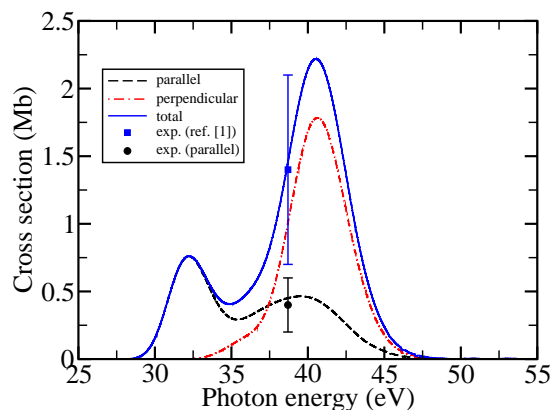


Fig. 1. Photodissociation of  $\text{HeH}^+$  into  $\text{He} + \text{H}^+$  (within the adiabatic approximation) compared to experiment [1]. (*Note:* the shown numerical results assume  $\text{HeH}^+$  to start in its rovibrational ground state, while a broad vibrational distribution is expected in the experiment).

# IONIZATION IN INTENSE LASER FIELD: INTENSITY-DEPENDENT ENHANCEMENTS AT INDUCED CHANNEL CLOSINGS

**Mihai Dondera**

Faculty of Physics, Bucharest-Magurele, MG11, R-76900, University of Bucharest,  
Romania

The high-energy part of the above threshold ionization spectra for atoms or ions exposed to laser pulses presents enhancements in the vicinity of certain values of the laser intensity. The phenomenon was observed experimentally for atoms of rare gases [1] in interaction with short laser pulses of high intensity.

Several theoretical studies were done to investigate the mechanisms of these quasi resonant variations of the peaks from the plateau of photoelectron spectra. The enhancements were explained in [2] as appearing from the decay of resonant states located near the polarization axis. Atomic systems are known for which the phenomenon is present even in the absence of excited states and it was suggested [3] that in their case light induced states can take over the role of excited states. An alternative explanation, not involving the existence of excited states, considers these enhancements as threshold effects associated with laser induced multiphoton channel closings (CC). A recent paper [4] predicts two distinct types of enhancements near CC and explains them as resulting from constructive interferences of a large number of long quantum orbits.

A significant progress in understanding the phenomenon was achieved within the Floquet theory framework. The plateau resonances have been related [5] with the resonances between the dressed ground state and excited states in the case of argon and no evidence was found for enhancements in photoelectron spectra which could be interpreted as due to CC. Pronounced enhancements of the above threshold detachment rates at CC were found in simulations [6] of the behavior of  $H^-$  and  $F^-$  ions in interaction with monochromatic laser fields.

We present results of an extensive numerical calculation of energy and angular distributions as functions of laser intensity near channel closings. These distributions are extracted from wave functions obtained by solving the time dependent Schrödinger equation in single active electron approximation for relevant cases. In simulations we consider potentials of Yukawa type and laser pulses with linear polarization, with or without a flat-top. For the case of a potential supporting a single bound state we study the dependence of these distributions on the other parameters of the laser pulse, with emphasis on the observation of the duration and shape roles. We analyze how the results change in the case of an Yukawa potential having one or more excited states.

*Keywords:* Laser pulse; Channel closings; Enhancements

## References

- [1] M.P. Hertlein, P.H. Bucksbaum and H.G. Muller, *J. Phys. B: At. Mol. Opt. Phys.* **30** (1997), L197; P. Hansch, M.A. Walker and L.D. Van Woerkom, *Phys. Rev. A* **55** (1997), R2535.
- [2] H.G. Muller, *Phys. Rev. A* **60** (1999), 1341.
- [3] J. Wassaf *et al*, *Phys. Rev. A* **67** (2003), 053405.
- [4] D.B. Milosevic *et al*, *Phys. Rev. A* **76** (2007), 053410.
- [5] R.M. Potvliege, Svetlana Vucic, *Phys. Rev. A* **74** (2006), 023412.
- [6] K. Krajewska, I.I. Fabrikant and A.F. Starace, *Phys. Rev. A* **74** (2006), 053407.

# COLD ATOMS PHOTOASSOCIATION WITH INTENSE LASER PULSES

Mihaela Vatasescu

Institute of Space Sciences, MG-23, 77125 Bucharest-Magurele, Romania

Photoassociation in cold atomic gases ( $T < 1$  mK) [1] is one of the leading techniques to create ultracold molecules [2]. Photoassociation experiments were mainly developed using continous lasers, but recently experimental results for pulsed photoassociation of cold atoms became available [3], as well as theoretical models [4]. Our work is part of the recent theoretical efforts investigating how tailored laser pulses could be used to control the photoassociation between two cold atoms in order to form cold molecules. We study the vibrational dynamics produced when two cold atoms are photoassociated in a diatomic molecule by a “moderately” strong laser pulse. The dynamics is simulated using a wavepackets method to solve numerically the time-dependent Schrodinger equation, and analysed in order to understand the time evolution of the system during and after the laser pulse. Results will be shown for a certain electronic transition in the  $\text{Cs}_2$  molecule. By analysing specific processes (acceleration of the vibrational population to the zone of the chemical bound, population of vibrational states, transfer of population and momentum between the electronic channels implied in the process) one can learn how the laser pulse could induce some desired states in the system.

*Keywords:* cold atoms and molecules; vibrational dynamics; pulsed photoassociation

## References

- [1] K.M. Jones, E. Tiesinga, P.D. Lett, P.S. Julienne, Rev. Mod. Phys. 78 (2006), 483
- [2] O. Dulieu, M. Raoult, E. Tiemann, J.Phys. B: At. Mol. Opt. Phys. 39, 19 (2006)
- [3] W. Salzmann, U. Poschinger, R. Wester, M. Weidemüller, A. Merli, S.M. Weber, F. Sauer, M. Plewicky, F. Weise, A. Mirabal Esparza, L. Wöste, and A. Lindinger, Phys. Rev. A 73, 023414 (2006); B. L. Brown, A.J. Dicks, and I.A. Walmsley, Phys. Rev. Lett. 96,173002 (2006); M. J. Wright et al., Phys. Rev. A 75, 051401(R), (2007)
- [4] J. Vala, O. Dulieu, F. Masnou-Seeuws, P. Pillet and R. Kosloff, Phys. Rev. A 63, 013412 (2001); E.Luc-Koenig, R. Kosloff, F. Masnou-Seeuws, M. Vatasescu, Phys. Rev. A 70, 033414 (2004); E.Luc-Koenig, M. Vatasescu, and F. Masnou-Seeuws, Eur. Phys. J. D.31, 239 (2004)

## PROPAGATION EFFECTS IN ATTOSECOND PULSE GENERATION

**V. Tosa**

Department of Molecular and Biomolecular Physics, National Institute for R&D of Isotopic and Molecular Technologies, Cluj-Napoca, Romania

The interaction of ultraintense and ultrafast laser pulses with noble atoms leads to the generation of high order harmonics, a process in which the electron is ionized by the driving laser, and, after being accelerated by the laser field, recombines with the core to emit a harmonic photon [1]. The process takes place two times in an optical cycle, giving rise to an attosecond pulse train in time domain and to odd order harmonics in frequency domain.

By using a non-adiabatic three-dimensional model for this process we studied the formation of the attosecond pulses in conditions close to the experiments performed nowadays. The model we developed [2] first solves the propagation equation for the laser field taking into account diffraction, optical Kerr effect and dispersion by neutral atoms and by electron plasma. We then use the solution of the propagation equation to calculate the single atom dipole in the strong field approximation, and, finally, we solve the propagation equation for the harmonic field having as source the atomic polarization. In addition to this model we present a time-dependent phase matching technique based on trajectory phase calculation which is used to analyze the macroscopic formation of the train in the near and far fields.

The formation of the attosecond pulses is strongly influenced by the propagation effects which manifest upon the driving laser field. For low intensities the spatial beam configuration and temporal/spectral pulse shape remain practically unaffected by the propagation. Increased pulse intensities produce distortions of the laser field. Space and time/frequency modifications of the laser pulse were investigated in detail in [2]. In time, the leading edge of the pulse remains unchanged, as it travels in a neutral medium of refractive index close to unity, while the rear portion lowers its intensity due to defocusing. The result is a certain shortening of the pulse duration and a shift of the peak intensity to earlier times within the pulse. In frequency, due to the self-phase modulation induced by the time dependent refractive index of the medium, the laser frequency increases with time (the laser chirp becomes positive) in the leading edge, and then decreases back to the nominal frequency in the trailing edge. Finally in space, these time/frequency distortions have a radial decrease, following the plasma density decrease with increasing  $r$ . It is obvious but important to mention that the changes in laser field intensity and phase will directly affect the phase of the single dipole, thus ultimately the APT features.

We analyze in this work the influence of the above propagation effects upon the formation of isolated attosecond pulse by an ultra-short laser pulse ( $\sim 5$  fs) and by longer pulses in a polarization gating configuration [3]. We show that ionization dynamics acts as an additional gate in the process of attosecond pulse formation, while propagation effects clean the single atom response and, in specific conditions, helps the formation of a single attosecond pulse.

### References

- [1] P.B. Corkum, Phys. Rev. Lett. **71**, (1993) 1994.
- [2] V. Tosa, H. T. Kim, I. J. Kim, and C. H. Nam, Phys. Rev A **71**, (2005) 063807; *ibid.* **71**(2005) 063808.
- [3] C. Altucci, V. Tosa, R. Velotta, Phys. Rev. A **75**, 061401 (2007)

## GENERATION OF ULTRA-SHORT X-RAY PULSES IN CLUSTER SYSTEM DURING IONIZATION BY FEMTO-SECOND OPTICAL PULSE

A. Glushkov<sup>a,b</sup>, O. Khetselius<sup>b</sup> and A. Ignatenko<sup>b</sup>

<sup>a</sup>Institute for Spectroscopy of Russian Academy of Sciences (ISAN), Troitsk, 142090, Russia

<sup>b</sup>Odessa University, P.O.Box 24a, Odessa-9, 65009, Ukraine

We present the results of modeling generation of the atto-second VUV and X-ray pulses during ionization of atomic and cluster systems by femto-second optical laser pulse. The concrete data are received for the Ar cluster response, the molecular 2D H<sub>2</sub><sup>+</sup> response for different inter nuclear distances (R=2.5, 3.5, 7.4, 16a.u.) with smoothed Coulomb potential and atomic (H) response (spectral dependence) under ionization of the system by femto-second optical pulse. Our calculation show that the generation of the atto-second X-ray pulses in the cluster system is more effective and profitable (as minimum the 2-3 orders) than in similar molecular atomic one. The generation of the atto-second pulses in the molecular system is more profitable too (as minimum the 1-2 orders) than in similar atomic one. The last achievements in this field demonstrate a possibility of construction of the compact X-ray radiation sources.

*Keywords:* X-ray; Cluster; Femto-Second Pulse

### References

- [1] A. Glushkov, L.N. Ivanov, Phys. Lett. A 170 (1992) 33; J.Phys.B 26 (1993) L279.
- [2] A. Glushkov et al, Int.Journ. Quant. Chem. 99 (2004) 889; 104 (2005) 562; J.Phys.CS 11 (2005) 199; 35 (2006) 425.

## DISORDER EFFECTS IN REFLECTANCE SPECTRA OF COLLOIDAL PHOTONIC CRYSTALS

E. Vințeler<sup>a</sup>, C. Farcău<sup>a,b</sup>, S. Aștilean<sup>a,b</sup>

<sup>a</sup>Faculty of Physics, Babeș-Bolyai University, Str M. Kogalniceanu 1, 400084 Cluj-Napoca, Romania

<sup>b</sup>Nanobiophotonics Laboratory, Institute for Interdisciplinary Experimental Research, Babeș-Bolyai University, T. Laurian 42, 400271, Cluj-Napoca, Romania

Photonic crystals are materials with a spatially periodic dielectric function in one, two or three dimensions [1]. In nature several insects reduce the reflection of light at interfaces using these crystals as antireflective coatings. In technology photonic crystals are important in fabrication of solar cells, optical fibers and other optical devices with reduced reflectance [2].

A relatively simple and inexpensive way of fabrication of colloidal photonic crystals via convective assembly technique can be achieved by using a home-built apparatus [3]. We were able to produce high-quality photonic crystals by self-assembling of several layers of close-packed polystyrene spheres on glass substrate.

Although fabrication of photonic crystals improved over the last few years, intrinsic defects of photonic lattice affect the shape of experimental reflectance spectra [4]. In order to compare experimental spectra with simulated photonic band structure, disorder effects are simulated by introduction of material absorption. By using the finite-difference time-domain (FDTD) method [5] we were able in the past to obtain a good agreement between experimental and simulated transmission curves by taking in account the glass substrate [6][7]. In this work we extend our analysis for reflectance curves for one, two and three-layered close-packed polystyrene spheres. We show that a key ingredient in understanding disorder effects is polystyrene absorption.

Keywords: Colloidal photonic crystals. Finite-difference time-domain

### References

- [1] E. Yablonovitch, Photonic Crystals: Semiconductors of Light, SCIAM, (2001), 47
- [2] V. Cămpăan, C. Farcău, E. Vințeler, S. Aștilean, Antireflective properties of polystyrene nanosphere self-assembled films, in Progress in Nanoscience and Nanotechnologies, Ed. Acad. Romane, Buc., (2007), 68-77
- [3] A. Kuttesch, C. Farcău, Z. Neda, S. Aștilean, Proc. SPIE, 6785, 678500 (2007).
- [4] L.A. Dorado, R.A. Depine, G. Lozano, H. Míguez, Phys.Rev. B76 (2007), 245103
- [5] J. D. Joannopoulos, S. G. Johnson, J.N. Winn, R. D. Meade, Photonic Crystals: Molding the Flow of Light (Second Edition), (2008)
- [6] C. Farcău, E. Vințeler, S. Aștilean, Experimental and Theoretical Investigation of Optical Properties of Colloidal Photonic Crystal Films, JOAM (2008) to appear.
- [7] E. Vințeler, C. Farcău, S. Aștilean, Designing The Colour of Photonic Crystals For Sensors Applications, JOAM (2008) to appear.

## INTERACTION OF LIGHT WITH METALLIC NANO HOLE ARRAYS

V. Canpean and S. Astilean

Nanobiophotonics Laboratory, Institute for Interdisciplinary Experimental Research and  
Faculty of Physics, Babes-Bolyai University, M. Kogalniceanu 1, 400084 Cluj-Napoca,  
Romania

A fundamental constrain in manipulating light at nanoscale is the extremely low transmission through subwavelength apertures. According to the theoretical results predicted by Bethe [1], transmission through a single aperture smaller than the wavelength of light scales as:

$$T \propto \left(\frac{r}{\lambda}\right)^4$$

where  $r$  is the radius of the subwavelength aperture and  $\lambda$  is the wavelength of light. Accordingly, for a hole of 150nm diameter, one expects a transmission efficiency on the order of  $10^{-3}$ . In 1998, Ebbesen and co-workers [2] found that the transmission of light through a *periodic array* of subwavelength holes is drastically enhanced. Using a silver film with periodic array of holes with diameter of 150nm, the authors observed an enhanced transmission with efficiencies about 1000 times higher than that expected. This result has generated numerous experimental and theoretical studies.

In this work we study the above phenomenon on thin gold films perforated with periodic arrays of nanoholes. For fabrication we implemented a nano-lithographic method inspired from the classical nanosphere lithography [3], in which we combine the self-assembling of polystyrene nanospheres with reactive ion etching (RIE) and metal deposition. The films morphology was characterized by AFM, whereas its transmission was measured using an optical fiber microspectrometer and simulated by FDTD method.

The physical mechanism responsible for the observed 3 times enhanced transmission can be understood by the contribution of mixed plasmon resonances: localized resonance and surface waveguide resonance [4]. The effect depends on the structural film parameters like hole diameter and film thickness. Apart from its fundamental interest in nano-optics, this transmission effect has potential applications in biophotonic, near-field microscopy and sensing.

**Acknowledgments** This work was partially supported by the Romanian National Authority for Research in the frame of the CEEX program (Project No. 71/ 2006) and by The National University Research Council in the frame of the PN-II program (Project No. TD-28/2007).

*Keywords:* nanostructures, plasmon resonance, enhanced optical transmission

### References

- [1] H. A. Bethe, Phys. Rev. **66** (1944) 163.
- [2] T. W. Ebbesen, H. J. Lezec, H. F. Ghaemi, T. Thio and P. A. Wolff, Nature **391** (1998) 667.
- [3] J. C. Hulteen and R. P. Van Duyne, J. Vac. Sci. Technol. A **13** (1995) 1553.
- [4] Z. Ruan and M. Qiu, Phys. Rev. Lett. **93** (2006) 233901.

## LUMINESCENCE PROPERTIES OF GOLD NANORODS

F. Toderas, M. Iosin and S. Astilean

Nanobiophotonics Laboratory, Institute for Interdisciplinary Experimental Research, Faculty of Physics, Babes-Bolyai University, Treboniu Laurian 42, 400271, Cluj-Napoca, Romania

Controlled synthesis of noble metal nanoparticles has attracted considerable attention because their optical properties are greatly size- and shape-dependent. Among the spherical particles, gold nanorods have been the subject of many investigations due to their different plasmonic properties. Recently, El Sayed et al. [1] reported luminescence from gold nanorods million times higher as compared with the gold metal. These unique properties of nanorods, namely multiple plasmon resonances and luminescence, are important for biosensors development [2], surface-enhanced Raman spectroscopy [2] and fluorescence enhanced spectroscopy [3].

In this work we report on the luminescence properties of gold nanorods synthesized by a seed growth method in the presence of cetyltrimethylammonium bromide (CTAB) solutions. For a fixed excitation line at 480 nm the spectral position of the maximum emission occurs at 570 nm and depends on gold nanorod aspect ratio.

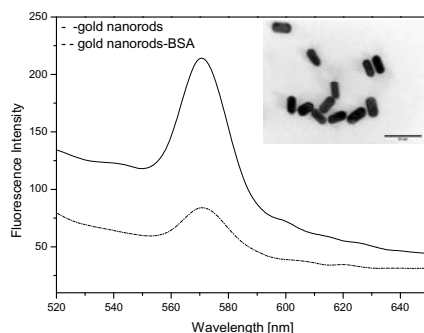


Fig. 1. Fluorescence spectra of gold nanorods in the presence of protein at 480 nm excitation line. The inset shows the transmission electron microscopy of gold nanorods.

We explore the ability of luminescence signal collected from gold nanorods to probe the attachment of biomolecule to metal surface. It is well known that the many molecules exhibiting thiol or amine groups bind specifically to the free ends of gold nanorod [3]. Indeed, in this study we found that binding of BSA is detectable from fluorescence spectra (see Fig 1). The intrinsic luminescence combined with strong plasmonic resonances opens the way to build novel multiplexed biodetection platforms based on gold nanorods.

*Keywords:* gold nanorods, surface plasmon, luminescence

**Acknowledgement** This work is supported by CNCSIS under the project PN-II-ID-PCE-2007-1, no 477/2007

### References

- [1] M. B. El Sayed, V. Volkov, S. Link, M. El Sayed, Chem. Phys. Lett. 317 (2000) 517-523.
- [2] Y. Yang, L. Xiong, J. Shi and M. Nogami, Nanotechnology 17 (2006) 2670-2674.
- [3] B. Pan, D. Cui, P. Xu, Q. Li, T. Huang, R. He, F. Gao, Colloids and Surfaces A: Physicochem. Eng. Aspects 295 (2007) 217-222.



## PLASMON-ENHANCED FLUORESCENCE OF DYE MOLECULES

**M. Iosin<sup>1</sup>, P.L. Baldeck<sup>2</sup> and S. Astilean<sup>1</sup>**<sup>1</sup> Nanobiophotonics Laboratory, Institute for Interdisciplinary Experimental Research,  
T. Laurian 42, 400271 and Faculty of Physics, Babes-Bolyai University, Cluj-Napoca, Romania<sup>2</sup> Laboratoire de Spectrométrie Physique, Université Joseph Fourier & CNRS UMR5588 Saint Martin d'Hères,  
France

Fluorescence spectroscopy is a central technology in bioscience. However, the detection of many biological molecules is usually limited by their low quantum yield, photostability and autofluorescence. Recently, a new strategy to achieve fluorescence enhancement has been demonstrated [1]. The approach is to use metallic nanoparticles, which drastically alter the emission of vicinal fluorophores as results of plasmon excitation [2]. The use of metallic nanostructure to enhance fluorescence has great potential for applications in the fields of medical diagnostics, biotechnology and applications for in-vivo imaging.

In this study, the fluorescence of the free rhodamine 6G (Rh6G) fluorophore in deionized water as well as in the mixtures with gold nanoparticles was measured using a Zeiss Axiovert microscope in epi-fluorescent geometry. A compact Xe lamp coupled to a monochromator was used as an excitation light source. R6G-Au mixtures were excited at different excitation wavelength in the range from 310 to 570 nm and R6G emission at 520 nm was collected using a highly sensitive CCD camera. A 3-fold amplification of the fluorescence signal in presence of colloid Au nanoparticles was observed for in resonance with plasmons. Two effects are responsible for fluorescence enhancement. First, the incident light field enhancement near metallic nanostructures, the phenomenon known as an enhanced local field. Second, the interaction of excited fluorophore dipole with metallic particle that results in enhanced radiative rate and rapid emission of the photon, the phenomenon we call RDE (Radiative Decay Engineering)

**Keywords:** Metal-enhanced fluorescence, Gold Colloids, Rhodamine 6G, Plasmons

**Acknowledgments.** This work was partially supported by the Romanian National Authority for Research in the frame of the CEEEX program (Project No. 71/ 2006) and by Agence Universitaire de la Francophonie (AUF)

**References:**

- [1] C. D. Geddes and J. R. Lakowicz, *J. Fluoresc.* **12**, 121, 2002.
- [2] J. R. Lakowicz, *Anal. Biochem.* **298**, 1 2001.

## THE STUDY OF RAMAN ENHANCEMENT EFFICIENCY AS FUNCTION OF NANOPARTICLE SIZE AND SHAPE

**Sanda C. Boca, Cosmin Farcau, Simion Astilean**

Nanobiophotonics Laboratory, ICEI, Babes-Bolyai University,  
T. Laurian 42, 400271 Cluj-Napoca, Romania

The interaction of light with noble metal particles much smaller than the wavelength, i.e. nanoparticles, is dominated by strong optical resonances due to excitation of surface plasmon modes [1]. One of the main consequences of plasmon excitation is the high electromagnetic field near the nanoparticle surface which is useful in enhancing the sensitivity of Raman spectroscopy in (bio)molecular detection [2]. It was demonstrated that colloidal gold mono- or multilayers self-assembled on solid substrates can strongly amplify the efficiency of Raman scattering of probe molecules attached to their surface [3].

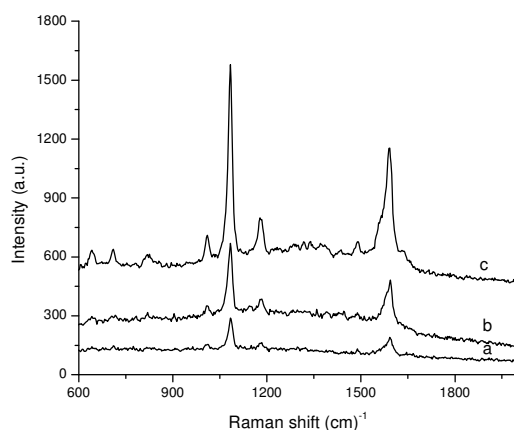


Fig. 1. Surface enhanced Raman spectrum of p-aminothiophenol adsorbed on different sizes gold nanoparticles: (a) 30 nm; (b) 45 nm; and (c) 60 nm.

This work is focused on studying the dependence of Raman enhancement of p-aminothiophenol molecules adsorbed on self-assembled gold monolayers as function of nanoparticle size and shape. Gold nanoparticles of different sizes (ranging from 18nm to 80nm) and shapes (round and ellipsoidal) were synthesized by reduction of tetrachloroauric acid ( $\text{HAuCl}_4$ ) in aqueous medium by varying the ratio between the reducing agent (trisodium citrate) and gold salt and were immobilized on functionalized glass substrates. The optical properties of the prepared samples were investigated by absorbance measurements taken before and after the adsorption of the molecule. We found that the Raman enhancement of probe molecules measured under 633 nm laser line strongly depends on the sizes of self-assembled gold nanoparticles as can be seen in figure 1.

**Acknowledgement:** This work was supported by CNCSIS under the project No. ID\_477/2007 in the frame of program PN-II-ID-PCE-2007-1.

*Keywords:* Gold nanoparticles, Raman scattering

### References

- [1] L. Novotny, B. Hecht, Principles of Nano-Optics, Cambridge University Press 2006.
- [2] J. Kimling, M. Maier, B. Okenve, V. Kotaidis, H. Ballot, A. Plech, J. Phys. Chem. B 110 (2006) 15700.
- [3] F. Toderas, M. Baia, L. Baia, S. Astilean, Nanotechnology 18 (2007) 255702.

## TEM, XRD and DSC analysis of Mn doped FINEMENT<sup>#</sup>

M.Moneta<sup>1\*</sup>, J.Balcerski<sup>1</sup>, P.Uznański<sup>2</sup> and P.Sovak<sup>3</sup>

<sup>1</sup>Uniwersytet Łódzki, Katedra Fizyki Ciała Stałego, PL 90-236 Łódź, Pomorska 149, Poland

<sup>2</sup>Centrum Badań Molekularnych i Makromolekularnych Polskiej Akademii Nauk  
PL 90-363, Łódź, Sienkiewicza 112, Poland

<sup>3</sup>Univerzita P.J.Šafárika v Košiciach Prírod. Fakulta, Park Angelinum 9, 04-101 Košice,

Properties of thin films (40nm) and foils (20 $\mu$ m) of FINEMET based amorphous and crystalline alloys Fe<sub>73.5-x</sub>Si<sub>13</sub>B<sub>9</sub>Cu<sub>1</sub>Nb<sub>3</sub>Mn<sub>x</sub> highly doped with Mn (x=9÷15) were studied. The transmission electron microscope (TEM) scanning electron microscope (SEM+EDX), X-ray diffraction (XRD) and differential scanning calorimetry (DSC) were analysed.

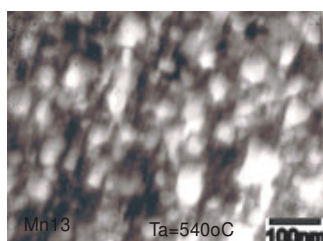


Fig.1 TEM SED picture

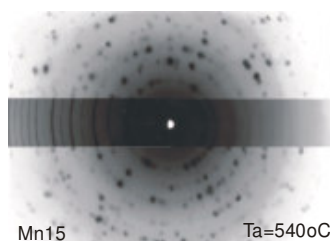


Fig.2 TEM diffraction pattern

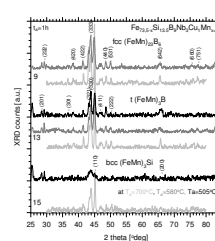


Fig.3. XRD pattern

As shown by DSC there is only one crystallization temperature at  $T_c=600^\circ\text{C}$ , however crystallization starts at  $T_o=500^\circ\text{C}$  as shown by TEM (Fig.1-2) and XRD (Fig.3). Three crystallographic structures were identified: Fe<sub>3</sub>Si, Fe<sub>23</sub>B<sub>6</sub>, Fe<sub>3</sub>B with lattice constants slightly different for foils and for thin films. The average size of crystallites approximately 35nm, 30nm and 25nm respectively, was shown to depend on Mn content x, annealing temperature  $T_a$ .

Keywords: Finemet; Mn doping; TEM; XRD;DSC

### References

1. R.Brzozowski, M.Wasiak, H.Piekarski, P.Sovak, P.Uznański and M.Moneta, J.Alloys Comp. (2008) accepted.

<sup>#</sup>supported by UŁ Grant 505/689 (2008)

\*e-mail: marek\_moneta@uni.lodz.pl

## **Surface and bulk plasmon excitations in Carbon Nanotubes. Comparison with the hydrodynamic model**

Mario Zapata Herrera<sup>+</sup> and J. L. Gervasoni<sup>\*</sup>

<sup>+</sup> Instituto Balseiro and Centro Atómico Bariloche, Comisión Nacional de Energía Atómica, 8400, Bariloche, Río Negro, Argentina.

<sup>\*</sup> Instituto Balseiro and Centro Atómico Bariloche, Comisión Nacional de Energía Atómica, 8400 Río Negro, Argentina. Also member of the Consejo Nacional de Investigaciones Científicas y Tecnológicas (CONICET), Argentina

The study of nanomaterials has given place in the last years to an enormous experimental and theoretical activity. One of the most important nanostructures are Carbon Nanotubes, which are of great interest due to their high conductivity and to their specific properties that are very sensitive to the geometric structure. Some theoretical studies predict that these materials exhibit properties of metals and semiconductors, depending on their geometric configuration.

In this work we study the structure and characterization of these nanostructures. We analyse the properties of the collective excitations of the free electron gas of Single Walled Carbon Nanotubes. We study in detail the surface and bulk modes excited in cylindrical nanostructures due to their interaction with charged particles. We analyze the surface and bulk plasmon excitations in nanowires and carbon nanotubes within the Dielectric formalism and the so-called Hydrodynamic model, which allows us to obtain different dispersion relations in both formalisms. We compare these models with other theoretical and experimental results, in particular with Energy Electron Loss Spectroscopy (EELS) spectra for plasmon excitations.

## ATOMIC FORCE MICROSCOPY CHARACTERIZATION OF GOLD NANOCRYSTALS

R. Stiuftuc, F. Toderas G. Stiuftuc and S. Astilean

“Babes-Bolyai” University, Faculty of Physics, Cluj-Napoca, Romania

Gold nanocrystals are promising candidates for optical, electronic and biological applications. They are of immense interest due to their intriguing surface plasmon resonance (SPR) property originating from the collective oscillation of conduction electrons in response to an optical excitation [1]. Nonspherical gold nanocrystals such as nanorods, nanotriangles, nanoplates, etc., show two plasmon bands: one in the visible region similar to spherical nanoparticles and another one in the higher wavelength region that sometimes extends well into the near-infrared (NIR) region of the spectrum. Metallic nanocrystals exhibiting such SPR band in the NIR region have potential applications in cancer hyperthermia and new cell imaging and as heat absorbing for solar energy production.

Among all the preparation methods biosynthesis of gold nanocrystals by plant extracts is a very promising route which allows the fabrication of nanoparticles with different shapes and dimensions ranging from a few nanometers to micrometers. On the other hand Atomic Force Microscopy is arguably the dominant technique for nanoscale characterization and/or manipulation. However, the ability to achieve quantitative chemical contrast by AFM is not as straightforward as topographic imaging [2]. Using the unique capabilities of Amplitude Modulation Atomic Force Microscopy we have characterized a broad range of gold nanocrystals biosynthesized by reduction of aqueous chloroaurate ions in pelargonium plant extract. Specifically, we have studied the phase shift dependence on the tip–surface separation, interaction regime, cantilever parameters, free amplitude and tip–surface dissipative processes and we have converted these results into energy dissipation values. Furthermore, energy dissipation maps provide a robust method to image material properties because they do not depend directly on the tip–surface interaction regime.

*Keywords:* Atomic Force Microscopy, Gold Nanocrystals

### References

- [1] Burda C., Chen X., Narayanan R., El-Sayed M. A. Chem. Rev. 105, (2005), 1025
- [2] Martinez N.F., R. Garcia, Nanotechnology 17 (2006) 167

## INFRARED SPECTRA OF SMALL WATER CLUSTERS: RELEVANCE OF INDUCED POLARIZATION

Titus Adrian Beu, Gabriel Cabau

*University "Babes-Bolyai", Faculty of Physics, Cluj-Napoca, 3400, Romania*

In order to calculate the vibrational spectra for small water clusters ( $n \leq 20$ ), two potential models were comparatively used for the description of intermolecular interactions: TIP4P and COS/B2.

One of the goals of the present study was to distinguish the effect of molecular polarization, and consequently we have chosen one potential model implying a fully rigid monomer with four sites, TIP4P, and one featuring three fixed sites and one movable polarization site – the COS/B2 model. In the latter model, the polarization is taken into account by a variable separation of charges on selected polarizable centers. One of the pair of polarization charges resides on a polarizable center, the O atom, while the other one is treated as an additional particle attached to the polarizable center by a parabolic restraint potential. The separation is calculated in response to the instantaneous electric field.

The original COS/B2 model parametrized by Haibo Yu et al. causes instabilities in the cluster structure calculations performed by deterministic energy minimization of random initial configurations. The instabilities can be avoided only by using a reparametrised model, with a reduced polarization charge (from  $-8e$ , originally, to  $-1.25e$ ). Obviously, using a smaller polarization charge results in increased polarization charge displacements. However, as Straatsma and McCammon observed, changing the polarization charge from  $-8e$  to  $-1e$  does not noticeably alter the radial distribution functions of the simulated bulk water. The difference in the potential energy and density are negligible and the dipole moment distributions remain very similar.

While for the small clusters ( $n \leq 10$ ) the potential energies obtained with the polarizable COS/B2 model are higher than the ones yielded by the TIP4P model, clusters bigger than  $n = 16$  appear to be more and more stable. Equally, the clusters obtained with COS/B2 appear to be more symmetrical, showing a preference for hexagonal or pentagonal prism structures instead of some of the rectangular TIP4P structures.

The IR frequency shifts have been calculated using a proven second order perturbation approach, which takes into account the effect of anharmonicities, intermolecular interactions and temperature, and the results have been compared with experimental IR spectra for size selected water clusters of sizes  $n < 10$ .

**PROPERTIES OF POSITIVE AND NEGATIVE IONS IN ANTHRACENE  
DERIVATIVES: A THEORETICAL STUDY**

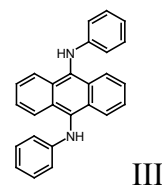
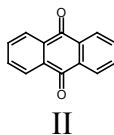
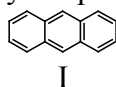
**A.V. Kukhta<sup>a</sup>, I.N.Kukhta<sup>a</sup>, O.L. Neyra<sup>b</sup>, E. Meza<sup>b</sup>**

<sup>a</sup> Electron Spectroscopy and Optics Group, B.I.Stepanov Institute of Physics, Nezalezhnastsi Ave. 70, 220072 Minsk, Belarus

<sup>b</sup> Spectroscopy and Laser Group, Popular University of Cesar, Valledupar, Colombia

Polycyclic aromatic compounds are a large class of conjugated  $\pi$ -electron systems of great importance in many research areas, such as materials science, astrochemistry, and molecular electronics. In the last case molecules having electron accepting and electron donating properties are often used strongly effecting charge transporting properties of thin films based on these materials.

In the contribution a systematic theoretical study of anthracene (compound I) and anthracene derivatives with electron accepting (compound II) and electron donating (compound III) properties in their anionic, neutral, and cationic charge states are presented. We used density functional theory (DFT) to obtain the ground-state optimised geometries, and time-dependent DFT (TD-DFT) to evaluate the electronic absorption spectra. Total-energy differences enabled us to evaluate the electron affinities and ionisation energies, the changes of HOMO and LUMO positions and their energy gap as well as the charge distribution in the studied neutral and ionic molecules. The chemical structures of molecules under study are presented below.



Keywords: anthracene derivative, ion, DFT study

## FORMATION OF LONG LIVED NEGATIVE IONS IN ANTHRACENE DERIVATIVES

**A.V. Kukhta<sup>a</sup>, S.A. Pshenichnyuk<sup>b</sup>, N.L. Asfandiarov<sup>b</sup>**

<sup>a</sup> Electron Spectroscopy and Optics Group, B.I.Stepanov Institute of Physics, Nezalezhnastsi Ave. 70, 220072 Minsk, Belarus

<sup>b</sup> Institute of Molecular and Crystal Physics, October Prosp. 51, 450075 Ufa, Russia

Wide applications of organic hydrocarbons in molecular electronics stimulated their studies by different tools. The formation of negative ions is known to effect strongly charge transporting properties of thin films based on these materials. A series of anthracene derivatives having different electron accepting and electron donating properties has been studied by means of electron capture negative ion mass spectrometry. The experimental details are described in [1].

The formation of negative ions of anthracene and anthraquinone is similar to observed earlier [2]. In the spectrum of 9,10-dianilidoanthracene three negative ions:  $[M-2H]^-$  ( $m/e$  358),  $[M]^-$  ( $m/e$  360), and  $[M-C_6H_5]^-$  ( $m/e$  283). The other peaks are at least one order less intensive. It can be derived three resonance regions at 0.2, 1.0 and 2.0 eV. The autodetachment lifetime is about 100 msec. The reasons of such negative ions are discussed.

Keywords: anthracene derivative, negative ion, mass spectrometry

### References

[1] A.V. Kukhta, D.V. Ritchik, N.L. Asfandiarov, V.S. Fal'ko, V.G. Lukin, S.A. Pshenichnyuk, Int. J. Mass Spectrom. 230 (2003) 41.

[2] N.L. Asfandiarov, A.I. Fokin, V.G. Lukin, E.P. Nafikova, G.S. Lomakin, V.S. Fal'ko and Y.V. Chizhov, Rapid Commun. Mass Spectrom. 13 (1999) 1116.



## INTERACTION OF LOW-ENERGY ELECTRONS WITH PHTHALOCYANINE AND PORPHIRINE MOLECULES IN THE GAS PHASE

**A.V. Kukhta<sup>a</sup>, S.M. Kazakov<sup>b</sup>**

<sup>a</sup> Electron Spectroscopy and Optics Group, B.I.Stepanov Institute of Physics, Nezalezhnastsi Ave. 70, 220072 Minsk, Belarus

<sup>b</sup> Chuvash State University, Moskovski Prosp. 15, 428015 Cheboxary, Russia

There is poor information about electron-molecule interaction for organic compounds as compared to atoms and small molecules though they find manifold applications in molecular electronics, radiation chemistry, biology, and medicine. At least, the study of low-energy electron scattering with organic molecules gives the possibility to find the structure of vibrational and electronic levels including direct population of optically forbidden states. In this presentation the relative efficiency of excitation into singlet and triplet states in the region between 1.5 and 10 eV, their dependence on projectile electron energies for the scattering of monoenergetic electrons with tunable energies from 0 to 50 eV at an angle of 90°, for a number of phthalocyanine and porphyrine molecules in the gas phase are presented. The experimental details are described in [1].

Keywords: phthalocyanine, porphyrine, electron energy loss spectrum

### References

[1] A.V. Kukhta, I.N. Kukhta, S.M. Kazakov, O.V. Khristophorov, O.L. Neyra, J. Chem. Phys. 127 (2007) 084316.

## SPECTROSCOPIC INVESTIGATIONS OF NEW METALLIC COMPLEXES WITH LEUCINE AS LIGAND

**Cs. Nagy<sup>a</sup>, A. Marcu<sup>a</sup>, A. Stanila<sup>b</sup>, D. Cozma<sup>a</sup>, D. Rusu<sup>c</sup> and L. David<sup>a</sup>**

<sup>a</sup> Faculty of Physics, "Babes-Bolyai" University, , 400084 Cluj-Napoca, Romania

<sup>b</sup> Agricultural Sciences and Veterinary Medicine Univ., 400018 Cluj-Napoca, Romania

<sup>c</sup> Faculty of Pharmacy, "Iuliu Hatieganu" Univ., 400032 Cluj-Napoca, Romania

The [Cu(L)<sub>2</sub>] $\cdot$ H<sub>2</sub>O (**1**), [Co(L)<sub>2</sub>] $\cdot$ 2H<sub>2</sub>O (**2**) and [Zn(L)<sub>2</sub>] $\cdot$ H<sub>2</sub>O (**3**) complexes with leucine (L) as ligand, were synthesized in water solution and analyzed by physical-chemical and spectroscopic means.

In the FT-IR spectrum of the ligand the  $\nu_s(\text{N-H})$  stretching vibration appears at 3052 cm<sup>-1</sup> and in the complexes spectra at: 3319 cm<sup>-1</sup>, 3245cm<sup>-1</sup> (**1**), 3325 cm<sup>-1</sup> 3268 cm<sup>-1</sup> (**2**), 3325 cm<sup>-1</sup> and 3263 cm<sup>-1</sup>(**3**) proving the involvement of the -NH<sub>2</sub>- group in the complex formation. The absorption band at 1608 cm<sup>-1</sup> was attributed to the  $\nu(\text{C=O})$  stretching vibration in the spectrum of the ligand and appears to be shifted toward higher wave numbers with 11 cm<sup>-1</sup>, 31 cm<sup>-1</sup> and 46 cm<sup>-1</sup> in the spectra of **1**, **2** respectively **3** proving the involvement of the carboxylic group in the covalent bonding to the metal ion [1]. The FT-IR data show that the amino acids bind to the metal ions through the  $\alpha$ -amino and two carboxylate groups.

The  $n \rightarrow \pi^*$  characteristic band assigned to the C=O bond appears at 277 nm in the ligand spectrum and is shifted toward UV domain with 7 nm, 5 nm and 11 nm in the complex **1**, **2** and **3** spectra, proving the presence of the ligand within the complex and the covalent nature of the metal-ligand bond.

In the visible domain the spectrum of complex **1** show a large band at 620 nm, assigned to the  $^2T_{2g} \rightarrow ^2E_g$  transition, specific to Cu (II) complexes with tetragonal distortion local symmetry due to the Jahn-Teller effect.

Powder ESR spectrum of complex **1** at room temperature is quasi-isotropic ( $g = 2.178$ ) and is characteristic for pseudotetrahedral symmetry around the copper ion. The shape and the value of the  $g$  tensor correspond to a CuN<sub>2</sub>O<sub>2</sub> chromophore. The powder ESR spectrum of complex **2** revealed the presence of monomeric compounds, with octahedral symmetry around the cobalt ion, the  $g$  tensor value is  $g = 2.195$ .

Spectral UV-VIS and ESR data confirmed the covalent metal-ligand bonds, the pseudotetrahedral symmetry around the copper and zinc ions and the octahedral environment for the cobalt ion.

The obtained structural data allow us to propose the molecular formulas for the studied metal complexes.

*Keywords:* Metal complexes; Leucine; ESR

### References

[1] A. Stanila, A. Marcu, D. Rusu, M. Rusu, Gh. Marcu, *J. Molec. Struct.*, 834-836 (2007), 364.

## STRUCTURAL INVESTIGATIONS OF SANDWICH-TYPE HETEROPOLYOXOMETALATE WITH DINUCLEAR VANADIUM CLUSTER

**O. Baban<sup>a</sup>, I. Hauer<sup>b</sup>, D. Rusu<sup>c</sup>, M. Rusu<sup>a</sup>, N. L. Mogonea<sup>b</sup> and L. David<sup>b</sup>**

<sup>a</sup> Faculty of Chemistry, "Babes-Bolyai" University, , 400028 Cluj-Napoca, Romania

<sup>b</sup> Faculty of Physics, "Babes-Bolyai" University, , 400084 Cluj-Napoca, Romania

<sup>c</sup> Faculty of Pharmacy, "Iuliu Hatieganu" University, 400032 Cluj-Napoca, Romania

The sandwich-type  $K_{10}[(VO)_2Sb_2W_{20}O_{70}] \cdot 20H_2O$  heteropolyoxotungstate was investigated by means of elemental analyses, thermogravimetric and spectroscopic (FT-IR, UV-VIS and EPR) methods.

The analysis of vanadium ion coordination mode was made comparing the FT-IR spectrum of the complex with the  $Na_9[SbW_9O_{33}] \cdot 14H_2O$  ligand. The stretching vibration of the terminal  $W=O_t$  bonds is shifted with  $8\text{ cm}^{-1}$  towards higher wave numbers in the FT-IR spectrum of the complex, which indicates the involving of the terminal oxygen atoms in the coordination to the vanadium ions. The  $\nu_{as}(W-O_e-W)$  vibration is shifted with  $11\text{ cm}^{-1}$  in complex FT-IR spectrum. This behavior arises from different deformations induced by the vanadium ions coordination in the frame of the trilacunary ligand. The shift of  $\nu_{as}(Sb-O_{b,c}-W)$ ,  $\nu_s(W-O_b-W)$ ,  $\nu_{as}(W-O_c-W)$  bands in the complex comparative to the ligand is due to the substitution of the lateral  $WO_6$  octahedral by the  $(VO)O_4$  square pyramid and the coordination of  $(VO)_{II}$  ions at  $O_{b,c}$  type oxygens [1].

The UV electronic spectra of the ligand and complex spectrum presents two bands assigned to ligand to metal charge transfer  $p_\pi \rightarrow d_\pi$  transitions in the  $W=O_t$  bonds and the electron transition  $d_\pi \rightarrow p_\pi \rightarrow d_\pi$  between the energetic levels of the tricentric bonds  $W-O_b-W$  [2].

The Visible electronic spectrum of the complex contain the  ${}^2B_2(d_{xy}) \rightarrow {}^2E(d_{xz,yz})$  and  ${}^2B_2(d_{xy}) \rightarrow {}^2B_1(d_{x^2-y^2})$  transition bands for vanadyl ions in  $C_{4v}$  local symmetry, at  $12040\text{ cm}^{-1}$  and respectively  $14705\text{ cm}^{-1}$  for the complex.

The powder EPR spectrum obtained in the X band at room temperature are typical for mononuclear oxovanadium species in an axial environment. The spectrum exhibits eight components both in the perpendicular and in the parallel bands due to the hyperfine coupling of the spin of one unpaired electron with the nuclear spin of the  ${}^{51}V$  isotope ( $g_\perp = 1.973$ ,  $g_\parallel = 1.912$ ,  $A_\perp = 69\text{ G}$ ,  $A_\parallel = 201\text{ G}$ ).

**Keywords:** Heteropolyoxometalate; FT-IR; ESR

### References

- [1] J. Canny, R. Thouvenot, A. Tézé, G. Hervé, M. Leparulo-Loftus, M.T. Pope, *Inorg. Chem.*, 30 (1991), 976.  
[2] T. Yamase, B. Botar, E. Ishikawa, K. Fukaya, *Chem. Letters*, 1 (2001), 56.

## SPECTROSCOPIC INVESTIGATION OF SOME $\text{UO}_2^{2+}$ -POLYOXOMETALATE COMPLEXES

**N. L. Mogonea<sup>a</sup>, O. Baban<sup>b</sup>, I. Hauer<sup>a</sup>, D. Rusu<sup>c</sup>, M. Rusu<sup>b</sup> and L. David<sup>a</sup>**

<sup>a</sup> Faculty of Physics, "Babes-Bolyai" University, 400084 Cluj-Napoca, Romania

<sup>b</sup> Faculty of Chemistry, "Babes-Bolyai" University, 400028 Cluj-Napoca, Romania

<sup>c</sup> Faculty of Pharmacy, "Iuliu Hatieganu" University, 400032 Cluj-Napoca, Romania

The lacunary polyoxometalates (POM) can be used for the incorporation of actinides into stable, non-volatile polyoxometalate complexes for subsequent separation and immobilization.

The  $\text{Na}_{10}[(\text{UO}_2)_2(\text{H}_2\text{O})_2\text{X}_2\text{W}_{20}\text{O}_{70}] \cdot n\text{H}_2\text{O}$  heteropolyoxometalates (**1**:  $\text{X} = \text{Sb}^{\text{III}}$ ,  $n = 28$ ; **2**:  $\text{X} = \text{Bi}^{\text{III}}$ ,  $n = 34$ ) were synthesized and investigated by thermal analysis, FT-IR and UV-Vis spectroscopy in order to determine the coordination, the ordering of cation electronic levels and their local symmetry.

By comparing FT-IR spectra of the uranyl complexes with the corresponding ligand ( $\text{L}_1 = \text{Na}_{12}[\text{Sb}_2\text{W}_{22}\text{O}_{74}(\text{OH})_2]$  and  $\text{L}_2 = \text{Na}_{12}[\text{Bi}_2\text{W}_{22}\text{O}_{74}(\text{OH})_2]$ ) the coordination of  $\text{UO}_2^{2+}$  ions to the POM lacunary units has been estimated. The shift of  $\nu_{\text{as}}(\text{X}-\text{O}_{\text{b,c}}-\text{W})$  and  $\nu_{\text{as}}(\text{W}-\text{O}_{\text{b,c}}-\text{W})$  vibration bands are due to the substitution of external  $\text{WO}_6$  octahedra with  $\text{UO}_2\text{O}_5$  pentagonal-bipyramids and to the coordination of  $\text{UO}_2^{2+}$  ions at the  $\text{O}_{\text{b}}$  and  $\text{O}_{\text{c}}$  atoms.

The UV electronic spectra of the  $\text{UO}_2^{2+}$ -POM complexes are similar to the ones of the ligands  $\text{L}_1$  and  $\text{L}_2$ . Each spectrum presents two bands assigned to the charge transfer from the ligand to the metal  $\text{p}_{\pi} \rightarrow \text{d}_{\pi}$  transitions in  $\text{W}=\text{O}$  bonds and  $\text{d}_{\pi}-\text{p}_{\pi}-\text{d}_{\pi}$  electronic transitions between the  $\text{W}-\text{O}_{\text{b}}-\text{W}$  bonds energy levels. The  $\text{p}_{\pi}-\text{d}_{\pi}$  electronic transition appears at  $\approx 47100 \text{ cm}^{-1}$  for the ligands and  $\approx 46700 \text{ cm}^{-1}$  for the complexes and  $\text{d}_{\pi}-\text{p}_{\pi}-\text{d}_{\pi}$  transitions into tricentric bonds at  $\approx 39000 \text{ cm}^{-1}$  for the ligands and  $\approx 36000 \text{ cm}^{-1}$  for the complexes. The shifting of the bands maximums for the complexes, comparing to the ones of the ligands are due to the distortion introduced by the  $\text{UO}_2^{2+}$  ions coordinated to the neighbor  $\text{WO}_6$  octahedrons [2].

The VIS electronic spectra of the complexes water solutions present the bands due to  $\text{O}=\text{U}=\text{O}$  internal transitions (at  $\approx 420$  and  $\approx 430 \text{ nm}$ ), charge transfer transitions (at  $\approx 468$  and  $\approx 481 \text{ nm}$ ) and U ( $f \rightarrow f$ ) electronic transitions at  $\approx 500 \text{ nm}$ .

The spectroscopic investigations of  $\text{Na}_{10}[(\text{UO}_2)_2(\text{H}_2\text{O})_2\text{X}_2\text{W}_{20}\text{O}_{70}]$ ,  $\text{X} = \text{Sb}^{\text{III}}$  (**1**),  $\text{Bi}^{\text{III}}$  (**2**) complexes indicate a sandwich-type structure formed by two  $\text{B}-\beta\text{-XW}_9\text{O}_{33}$  fragments binding by two uranyl ions and two  $\text{WO}_2$  units.

*Keywords:* Polyoxometalate; Uranyl; FT-IR

### References

- [1] C.J. Gómez-García, E. Coronado, P. Gómez-Romero, N. Casañ-Pastor, *Inorg. Chem.* 32 (1993), 89.  
 [2] T. Yamase, *Chem. Rev.* 98 (1998), 307.

## Surface morphology influence on D retention in Be films prepared by thermionic vacuum arc method

A. Anghel, C. Porosnicu, M. Badulescu, I. Mustata, C. P. Lungu  
*National Institute for Lasers, Plasma and Radiation Physics, Bucharest, Romania*  
 K. Sugiyama, S. Linding, K. Krieger, J. Roth  
*Max-Planck-Institut für Plasmaphysik, Garching, Germany*  
 A. Nastuta, G. Rusu, G. Popa  
*“Al. I. Cuza” University, Iasi, Romania*

In a plasma-confinement device, material eroded from plasma facing components will be eroded, transported and redeposited at other locations inside the reaction chamber. For the design of ITER a first wall made of beryllium is planned while the divertor region will consist of tungsten and carbon [1]. Since beryllium from the first wall will be eroded, ionized in the scrape-off layer plasma and finally will be redeposited on divertor surfaces flowing along the magnetic field, it is important to study the properties of divertor armour materials (C, W) coated with beryllium.

Be films deposited on graphite substrates were prepared using thermionic vacuum arc technology developed at NILPRP Bucharest. The coating device consists of a tungsten filament surrounded by an electron focusing Wehnelt cylinder heated by an external high current source as cathode and an anode made of the material to be deposited (beryllium in this case). The electrons emitted by the cathode heat up and evaporate the anode providing the source for a pure Be plasma, which is ignited by applying a high dc voltage (typically 1-3 kV) to the anode [2].

By applying different bias voltages (-200 V to +700 V) to the substrates during deposition, the morphology of the obtained films can be modified. In this study, a comparison of the films properties as a function of the bias voltage applied to the substrate is done. The films' morphology was characterized by means of AFM, SEM, XRD. It was found that the coatings prepared using negative bias voltage at the substrate during deposition are more compact and have a smoother surface with an average roughness of 7 nm compared to the samples prepared with positive bias voltage.

Also, the thickness and composition of each film were confirmed by Rutherford Backscattering Spectrometry (RBS) and deuterium implantation was performed at IPP Garching in the High Current Ion Source. After implantation, the amount of D retained in the films was determined by Nuclear Reaction Analysis (NRA) using the reaction  $D(^3\text{He}, \alpha)p$ . The obtained  $\alpha$  particle spectrum was converted to D depth profiles using the SIMNRA code [3].

### References:

- [1] ITER Physics Expert Group, ITER physics basis, Nucl. Fusion 39 (1999) 2137-2664
- [2] C P Lungu, I Mustata, V Zaroschi, A M Lungu, A Anghel, P Chiru, Marek Rubel, Paul Coad, G F Matthews and JET-EFDA Contributors, *Phys. Scr.* 2007 **T128** 157.
- [3] M. Mayer, SIMNRA User's Guide, Tech. Report IPP 9/113, Max-Planck-Institut für Plasmaphysik.

**CHARACTERISATION OF A NEW PLASMA JET  
BASED ON ATOMIC AND MOLECULAR PROCESSES**

**S. D. Anghel, A. Simon, A. I. Radu and I.J. Hidi**

Faculty of Physics, “Babes-Bolyai” University, Cluj-Napoca 400084, Romania

Atmospheric pressure plasma jet [1], has been used to etch polyimide, tungsten, tantalum, and silicon dioxide and to deposit silicon dioxide and silicon nitride films and to decontaminate chemical and biological warfare. One of the methods used to study the main characteristics of a plasma jet is based on atomic and molecular processes in the plasma bulk. The aim of this work is to study the thermal characteristics and electron density based on atomic and molecular emission of a new plasma jet at atmospheric pressure. The novelty of our jet is its generation with a single electrode, the plasma gas flowing perpendicularly to the RF powered electrode (11 MHz,  $10^3$  V).

The plasma emission is used to jet characterization. Optical emission of the plasma was collected in two ways: the normal viewing mode and the axial viewing mode. The plasma characteristic parameters were studied as function of helium flow-rate, plasma power and position of the investigated zone. The electron excitation temperature of He atoms,  $T_{\text{excHe}}$  (2000 – 3500 K) and the temperature of excitation of vibrational states of  $\text{N}_2$  molecules,  $T_{\text{vibrN}_2}$  (4000 – 5000 K) were calculated by the Boltzmann plot method. The temperatures of excitation of rotational states of OH radicals,  $T_{\text{rotOH}}$  (550 – 750 K) and of  $\text{N}_2^+$  molecules,  $T_{\text{rotN}_2^+}$  (550 – 850 K) were estimated by finding the best fit of the measured molecular spectra with the synthetic spectra. These temperatures indicate the non-izothermal character of our plasma jet. The electron number densities ( $10^{12}$  –  $10^{13}$   $\text{cm}^{-3}$ ) were determined from  $\text{H}_\alpha$  emission line (656.27 nm) broadening.

For qualitative observations regarding the behaviour of the plasma species we used the relative intensities of the representative lines of He - 667.81 nm as plasma gas,  $\text{N}_2$  - 337.13 nm as dominant component of the diffusing air, O - 777.41 nm and H - 656.27 nm as resultants of  $\text{H}_2\text{O}$  dissociation (residual water can be present in plasma gas and in diffusing air) and  $\text{N}_2^+$  - 391.44 nm as an indicator of existence of helium metastables.

**References**

[1] A. Schutze, J.Y. Jeong, S.E. Babayan, J. Park, G.S. Selwin and R.F. Hicks, *IEEE Trans. Plasma Sci.* **26** (1998) 1685.

# ENERGY APPROACH TO CALCULATING ELECTRON-COLLISION STRENGTHS AND RATE COEFFICIENTS IN MULTICHARGED IONS PLASMA

**A. Glushkov<sup>a,b</sup>, O. Khetselius<sup>b</sup>, A. Loboda<sup>b</sup> and E. Gurnitskaya<sup>b</sup>**

<sup>a</sup>Institute for Spectroscopy of Russian Academy of Sciences (ISAN), Troitsk, 142090, Russia

<sup>b</sup>Odessa University, P.O.Box 24a, Odessa-9, Ukraine

The problem of diagnostics for the collisionally pumped plasma and search of the optimal plasma parameters of X-ray lasing are studied. Two principal theoretical problems must be solved in order to develop a special code adequate to predict the plasma parameters needed to generate a soft-X-ray or extreme UV amplified spontaneous emission: i). accurate calculation of electron-collision excitation cross-sections, rate coefficients for elementary processes in the plasma that are responsible for the formation of emission lines spectra; ii). kinetics calculation to determine level populations, inversions, line intensities, gain coefficients at definite plasma parameters. We present the uniform energy approach, formally based on the QED perturbation theory [1], [2] with using gauge invariant scheme of generation of the optimal relativistic one-electron representation, for the calculation of electron collision strengths and rate coefficients. The aim is to study, in a uniform manner, elementary processes responsible for emission-line formation in plasmas. The electron collision excitation cross-sections and rate coefficients for some plasma Ne-like multicharged ions are calculated. To test the results of calculations we compare them with other authors' calculations and with available experimental data. The inclusion of Na-like states, accounting for diffusion-like processes, can increase the population inversion for the "lasing candidates" by at least a factor of two for a wide range of plasma conditions. Besides, we are calculating the functions, which describe the population distribution within each Rydberg series dependent on the Rydberg electron energy. These functions bear diagnostic information. Detailed calculations will be done for the homogeneous steady-state Maxwellian plasma.

*Keywords:* Electron-ion; Collision; Plasma

## References

- [1] A. Glushkov, L.N. Ivanov, Phys. Lett. A 170 (1992) 33; J.Phys.B 26 (1993) L279.
- [2] A. Glushkov et al, Int.Journ. Quant. Chem. 99 (2004) 936; 104 (2005) 562; J.Phys.CS 11 (2005) 188; 35 (2006) 420.

## RESONANCE AND MULTI-BODY PHENOMENA IN HEAVY IONS COLLISIONS

**A. Glushkov<sup>a,b</sup>, O. Khetselius<sup>b</sup> and A. Loboda<sup>b</sup> and Yu. Dubrovskaya<sup>b</sup>**

<sup>a</sup>Institute for Spectroscopy of Russian Academy of Sciences (ISAN), Troitsk, 142090, Russia

<sup>b</sup>Odessa University, P.O.Box 24a, Odessa-9, Ukraine

A great interest to this topic has been, in particular, stimulated by inaugurating the heavy-ion synchrotron storage cooler ring combination SIS/ESR at GSI [1]. The known discovery of existence of a narrow and unexpected  $e^+$  line in the positron spectra obtained from heavy ions collisions near the Coulomb barrier. Here a consistent unified QED approach is developed and applied for studying the low-energy heavy ions collision, including the electron-positron pair production (EPPP) process too. To calculate the heavy ions (atoms, nuclei) (EPPP) cross-section we use modified versions of the relativistic energy approach, based on the S-matrix Gell-Mann and Low formalism and QED operator perturbation theory [2]. The nuclear subsystem and electron subsystem has been considered as two parts of the complicated system, interacting with each other through the model potential. The nuclear system dynamics has been treated within the Dirac equation with effective potential. All the spontaneous decay or the new particle (particles) production processes are excluded in the 0th order. Resonance phenomena in the nuclear system lead to the structurization of the positron spectrum produced. Analysis of data for cross-section at different collision energies (non-resonant energies, resonant ones, corresponding to energies of s-resonances of compound U-Cf, U-U, U+Ta system) is presented. The special features are found in the differential cross-section for the nuclear subsystem collision energies, for example, for U-U system as follows: (a)  $E_1 = 162.0$  keV (3rd s-resonance), (b)  $E_1 = 247.6$  keV (the 4th s-resonance), (c)  $E_1 = 352.2$  keV (5th upper s-resonance).

*Keywords:* Heavy ions; Collision; Theory

### References

- [1] J.Reinhardt, U. Muller, W.Greiner, Z. Phys.A 303 (1981) 173; V.Zagrebaev, W.Greiner, J. Phys. G. 34 (2007) 1; V.Zagrebaev, V.Samarin, W.Greiner, Phys.Rev.C.75 (2007) 035809; A.Glushkov, JETP Lett.55 (1992) 108; Low Energy Antiproton Phys., AIP Serie.796 (2005) 206 ; A.Glushkov, L.Ivanov, Phys.Lett.A.170 (1992) 36 ; L.Ivanov, A.Glushkov et al, Preprint Inst.for Spectroscopy RAS, AS-5, Moscow,1991; L.Ivanov, T.Zueva, Phys.Scr. 43 (1991) 374;
- [2] A.Glushkov et al, In: New Projects and New lines of research in Nuclear Physics, eds.Fazio G., Hanappe F. (World Sci. Singapore, 2003); Nucl. Phys.A. 734 (2004) 21; Int.J. Quant.Chem. 99 (2004) 879, 936; 104 (2005) 496,512, 562 ; J.Phys.CS. 11 (2005) 188,199.



## MICROORGANISM SENSITIVITY TO IONS AND FREE RADICALS DELIVERED BY PLASMA DISCHARGE

Antonia Poiata<sup>(1)</sup>, Iuliana Motrescu<sup>(2)</sup>, Cristina Tuchilus<sup>(1)</sup>, A. Nastuta<sup>(2)</sup> D. E. Creanga<sup>(2)</sup>, G. Popa<sup>(2)</sup>

<sup>(1)</sup> Faculty of Pharmacy, "Gr. T. Popa" University, Iasi, Romania

<sup>(2)</sup> Department of Physics, "Al. I. Cuza" University, Iasi, Romania

e-mail: iulia@plasma.uaic.ro

The interaction of ionized chemical species -generated during cold plasma atmospheric discharge with molecular and cellular structures in microorganisms was investigated, due to the possible extent of plasma applications in controlling microbial contamination. Among the particles associated to controlled gaseous discharge high concentrations of free radicals can be found (above half a trillion i.e.,  $5 \cdot 10^{11}$  /cm<sup>3</sup>), that can quickly overwhelm the natural defenses of living organisms, leading to their destruction [1-2]. Plasmas usefulness in surface decontamination processes has been reported especially for gram-positive bacteria.

Our research has involved both gram-positive and gram-negative germs treated in helium plasma (asymmetric dielectric barrier discharge) for various time durations between 25 s and 100 s. The investigated microbial species were *Staphylococcus epidermidis*, *Bacillus cereus* ATCC 14579, *Escherichia coli* ATCC 25922 and *Candida sake*, cultivated on special agarized medium. The increased sensitivity to the increase of the distance between the experimental device electrodes (from 2.5 to 3.5

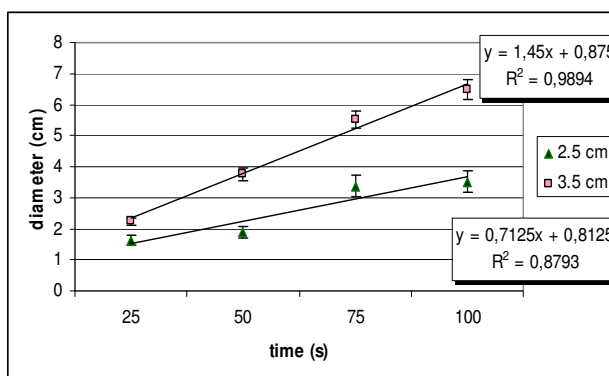


Fig.1. *E. coli* inactivation growth following the interaction with helium plasma

cm.) was noticed according to the slope values of the regression lines corresponding to the graphs  $d(t)$  for every studied bacteria strain ( $d$  being the diameter of the colony growth inactivation). The counting of the surviving colonies around the spot of total microorganism killing provided an estimation of the percentage sterilization efficiency in every case. Discussion was carried out considering the peculiarities of the bacterial cell wall for gram-positive and gram-negative microorganisms in relation with their survival capacity following the interaction with helium plasma.

Key words: asymmetric dielectric barrier discharge, bacteria sterilization

### References

- [1] Morris, A. D; McCombs, G. B; Tolle, S. L; Laroussi, M.; Hynes, W. L., Journal of Dental Hygiene, Nr 4, 1st Oct 2007 , pp. 103-103(1)
- [2] Vleugels, M.; Shama, G.; Deng, X.T.; Greenacre, E.; Brocklehurst, T.; Kong, M.G. IEEE Trans. on Plasma Sci., Vol. 33, Issue 2, April 2005 Page(s): 824 - 828

## ON THE DYNAMIC OF PLASMA PLUME IN HIGH-FLUENCE LASER ABLATION

**C. Ursu<sup>a, b</sup>, S. Gurlui<sup>a</sup>, M3. Ziskind<sup>b</sup>, G. Popa<sup>a</sup> and C. Focsa<sup>b</sup>**

<sup>a</sup>Faculty of Physics, “Al. I. Cuza” University, Blvd. Carol I no.11, Iasi – 700506, Romania

<sup>b</sup>Laboratoire de Physique des Lasers, Atomes et Molécules (UMR 8523), Centre d’Etudes et de Recherches Lasers et Applications (FR CNRS2416), Université des Sciences et Technologies de Lille, 59655 Villeneuve d’Ascq cedex, France (e-mail :

[Cristian.Focsa@phlam.univ-lille1.fr](mailto:Cristian.Focsa@phlam.univ-lille1.fr)

The dynamic of laser produced plasma have been experimentally and theoretically investigated. Different targets types have been irradiated in vacuum ( $10^{-7}$  mbar) by the 2<sup>nd</sup> harmonic (532 nm) of a ns Nd:YAG laser, with fluence in the range 0.7-5 J/cm<sup>2</sup>. Both time and space evolutions of the created space charge structures have been studied by means of both electrical (Langmuir probe)[1] and spectral [2] methods. Recording the temporal and spatial evolution of the corresponding spectral lines has followed the dynamic of different plasma plume components. The axial profile of excitation temperature has been investigated using the relative line intensity method, too. These measurements emphasized a specific behavior of each spectral line, with distinct spatial intensity profiles, leading to different velocities of the associated species. Comparison and convergence of results obtained in emission spectra and ICCD fast imaging will be presented. Considerations are also presented on relationship between plasma plume characteristics and erosion of the target in the region where plasma is originating.

Key words: plume, relative line intensity method, ICCD, erosion.

### References

- 1.J.D.Swift and M.J.R.Schwar, Electrical probe for plasma diagnostic, ILLFF Book, 1970.....
- 2.H. Grien, Plasma spectroscopy, McGraw Hill, 1964 ....

## ON THE CARBON AND TUNGSTEN SPUTTERING YIELD IN A MAGNETRON DISCHARGE

V. Tiron, S. Dobrea, C. Andrei and G. Popa

Faculty of Physics, “Al. I. Cuza” University, Iasi, 700506, Romania

Physical sputtering is one of the most serious processes of erosion of the innermost surfaces of fusion machines. The most important elemental species of wall material in fusion machines are the light elements as Be and C and heavy elements as W, material in the form of tiles covering the metal vessel [1]. Gases as Ar and He are used and considered in ITER as a means of radiation cooling in the divertor, respectively, as the reaction product in the fusion process [2].

The aim of this study is to reveal the influence of the projectile energy on the erosion of C and W target material. In this way, the magnetron discharge may serve as an alternative for ITER divertor diagnostics. The experimental results are presented regarding sputtering yield of the carbon and tungsten using a dc magnetron discharge in argon and helium atmosphere at different gas pressure in the range of 10 to 100 mTorr and discharge power density up to  $5 \cdot 10^5 \text{ W/m}^2$ . To provide the same value of current density on the target surface, the discharge current intensity was used as the control parameter.

In this investigation, carbon and tungsten sputtering yields were measured experimentally using a quartz crystal microbalance (QCM) and two conventional measurements methods based on gravimetric mass loss and profilometry. The C and W sputtering yields measured under  $\text{Ar}^+$  and  $\text{He}^+$  bombardment at normal incidence displayed satisfactory agreement with previously published data over the energy range studied (200eV-700eV). Good agreement of the erosion profile was obtained compared with the ion current density profile on the target surface.

Keywords: plasma-material interaction; sputtering yield; magnetron discharge

### References

- [1] W. Eckstein, *Journal of Nuclear Materials*, **248** (1997) 1-8
- [2] A. Kallenbach, P.T. Lang, R. Dux, C. Fuchs, A. Herrmann, H. Meister, et al., *J. Nucl. Mater.* **337–339** (2005) 732.

## DIAGNOSTICS AND ACTIVE SPECIES FORMATION IN AN ATMOSPHERIC PRESSURE HELIUM STERILIZATION PLASMA SOURCE

**Alpar Simon; Sorin Dan Anghel; Mihaela Papiu; Otilia Dinu**

Babes-Bolyai University, Faculty of Physics, M. Kogalniceanu street 1,  
400084 Cluj-Napoca, Romania

Systematic spectroscopic studies and diagnostics of an atmospheric pressure radiofrequency (10 MHz) He plasma is presented.

The discharge is an intrinsic part of the resonant circuit of the radiofrequency oscillator and was obtained using a monoelectrod type torch, at various gas flow-rates (0.1 - 6.0 l/min) and power levels (0 - 4 W).

As function of He flow-rate and power the discharge has three developing stages. Point-like plasma is formed at low flow-rates (usually below 0.5 l/min) and low power levels. Increasing the flow-rate, the plasma power increases and the plasma develops in its volume having a ball like shape. Further increase of the flow-rate causes gradual change in the plasma shape. Over 1.5 l/min it will extend axially becoming an ellipsoid. At higher flow-rates (over 2.0 - 2.5 l/min), the plasma power presents saturation tendencies due to convection and conduction cooling of the flowing He gas.

The emission spectra of the plasma were recorded and investigated as function of developing stages, flow-rates and plasma power. The most important atomic and molecular components were identified and their evolution was studied as function of He flow-rate and plasma power towards understanding basic mechanisms occurring in this type of plasma.

The characteristic temperatures (vibrational  $T_{vibr}$ , rotational  $T_{rot}$  and excitation  $T_{exc}$ ) and the electron number density ( $n_e$ ) were determined. It was found that  $T_{vibr}$  (for  $N_2$ ) vary between 3600 to 5300 K,  $T_{exc}(He)$  between 1650 and 2200 K,  $T_{rot}(N_2^+)$  between 560 and 640 K, indicating the non-equilibrium character of the discharge. The electron number densities were found to be in the range of  $10^{11} - 10^{13} \text{ cm}^{-3}$ .

The discharge was used successfully for sterilization and surface properties modifications.

Key words: atmospheric pressure; helium plasma; very low power; emission spectroscopy; diagnostics; sterilization; surface modification

## STUDIES ABOUT THE ACRYLIC ACID PLASMA POLYMERS

**I. Topala, N. Dumitrascu, Gh. Popa**

Plasma Physics Laboratory, Blvd. Carol I No. 11, Faculty of Physics,  
Alexandru Ioan Cuza University, Iasi, Romania

Interactions between electron, ions and UV photons from plasma and monomeric gases lead to bond breaking and appearance of polymerizable compounds. Therefore, on substrates arranged in different regions of the discharge, deposition of plasma polymer films occurs, as a three dimensional network of molecular chains. The physico-chemical properties of these polymers are different from the polymers obtained by conventional polymerization reactions [1]. Nowadays, plasma polymerization is a useful tool to obtain thin polymer films on various substrates. These new plasma polymers may provide benefic surface properties such as corrosion resistance, specific optical characteristics, higher biocompatibility and controlled processes at the interface with active biological compounds [2]. Promising results are obtained lately by plasma polymerization in discharges at atmospheric pressure, such as dielectric barrier discharges.

In this work we present results concerning the plasma polymerization of acrylic acid using a dielectric barrier discharge (DBD) in helium, driven by high voltage monopolar pulses with 2 kHz frequency. Discharge diagnosis was performed by electrical measurements and spatially resolved optical emission spectroscopy. The plasma polymers films were investigated by contact angle measurements, IR and UV-Vis absorption spectroscopy and scanning electron microscopy.

The working regime of our DBD at atmospheric pressure was the glow discharge mode, confirming by the discharge current shape and the specific discharge regions. For example, using optical investigations it was identified the known glow discharge regions such as the negative glow and positive column. Besides helium, in the discharge volume were identified other excited species such as atomic oxygen, molecular and ionic nitrogen and hydroxyl free radicals. From the spatial distribution of excited helium lines (commonly with excitation energy of 22.72 eV) it can conclude that high energy electrons are generated in the cathode region of DBD. Also, using the Boltzmann plot of molecular nitrogen vibrational bands intensities it was calculated the vibrational temperature distribution in the discharge gap. An important parameter concerned of the polymerization reaction, respectively the gas temperature, was evaluated from the rotational spectra of the nitrogen molecular ion and the results show values around 340 K in the cathode region and 380 K in the anode region.

The analysis of acrylic acid plasma polymers films proved a hydrophilic character, the water contact angle being less than 20°. Regarding their surface energy, the films show high values of the polar component (more than 50mN/m), and low values of the dispersive component (17 mN/m), as comparing with the polymers films produced by classical methods. The ATR-FTIR spectra of the films confirm strong absorbance in the OH region (3600 – 3000 cm<sup>-1</sup>), in a good correlation with the hydrophilic character. The films show no significant absorbance in the visible range and strong absorption bands in UV, below 325 nm. The surface morphology, investigated by scanning electron microscopy, is smooth at micrometric scale, free of defects and inhomogeneities.

Keywords: Plasma Polymerization; Dielectric Barrier Discharge; Acrylic Acid

### References

- [1] H. Yasuda, Plasma Polymerization, Academic Press (1985) 334.
- [2] R. d'Agostino, P. Favia, C. Oehr, M.R. Wertheimer, Plasma Processes and Polymers 2 (2005) 7.

## STUDIES AND CALCULATION OF ENERGY FILTER PARAMETERS

**A.S.Agafonova<sup>a</sup>, V.A.Surkov<sup>b</sup>**

<sup>a</sup>Institute of Electron Physics, Ukr. Nat. Acad. Sci., Uzhgorod 88017, Ukraine

<sup>b</sup>SELMi Corp., Sumy, Ukraine, *E-mail*: [an@zvl.iep.uzhgorod.ua](mailto:an@zvl.iep.uzhgorod.ua), [sur@selmi.sumy.ua](mailto:sur@selmi.sumy.ua)

For the increase of isotopic sensitivity and improvement of isotopic ratio in monopole mass spectrometers special energy filters (EFs) are used. In a commercial MX7304A mass spectrometer [1] a compact doubled energy filter was employed, consisting of two L-shaped and one flat electrode with end apertures. The L-shaped electrodes were at the same potential, while the flat electrode and the end apertures – at the Earth potential [2]. It is designated to reduce the ion scatter in energy as well as to shift the input hole of the monopole electrode unit with respect to an external source of ions and accompanying neutral particles. Recently this EF was applied for work with secondary ion and neutral beams. Though the real structure of the EF was different from that calculated analytically, its parameters have not been optimized. The aim of the present paper is the EF parameter optimization and its adjustment with a monopole analyser. The calculations were performed using a SIMION software for ion optical system modelling. In order to optimize the filter structure and to determine its parameters depending on the charged particle energy, we have numerically solved the three-dimensional parametrization problem what has enabled the optimal EF geometry to be found and the distribution of potentials on the electrodes to be determined.

The optimization of the actual structure with the account of the ion beam parallel alignment being preserved, has enabled us to find that the L-shaped electrode should be under different potentials and the distance between the input and output holes is reduced almost twice. This resulted in the device transmission increase almost by an order of magnitude. For the increase of the distance between the input and output holes the EF length had to be increased by factor of 1.5, the tolerated dimensions of the input and output holes being also increased. The numerical calculations have shown that if the input and output hole diameters in the EF electrodes are 1.2 mm and the dispersion slit width in the flat electrode is 0.48 mm, then the energy filter resolution should be not worse than  $\rho = \Delta E/E = 0.009$  without a decrease of the ion transmission value.

1. MX7304A mass spectrometers. Technical specifications. Sumy. 2005.
2. T.Ya.Fishkova, Zh. Tekhn. Fiz., 1988, v.58, No. 5, p. 925-929.

## MASS SPECTROMETRIC STUDY OF A GLUCOSE MOLECULE

A.N.Zavilopulo, L.G.Romanova, O.B.Shpenik, A.S.Agafonova

Institute of Electron Physics, Ukr. Nat. Acad. Sci., 21 Universitetska str.,  
Uzhgorod 88017, Ukraine, E-mail: [an@zvl.iep.uzhgorod.ua](mailto:an@zvl.iep.uzhgorod.ua)

A specific feature of mass spectrometry of organic molecules is the difficulty of adequate assignment of spectral peaks to corresponding molecular fragments. Here we report on the results of mass spectrometric studies of a glucose molecule, an organic compound, playing an important role in living organisms, what is a good reason to stimulate its all-round studies. The experimental setup, based on a MX-7304A type monopole mass spectrometer, and the measurement method are similar to [1]. Ions, extracted from the area of interaction of an electron beam and a molecular beam, are focused by the ion optical analyser system, separated according to their masses, and detected by a computer-driven registration system. Masses of fragments of the molecules under investigation were identified, using the reference species (He, Ar, Kr, Xe, and N<sub>2</sub>). The intensity of background ion peaks (not contained in the glucose molecule) did not exceed 0.5% of the intensity of the highest peak in the mass spectrum.

The mass spectrum of the glucose molecule (D-glucose - C<sub>6</sub>H<sub>12</sub>O<sub>6</sub>) contains group of lines with the interval between them of 1-2 a. m. u., typical for organic compounds. The following ion fragment lines are predominant: CHO<sup>+</sup>, CH<sub>3</sub>O<sup>+</sup>, C<sub>2</sub>H<sub>3</sub>O<sup>+</sup>, C<sub>3</sub>H<sub>3</sub>O<sup>+</sup>, C<sub>3</sub>H<sub>6</sub>O<sup>+</sup>, C<sub>4</sub>H<sub>7</sub>O<sup>+</sup>, C<sub>4</sub>H<sub>9</sub>O<sup>+</sup> (Fig.1). The relative intensity of the C<sub>6</sub>H<sub>12</sub>O<sub>6</sub><sup>+</sup> molecular ion peak is almost by factor of 100 smaller than that of the C<sub>4</sub>H<sub>9</sub>O<sup>+</sup> fragment ion. One can suppose that at the collision with electrons, the molecular fragment, not contained in the heterocycle, namely C<sub>2</sub>H<sub>3</sub>O<sup>+</sup>, should be the first to split off. The high intensity of the peak, corresponding to this fragment ( $m/z = 43$ ), indirectly confirms the predominantly cyclic spatial configuration of the molecule under investigation. Besides, dissociative ionization of the glucose molecule C<sub>6</sub>H<sub>12</sub>O<sub>6</sub> also takes place by means of the glucopyranose ring fragmentation (in most cases after the elimination of one or two molecules of water by the glucose molecule).

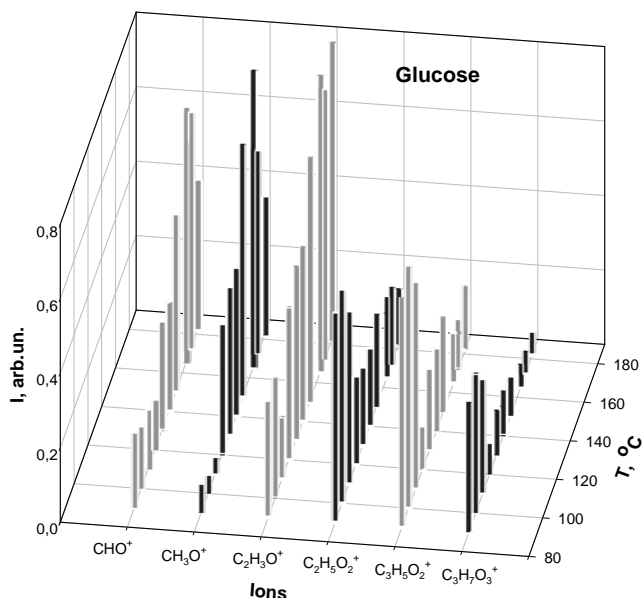


Fig. 1 Mass spectra of glucose molecules

*This work was supported in part by the CRDF Grant # UKC-2832-UZ-06.*

**Keywords:** mass spectrum; fragment ions, glucose

1. A.N.Zavilopulo, O.B.Shpenik, V.A Surkov Anal.Chim.Acta 573-74, (2006), pp. 427-431.

**MASS SPECTROMETRIC DETERMINATION  
OF RESIDUAL AMOUNTS OF PH<sub>3</sub> AND SO<sub>2</sub>F<sub>2</sub> IN FOOD**

<sup>a</sup>A.N. Zavilopulo, <sup>b</sup>V.A. Mamontov, <sup>a</sup>L.G. Romanova, <sup>a</sup>M.I. Mykyta

<sup>a</sup>Institute of Electron Physics, Ukr. Nat. Acad. Sci., Uzhgorod 88017, Ukraine

<sup>b</sup>Transcarpathian Territorial Centre of the Plant Quarantine, Institute of Plant Protection, Ukr. Acad. Agr. Sci.  
Uzhgorod 88017, Ukraine, *E-mail*: [an@zvl.iep.uzhgorod.ua](mailto:an@zvl.iep.uzhgorod.ua)

Obtaining information on the composition and concentration of organic toxic agents in the environmental objects (air, water, soil, water reservoir sediments, etc.) is the decisive type of environmental examinations. In the framework of environmental, health, and chemical examinations, analytical problems can be reduced to two types: determination of the object pollution by specific substances and determination of the object pollution at the conditions when the presence of practically any substance could be expected. There are two main approaches to such problems. The first approach consists in the fact that analysis regarding the content of a specific substance or group of substances is carried out in order to reveal their presence and quantitatively determine their concentration. In the second case, no specific preset components are determined, but the qualitative composition is studied with a subsequent evaluation of concentrations of the identified substances.

Determination of residual amounts of poisonous chemicals in foodstuffs after their disinfection is strictly required to obtain a certificate for their applicability. Phosphine (PH<sub>3</sub>) and sulfuryl fluoride (SO<sub>2</sub>F<sub>2</sub>), being highly toxic for living organisms, are used for gas disinsection (fumigation) of vegetable food, granaries, grain elevators, vehicles from quarantine pests and other dangerous vermin. Here we report on mass spectrometric studies of molecules of gaseous phosphine and sulfuryl fluoride and samples of juice of cherries, subjected and not subjected to these fumigators. As a rule, chemical methods are used for quantitative determination of these substances; however, not always the results are satisfactory. In particular, this concerns SO<sub>2</sub>F<sub>2</sub>, whose molecules are characterized by high chemical passivity, and their residual amounts can hardly be determined by conventional techniques of analytical chemistry. Application of mass spectrometry for these purposes is of a certain interest. Analyzing mass spectra, obtained using a monopole mass spectrometer, one should note them to be somewhat different from those quoted in the NIST database: the phosphine mass spectrum contains molecular hydrogen and in the sulfuryl fluoride mass spectrum pronounced F<sup>+</sup> and F<sub>2</sub><sup>+</sup> peaks are observed.

Besides the determination of traces of PH<sub>3</sub> and SO<sub>2</sub>F<sub>2</sub> in the juice of fumigated and non-fumigated cherries, we have also performed measurements of full and dissociative ionization of these substances. Using a special method [1], from their threshold dependences we have determined the potentials of appearance for the H<sup>+</sup>, P<sup>+</sup>, HP<sup>+</sup>, H<sub>2</sub>P<sup>+</sup>, H<sub>3</sub>P<sup>+</sup> fragment ions for phosphine and for S<sup>+</sup>, F<sup>+</sup>, F<sub>2</sub><sup>+</sup>, SO<sup>+</sup>, SO<sub>2</sub><sup>+</sup>, SOF<sup>+</sup>, SO<sub>2</sub>F<sup>+</sup>, SO<sub>2</sub>F<sub>2</sub><sup>+</sup>, SO<sub>2</sub>F<sub>2</sub>H<sup>+</sup> fragment ions for sulfuryl fluoride (Fig.1).

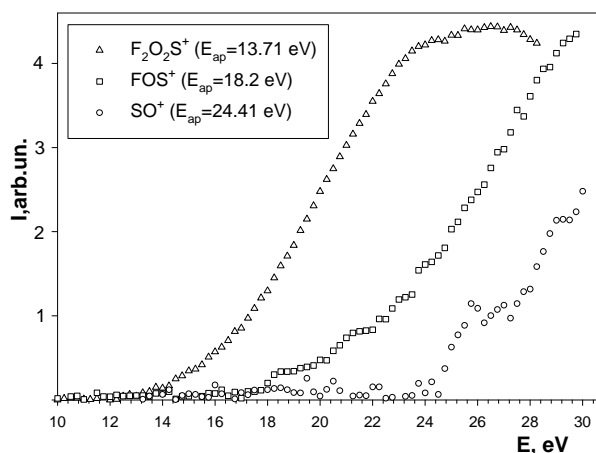


Fig.1. The threshold dependences of relative ionization cross-section of the sulfuryl fluoride and its fragment ions



## MASS SPECTROMETRY OF ASCORBIC ACID

A.N.Zavilopulo, A.S.Agafonova, L.G.Romanova, M.I.Mykyta

Institute of Electron Physics, Ukr. Nat. Acad. Sci., 21 Universitetska str.,  
Uzhgorod 88017, Ukraine, E-mail: [an@zvl.iep.uzhgorod.ua](mailto:an@zvl.iep.uzhgorod.ua)

Mass spectrometry ranks very high among the variety of widely applied physical methods of studies of bioorganic compounds. Mass spectrometric studies, related to the investigation of processes of dissociative ionization and ways of fragmentation of bioorganic compounds, deserve particular attention. The subject of our investigation was one of the most vitally important molecules – ascorbic acid. Ascorbic acid, or vitamin C ( $C_6H_8O_6$ ) is a lactone of hexonic acid with a structure close to that of L-glucose. Due to the presence of two asymmetrical carbon atoms in the 4 and 5 positions, the ascorbic acid forms 4 optical isomers and two racemates. Vitamin C is a crystalline compound with the melting point at 462-464 K, easily dissolved in water with the formation of acidic solutions. One should note the presence of quite a few papers devoted to its spectroscopy, especially mass spectroscopy.

We have performed mass spectrometric studies of the  $C_6H_8O_6$  molecule. The measurements were carried out, using a setup with a monopole mass spectrometer MX-7304A, the technique being described in detail in [1]. Since no temperature data were available from the known mass spectrometric catalogues regarding the mass spectrometer operating modes for the ascorbic acid molecule, and temperature is a factor, affecting the peak intensities in the mass spectra, we have performed mass spectra measurements at the temperatures from 360 to 450 K. For identification of the ascorbic acid molecule fragments, a special attention was paid to the calibration of the mass scale, using the known noble gas (Ar, Xe, and Kr) masses. The mass spectra were measured for two values of the ionizing electron energies – 40 and 70 eV.

The studies have shown the peak intensity in the spectra to be proportional to the temperature increase and reaches a maximum in the temperature range  $432 \div 442$  K. In the ascorbic acid mass spectra an intense peak is present at  $m/z$  116 ( $[C_4H_3O_5]^+$ ) in comparison with the molecular ion peak ( $m/z=176$ ). The most probable scheme for the molecule fragmentation is proposed (Fig.1).

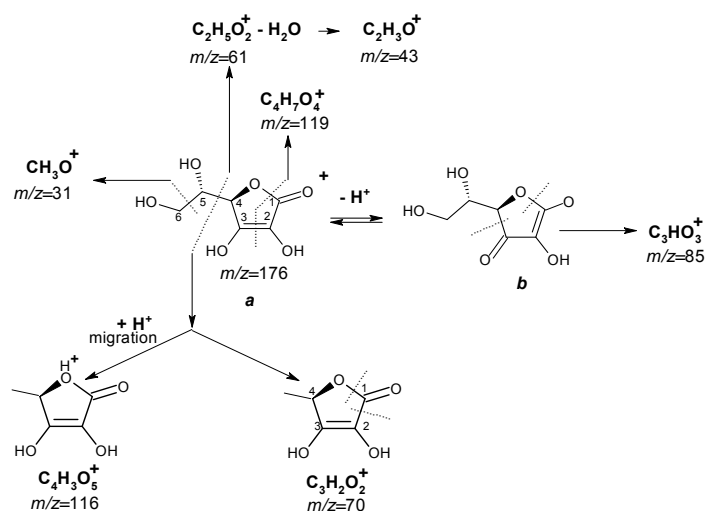


Fig.1 Fragmentation paths of ascorbic acid.

This work was supported in part by the CRDF Grant # UKC-2832-UZ-06.

1. A.N.Zavilopulo, F.F.Chipev, O.B.Shpenik, Technical Physics, V.50, No 4, 2005, pp. 402–407.

## PRESOWER DETECTOR IMPLEMENTATION IN $\pi^+\pi^-$ HADRONIC ATOM BREAKUP STUDIES

M. Pentia, D.E. Dumitriu, M. Gugiu, C. Ciocarlan,  
S. Constantinescu, and C. Caragheorghopol

Department of Nuclear Physics - Tandem,  
"Horia Hulubei" National Institute of Physics and Nuclear Engineering,  
Atomistilor St. 407, P.O.Box MG-6 Măgurele, 077125 Bucharest, Romania

DIRAC experiment at CERN [1] looks upon pionium ( $\pi^+\pi^-$  hadronic atom) lifetime by measuring its breakup (ionization) probability. The pion pairs detection from the atom breakup processes is the main task of the DIRAC setup. This is realized with a double arm magnetic spectrometer. In this context the main task of the preshower detector, together with the Cherenkov detector, is to reach an overall electron rejection efficiency  $\sim 99.5\%$ , in the region of low energy ( $1 \div 3$  GeV), where the pion/electron separation is important.

The preferred technique for pion/electron separation is to probe the shower development for particle discrimination. Electrons and pions are counted by detecting the preshower signal in plastic scintillator slabs placed behind a 2 or 5 radiation lengths thick Pb converter. The particles (electrons and photons) detection of the electromagnetic shower produced by a relativistic electron, gives a high amplitude (ADC) signal, as long as the pion detection, as minimum ionizing particle, gives a low amplitude signal. The preshower Pb converter is too shallow for pions to produce hadronic shower [2]. So, the pion shower contribution is negligible.

We studied the electron and pion detection by measuring their shower production in the early stages, to get the entire information on pion/electron separation and to find a proper methodology for electron background rejection. We report the Monte-Carlo simulations and test beam data of  $\pi^-$  and  $e^-$  at various energies for optimal configuration settings. The objective for simulation studies in designing the PSh detector has been the optimization of converter and scintillator slab thickness in order to do the best pion/electron separation in the  $1 \div 8$  GeV energy range.

We have studied the dependence of the amplitude spectra properties on particle momentum and on converter and scintillator thickness using GEANT package (<http://cern.ch/geant4/geant4.html>). The electron rejection was estimated to be better than 85% with a pion loss less than 5% in the momentum range  $1 \div 4$  GeV/c using a preshower detector with Pb converter thickness  $w_{Pb} = 2.5$  cm and scintillator slab  $w_{Sc} = 1$  cm.

*Keywords:* preshower detector, hadron/electron separation, hadronic atoms

### References

- [1] B. Adeva, L. Afanasyev, M. Benayoun, ..., M. Pentia et al., Physics Letters B 619 (2005) 50
- [2] C Santamarina, M Schumann, L. G. Afanasyev, T Heim, J. Phys. B 36 (2003) 4273

## COMPUTATIONAL CHEMISTRY *ir* SPECTRA SIMULATION OF DEUTERATED TRIGLYCIN SULFATE II FOR NEUTRON QUASIELASTIC INCOHERENT SCATTERING ON MICROCRYSTALS

C.A. Simion<sup>a</sup>, V. Tripăduș<sup>b</sup>, A. Niculescu<sup>c</sup>

<sup>a</sup> Life Sciences and Environmental Physics Dept., 407 Atomistilor St. PO Box – MG 06 Magurele Ilfov 077125, “Horia Hulubei” National Institute for Physics and Nuclear Engineering, Romania

<sup>b</sup> Departament of Nuclear Physics-Tandem, 407 Atomistilor St. PO Box – MG 06 Magurele Ilfov 077125, “Horia Hulubei” National Institute for Physics and Nuclear Engineering, Romania

<sup>c</sup> Institute of Organic Chemistry "C. D. Nenitzescu" of the Romanian Academy, NMR Laboratory, 212B Splaiul Independentei, Bucharest, Romania

There are three Triglycine sulfate molecular units in the microcrystalline powder (GI, GII, and GIII); the first molecular structure is an amphionic form with an out-of-plane  $-\text{NH}_3^+$  group, the another two components being mono-protonated planar structures Triglycine sulfate molecules crystallize at room temperature in monoclinic form -  $P2_1$  space group, having a polar direction among the two-fold screw axis. The spontaneous polarization disappears near  $47^\circ\text{C}$  in the same time with the space group modification from  $P2_1$  to  $P2_1/m$ . The two main motions which determine the order-disorder ferroelectric phase transition are the GI amino group ( $-\text{NH}_3^+$ ) swinging, and the tunneling of hydrogen atom involved in GII – GIII hydrogen bonding respectively [1]. In this order, recording of quasielastic neutron scattering spectra on a range of temperatures near to  $49.5^\circ\text{C}$  requires a deuteration of the microcrystalline Triglycine sulfate powder [2]. Labile protons of GI amino group are exchanged through the deuteration process. The substitution of Hydrogen with Deuterium permits a better understanding of a jump rotational motion of the proton of the amino group in a hindered potential.

For a complex interpretation of the *ir* experimental spectra, a computational chemistry method is used. This method allows a sequential virtual deuteration process to develop for each position in the molecules as well as a complete correlation between theoretical and experimental data. An un-equivoque attribution was possible for all signals, confirming the deuteration at GI out-of-plane  $-\text{NH}_3^+$  group (disparition of “ammonium band” from  $\sim 3100 - 3200 \text{ cm}^{-1}$  (m-i, large) related to sym  $\nu_{\text{NH}_3^+}$  as,  $\nu_{\text{NH}_3^+}$ , and the apparition of a large  $\sim 2200 \text{ cm}^{-1}$  (m) band related to the symmetrical  $\nu_{\text{ND}_3^+}$  as,  $\nu_{\text{ND}_3^+}$ .

Using a computational chemistry method we have been demonstrate the existence of a large band near  $2375 \text{ cm}^{-1}$  (m) substituted by a small signal at  $2374.97 \text{ cm}^{-1}$  (m-i, large) (some un-deuterated fraction) and a large signal at  $\sim 2200.57 \text{ cm}^{-1}$  (m) correlated with the deuteration of labile amino protons belonging to all three units of Triglycin sulfate .

*Deuterated Triglycin sulfate, phase transition, ir spectra, computational chemistry*

### References

- [1]. R.R. Choudhury, R. Chitra, M. Ramanadham, J. Phys.: Condens. Matter, 15, (2003), 4641 – 4650.  
 [2]. V. Tripăduș, A. Rădulescu, A. Buchsteiner, S. Janssen, D. Aranghel, C. Simion, Roum. J. Phys., 51 (5-6), (2006), 557-565.

## APPLICATION OF COMPTON SCATTERING IN ORGANIC SCINTILLATORS FOR THE ENERGY CALIBRATION IN $\beta$ AND NEUTRON SPECTROSCOPY

L. Daraban

Faculty of Physics, Babes-Bolyai University, Cluj-Napoca, Romania

The plastic scintillator  $\beta$ -spectroscopy was applied to the radioactive waste measurements by using a large area plastic scintillator. One of most important problem is the calibration of the multichannel analyzers regarding to  $\beta$ - ray energy units, was applied by generating of some Compton distributions of electrons produced by gamma radiations with well-known energies in the organic scintillator. The values  $E_{\text{emax}}$  of the Compton edge's energy [1], corresponding to each distribution is calculated and the channels of the analyzer are calibrated with this values. A computer program was used for locating the Compton edge as the most abrupt descendent part of the spectrum. A good linear calibration curve was obtained for  $\beta$ -spectra processing by Fermi-Kurie method for some well-known radionuclides.

Stylben  $C_{14}H_{12}$ , is one of the best organic scintillators for the measurement of neutrons energy by the proton recoil method. But the light efficiency produced by protons is lower than the one produced by electrons having equal energies. If the calibration with Compton electrons gives a linear dependence with their energy ( $dL/dE = \text{ct.}$ ), in the case of exciting a stylben crystal with heavy particles, the luminosity function  $L(E)$  varies with the energy faster than a linear function, as higher the LET is  $dE/dx$ . In this organic scintillator, a correlation between the energies of different types of particles, which give the same luminosity was established. This is useful for calibrating the neutron spectrometers equipped with an organic scintillator, because in order to calibrate the energetic scale of the recoil protons, Compton electrons can be used. We established an equivalent formula between the energy of a proton and that of an electron, which gives the same number of photons of scintillation in the crystal.

By operating a neutron spectrometer with stylben crystal or with a plastic scintillator NE-102, the calibration at proton energies equivalent was obtained by using Compton electrons produced by the gamma radiation of  $^{60}\text{Co}$ ,  $^{137}\text{Cs}$  and that of 4.43 MeV from the dezexcitation of  $^{12}\text{C}$  in the neutron sources Am-Be. The control of the validity of the calibration method was confirmed by the monoenergetic neutrons spectrum at 14.6 MeV of the D-T reaction from the neutron generator.

### References

- [1] N. Kudomi, Nucl.Intr.& Meth.in Phys. Res., A430 (1999) 96-99.

## Authors Index

### A

Abbas, I. ....	113
Ackerman, G. ....	73
Acuña, M. ....	77
Agafonova, A.S. ....	126, 127, 174, 175, 177
Aguilar, A. ....	73
Ancarani, L.U. ....	70
Andersen, H.H. ....	52
Andrei, C. ....	171
Anghel, A. ....	165
Anghel, S.D. ....	166, 172
Arbó, D.G. ....	40, 111, 114, 143, 144
Arista, N.R. ....	44
Asfandiarov, N.L. ....	160
Aștilean, S. ....	150, 151, 152, 153, 154, 157
Aumayr, F. ....	41, 105
Azriel, V.M. ....	59, 132

### B

Baban, O. ....	163, 164
Badulescu, M. ....	165
Balcerski, J. ....	155
Baldeck, P.L. ....	153
Bandurina, L. ....	84
Banković, A. ....	121
Baran, J. ....	136
Barrachina, R.O. ....	32, 35, 61, 133, 134
Bereczky, R.J. ....	105
Berényi, D. ....	21
Bernardi, G. ....	134
Berrah, N. ....	73
Beu, T.A. ....	108, 158
Bilodeau, R.C. ....	73
Biri, S. ....	106
Blaum, K. ....	96
Boca, M. ....	142
Boca, S.C. ....	154
Böhm, S. ....	138
Bondar, I.I. ....	112, 113
Borbély S. ....	40, 144
Borovyk Jr., A. A. ....	140
Braeuning–Demian, A. ....	26, 82
Brawley, S. ....	50
Bučar, K. ....	39, 64
Buck, U. ....	46

Buica, G. ....	110
Bundesmann, J. ....	42
Burgdörfer, J. ....	37, 111

### C

Cabau, G. ....	158
Campeanu, R.I. ....	51, 124
Canpean, V. ....	151
Caragheorgheopol, C. ....	178
Carravett, V. ....	47
Cassidy, D. ....	136
Champion, C. ....	78, 131
Charlton, M. ....	52
Chernushkin, V.V. ....	93
Chernyshova, I.V. ....	129, 130
Chesnel, J.-Y. ....	31, 32, 107, 134
Chiper, A.S. ....	103
Chiș, V. ....	124
Ciappina, M.F. ....	23
Ciocarlan, C. ....	80, 178
Ciortea, C. ....	80
Colavecchia, F.D. ....	70
Constantinescu, S. ....	178
Cooke, D. ....	50
Coreno, M. ....	29, 47
Cozar, O. ....	115, 116, 117, 118
Cozma, D. ....	162
Creanga, D.E. ....	169
Culea, E. ....	115
Culea, M. ....	115, 116, 117, 118

### D

Dal Cappello, C. ....	70, 78
Daraban, L. ....	180
Das, S. ....	136
Dassanayake, B.S. ....	136
David, L. ....	162, 163, 164
Deumens, E. ....	28
Dimitriou, K.I. ....	111
Ding, Z.J. ....	36
Dinu, O. ....	172
Dobrea, S. ....	171
Dogan, M. ....	88
Dondera, M. ....	146
Dovhanych, M. ....	76

DuBois, R.D.....	123
Dubrovskaya, Yu. ....	168
Dudu, D.....	120
Dujko, S. ....	137
Dumitrascu, N.....	173
Dumitriu, D.....	80, 82, 178
Dumitriu, I.....	73
Dumitriu, Irina. ....	145
Dupljanin, S. ....	137
Dürr, M. ....	23

## E

Elkafrawy, T. ....	136
Enulescu, A.....	80
Erdevdy, M.M.....	101, 128
Erengil, Z.....	88

## F

Facsko, S.....	104
Fainstein, P.D.....	136
Farcău, C.....	150, 154
Fedorko, R.O.....	60
Ferger, T. ....	23
Feyer, V.....	29, 47
Filipović, D.M.....	74, 75
Fink, D. ....	42
Fiol, J.....	35, 77
Fischer, D.....	23, 58
Florescu, V.....	142
Fluerasu, D.....	80, 82
Focke, P.....	134
Focsa, C.....	170
Fregenal, D.....	134
Frémont, F.....	31, 32, 107, 134
Fritzsche, S.....	56, 63

## G

Galassi, M.E.....	136
Gasaneo, G.....	70
Gavin, J. ....	123
Gavrila, M.....	38, 142
Gedeon, S.....	62
Gedeon, V. ....	84
Gervasoni, J.L.....	44, 156
Ghişoiu, I.....	108
Gibson, N.D.....	73
Glukhov, I.L.....	95
Glushkov, A.....	53, 97, 149, 167, 168

Gochitashvili, M. ....	72
Gomonai, A.....	71
Gorczyca, T.....	73
Groeneveld, K.O.....	22
Gromov, E.V.....	29
Gugiu, M.....	80, 178
Gulyás, L.....	122
Gumberidze, A.....	54
Gümüş, H. ....	87
Gurlui, S.....	170
Gurnitskaya, E.....	167

## H

Hajaji, A.....	31, 32, 107, 134
Hanssen, J. ....	131
Hasan, A. ....	23
Hauer, I. ....	163, 164
Heller, R.....	104
Hellhammer, R.....	42
Heneral, A.A. ....	92
Herrera, M.Z. ....	156
Hidi, I.J.....	166
Holste, K. ....	81, 140
Hori, M. ....	119
Horváth, L.....	108
Hunniford, C.A. ....	52
Hutyach, Yu.....	71

## I

Ichioka, T. ....	52
Igarashi, A.....	122
Ignatenko, A.....	149
Imao, H. ....	52
Imre, A. ....	71, 109
Iordache, A.....	117
Iosin, M.....	152, 153
Itoh, A. ....	83
Iván, I. ....	106
Ivanov, E.A. ....	120

## J

Járai-Szabó, F.....	85
Jovanović, J.V.....	86
Juhász Z. ....	106, 107

## K

Kabachnik N. M.....	63
---------------------	----

Kabadayi Önder .....	87
Kavčič M. ....	39, 64
Kayani A. ....	136
Kaymak N. ....	88
Kazakov S.M. ....	161
Kelemen V. I. ....	75, 76
Kelman V.A. ....	92, 141
Khetselius O. ....	97, 98, 99, 149, 167, 168
Kilic HS .....	88
Kirchner T. ....	23
Knudsen H. ....	52
Koike F. ....	43
Kontros J.E. ....	101, 128, 129, 130
Kövér Á. ....	50, 140
Kowarik G. ....	105
Kozhuharov C. ....	55
Kristiansen H.-P. E. ....	52
Kukhta A.V. ....	159, 160, 161
Kukhta I.N. ....	159
Kupliauskienė A. ....	65, 66
Kuroda N. ....	52

## L

Lahmam-Bennani A. ....	25
Laricchia G. ....	50
Lazur V. ....	62
Leclercq C. ....	31
Lehene C. ....	116
Lekadir H. ....	78
Lekadir H. ....	131
Li H.M. ....	36
Li Y.G. ....	36
Loboda A. ....	167, 168
Lomsadze B. ....	72
Lomsadze R. ....	72
de Lucio O. G. ....	123
Lungu C. P. ....	165

## M

Macri P. A. ....	61, 114, 133
Malović G. ....	90, 121
Mamontov V.A. ....	176
Mao S.F. ....	36
Marcu, A. ....	162
Marić, D. ....	90
Marinković, B.P. ....	74, 75
Marler, J.P. ....	121
Martin, F. ....	33
Marushka, V.I. ....	60

Mátéfi-Tempfli, M. ....	106
Mátéfi-Tempfli, S. ....	106
Maydanyuk, N. ....	23
McCollough, R.W. ....	52
Mesaros, C. ....	118
Meza, E. ....	159
Mihelič, A. ....	39
Miraglia, J.E. ....	143
Mizuno, T. ....	83
Mogonea, N.L. ....	163, 164
Møller, S.P. ....	52
Möller, W. ....	104
Moneta, M. ....	155
Moshhammer, R. ....	23, 34
Motrescu, I. ....	169
Mukoyama, T. ....	79
Müller, A. ....	81, 140
Murtagh, D.J. ....	50
Mustata, I. ....	165
Mykyta, M.I. ....	127, 176, 177

## N

Nagata, Y. ....	52
Nagy, Cs. ....	162
Nagy, L. ....	40, 85, 124, 135, 144
Naja, A. ....	25, 31
Nastuta, A.V. ....	103, 169
Neyra, O.L. ....	159
Niculescu, A. ....	179
Nikitović, Ž. ....	67
Nina, A. ....	89
Nitisor, S. ....	120

## O

Öhrn, Y. ....	28
Opachko, A. ....	139
Orbán, A. ....	68
Orban, I. ....	138
Ortikov, R.O. ....	102
Ovcharenko, E. ....	71
Ovsiannikov, V. D. ....	93, 95

## P

Palásthy, B. ....	64, 69
Pálinkás, J. ....	106
Panchenko, L.K. ....	91
Panchenko, O.F. ....	91
Papiu, M. ....	172

Parilis, E.S.....	48
Paripás, B.....	64, 69
Pavlyuchok, O.V.....	125
Pejčev, V.....	74, 75
Pena, M.D.....	80
Pentia, M.C.....	80, 178
Perehanets, V.....	60
Persson, E.....	111
Pešić, Z.....	73, 104
Petrović, Z. Lj.....	67, 86, 89, 90, 121, 137
Petukhov, V.P.....	100
Piraux, L.....	106
Piticu, I.....	80
Plekan, O.....	29, 47, 92, 141
Poiata, A.....	169
Popa, Gh.....	103, 169, 170, 171, 173
Popik, T.Yu.....	102
Póra, K.....	135
Porosnicu, C.....	165
Prince, K.C.....	29, 47
Pshenichnyuk, S.A.....	160

## R

Rabasović, M.S.....	74
Radmilović-Radjenović, M.....	89, 90
Radu, A.I.....	166
Raspopović, Z.....	67
Remeta, E.....	75, 76
Richter, R.....	29, 47
Ricsóka, T.....	140
Ricz, S.....	81, 140
Robson, R.E.....	121
Rodríguez, V.D.....	114
Rolles, D.....	73
Romanova, L.G.....	127, 175, 176, 177
Rusen, I.....	120
Rusin, L.Yu.....	59, 132
Rusu, D.....	162, 163, 164
Rusu, G.B.....	103
Rusu, M.....	163, 164

## S

Sabin, J.R.....	28
Saenz, A.....	145
Sarkadi, L.....	68
Šašić, O.....	67, 137
Scafes, A.C.....	80
Schabinger, B.....	96
Schippers, S.....	24, 81, 140
Schirmer, J.....	29

Schuch, R.....	138
Schulz, M.....	23
Segui, S.....	44
Šević, D.....	74, 75
Shafranyosh, I.I.....	60, 125
Shafranyosh, M.I.....	125
Shimon, L.L.....	125
Shpenik, O.B.....	101, 102, 126, 127 128, 129, 130, 175
Shpenik, Yu.O.....	92, 141
Simion, C.A.....	179
Simon, A.....	166, 172
de Simone, M.....	29, 47
Simulik, V.....	139
Sise, O.....	88
Snegurskaya, T.A.....	60
Snegursky, A.V.....	109
Soret, J.....	31
Sovak, P.....	155
Staicu Casagrande, E.M.....	25
Stancalie, V.....	94
Stanila, A.....	162
Stecovych, V.V.....	125
Stiufiuc, G.....	157
Stiufiuc, R.....	157
Stöhlker, Th.....	56, 63
Stojanović, V.....	67, 86, 89
Stolterfoht, N.....	28, 42
Sturm, S.....	96
Suárez, S.....	32, 134
Sukhoviya, M.I.....	125
Sulik, B.....	31, 106, 107
Suran, V.V.....	112, 113
Surkov, V.A.....	174
Surzhykov, A.....	56, 63
Svinarenko, A.....	97
Svitlichnyi, E.A.....	141

## T

Taboridze, O.....	72
Takács, E.....	106
Tanis, J.A.....	30, 31, 136
Thomsen, H.D.....	52
Tiron, V.....	171
Toderas, F.....	152, 157
Toderian, S.....	120
Tőkési, K.....	40, 52, 64, 105, 106, 143, 144
Topala, I.....	173



Torii, H.A.....	52
Tosa, V. ....	148
Tošić, S. D.....	74, 75
Tóth, I.....	124
Tripăduş, V. ....	179
Trofimov, A.B. ....	29
Trotsenko, S.....	138
Trujillo, R.C.....	28
Tsiskarishvili, N.....	72
Tsuchida, H.....	83
Tuchilus, C.....	169
Tutlys, V. ....	65

Zeng, R.G.....	36
Zhang, Z.M. ....	36
Zhmenyak, Yu.V.....	92, 141
Ziskind, M.....	170
Žitnik, M. ....	39, 64
Živanov, S.....	90

## U

Uggerhøj, U.....	52
Ullrich, J.....	23
Ursescu, D.....	57
Ursu, C. ....	170
Uznański, P. ....	155

## V

Vall-Ilosera, G. ....	29
Varga, D.....	140
Vata, I.....	120
Vatasescu, M.....	147
Vikor, Gy. ....	106
Vințeler, E.....	150
Vukstich, V.S.....	109

## W

Walter, C.W.....	73
Walters, H.R.J.....	49
Werth, G.....	96
Whelan, C.T.....	45
Wilhelm, R.....	104
Williams, A. ....	50
Winkworth, M.....	136

## Y

Yamada, T.....	83
Yamazaki, Y. ....	27, 52
Yildirim, M.....	88

## Z

Zajak, T.....	139
Zavilopulo, A.N. ..	126, 127, 175, 176, 177
Zaytseva, I. L. ....	29